Pavement Temperature Effects on Overall Urban Heat Island

by

Tina Pourshams-Manzouri

A Thesis Presented in Partial Fulfillment
of the Requirements for the Degree
Master of Science

Approved April 2013 by the
Graduate Supervisory Committee:

Kamil Kaloush, Co-Chair
Zhihua Wang, Co-Chair
Claudia Zapata
Michael Mamlouk

ARIZONA STATE UNIVERSITY

May 2013

ABSTRACT

In recent years, an increase of environmental temperature in urban areas has raised many concerns. These areas are subjected to higher temperature compared to the rural surrounding areas. Modification of land surface and the use of materials such as concrete and/or asphalt are the main factors influencing the surface energy balance and therefore the environmental temperature in the urban areas. Engineered materials have relatively higher solar energy absorption and tend to trap a relatively higher incoming solar radiation. They also possess a higher heat storage capacity that allows them to retain heat during the day and then slowly release it back into the atmosphere as the sun goes down. This phenomenon is known as the Urban Heat Island (UHI) effect and causes an increase in the urban air temperature.

Many researchers believe that albedo is the key pavement affecting the urban heat island. However, this research has shown that the problem is more complex and that solar reflectivity may not be the only important factor to evaluate the ability of a pavement to mitigate UHI.

The main objective of this study was to analyze and research the influence of pavement materials on the near surface air temperature. In order to accomplish this effort, test sections consisting of Hot Mix Asphalt (HMA), Porous Hot Mix asphalt (PHMA), Portland Cement Concrete (PCC), Pervious Portland Cement Concrete (PPCC), artificial turf, and landscape gravels were constructed in the Phoenix, Arizona area. Air temperature, albedo, wind speed, solar radiation, and wind direction were recorded, analyzed and compared above each pavement material type.

The results showed that there was no significant difference in the air temperature at 3-feet and above, regardless of the type of the pavement. Near surface pavement temperatures were also measured and modeled. The results indicated that for the UHI analysis, it is important to consider the interaction between pavement structure, material properties, and environmental factors.

Overall, this study demonstrated the complexity of evaluating pavement structures for UHI mitigation; it provided great insight on the effects of material types and properties on surface temperatures and near surface air temperature.

DEDICATION

I dedicate this work to my lovely family, Soraya, Fereydoun, and Tania, for their endless love, support and encouragement.

ACKNOWLEGEMENT

I would like to express my sincere thanks to Dr. Kamil Kaloush, my committee co-chair, for his continuous encouragement and guidance through my undergraduate and graduate studies. He was not only a co-chair but rather a mentor and an advisor, who would always support and guide me in any way possible. My graduate years and this research work would have not been successful if not for his continuous dedication to help encourage and support.

I would like to thank Dr. Zhihua Wang, my committee co-chair, for his support and guidance throughout the project. His greatest effort in providing me with all the necessary resources cannot be left unrecognized. Without his knowledge and support the success of this project was not possible.

I would also like to thank Dr. Mike Mamlouk and Dr. Claudia Zapata, Committee members, who have always guided me through my undergraduate and graduate studies.

I am heartily thankful to, Dr. Soe Myint, Jeff Stempihar, Waleed Zeiada, Moein Saleh, David Ramsey, Sam Enmon, Jiachuan Yang, Jiun Song, Carolina Rodezno my parents, friends, family and all those who supported me through this project.

Last but not least, special thanks to, Decorative Paving solutions, American Asphalt, Vulcan Materials, CEMEX, and For Ever Lawn for their support and sponsorships through the construction of this project. Special Thanks to the Asphalt Pavement Alliance (APA) who provided funding for this special research project.

TABLE OF CONTENT

Page

CHAPTER Page

CHAPTER Page

LIST OF TABLES

LIST OF FIGURES

Figure Page

CHAPTER 1

1.1 INTRODUCTION

In recent years, an increase of environmental temperature in urban areas has raised many concerns. These areas are subjected to higher temperatures compared to rural surrounding areas. Modification of land surface and use of materials such as concrete and/or asphalt are one of the contributing factors influencing the ecology system and therefore the environmental temperature in the urban areas. Such engineered materials have relatively higher solar energy absorption and tend to trap a relatively higher incoming solar radiation. As the result they contain a higher thermal energy storage that allows them to retain heat during the day and then slowly release it back into the atmosphere at night. This phenomenon is known as Urban Heat Island (UHI) effect and causes an increase in the surrounding air temperature during the day and night (1,2).

The U.S. Department of Energy conducted a study in 1993 that showed an increasing trend in urban temperatures and energy consumption where engineering materials were used to replace agricultural lands (3). The US Environmental Protection Agency (EPA) initiated the implementation of some sustainable practices that would help in mitigating the UHI effect (4). The U.S. Department of Energy has also conducted a literature review of international studies on UHI countermeasures (5). Studies reported that due to such phenomena during the summer time, the extreme temperatures demands for a higher air conditioning usage inside buildings. The extent of its effect is greatly dependent on environmental factors such as shading, weather conditions, open and green spaces, and the infrastructure surface material. Therefore, these factors can be considered

during the construction of new development in such a way that would reduce the UHI effect and energy consumption. Many studies suggest that one way to mitigate the UHI effect is to use materials that contain a higher solar radiation that may lead to a smaller heat storage capacity. Specifically, studies suggest the replacement of the darker color material with a lighter ones and increasing the vegetation around the surrounding. However, for pavements, the problem is more complex than just the reflectivity of the material. Research work at the National Center of Excellent for SMART Innovation at Arizona State University (ASU) showed that the material solar reflectivity (albedo) alone is not the only factor that should be considered for the UHI mitigation (6).

In February of 2012, the Asphalt Pavement Alliance (APA) and ASU outlined a scope of continued research on "Asphalt Pavement Temperature Effects on overall Urban Heat Island." The main goal of this Phase II study was to evaluate the effect of pavement surface type on above and near surface air temperatures. This effort was the result of a 2010 Phase I study conclusions that indicated a porous Hot Mix Asphalt (HMA) layer with low albedo can have a lower nighttime surface temperature compared to a conventional pavement layer with higher albedo (7).

1.1.1 Objective

The main objective of this study was to analyze and research the influence of pavement materials on the near surface pavement temperature and the extent at which the surrounding air temperature will be affected. Phase I consisted of analyzing the thermo-physical properties of Porous Hot-mixed Asphalt (PHMA) and looked into modeling and comparing diurnal pavement surface temperature. In the Phase II study, a major undertaking was the construction of four full-scale pavement slabs consisting of dense

graded HMA, porous HMA, conventional Portland Cement Concrete (PCC), and pervious PCC. These slabs were constructed by the end of summer 2012 in Tempe, Arizona, near the ASU campus (Figure 1). The slabs dimensions were 12 x 12 feet, with a thickness of 5 inches. Each slab was instrumented with a weather stations and pavement temperature sensors. In addition, two test areas of similar dimensions were also constructed using landscape gravel and artificial turf; these are typical urban landscapes found in Phoenix, Arizona.

Figure 1 – Full-Scale Test Setup in Tempe, Arizona

1.1.2 Scope of Work

Phase II was divided into the following three main tasks with the goal of determining the effect of pavement temperature, among other factors on near surface air temperatures:

Task 1: Research and document existing models and software capable of predicting near surface air temperature as a function of adjacent surface temperature.

Task 2: Collect near surface air temperature for various pavement types.

Task 3: Models development and validation.

CHAPTER 2

2.1 LITERATURE REVIEW

Paving materials each consist of different thermo-physical characteristics. A mixture design accounts for air voids, asphalt or Portland cement, aggregates gradation, and modifications such as using fibers, polymers or crumb rubber. Some researchers believe that surface reflectivity is the most important parameter in mitigating the Urban Heat Island (UHI) effect. Other researchers believe that porosity of a pavement can greatly influence the degree at which the solar energy is being absorbed. Therefore, permeable materials with higher percentage of voids have the ability to insulate the ground, and reduce the urban heat island impacts. On the other hand, the voids allow the infiltrated water to evaporate, resulting in cooler (8).

Pavements contribution to UHI is much more complex than surface material type and reflectivity. Although reflectivity (albedo) plays an important role in pavement surface temperature, prudence should be exercised when using it as a sole parameter to describe pavements contribution to UHI or for a "cool pavement" designation. Literature has shown that porous pavements with open void structure do not have higher reflectivity, but have evaporative cooling and insulating effects which cause the surface temperature to be lower at night than conventional materials with higher reflectivity (6). In addition, the ASU Phase I modeling effort indicated that different pavement structures (materials and thicknesses) can have similar surface temperatures throughout the day (7).

In fact, the complexity of the UHI effect makes it a challenging task to isolate the

effects of pavement surfaces alone as a contributing factor. For example, the main driving factors which contribute to UHI include any or all of the following (2):

- ***Canyon Geometry***

  Buildings form "canyons" that tend to trap thermal energy near the bottom surface.

- ***Thermal Properties***

  The materials, concrete, asphalt, roofs, and walls tend to be denser and absorb and retain more thermal energy than nature surface cover.

- ***Anthropogenic Heat***

  Heat released from combustion of fuels, electrical energy used for lighting and driving motors, and human and animal biological metabolism can elevate the temperatures within dense urban areas.

- ***The Urban Greenhouse Effect***

  The warmer air and air pollution within cities act as a micro-greenhouse effect, preventing heat from radiating from the warm surfaces.

- ***The Effective Reflectivity (Albedo)***

  The total reflectivity of a city is reduced due to trapping effect of short-wave radiation of its building canyons.

- ***Reduction of Evaporating Surfaces***

  As a city expands natural vegetation is removed at a greater rate than it is replaced. This loss of moisture can adversely affect temperatures within the city.

- ***Reduced Turbulent Transfer of Heat***

  In some areas of the city, wind patterns can actually be blocked, causing pockets with little wind flow and mixing. This reduced mixing of air greatly reduces the heat release from streets.

Consideration of the effects of pavement types and temperatures on near surface air temperatures include many environmental and physical parameters. In addition, the effects of age and traffic play a significant role as clearly shown in Figure 2. In this figure, different pavement surface types show the same temperatures in the phoenix area. In addition, the same pavement surface material has lower surface temperatures due to the aeration effects of traffic compared to the HOV lane with no traffic allowed a the time this image was captures. Some of the environmental considerations include air, surface, and subsurface temperatures, cloud cover, direct sun light and solar radiation, humidity level, wind velocity, and surrounding land cover. Physical parameters include material constituents, surrounding materials and anthropogenic heat sources, build up concentration levels and ground heat flux.

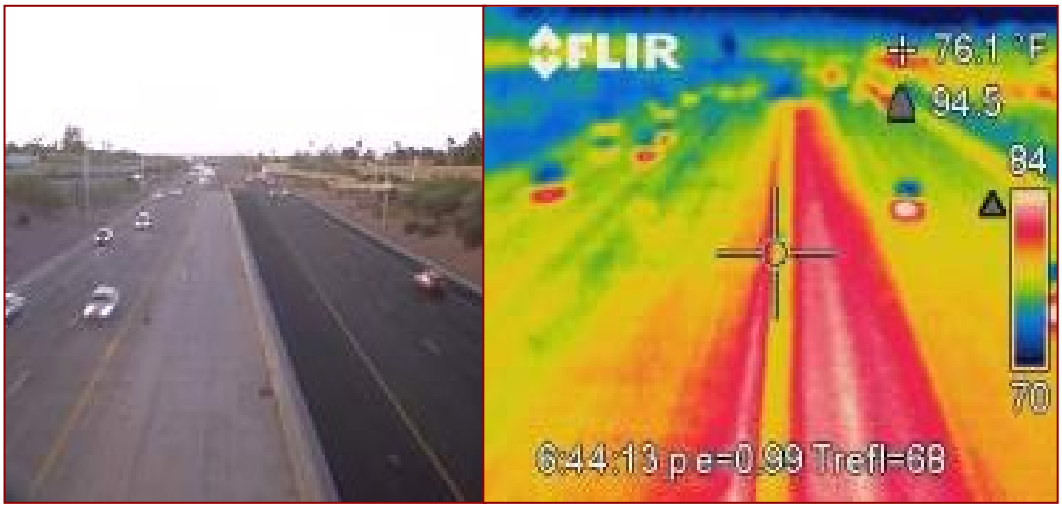

Figure 2 – Traffic Effects on Pavement Surface Temperature

2.1.1 Conventional VS. Porous Asphalt Mixture

The term porous hot-mix asphalt (PHMA), in general, refers to a mixture with large maximum aggregate size with high percentage of air void. Such mix designs the particles smaller than No. 30 sieve (600 microns) are reduced, allowing for an open-graded structure. This type of mixture in general contains small percentage of the middle size aggregates (9). Such materials have a similar gradation compare to the open-graded friction course (OGFC). However, PHMA contains larger maximum aggregate size. According to the Federal Highway Administration's (FHWA) open-graded mixes consist of mix designs with a large amount of air voids, in general, aggregates of 3-10mm (10).

PHMA was originally designed to reduce floods, storm sewer load and raise water tables (11). These types of pavements provide rapid water drainage from roadway by providing lateral movement of water off the roadways. In other words, an open graded structure allows for a higher skid resistance and less tendency to accumulate water compare to the traditional dense graded asphalt mixes, improving the driving condition during the wet seasons (12). In addition, porous pavements have high macrotexture at early age that significantly reduces the potential of hydroplaning condition (13). The porous material are also known more absorptive and are used to reduce the noise intensity of the highways (14).

In general, a PHMA requires the certain criteria and design consideration. The following provides an overview of the standard porous cross section, according to National Asphalt Pavement Association (NAPA) (11):

- An open structure that allows water to pass through

- A stabilizing course that is consisted of a clean crushed stone to stabilize the surface for paving equipment. It is important to note that all the crushed stones are all single size gradation.
- A stone recharge behaves as a structural layer that would also temporarily stores water as it infiltrate into the subsurface. This is consisted of clean single-sized crushed large stones that contain about 40 percent voids. These stones are larger than eh stabilizing course stones that are used in the top layer.
- Geotextile fabric that allows only water to filtrate but restrained the migration of fine material to the surface below.
- An uncompacted subgrade. This is beneficial to maximize the infiltration rate of soil.

The open structure of PHMA is due to lower concentration of fines in comparison to the traditional HMA that does not allow water to infiltrate into the pavement structure. Smaller percentage of fine materials allow for less contact of particles. The single graded underlying stone recharge bed may be consisted of only large particles size or smaller size stones, as this section acts as a storage volume for the storm water. Therefore, in terms of the storm water, single size and clean stone is preferred, because dirt or dusty stones may clog the voids and the infiltration bed actual paper. It is important to note that the bottom of the recharge bed is not compacted and is generally a level surface. This is because the water that infiltrate down into the pavement structure could easily and evenly distributed out of the discharge bed and into the ground (15).

In many areas in Europe, two layers of OGFC or porous pavements are used as a noise-reducing method instead of noise barrier walls. These types of mixes contain large stone mix, usually ranging between 16 to 22 mm, in the first layer and smaller mix size, usually ranging between 5 to 8 mm, in the second layer (16). This arrangement creates a bottleneck effect that allows sound waves to pass through small voids in the top layer, bounce and trap in the larger voids of the bottom layer until the sound wave dissipates. Such mixture designs have lower permeability than the traditional US mixes however, undergoes a higher durability under rapid load conditions.

2.1.2 Conventional VS. Pervious Portland Cement Concrete

Due to the recent amendments of the Clean Water Act, many Best Management Practices (BMPs) are used to improve the storm water conditions (17). Pervious Portland Cement Concrete (PPCC) is one of the practices that are being used. The name is driven from the structure of the material that allows the water to infiltrate into the soil (porous). Similar to the PHMA, PPCC contains a large volume of pore spaces that allows for evaporation of water and therefore acts as a temperature buffered. Some studies suggest that PPCC can be considered as a cool pavement in the areas with the warmer climate conditions (18).

In early1990's, the mixture designs used in US were usually consisted of coarse aggregate with the permeability of up to 0.6 cm/sec (1700 ft/day). However such design suffered from low compressive strength ranging from 6.7- 17.5 MPa (17). This is when the European industry had many successes in utilizing the PPCC. In order to improve the strength of the concrete with keeping the primary objective of adequate permeability in

mind, many tests were conducted in United States. According to a study completed at CP Tech Center, balanced gradation of high-quality coarse aggregate, sand and cement to extend at which it would coat all the aggregate is required in order to obtain a well performing mixture. On other hand, addition of Polypropylene fiber can improve the strength of the concrete while maintaining its permeability. A typical PPCC mix design that is durable during freeze-thaw condition contains about 20% voids at 3,051 kg/m3 (17).

2.2 MATERIAL THERMAL PROPERTIES

In the terms of pavements and albedo, as the sunlight is absorbed by the pavement i converts to thermal energy, heating the pavement. Studies completed in the past suggest that higher albedo is associated with lower thermal energy. Lower thermal energy will cause a reduction in the heat island effects and energy by reducing the use of air conditioning. However, it is important to understand other key thermo-physical properties in order to evaluate such behavior. Other important factors that will affect the pavement thermal behavior include thermal conductivity, heat capacity, thermal diffusivity, porosity, thickness and the underlying layers such as the subgrade material.

In general, the thermo-physical properties of the matter are related to the energy transport through the system and the thermodynamic behavior of such system. Therefore such properties can be separated into two categories (19).

On the micro scale, heat flow represents the movement of thermal energy that is related to molecular kinetic energy. Therefore, higher temperature is related to a higher linear motion of molecules and vibrational mode, resulting in a higher kinetic energy.

According to the basic physics, energy transfers from the higher regions to the region with a lower energy level. Heat transfer mechanism can be categorized into three subgroups: conduction, convection and radiation.

In simple terms, conduction is the movement of thermal energy from regions with higher molecular energy to regions with less energy level. Convection, on the other hand, is the transportation of heat through fluid motion that can cause volumetric expansion, causing the fluid parcel to become buoyant and displace. The term radiation refers to the extent of the thermal energy that is not absorbed by the media but rather the energy is carried by photons of light as a visible portion of electromagnetic spectrum and radiated into the atmosphere (19).

On the other hand, the thermodynamic properties are directly related to the second order differential of the thermodynamic potential of the given material. Some examples include the compressibility, and specific heat capacity. The thermodynamic properties are those that are related to the equilibrium state. In simple terms, compressibility refers to the relative change in the volume of the matter in response to change in pressure or stress. Specific heat capacity refers to the quantitative amount of heat that is needed to change the temperature of a matter by a given amount. These are all closely related to the density of the substance.

In terms of the pavement materials, the thermal conductivity and emissivity is closely related to the heat transfer mechanism of the materials. On the other hand the volumetric heat capacity and thermal diffusivity is closely related to the thermodynamic property of the materials. These properties and terms are discussed further in the following sections.

2.2.1 Thermal Conductivity

Thermal Conductivity, *k*, is referred to the ability of the material to conduct heat. It is the transfer of the energy from a region with the higher energy level to a region with less energetic particles. The process is completed through the random interactions of the particles at the molecular level (19). As it was stated earlier, conductivity of the material is related to the heat transfer process. According to Fourier's law, the heat flux is related to the temperature gradient through a surface (in one dimensional application) and the thermal conductivity of the material. The following expresses the conduction equation (19):

$$q_x'' = \frac{-kdT}{dx}$$

Where,

q_x'' = heat flux (Wm^{-2})

$\frac{dT}{dx}$ = temperature gradient in the x direction

k = the thermal conductivity ($Wm^{-1}K^{-1}$)

In general, the average maximum temperature during the day decreases with increasing the pavement thermal Conductivity. This is due to the fact that a material with a high conductivity can act as heat sink; the heat gain from the solar radiation at the surface is rapidly transferred into the ground, leaving the surface pavement temperature cooler. This mechanism is also an explanation for an increase in minimum surface temperature with respect to k during the night. As the heat is observed at the greater depths of the ground during the day, the effective thermal mass of the ground is increased, increasing the minimum temperature during the night.

2.2.2 Albedo

Albedo, α, is a measure of the amount of light reflected from an object. Therefore, it can be defined as the ratio of the light reflected to the amount of light shone on the object. A lower albedo indicates that more light is absorbed and it is related to the absorptivity of the surface (α_{abs}). This relationship can mathematically be shown as the following:

$$\alpha = 1 - \alpha_{abs}$$

The absorptivity of the surface ranges from value 0 to 1, where zero indicates that all the energy is reflected and therefore no energy is absorbed by the surface. Almost all materials (excluding the transparent materials) radiate a portion of the incoming solar radiation. As the portion of solar radiation is observed by the surface, the thermal energy of that material increases. The absorptivity of the material indicates the rate at which the energy is absorbed. The following equation describes such relationship:

$$G_{abs} = \alpha_{abs} G$$

Where:

G_{abs} = total radiation absorbed by the surface per unit area

G = total radiation per unit area incident to the surface

α_{abs} = absorptivity of the surface

It is important to note that the albedo factor is solely depended on the presence of the sun. Therefore, it significantly and directly affects the daytime maximum temperature. As the result, less energy is absorbed during the day reducing the nighttime minimum temperature (20).

2.2.3 Emissivity

Emissivity, ε, is the ratio of energy radiated by the surface compare to the radiation emitted by a black body at the same temperature. Emissive power is defined as the rate at which the energy is emitted per unit of area and commonly noted as E (Wm^{-2}) (19). According to Stefan-Boltzmann law, the total energy that is radiated from a unit surface of a black area per unit of time is directly proportional to the forth power of that same body thermodynamic temperature:

$$E_b = \sigma T_s^4$$

Where:

E_b = the total emissive power of a blackbody or ideal radiator

σ = Stefan-Boltzmann Constant = 5.67×10^{-8} W/m^2*K^4

T_s = absolute temperature (K)

It is important to note that a surface in general does not absorb all the radiation and therefore, the amount of energy that is emitted is less than a black surface. This is characterized by a factor known as emissivity, ε, that it always has a value less than one (19):

$$E=\varepsilon\sigma T_s^4$$

Where,

ε = the emissivity of the surface

E = the emissive power of any surface with emissivity ε

The body material, surface texture and finish greatly affect the emissivity of that body. Emissivity value can be used to compare the amount of energy that is emitted by a

surface relative to a blackbody. This will give some inside on the efficiency of the surface of the interest.

2.2.4 Volumetric Heat Capacity and Specific Heat

Volumetric Heat Capacity, is the ability of the material at the given volume to store energy; heat. The amount of heat that is needed to raise the temperature of one gram of a material by 1˚C is commonly referred to as Specific heat (c_p) in $JKg^{-1}K^{-1}$.

2.2.5 Density

Density *(p)* is referred to the ratio of mass to volume of a substance. The following equation mathematically represents this variable:

$$\rho = \frac{m}{V}$$

Where,

m = the mass of the material (kg or lb)

V = volume of the material (m^3 or ft^3

This is an important material property that greatly affects the temperature and the thermal diffusivity.

2.2.6 Thermal Diffusivity

Thermal diffusivity, α_{diff}, is a ratio of the thermal conductivity to its volumetric heat capacity. This is the rate at which heat propagate through the medium. Therefore, the average maximum surface temperature reduces while the minimum temperature increases with increasing diffusivity. In other words, thermal diffusivity, explains the ability of the material to conduct heat relative to its ability to store heat. The following equation mathematically explains this property energy (19):

$$\alpha_{diff} = \frac{k}{\rho c_p}$$

Where,

α_{diff} = thermal diffusivity

k = thermal conductivity

ρ = density

c_p = specific heat

2.2.7 Permeability

Permeability is the measure of the ability of the material to transmit water. In other words, how easy water can flow through a volume of material. Permeability can affect the strength and the deformation of soils. It is important to note that many factors such as aggregate texture and structure can affect its permeability (20, 21). Pore size and the number of pores closely relate the pavement structure and texture. In general the finer the particle texture is, the higher the particle contact area is and therefore the slower the permeability is. On the other hand the porosity of a material is commonly defined as the ratio of the volume of pores to the substance's total volume (21, 22). It is important to note that the porosity is also related to the voids size and the particle contact area. Therefore, the heat/energy flux of substance can be greatly affected by the porosity of that material. In general, the material with lower porosity has a higher heat transfer performance (less temperature variability throughout the median). This is because lower porosity indicates higher surface contact between the particles and therefore higher solid structure. As a result, the thermal conductivity of such material increases, causing a higher and more efficient heat flux transfer through the median (23).

2.3 THERMAL CHARACTERISTICS PAVING MATERIAL MODEL

In 2007, a one-dimensional mathematical heat transfer model was developed at Arizona State University (24). This model calculate/predict the pavement temperature for duration of 24 hours based on several climatic and material input variables such as: 24 hours air temperature, wind velocity, dew-point temperature, solar radiation, and material thermo-physical properties. This model accounts for radiation, convection and conduction of heat through the pavement. According to this study, the thermal conductivity, heat capacity and diffusivity affect the maximum temperature during the 24 hours cycle. In addition, the albedo and emissivity of the pavement play only an important role on both the maximum and the minimum temperature during the day. The study also found that albedo has the most impact on the maximum temperature, whereas the emissivity has the most impact on the minimum temperature of the pavement. A summary graph from this study is shown in Figure 3 (24).

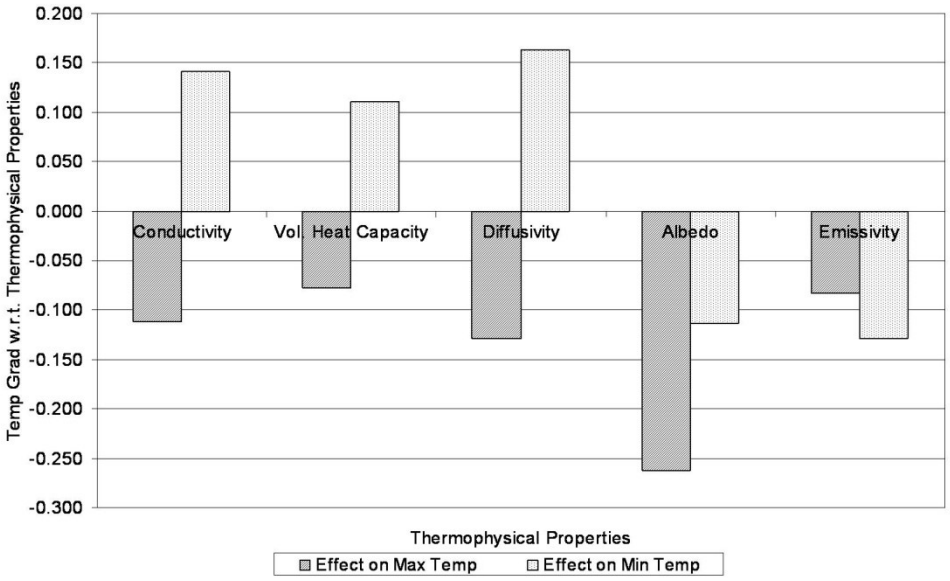

Figure 3 – Effect of Thermo Physical Properties on the Maximum and Minimum Temperature (24)

In 2010, Brent Hedquist conducted a Micro-scale evaluation of UHI in Phoenix area (25). In this study thermo-physical and climatic was used to perform an ENVI-met simulation study. In addition, an Infra radiate camera was used over the city of phoenix to aid the analysis. ENVI-met is a 3D microclimatic numerical model that can be used for UHI mitigation strategies. According to this study, impermeable materials such as asphalt and concrete (building or pavements) had negative impact on the night temperature (higher temperature). On the other hand, building shading and evapotranspiration had a positive effect on lowering the temperature during the afternoon. He also found that even a light wind speed, depending on the direction of flow can have a positive effect by transporting the cooler air from pervious material and greenery surfaces to higher temperature areas (25). During this study, human comfort level in an outdoor

environment was also analyzed using ENVI-met. The result revealed a positive correlation between shading, tall buildings and human comfort during hot temperature days (25).

A study in Singapore showed a clear evidence of UHI effect in the dense, high rise areas. According to this study, solar radiation was the main dominating factor for the day time temperature. Lower temperature was observed in the areas located between tall buildings compare to the locations with low-rise buildings. The study shows that although the urban canyon provides the lower day time temperature, such an area tends to trap heat. This is due to the reduced albedo and several solar reflections. The study showed a significant difference in the air temperature when using high and low reflectance materials, at lower wind speeds within the canyon. It was found that the air temperature significantly increases in the presence of low reflective materials. In addition, a comprehensive assessment was carried that shows high-rise towers will enhance the wind speed within the canyon, resulting in a lower the air temperature (26).

In a study conducted in California at UC Davis, nine 13x13ft test sections were designed to compare the cooling effect of three pavement designs: conventional impermeable (dense graded), novel permeable and novel permeable (both open graded). Pavement and near surface air temperatures were both monitored during dry and wet condition. Cooling degree hours (CDH) and the Heating degree hours (HDH) were measured during the study. CDH is a measure of degree and the time where the air temperature is higher than a specific temperature. On the other hand, the HDH refers to the measurement of the degree and the time where the air temperature is lower than the specific base temperature. Both of these measurements are used to calculate the energy

consumption to cool and heat an adjacent building respectively. The study showed that the permeable pavement (open graded) potentially causes a lower energy consumption by the adjacent building. This is due to the fact that such materials withhold a moderate surface and near surface air temperature throughout the day, helping to mitigate the UHI effect (27). In addition, author concludes that the air temperature decreases with an increase in the elevation, to the point where there is no significant difference between the ambient air temperature above the asphalt and the concrete pavement. However, the author explains that the higher near surface temperature (below 2m). It is explained that the air temperature near the surface is more influenced by the pavement temperature where there is low wind speed (27).

In a study conducted by Wang et al, an analytical model for solving temperature and heat fluxes in solid media (e.g. pavements, landscape gravels, soils, etc.) was developed. The author states that the model predictions were validated against field measurements in different cities, and were found to be accurate and reliable. In comparison to the conventionally used discrete (finite difference) model used in, e.g. Energy-Plus, this model captures realistic and more accurate pavement temperatures through the entire depth (28).

In a different study, the same author presents a physically based urban land surface model that solves the heat exchange among roads, walls, roofs and the overlying atmosphere. Author explains that parameterization schemes are developed to account for the radiation trapping and the shading effect inside urban canyon, i.e. between roads and building walls. Building energy consumptions can be estimated from the heat flux conducted through the building envelop (walls and roofs). Different mitigation strategies,

such as the usage of cool roof (with increasing albedo) and green (vegetated) roofs, are investigated and compared. This model has the potential to investigate the effect of pavement surface temperature on adjacent building energy consumption (29).

2.4 ASU THERMAL CONDUCTIVITY TEST PROCEDURE

The standard procedure for measuring thermal conductivity is outlined in ASTM C 177-04. This method requires the temperature at steady state to determine *k* and mandates slab specimen geometries. It is not recommended for highly inhomogeneous materials as the size of aggregates in a pavement layer can sometimes exceed 25 mm (1 in.). Specifying plate thicknesses that are considerably larger than the maximum aggregate diameter in the mix will cause non-uniform heat flux through the material and possibly affect the test results. To maintain one-dimensional conduction heat transfer through a slab of 25 mm (1 in.) thickness would require sides of at least 30 cm (12 in.) or more. These large dimensions present several difficulties in the fabrication of laboratory asphalt or concrete samples. In addition, obtaining this size of pavement specimen from in-service pavement would disturb a large section of the pavement and add additional costs to traditional material sampling techniques.

The ASU's National Center of Excellence for SMART (Sustainable Materials and Renewable Technologies) Innovations developed a test method for accurately measuring the thermal conductivity of pavement materials using cylindrical specimen geometry, commonly used for mechanical testing of paving materials. This new experimental method allows thermal and mechanical properties to be determined from identical material geometry with minimal additional sample preparation. In addition, materials can

be obtained from the field using standard sampling techniques (30, 31). Figure 4 provides illustrations of the specific heat capacity and thermal conductivity tests utilizing cylindrical test specimens (30).

a) b)

Figure 4 – Evaluation of Thermal Properties of HMA and Porous HMA at ASU (a: Thermal Conductivity and b) Specific Heat Capacity)

The thermal conductivity test developed at ASU, revealed that the thermal conductivity parameter of asphalt materials is very complex. Therefore, use of the general k-values found in the literature may affect the analysis of the paving material resulting in improper conclusions.

CHAPTER 3

3.1 PHASE I

3.1.1 Objective

The main objective of this Phase I effort was to research and model the extent to which OGFC and PHMA pavements influence pavement surface temperatures and thus contribute to the overall UHI effect. This was accomplished through pavement surface temperature modeling and laboratory measurement of thermal conductivity of PHMA and OGFC mixtures.

3.2 BACKGROUND

3.2.1 Definition of Mixtures

The terms open-graded friction course (OGFC) and porous hot-mix asphalt (PHMA) are commonly referred to as the same material. While the mixtures express similarities, the two types of asphalt concrete mixtures actually serve two different purposes. An OGFC mixture has a smaller maximum aggregate size and also has a very small percentage of aggregate in the mid-range sieve sizes. This open aggregate structure has been found to be very beneficial in allowing water to drain through the asphalt layer which; in turn, reduces tire spray and provides better friction. In addition, the use of an asphalt rubber, open-graded friction course has been shown to reduce traffic noise (32). In comparison, PHMA has a similar gradation as the open-graded structure; however, the maximum aggregate size is bigger which produces a very open structure. This porous

mixture allows water to freely pass through and when used in conjunction with an underlying reservoir is effective in managing storm water. According to the National Asphalt Paving Association (NAPA), a porous mixture can be classified according to the gradation provided in Table 1 – NAPA Porous Asphalt Gradation Specification with air voids greater than 16% (33).

Table 1 – NAPA Porous Asphalt Gradation Specification

Sieve Size		Gradation Limits % Passing	
Standard	**mm**	**Upper**	**Lower**
3/4	19.0	100.0	-
1/2	12.5	85.0	100.0
3/8	9.5	55.0	75.0
No. 4	4.8	10.0	25.0
No. 8	2.4	5.0	10.0
No. 200	0.1	2.0	4.0

3.2.2 Pavement Material Thermal Properties

Evaluating the thermal behavior of urban materials requires understanding of the key thermo-physical properties of matter that govern thermal phenomenon. There are two distinct categories of these properties: those related to transport of energy through a system and those related to the thermodynamic or equilibrium state of a system (19). Transport of energy through a system, also referred to as heat transfer, can occur by means of radiation, conduction and convection. Heat transfer properties of materials relating to radiation include albedo (α) and emissivity (ε). Thermodynamic properties differ from transport properties in that they are concerned with the equilibrium state of a system. These properties include density (ρ) and specific heat capacity (cp) which form

the basis for volumetric heat capacity and thermal diffusivity. These properties and terms are discussed in further detail in the following sections.

A portion of solar radiation, incident to a pavement surface, will be absorbed by the surface and increase its thermal energy. The rate at which this energy is absorbed per unit of surface area is dependent on the absorptivity (α_{abs}) of the surface material that ranges from zero to one (19). A value of zero implies that no energy is absorbed by the surface. The rate at which energy is reflected by the surface is known as the albedo (α) of the surface. It takes into account the full spectrum of solar radiation and not just those in the visible range (3,24).

A portion of the thermal energy contained within a pavement is constantly being emitted as radiation back into the atmosphere. The rate at which the energy is emitted per unit area is referred to as the surface emissive power, E (Wm^{-2}) (24). Emissivity, ε, is the ratio of energy radiated by the surface compared to the radiation emitted by a black body at the same temperature. The emissivity of a surface greatly depends on the surface material and its finish.

Density (ρ) and specific heat (cp) are widely used in thermal analysis. Density is a measure of mass per volume of a substance and can affect the temperature of paving materials. Specific heat (cp) is defined as the amount of heat energy required to raise the temperature of one gram of a substance by $1^{o}C$. Thermal conductivity is the rate constant that governs the heat flux through a body and is a transport property characteristic of the material. In essence, it is the ability of a material to conduct heat. Finally, the porosity of a material is commonly defined as the ratio of the volume of pores in a substance to its

total volume (34). Porosity can affect the surface energy fluxes due to changes in voids and particle contact.

The literature provides limited thermal properties of paving materials and in most cases the specifics of the materials tested are not reported. These properties can be drastically affected by the physical properties of the materials. Table 2 summarizes select thermal material properties found in the literature for different Hot Mix Asphalt (HMA) and Portland Cement Concrete (PCC) pavement materials. It is important to note that studies rarely reported or measured all material thermal properties.

Table 2 – Pavement Material Thermal Properties

Material	Thermal Conductivity (W/mK)	Specific Heat *c* [J/(kg*°K)]	Albedo	Density (kg/m^3)	Source
Porous Asphalt	2	900	-	2157	**(35)**
Water Holding Porous Asphalt	1.46	520	-	2360	**(35)**
Asphalt	1.2	921	0.1	2238	**(30)**
	2	900	-	2300	**(35)**
	0.8-1.6	879-1600	-	-	**(36)**
	1.3-1.42		-	-	**(13)**
	1.45-1.81	1475-1835	-	2350	**(37)**
	-	-	0.05 – 0.10 (new) 0.10 – 0.15 (aged)	-	**(38)**
	1.21	921		-	**(39)**
	1.003-1.747	-	-	-	**(40)**
PCC	1.1	950	0.25	2100	**(41)**
Porous PCC	1.1	950	0.18	2100	**(42)**

3.2.3 Pavement Temperature Modeling Studies

A study conducted by Asaeda (42) attempted to understand the surface heating processes of various pavements. Thermal characteristics and behavior of materials of porous and traditional dense pavements were studied and field experiments were conducted with various types of alternate pavement materials. A one-dimensional numerical model was developed to simulate processes of heat and moisture transfer at the porous surfaces and in the underlying soil. Authors concluded that the surface of normal porous pavement is rather dry and almost no evaporation was observed at this surface. Also, they found that the normal porous and non-porous pavement surfaces can absorb a large amount of the incoming net radiation, which increases its pavement surface temperature during the daytime.

Nakayama and Fujita (35) presented an interesting study dealing with the evaluation of pavements comprised of traditional versus new materials regarding thermal and evaporation properties. They used a model called NICE (NIES Integrated Catchment-based Eco-hydrology) to simulate the water and heat budgets for the various materials and to reproduce the cooling effect by evapotranspiration of water-holding pavement (consisting of porous asphalt and water-holding filler made of steel by-products based on a silica compound). In the study, they used experimental results conducted by JFE Steel Corporation (43). Several blocks of different materials were fastened to the rooftop of the building to study the differences in their responses to the environment. Some of these materials included concrete, porous pavements and water holding pavements. The surface temperatures of the infiltration and water-holding blocks were much lower than those of the other engineered pavements. In particular, they were about 5–10 ◦C cooler than the

temperature of the rooftop in the hottest part of the day, mainly because of the cooling effect of evaporation from the materials. The simulation showed that the surface temperature decrease in water-holding pavement is closely related to evaporation from the surface, the water volume of the pavement and the surface reflectance.

3.2.4 Case Studies

In 2006, Belshe et al (32) conducted a study to evaluate the thermal effects of asphalt-rubber OGFC overlays on PCC pavements. This practice is typically used in the State of Arizona in order to improve skid resistance, restore smoothness and provide noise reduction. The study instrumented several pavements with temperature sensors to document the thermal gradient in the PCC with and without asphalt-rubber OGFC overlays. Using obtained temperature data throughout the depth of the pavement; stresses were computed by utilizing typical slab theory equations. The study concluded that use of an asphalt rubber OGFC overlay reduced the stresses in the PCC due to thermal gradients by approximately 25% during the day and 8% during the nighttime. These results are for a typical extreme summer day in Phoenix, Arizona. It was also noted that the effects of traffic aeration reduced the magnitude of thermal gradients due to lower surface temperatures. Despite the low albedo of OGFC, the material acted as a thermal blanket over the PCC and reduced thermal stresses.

Similar studies on pervious concrete and its thermal behavior are also reported in the literature. Researchers at ASU (41) carried out a study on a pervious Portland cement concrete (PPCC) parking lot in order to determine the role of pervious pavements in UHI mitigation. The study concluded that the PPCC exhibited higher daytime temperatures than conventional PCC. The authors speculated a combination of factors including lower

albedo, rougher surface texture trapping air and heat, and high air voids in the mix. However, the PPCC achieved a lower nighttime temperature when compared to the PCC and thus aids in mitigation of UHI at nighttime. Results of this study correspond well with modeled observations by Haselbach (8) in South Carolina where PPCC experienced higher daytime surface temperatures than PCC and asphalt concrete. Authors also noted the base material was cooler under the PPCC which demonstrates an insulating effect of porous pavement. This insulating effect is directly related to the thermal conductivity of the materials, and therefore is a result of reduced heat transfer through a pavement with a large air void structure. It was observed that the heat transfer rate of PPCC is approximately 59% of the heat transfer rate of PCC. Again, work by Kevern et al (17) and expanded by Haselbach et al (6) demonstrated that PPCC cooled faster than PCC. However, the low temperatures of the two pavements were similar, indicating less heat storage capacity of the PPCC.

3.3 THERMAL CONDUCTIVITY TESTING

Many different factors play a role in the thermal conductivity of a given material. In the past, these thermal transport characteristics have not been given much attention during pavement design or mixture design and are not easily available in the literature. The thermal conductivity of a pavement is generally dependent on the type of mix, aggregates used, percentage of each component in the mix and its level of compaction. In terms of aggregate base materials or subgrade materials, the thermal conductivity is a function of material type, mineral content, moisture content, particle size and overall

density (44). Therefore, the thermal conductivity of paving materials can be a very difficult parameter to obtain and generalize for different asphalt pavement types.

A review of the literature proved that thermal properties of asphalt mixtures are rather limited and can be misleading since mixture properties or types are not always reported. In order to verify data and to evaluate the thermal conductivity of a porous asphalt mixture, laboratory specimens were prepared using asphalt mixtures obtained from actual field projects in the State of Washington, Wyoming and Arizona. These mixtures were selected because their gradations resembled the porous asphalt specification defined by the National Asphalt Paving Association (NAPA). Table 3 presents asphalt mixture properties used in this thermal conductivity study.

Table 3 – Summary of Mixture Properties and Gradation

Mix Property	Mixture		State of Washington	Wyoming	Arizona
	Gradation Type		Porous	Open	Gap
	PG Binder Grade		64-22	64-34	64-16 AR**
	% Binder		5.4	5.7	8.5
	G_{mm}		2.587	2.416	2.337
	Ave. Air Void %		21	12.3	4.9
	Modification		None	1 lb/ton (0.5 kg/MT) fibers*	18% AR **
	Thermal Conductivity, k (W/m-K)		0.57	0.38	0.9
Mix Gradation	Sieve Size		Percent passing		
	US	SI			
	3/4	19	100	100	-
	1/2	12.5	92	82	100
	3/8	9.5	59	57	87
	No. 4	4.8	16	22	27
	No. 8	2.4	8	12	18
	No. 16	1.2	6	7	14
	No. 30	0.6	5	6	11
	No. 50	0.3	5	4	7
	No. 100	0.2	4	3	5
	No. 200	0.1	3.2	2	3.6

* Blend of polypropylene and aramid fibers
** AR – Asphalt Rubber with type B crumb rubber

The standard procedure for measuring thermal conductivity is outlined in ASTM C 177-04 “Standard Test Method for Steady-State Heat Flux Measurements and Thermal Transmission Properties by Means of the Guarded-Hot-Plate Apparatus”. This method requires the temperature at steady state to determine thermal conductivity, k and mandates slab specimen geometries. However, obtaining such specimens from in-service pavement is very difficult and not recommended for highly inhomogeneous materials where the size of aggregates can exceed 1-inch (25mm). A new experimental method developed by ASU National Center of Excellence for SMART (Sustainable Materials and

Renewable Technologies) Innovations allows thermal and mechanical properties of materials to be determined using specimens obtained using standard sampling techniques with minimal additional sample preparation. Detailed discussion of the test methodology can be found in (30). In summary, a 1-inch (25mm) vertical hole is cored through the center a 4-inch (100 mm) diameter specimen that measures 7 inches (178 mm) in height. A heating element is introduced into the hole and thermocouples are mounted on the outside of the specimen.

The average thermal conductivity values, k (W/m-K) obtained in this study for the State of Washington, Arizona and Wyoming mixtures are 0.57 (cov=5.1%), 0.90 (cov=16.2%) and 0.38 (cov=0.9%), respectively. These test values are significantly lower than the range of values found in the literature (35). However, values reported in literature rarely are accompanied by mixture properties. Two of these mixtures tested were similar in porous nature, however; differences in constituent materials and air voids played a major role in the k-values. For example, the Washington State mixture had the highest air voids of the three mixtures, but did not show the lowest thermal conductivity values. In comparison, the Wyoming mixture had polypropylene and aramid (Kevlar) fiber modification. This combination, along with the type of aggregate, resulted in the lowest k-value of the three mixtures tested. The Arizona mixture had the lowest air voids and thus; the high thermal conductivity value is reasonable since more particle contact accelerates heat transfer. As a result, the thermal conductivity parameter of asphalt material is greatly influenced by the constituent materials. Therefore, use of the general k-values may result in improper analysis of a paving material.

3.4 PAVEMENT TEMPERATURE MODLEING

In order to examine the effect of different factors on pavement surface temperature, a one-dimensional mathematical model developed at ASU by Gui et al. (24) was used to predict pavement near-surface temperatures using hourly measured solar radiation, air temperature, dew-point temperature, and wind velocity data.

The climatic data used in this analysis were collected from the Arizona Meteorological Network (AZMET) Phoenix Encanto weather station for August 14-16, 2010, representing the hottest days in 2010. The ASU model calculated the pavement temperature in two-minute increments for each of these days at the depth of 0.5 inches (12.5mm) into the pavement and used a 3-day average value to plot the diurnal pavement temperatures.

Three types of pavements were considered: porous hot mix asphalt, hot mix asphalt (HMA) and Portland cement concrete (PCC). Each pavement type was analyzed with the ASU model using a typical albedo range for the material types. Table 4 provides a summary of the pavement properties used as input into the ASU model to predict and compare pavement surface temperatures. Recognizing that the material properties of the subgrade are highly dependent on the type of material, mineral content, particle size and moisture content values, typical values were selected to represent a dry clay subgrade and aggregate base (44). Models are available to predict the thermal properties of subgrade material but are complex and out of the scope of this study (44).

Table 4 – Material Input Properties

Pavement Structure		1	2	3
Layer 1				
Material	-	HMA	PHMA	PCC
Albedo	-	0.05, 0.1, 0.2	0.05, 0.1, 0.2	0.15, 0.25, 0.35
Emissivity	-	0.91	0.91	0.91
Density	(kgm^{-3})	2238	2146	2350
Specific Heat	($Jkg^{-1}K^{-1}$)	921	800	1000
Conductivity	($Wm^{-1}K^{-1}$)	1.2	0.4	1.5
Thickness	(in)	2, 4, 8, 12	2, 4, 8, 12	2, 4, 8, 12
Interface Resistance	-	0.001	0.001	0.001
Layer 2				
Material	-	Aggregate	Aggregate	Aggregate
Density	(kgm^{-3})	2200	2200	2200
Specific Heat	($Jkg^{-1}K^{-1}$)	890	890	890
Conductivity	($Wm^{-1}K^{-1}$)	1.3	1.3	1.3
Thickness	(in)	6	6	6
Interface Resistance	-	0.001	0.001	0.001
Layer 3 (Ground)				
Material	-	Dry Clay	Dry Clay	Dry Clay
Density	(kgm^{-3})	1700	1700	1700
Specific Heat	($Jkg^{-1}K^{-1}$)	920	920	920
Conductivity	($Wm^{-1}K^{-1}$)	0.9	0.9	0.9
Additional Factors				
Sky View Factor	-	0.95	0.95	0.95
Solar View Factor	-	0.85	0.85	0.85

3.4.1 Evaluation of Porous Hot Mix Asphalt

One goal of this study was to compare the diurnal pavement surface temperatures for PHMA, HMA and PCC. Based on the information presented in the literature review section, studies on pervious concrete indicated higher daytime surface temperatures but lower nighttime temperatures when compared to PCC. It was anticipated that PHMA would perform in a similar manner due to the open void structure of the material and with the absence of significant evapotranspiration effects.

Pavement surface temperatures were modeled for 2, 4, 8 and 12-inch (51, 102, 203 and 305 mm) pavement thicknesses on dry clay subgrade. Although the 8 and 12-inch (203 and 305 mm) sections are unlikely to be used in urban settings (except in cases of heavy loading), they were included in this study to evaluate the thickness effect on surface temperatures. Figure 5 presents an example of the diurnal pavement surface temperature comparison for PHMA and HMA.

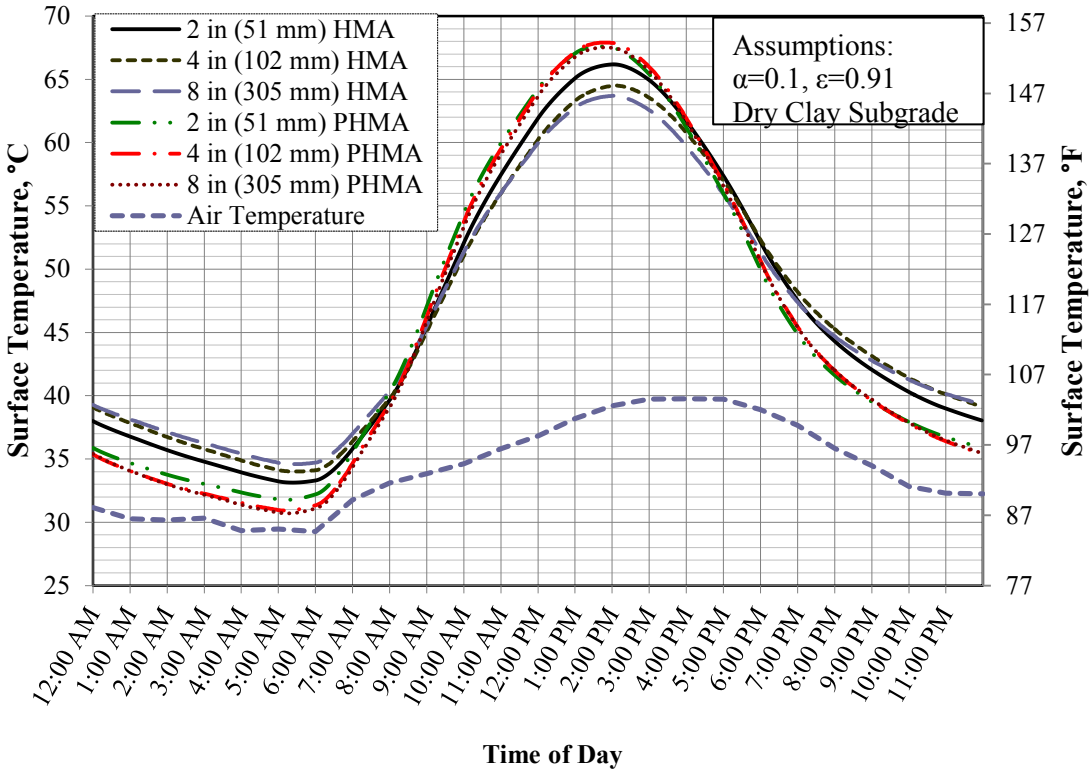

Figure 5 - Pavement Surface Temperature Comparison for PHMA and HMA, August 15, 2010 in Phoenix, Arizona

Although the PHMA has higher daytime surface temperatures, it is evident from Figure 5 that PHMA has cooler surface temperatures for a significant portion of the 24-hour day. This is the case for all pavement thickness values used in this study. It is important to note that after a thickness of about 8 inches (203 mm), the pavement surface temperatures become asymptotic and pavement thickness plays a reduced role in pavement temperatures. These findings are consistent to those reported by Gui et al (24).

High PHMA surface temperatures during peak hours are not surprising because the lower thermal conductivity of the porous material will keep the surface temperature elevated. Also, the open void structure exposes additional surface area to solar radiation

resulting in higher peak daytime temperatures. Rough surface texture may contribute to the hotter daytime temperatures by trapping warm air and heat. Finally, the insulating effect caused by the large air void structure of PHMA results in less conduction to the ground. Similar observations have also been documented in porous PCC pavements (41,42).

3.4.2 Thermal Evaluation of Various Pavement Materials

Pavement temperature modeling was performed for PHMA, HMA and PCC using input values provided in Table 4. The same pavement thickness values were used but albedo values were varied within typical ranges for each type of materials. However, the analysis was completed two times, once considering no base material and again using a 6 inch (152 mm) aggregate base material under the pavement to model a more realistic pavement section. Table 5 presents the modeled results for maximum and minimum pavement surface temperatures for pavement structure with and without an aggregate base layer. The shaded colors in each cell help to indicate pavement structure combinations that provide similar maximum or minimum pavement surface temperatures. In this table, PHMA, HMA and PCC represent porous hot mix asphalt, hot-mix asphalt and Portland cement concrete, respectively.

Table 5 – Maximum and Minimum Pavement Surface

	Pavement Type (Thickness)	Max. Temperature (C°)			Min. Temperature (C°)		
No Base Material	**PHMA**	**α=0.05**	**α=0.1**	**α=0.2**	**α=0.05**	**α=0.1**	**α=0.2**
	2 in (51 mm)	69.5	67.6	63.7	32.1	31.8	31.1
	4 in (102 mm)	69.9	67.9	64.0	31.2	30.9	30.3
	8 in (203 mm)	69.5	67.5	63.6	31.0	30.7	30.1
	12 in (305 mm)	69.5	67.5	63.6	31.0	30.7	30.1
	HMA	**α=0.05**	**α=0.1**	**α=0.2**	**α=0.05**	**α=0.1**	**α=0.2**
	2 in (51 mm)	68.1	66.2	62.4	33.5	33.1	32.4
	4 in (102 mm)	66.3	64.5	60.8	34.4	34.0	33.2
	8 in (203 mm)	65.5	63.7	60.1	35.0	34.6	33.7
	12 in (305 mm)	65.5	63.7	60.1	34.8	34.4	33.5
	PCC	**α=0.15**	**α=0.25**	**α=0.35**	**α=0.15**	**α=0.25**	**α=0.35**
	2 in (51 mm)	63.6	59.8	56.0	33.2	32.3	31.5
	4 in (102 mm)	61.4	57.8	54.2	34.3	33.5	32.6
	8 in (203 mm)	60.4	56.9	53.4	35.3	34.3	33.3
	12 in (305 mm)	60.5	57.0	53.4	35.2	34.2	33.2
6 in (152 mm) Aggregate Base	**Pavement Type (Thickness)**	**Max. Temperature (C°)**			**Min. Temperature (C°)**		
	PHMA	**α=0.05**	**α=0.1**	**α=0.2**	**α=0.05**	**α=0.1**	**α.=0.2**
	2 in (51 mm)	67.6	65.7	61.9	31.8	31.4	30.8
	4 in (102 mm)	68.8	66.9	63.0	30.0	29.8	29.3
	8 in (203 mm)	68.6	66.7	62.8	29.9	29.7	29.2
	12 in (305 mm)	68.8	66.9	63.0	30.2	30.0	29.5
	HMA	**α=0.05**	**α=0.1**	**α=0.2**	**α=0.05**	**α=0.1**	**α.=0.2**
	2 in (51 mm)	65.7	63.9	60.3	34.1	33.7	32.8
	4 in (102 mm)	65.1	63.3	59.7	34.0	33.6	32.8
	8 in (203 mm)	64.5	62.7	59.2	33.7	33.3	32.5
	12 in (305 mm)	64.3	62.6	59.0	33.5	33.1	32.3
	PCC	**α=0.15**	**α=0.25**	**α=0.35**	**α=0.15**	**α=0.25**	**α=0.35**
	2 in (51 mm)	61.5	57.9	54.2	33.7	32.8	32.0
	4 in (102 mm)	60.3	56.8	53.2	34.1	33.2	32.3
	8 in (203 mm)	59.5	56.0	52.6	34.1	33.2	32.3
	12 in (305 mm)	59.3	55.9	52.4	33.8	33.0	32.0

NOTE: ˚F = 9/5 *(˚C) + 32

Independent of the type and the thickness of the pavement, it is clear from the results that a higher albedo results in a lower maximum daily surface temperature. In

addition, the minimum daily temperature values for each type of pavement also decrease as albedo increases. Considering the PHMA, the highest surface temperature is associated with the lowest albedo value, and the lowest surface temperature is associated with the highest albedo value.

It is evident from the analysis that the albedo has an important impact on the maximum daily temperature of all pavement surfaces. However, the type of material and properties of the pavement structure have a greater impact on the minimum nighttime temperatures. Factors such as pavement thickness, density, specific heat capacity and thermal conductivity all become important as they affect the ability of a pavement structure to retain heat. Therefore, it becomes important to evaluate the entire pavement structure and material properties when selecting paving materials to mitigate urban heat island. Daytime versus nighttime conditions should be carefully evaluated for the pavement under consideration.

In a comparison of different pavement layer thicknesses, it can be noted that the surface temperature generally decreases as the pavement thickness increases. This trend appears reasonable given the additional material to conduct heat. As a consequence, the maximum surface temperature of a thicker pavement decreases during the day but may cause an undesired increase in the minimum temperature during the night.

In a more detailed comparison using Table 5, consider a 4-inch (102 mm) PHMA pavement (α = 0.1) that has a maximum daytime temperature of 67.9°C (154.2˚F). PHMA is 3.4°C (6.1˚F) and 10.1°C (18.2˚F) hotter than a 4-inch (102 mm) HMA (α = 0.1) and PCC pavement (α = 0.25), respectively. However, this same PHMA pavement has a nighttime minimum temperature of 30.9°C (87.6˚F) which is cooler than the same

HMA and PCC structures by 3.1°C (5.6˚F) and 2.6°C (4.7˚F), respectively. Thus, PHMA has the ability to dissipate heat more rapidly than other pavements due to the insulating effect of the PHMA as described earlier. Again, lower nighttime temperatures help to mitigate the effects of UHI.

It can also be observed that a pavement with high albedo does not necessarily translate into lower nighttime temperatures. This was evident in the preceding example and can be further explored by looking at a higher albedo PCC (α = 0.35) and a lower albedo PHMA (α = 0.05); both with 4-inch (102 mm) thickness. Again, the low albedo PHMA has significantly higher daytime temperatures, which is reasonable given the amount of solar radiation that can be absorbed by the material. However, during the nighttime, the PHMA (α = 0.05) is cooler than the same thickness HMA (α = 0.20) and PCC (α = 0.35) by 2°C (3.6˚F) and 1.4°C (2.5˚F), respectively.

Similar trends are observed when a 6-inch (152 mm) aggregate base was included in the modeling. The notable difference was that the addition of the aggregate base reduced the minimum temperatures of the PHMA (same material properties) by a greater amount than PCC and HMA. Again, this can be attributed to the insulating effect of the porous structure in that the materials below are exposed to less heat via conduction and thus release less heat during the night.

3.4.3 Effects of Pavement Structure

Throughout this analysis, it is evident that surface temperature of pavement materials is a much more complex interaction than simply analyzing a single aspect or factor alone. Granted albedo has the greatest effect on pavement surface temperature during day conditions. However, selection of pavement materials to mitigate UHI must

consider nighttime temperatures as well. In general, the reference to UHI mitigation is directed more toward the nighttime phenomenon. The preceding analysis showed examples on how the selection of the entire pavement structure and material type can affect surface temperatures of pavements during day as well as night conditions.

Studies in the literature are vague on the specific thermal properties of paving materials used including subgrade and aggregate materials. The specific heat capacity and thermal conductivity of aggregates and subgrade materials are very dependent on factors such as moisture content and type of minerals present (44). In the case of PHMA, it would seem reasonable that additional moisture increases the thermal conductivity of the subgrade resulting in higher temperature. However, this is offset in that pavements with open void structures also allow evapotranspiration, which in turn cools the pavement surface (8). Evaporation through the porous pavement has also been shown to reduce the moisture content of the underlying soil (41), thus reducing the volumetric heat capacity of the soil.

Thickness (or thermal mass) plays a key role in the mitigation of UHI especially for nighttime temperatures. However, surface temperatures approach constant values after a certain pavement thickness value, which confirms observations by Gui et al. (24).

3.5 AIR TEMPERATURE ABOVE PAVEMENT (PILOT STUDY)

A pilot study was completed to analyze the effect of pavement surface temperature on near-surface air temperatures. Air temperature was measured at 1-foot interval above the pavement surface using 9 temperature sensors (accuracy of +/- 1C). Temperature data were collected from different locations near Arizona State University at Tempe campus. It was noted that there is not a significant difference after 5’ level.

However, due to the time and equipment limitation the data were collected at different days making comparison of air temperatures and pavement surface temperatures impractical. Although the results were promising, it led to further investigation and construction of pavement test sections in Phase II.

CHAPTER 4

4.1 PHASE II - EXPERIMENTAL WORK

A major effort and unique characteristic of this Phase II effort was the ability to construct full-scale test pads near the ASU campus in Tempe, Arizona. Previous work relied on data collected at different locations and differences in weather conditions and surrounding conditions (buildings, etc.) made comparison of air temperatures and pavement surface temperatures impractical. Four full-scale pavement slabs consisting of HMA, PHMA, PCC and PPCC were constructed near the ASU campus in Tempe, Arizona. These slabs were constructed at dimensions of 12’ x 12’ with a thickness of 5 inches. The slabs were instrumented with weather stations and pavement temperature sensors. In addition, test slabs were also constructed with landscaping gravel and artificial turf; typical surfaces found in the Phoenix metropolitan area.

Table 6 and Table 7 provide a summary of the HMA and PHMA Mixture Properties and aggregate gradation, respectively. In addition, Table 8 provides some typical values for PPCC and PCC.

Table 6 – Mixture Properties of HMA and PHMA

Mix Property	Mixture	
Gradation	PHMA	HMA (Dense)
PG Grade	64-22	
% Binder	5.4	5.7
G_{mm}	2.438	2.452
Ave. Air Void %	21	5.3
Modification	None	None
Thermal Conductivity, k (W/m-K)	0.57	1.2

Table 7 – Aggregate Gradation for HMA and PHMA

Sieve Size		**% Passing**	
Standard	**mm**	**PHMA**	**HMA**
3/4	19	100	100
1/2	12.5	92	90.6
3/8	9.5	60	76.4
No. 4	4.8	16	65.6
No. 8	2.4	9	46
No. 200	0.1	2	4.54

Table 8 – Typical Materials Properties for PPCC and PCC (7)

Material	Thermal Conductivity (W/mK)	Specific Heat [J/(kg*°K)]	Reflectance	Emissivity	Albedo	Density ρ (kg/m^3)	Porosity	Source
Gray PCC					0.35 – 0.40 (new)			ACPA (2002)
					0.20 – 0.30 (weathered)			ACPA (2002)
White PCC					0.70 – 0.80 (new)			ACPA (2002)
					0.40 – 0.60 (weathered)			ACPA (2002)
PCC	1.1	950			0.25	2100		Carlson et al (2008)
PPCC	1.1	950			0.18	2100		Carlson et al (2008)
Concrete	2.56	1050	0.32	0.99		1785*	0.01	Nakayama and Fujita (2010)

Construction took place in summer 2012 and also included an educational component. Undergraduate and graduate students from the civil engineering Highway Construction/Materials class were onsite to observe construction and to help sample materials to be tested at the ASU SMART lab (Figure 6).

Figure 6 – Construction of Porous HMA and Sampling of PCC Materials

During construction, pavement slabs and the gravel were instrumented with thermo-couple sensors (Figure 7) to monitor pavement temperatures at different depths. Sensors were fixed using PVC pipe and care was taken not to disturb the location and heights during construction. Figure 8 shows the final test section layout along with the weather station equipment at each location.

Figure 7 – Pavement Temperature Sensors Installation

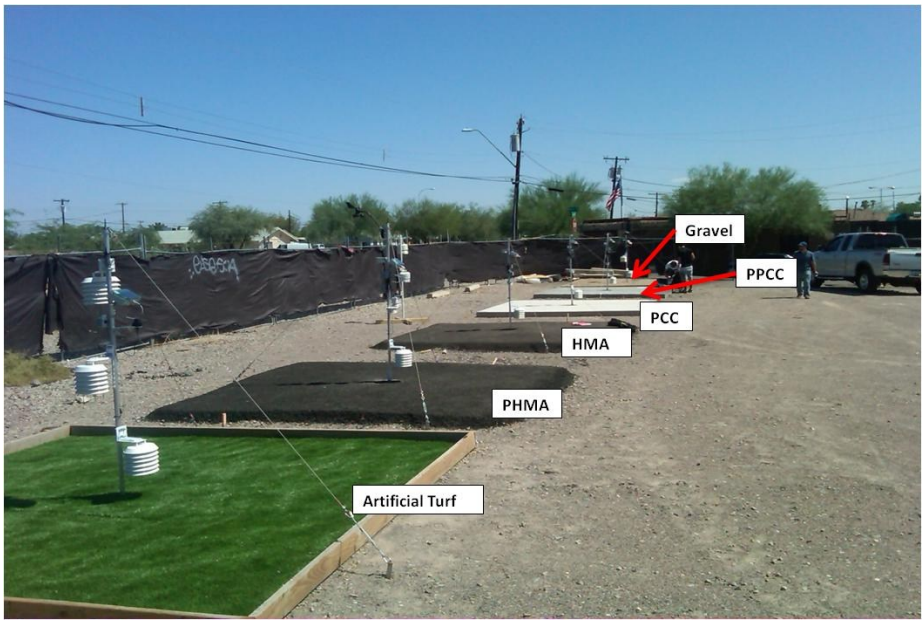

Figure 8 – Full-Scale Pavement Test Slabs in Tempe, Arizona

4.1.1 Weather Stations

One weather station (Figure 9) was installed above each of the slabs, gravel and artificial turf test sections. Each station was capable of measuring temperature and humidity at 1, 3 and 5 feet above the pavement surface along with pavement surface temperature. It is important to note that for simplification abbreviation of each measurement is used. For example, temperature at 1' is represented by T1, humidity by H1 and so forth. In addition, solar radiation, wind speed/direction and rain data were collected on-site. The accuracy of the sensors is: about +/- 2% for humidity measurements, +/- 5% for the solar radiation and +/- 0.5˚C for temperature measurements in the range of 5-40 ˚C.

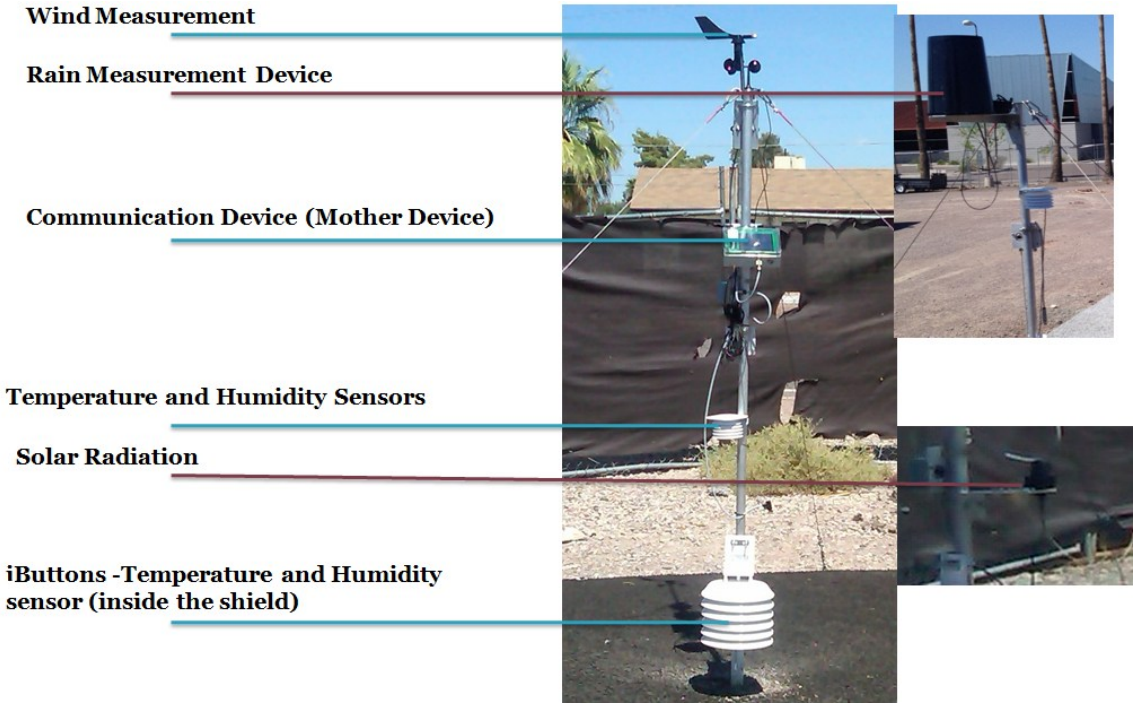

Figure 9 – Typical Weather Station

Weather station data were collected wirelessly from each station and were visible on the website: www.climaps.com. Figure 10 provides a sample of real-time data that is collected from the weather stations (Note: Website data is reported in GMT).

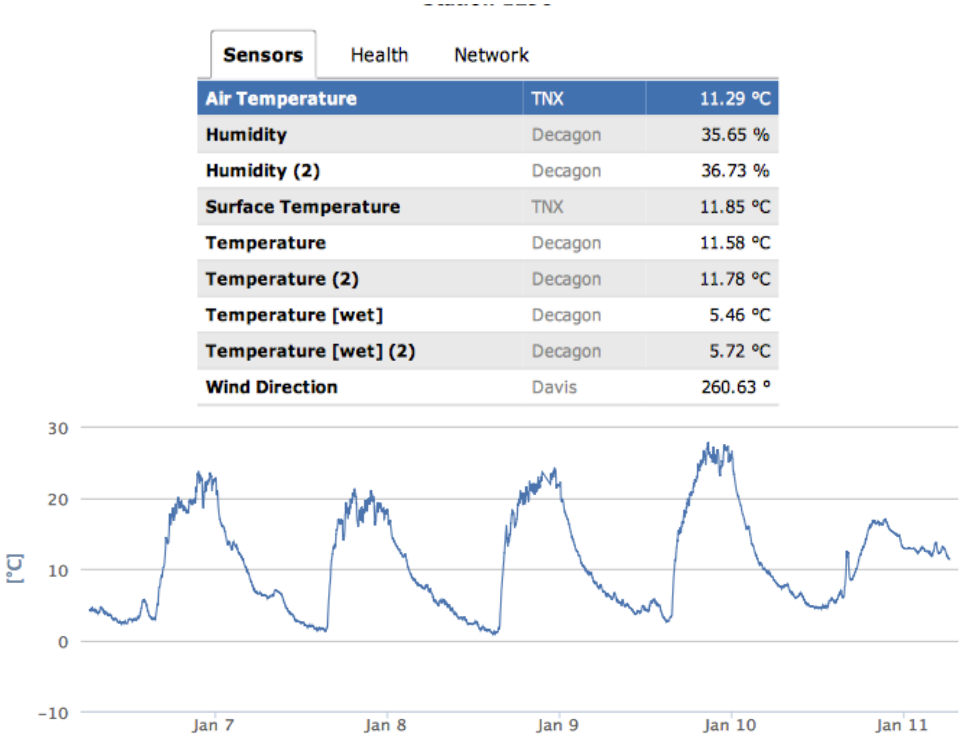

Figure 10 – Example Data From Website

4.1.2 Albedo Device

Albedo was measured on all six surfaces using a spectrometer. This equipment was able to capture the full wavelength range of 350-2500 nm, and included average albedo reading for the specific surface. Calibration was performed using a pure white reference panel prior to taking measurements on any slab. Table 9 provides a summary of the construction activities and modifications made during the monitoring period.

Table 9 – Summary of Tasks

Date	Local (AZ) time	Action	Notes & remarks
7/31/2012	7 AM-2 PM	Site construction	HMA and PCC Slabs
9/17/2012	--	HMA Pavement temperature sensors stopped working	Data were collected for 1 week.
9/17/2012	12:30PM	Stations PPCC, PCC, Turf (surface temperature and solar radiation only) were deployed	
9/18/2012	noon	Stations Gravel-HMA were deployed	Gravel slab was installed.
9/24/2012	6PM	Station PHMA was deployed to replace the old station	Station PHMA was found not working since its deployment on 9/18/12
10/2/2012	--	All stations can be accessed online	
10/3/2012	2PM	Station PHMA under test	tests including: connectivity of sensors, station boot and recharge of batteries
10/4/2012	6AM	Station PHMA lost connection to all sensors and battery info	PHMA needs to be further tested
10/9/2012	--	Turf ibutton sensor at 5' stopped working and it was replaced	All previous Turf data were lost
10/16/2012	7 AM-5 PM	Albedo measurement	every hour from ~7:30am to ~ 4:30pm
11/27/2012	10:30 AM	Re-organization of air sensors	Sensors at 3 ft. of stations PCC/HMA/PHMA were removed; sensor at 3 ft. was moved to 1ft at PPCC; sensor was added at 5ft at Turf
11/29/2012	5 PM	All stations rebooted to reconnect	All station at 5 ft. back to the network

CHAPTER 5

5.1 PHASE II - RESULTS

5.1.1 Albedo Measurements

Four measurements were taken hourly on each slab, between 7 a.m. and 4:30 p.m. on the same day. Figure 11 shows an average of four albedo readings at noon for all 6-test sections. In this figure, the reflectivity (albedo) is shown at different wavelengths. Considering all wavelengths, PCC appears to have the highest albedo reading. PPCC and Gravel tend to have similar albedo value, lower than PCC but higher than PHMA, HMA and Turf. It is important to note the different shape of the reflectivity of the turf section, some higher albedo reading at different wavelengths is due to the color moisture content present in the soil (dispersed over the turf as it is a routine for the turf placement). All other measurements can be found in Appendix A.

Similar trend is observed when looking at the average albedo measurement throughout the day. Table 10 and Figure 12 present a comparison of hourly albedo for all test slabs. Albedo reading was measured hourly over a range of wavelength as it was show in Figure 11. The average value across all different wavelengths was taken for each hour and they are reported in Table 10. This is also shown graphically in Figure 12.

Although, PHMA and PPCC are similar in color compared to HMA and PCC respectively, they appear to have different albedo values. It is important to note that due to open (pore) structure of PHMA and PPCC the albedo values captured during this experiment are lower than anticipated values. This is because the open structure of such materials causes an inconsistent reflection in random directions that cannot be captured by the device.

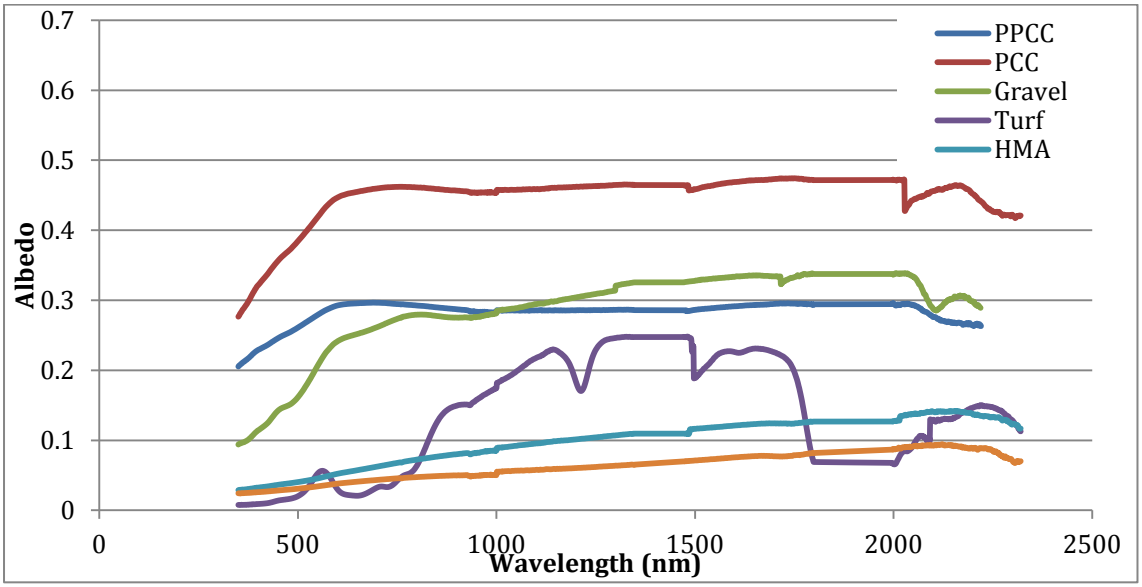

Figure 11 – Albedo Measurements (Readings at Around Noon)

Table 10 – Summary of the Albedo Measurement on October 16th 2012

Time	HMA	PHMA	PCC	PPCC	Gravel	Turf
7:30AM	0.116	0.063	0.490	0.283		0.099
8:30AM	0.100	0.060	0.488	0.256	0.235	0.111
9:30AM	0.093	0.058	0.487	0.263	0.233	0.125
10:30AM	0.093	0.059	0.453	0.285	0.269	0.125
12PM	0.095	0.061	0.453	0.282	0.278	0.132
1PM	0.097	0.057	0.444	0.291	0.296	0.110
2PM	0.090	0.061	0.466	0.246	0.266	0.125
3PM	0.099	0.068	0.460	0.306	0.250	0.125
4PM	0.099	0.065	0.497	0.267	0.321	0.131
Average:	0.098	0.061	0.471	0.275	0.269	0.120

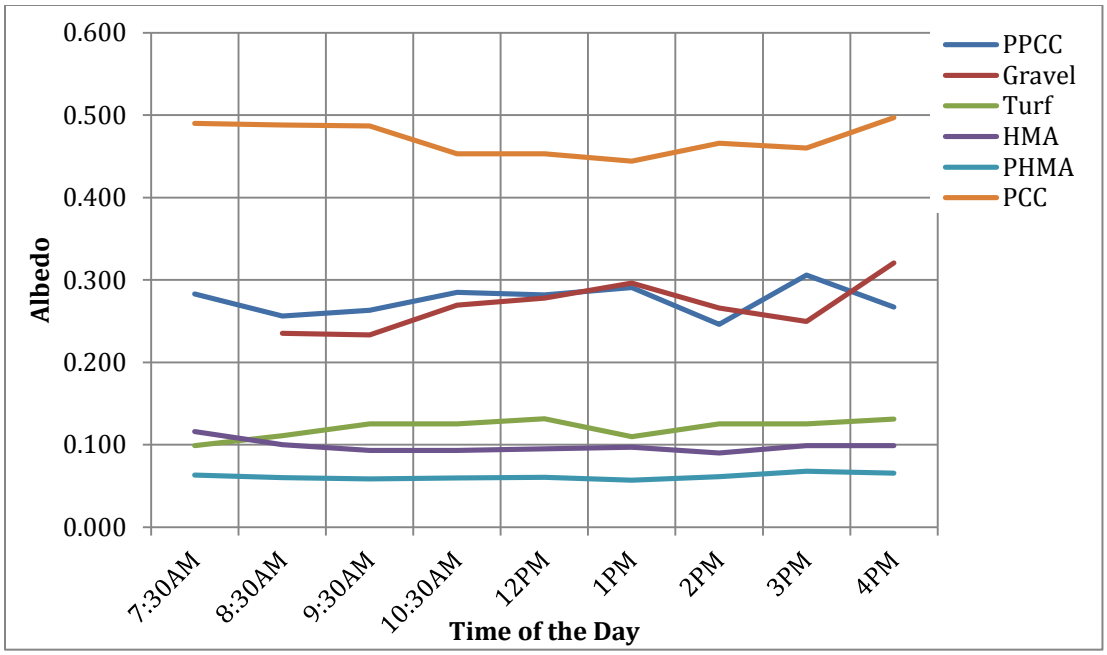

Figure 12 – Hourly Albedo Comparison

PCC appears to have the highest albedo measurement, followed by: PPCC and Gravel, Turf, HMA and PHMA throughout the day. Although the colors of the PPCC and Gravel test sections are different they seem to have a similar albedo value. This similarity could be due to the structure of the PPCC. As it was stated earlier, the open structure of the PPCC and gravel causes an inconsistent reflection of the radiations in random directions. As a result, the device captures a lower percentage of the reflection.

5.1.2 Near Surface Air Temperature

Thermal imaging data (Figure 13) were collected on the same day and time using a FLIR thermal imaging camera. These images corresponded well with the general surface temperature trends for each type of material. PHMA and the turf section appear to have the highest surface temperature 63.04 ˚C, and 62.92 ˚C, respectively. According to Figure 13, HMA has a surface temperature of 57.56 ˚C, Gravel 56.20 ˚C, PPCC 51.90 ˚C and PCC has the coolest surface temperature at 41.20 ˚C . Based on the obtained data, turf surface temperature tends to be higher than HMA surface. The actual surface temperature measurements will be discussed later in this chapter.

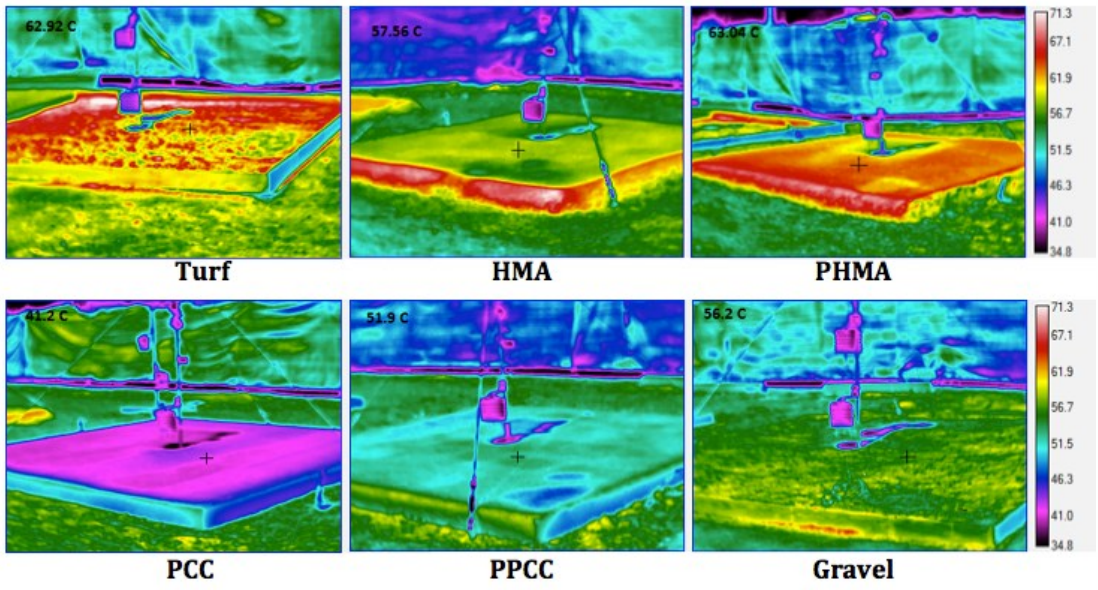

Figure 13 – Thermal Image Data From Full-Scale Test Site

5.1.3 Weather Station Temperature Data

As it was stated earlier, the data was collected wirelessly from each station and was accessible on the website: www.climaps.com. A sample output of the data is shown in Appendix B.

In order to have a better understanding of the collected data, the air temperature at each elevation at a given time of the day was plotted for several days. Figure 14 provides an example of such a graph, showing the air temperature at 3' for HMA, PHMA, PCC, and PPCC for 3 different weeks during the months of September, October, and November. The figure also displays the wind speed during these time periods. Similarly, Figure 15 shows the air temperature at 5' for all 6 sections at noon as well as the solar radiation. This analysis was also completed considering the surface temperature, air temperature at 1' and 5' at 4 am (before sunrise) and at 5 pm for all three sample-weeks. All graphs can be found in Appendix C.

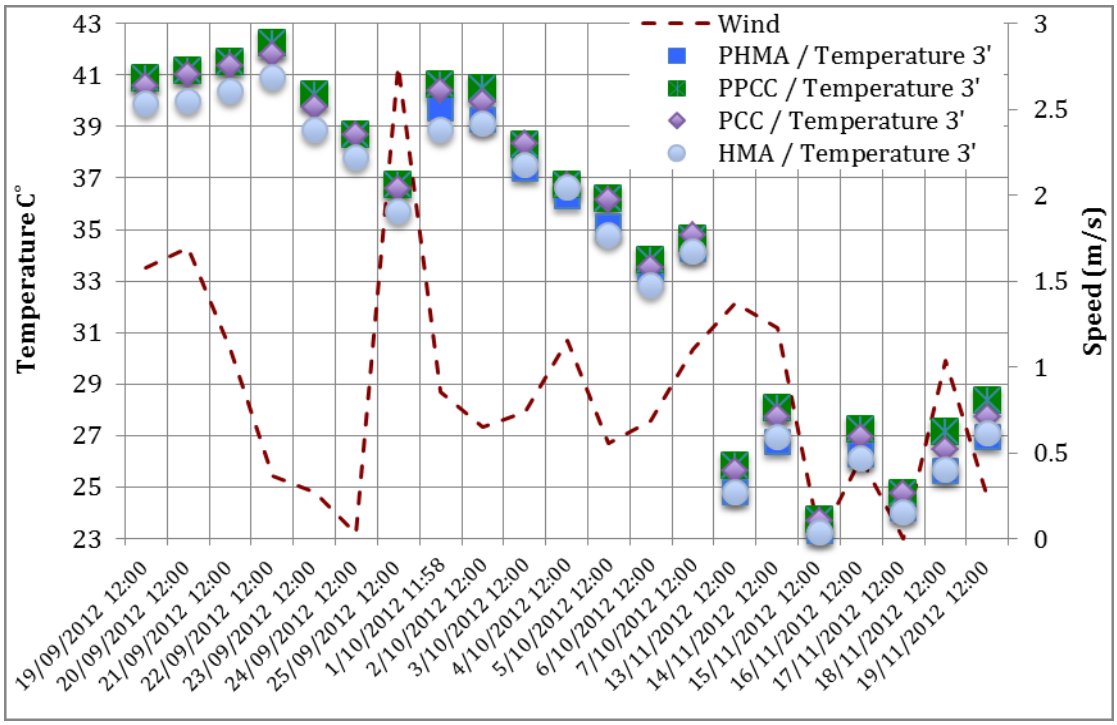

Figure 14 - Air Temperature at 3' and Wind Speed at Noon

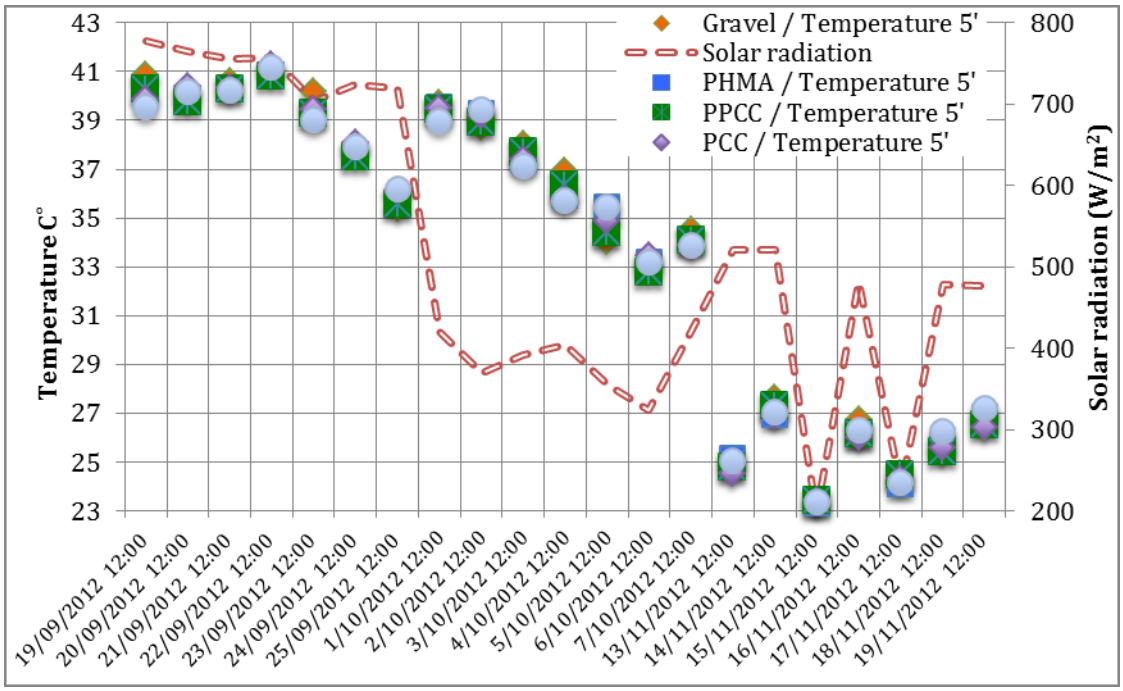

Figure 15 – Air Temperature at 5' and Solar Radiation at Noon

According to Figure 14 and Figure 15, higher temperatures corresponded with lower wind speed. It is also observed the air temperature is lower during the month of November, although the wind speed appears to be relatively low. This is explained by considering the solar radiation in November. According to Figure 15, the solar radiation is generally lower in November compared to September or October. Higher solar radiation corresponds to higher surface temperature/air temperature, regardless of wind effect. In addition, the air temperature difference above all 6 slabs decreased as the elevation increased from 3' to 5'. The temperature differences among all test slabs were less than 1 degree C. Therefore, the data shows that air temperature starts to level off at around 3', indicating that air temperature starts to reach equilibrium and there is no significant difference above this elevation. This trend is clearly visible in Figure 16 and Figure 17. These two Figures provide a sample graph considering the surface Temperature, T3 and T5 for HMA and PCC during the sample days at noon. All other plots for all slabs with measurements at noon, 4am and 5pm can be found in Appendix D.

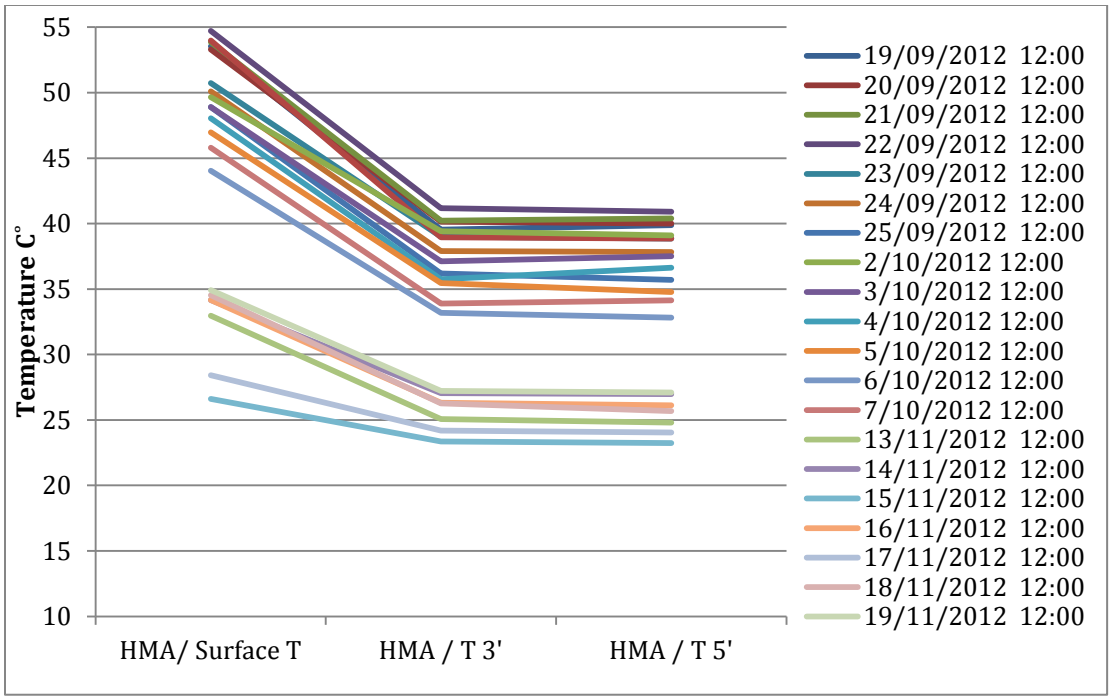

Figure 16 – Relative Comparison of Surface T, T3 and T5 at Noon for HMA

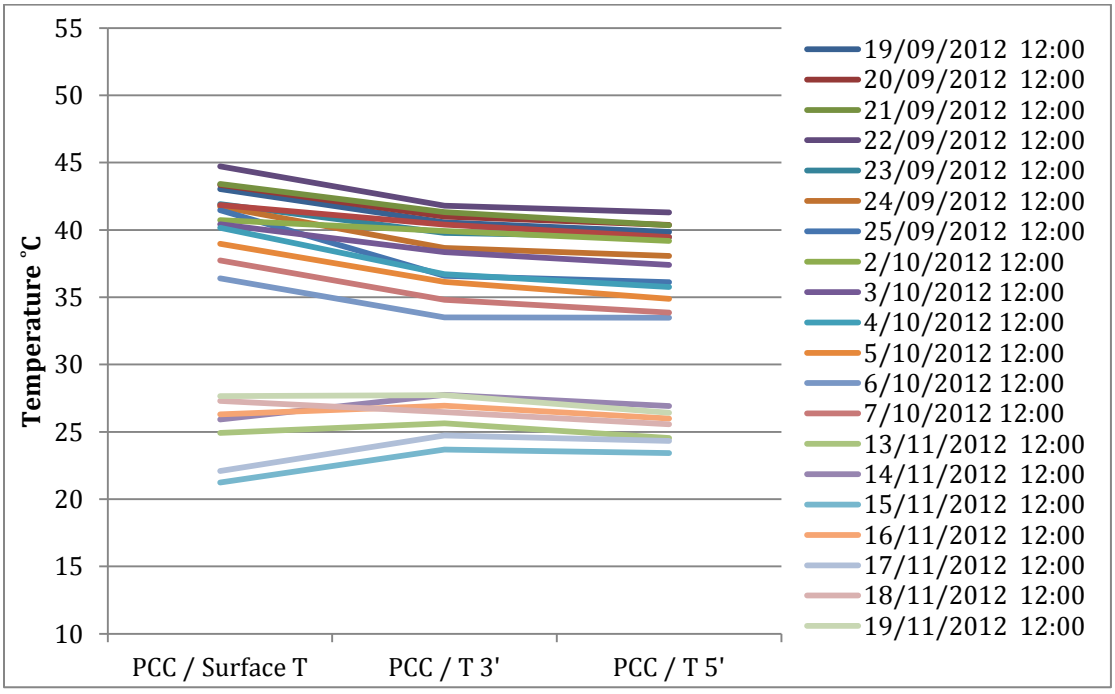

Figure 17 – Relative Comparison of Surface T, T3 and T5 at Noon for PCC

Figure 18 demonstrates a 24-hour air temperature cycle above the porous HMA. In this figure, the surface temperature (green), Air temperature at 3’ (blue) and 5’ (red) are shown. According to this graph, the air temperature at 3’ and 5’ are about the same throughout the day. During the warmest time of the day, surface temperature is about 15˚C warmer than the air temperature at 3’ and 5’. Similarly, the trend indicates no significant air temperature differences between 3’ and 5’ above the pavement surface. In addition, Figure 19 shows a 24-hour cycle of air temperature at 5’. According to this graph, the air temperature reaches a constant value at about 5’ across all six-test slabs.

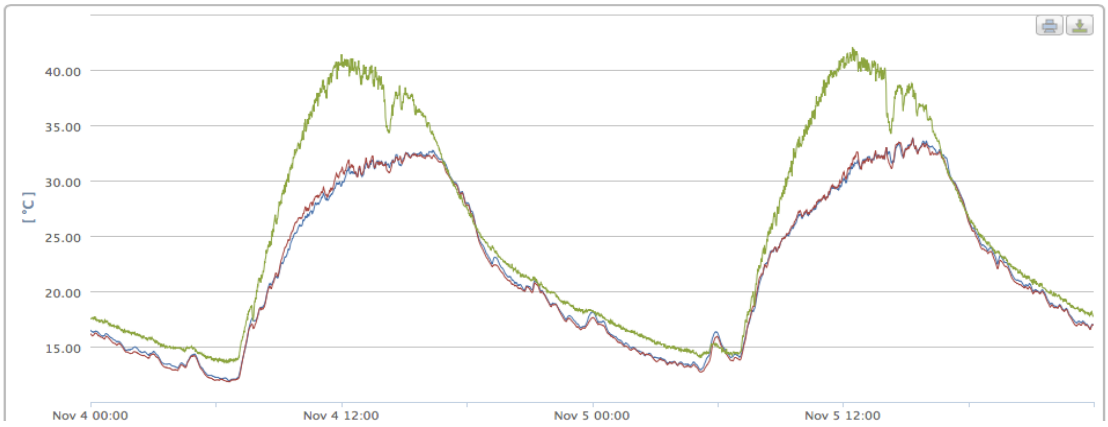

Figure 18 – PHMA (Surface T, T3 and T5), a 24 Hours Cycle

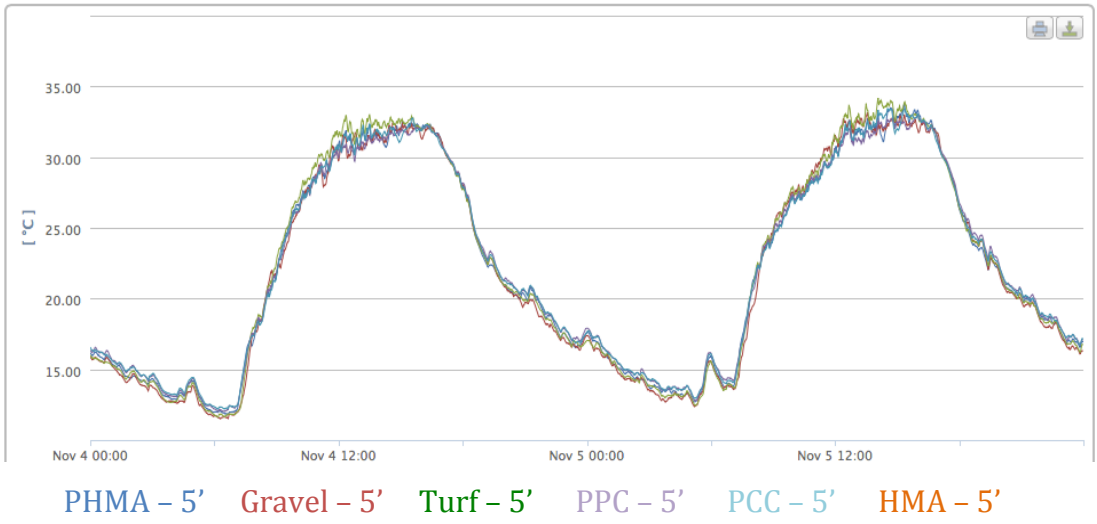

Figure 19 –Air Temperature at 5' for All 6 Sections, a 24 Hours Cycle

Figure 20 provides a comparative plot of above pavement air maximum temperatures for hot and cool days recorded during the monitoring period. The hot day was for October 2, 2012 with an air temperature of about 38.5 C (101.3F). During this hot day, the artificial turf and gravel exhibit the hottest surface temperatures followed by the HMA, PHMA, PPCC and PCC during the day. However, it is interesting to note that the air temperatures above the surfaces are approximately equivalent at 3' and 5' heights despite the significant differences between pavement surface temperatures. A similar air temperature trend is evident on the cooler day (November 4, 2012 with an air temperature of about 30 C (86 F)). It is important to note that the reported air temperature of 38.5 C for Oct 2nd and 30 C for Nov. 4th are the reported maximum air temperature by the official Sky Harbor Weather Station in the Phoenix area, however the air temperature readings at 3' and 5' on the site are relatively higher.

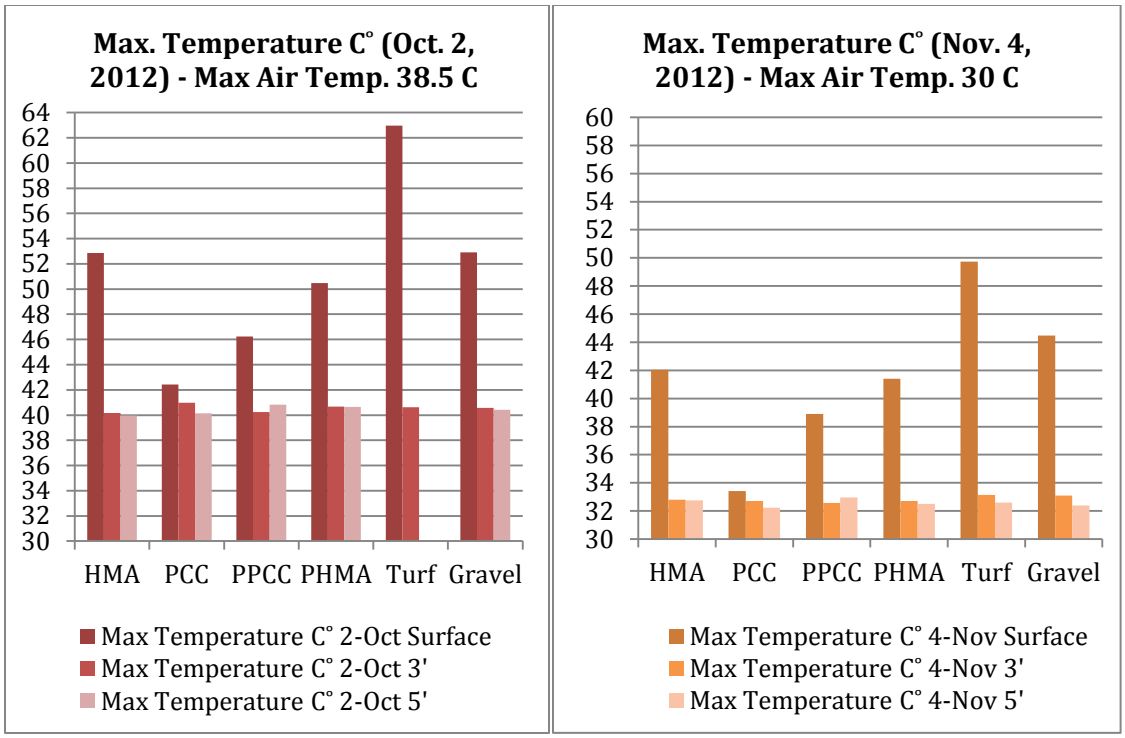

Figure 20 – Maximum Above Surface Air Temperature Comparison for a Hot and a Cool Day in Phoenix, AZ.

Similarly, Figure 21 shows the minimum above pavement air temperatures for the same days, noted at around 6am. Trends indicate no significant air temperature differences between 3' and 5' over the pavement slabs (less than 1degree). Early morning and before sunrise (at around 6am) the HMA has the highest minimum surface temperature followed by: PCC, PPCC, PHMA, gravel and turf.

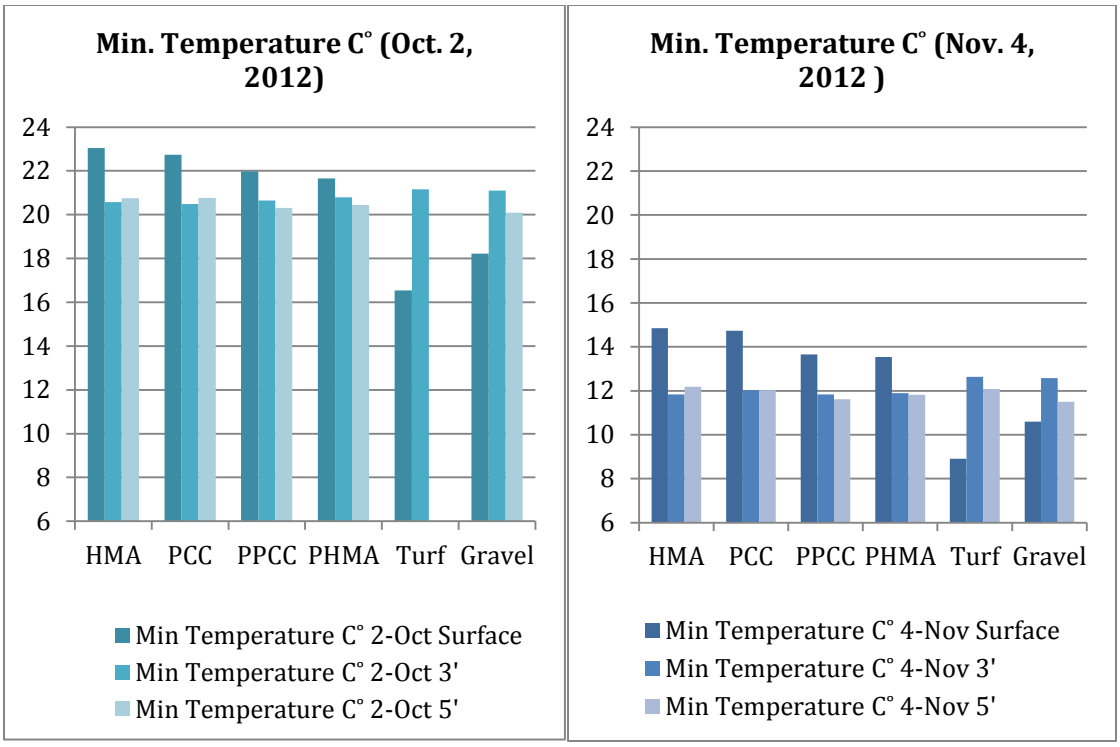

Figure 21 – Minimum Above Surface Air Temperature Comparison for a Hot and a Cool Day in Phoenix, AZ.

Based on the collected data, the maximum temperature for all 6 slabs is recorded at about noon and the coolest temperature is about 4am. From an UHI perspective, the nighttime temperature (the time after sunset and before sunrise) is critical as the heat stored in the materials during the day returns back into the air, causing an increase in the air temperature during the night. Based on the observed trends, the section that shows a higher surface temperature during the day tends to have a cooler surface temperature at night, hence less capacity to store heat. Therefore, such materials have less negative contribution to UHI effect. The maximum and the minimum temperature analyzed for two additional days, Sep. 27th and Nov. 26th, also follow the same trend. All the graphs can be found in Appendix D.

Moreover, based on the collected data, there are minimal differences in air temperatures at 3’ and 5’ above a pavement surface. However, differences exist between air temperatures above different pavement types at surface and below 3’ elevations. As it was discussed in this chapter, temperature measured at the surface of each slab differs significantly from the air temperature measured at 3’ above the same slab, indicating that any temperature difference exist below 3’. Factors such as wind speed, solar reflectivity, rain and humidity have a significant role in air temperatures above pavement along with the pavement surface material type. As it was shown in Figure 14 and Figure 15, higher wind speed corresponds with a lower air temperature and higher solar reflection corresponds with a higher air temperature. This corresponds to the findings in the literature reviews as well, other studies showed that the pavement surface temperature becomes more critical in the areas where there is no or minimum wind speed (26). Unfortunately rain factor was not analyzed in this study as the rainy season was beyond the duration of this study. However, as it was discussed in the literature reviews, studies show that moisture present in the pavement (especially porous materials) corresponds with a lower air temperature above the surface (27).

These conclusions support the view that pavement surface reflectivity or any single parameter alone should not be used to define a “cool pavement” or to evaluate the effect of pavement surface type on overall urban heat island.

CHAPTER 6

6.1 PHASE II - STATISTICAL ANALYSIS

In Chapter 5, visual analysis of the raw data was provided and the observed trends were discussed. In this chapter, a series of statistical analyses was done to have a better understanding of the results. In addition, the statistical analysis provides some insight about the relationships between the pavement temperature and air temperatures above the surface.

6.1.1 T-paired Test

In this study, the data was collected continuously at fixed locations above the different pavement types. As a result, the temperatures need to be compared at the given time and the elevation. Therefore, T-paired test was used to determine if there is a significant difference between: 1) air temperature at 3' and 5' above each section, and 2) air temperature across all the test sections. In order to complete this task, the sets of data (air temperature above different types of the surfaces) were compared one by one. For this test the average difference between all pairs are considered. The following equation shows the mathematician description of such test (45):

$$t = \frac{X_D - \mu_0}{s_D / \sqrt{n}}$$

Where:

S_D: Standard deviation of the average difference

X_D: Average difference

n: sample size

In order to complete this analysis, Minitab software (a statistical software) was used. It is important to note that the accuracy of the sensors used in this study is +/- 0.5˚C. Therefore, for statistical analysis purposes, the analyses were completed using a temperature difference threshold of 0.1˚C.

The null hypotheses for this analysis is that there is not a significant difference between the average air temperature or surface temperature among the pavement types, assuming that the difference is less than 0.1˚C. Here, the alternative hypothesis is that the average difference between the test sections is more than 0.1˚C. The confidence interval is set at 95%. Therefore, if the P-value is less than 0.05 the null hypothesis is rejected, indicating that average temperature differences are more than 0.1˚C and thus the difference is significant. Below is an example of a Minitab output. All the results can be found in Appendix E.

Paired T-Test and CI: HMA/ Surface Temperature, PPCC / Surface Temperature

Paired T for HMA/ Surface Temperature - PPCC / Surface Temperature

	N	Mean	StDev	SE Mean
HMA/ Surface Temperature	62763	31.0653	9.4592	0.0378
PPCC / Surface Temperature	62763	28.8915	8.3505	0.0333
Difference	62763	2.17383	2.09247	0.00835

95% lower bound for mean difference: 2.16009
T-Test of mean difference = 0.1 (vs > 0.1): T-Value = 248.29 P-Value = 0.000

Table 11, Table 12 and Table 13 provide a summary of the t-paired test for pavement surface temperature, air temperature at 3’ and air temperature at 5’, respectively. P-Value greater than 0.05 indicates that the average difference is less than 0.1 C, and thus no significant difference between the test sections.

Table 11 – T-paired Test Results for Pavement Surface Temperature

Surface T: P-Value, where H0 < 0.1C						
	PPCC	PCC	HMA	PHMA	Gravel	Turf
PPCC		0	0	1	0	0
PCC	0		0	0	1	1
HMA	0	0		0	0	0
PHMA	1	0	0		0	0
Gravel	0	1	0	0		1
Turf	0	1	0	0	1	

Table 12 – T-paired Test Results for Air Temperature at 3'

T3: P-Value, where H0 < 0.1C						
	PPCC	PCC	HMA	PHMA	Gravel	Turf
PPCC		1	1	1		
PCC	1		1	1		
HMA	1	1		1		
PHMA	1	0.99	1			
Gravel						
Turf						
missing data						

Table 13 - T-paired Test Results for Air Temperature at 5'

T5: P-Value, where H0 < 0.1C						
	PPCC	PCC	HMA	PHMA	Gravel	Turf
PPCC		1	1	1	1	
PCC	1		1	1	1	
HMA	1	1		1	1	
PHMA	1	0.99	1		1	
Gravel	1	1	1	1		
Turf						
missing data						

Considering the pavement surface temperature, there is a significant difference among most of the pavement types. However, it is interesting to note that according to the results there is not a significant difference in the surface temperature of: PHMA vs. PPCC, Gravel vs. Turf, PCC vs. Turf and PCC vs. Gravel. This indicates that although Turf surface temperature tends to have a high fluctuation throughout the day, the average difference between Turf and PCC is not more than 1˚C. In addition, this is true for PCC and Gravel, the average difference between PCC and Gravel surface temperature is not significant.

Considering the air temperature at 3', all the P-values are greater than 0.05. This indicates that the temperatures are similar and there is no significant difference among any of them. It is important to note that the air temperature data at 3' above the Turf and the Gravel are missing and are not analyzed. A similar result is obtained for air temperature above 5'. There is no significant difference between the air temperatures among all test section (excluding the missing values above the turf).

6.1.2 Regression Analysis

Different criteria can be used to find a linear model, in this analysis, the minimum least square of the error criterion is used. Regression analysis is completed to have a better understanding of the interaction and the dependency of the variables. The linear models obtained through this analysis, are considered as the following (46):

$$Y_i = \beta_0 + \sum_{j=1}^{p} \beta_j X_{i,j} + \varepsilon_i$$

Where:

Y_i: $response\ variable$ ($dependent\ variables$)

$X_{i,j}$: $p\ regressors$, $(X_{i,1} \ldots X_{i,p})$

β: $the\ unkonwn\ coefficients$ ($estimated\ by\ least\ squares$)

ε_i: $mean\ zero\ error$

It is important to note, that if the error of the model follows normal distribution (as it is true for this study), the obtained results are similar to the Maximum Likelihood Estimation (MLE).

A multiple-linear regression was completed to fit an air-temperature prediction model considering pavement types. The measured temperatures (surface, 3' and 5') are selected as the dependent variables. All other variables are assumed to be the independent variables: Time, Elevation, Wind Speed, Wind Direction, Solar Radiation, Humidity, Density, Albedo, Specific Heat Capacity, and Conductivity. Density, specific heat capacity and thermal conductivity were combined into a diffusivity term. For the surface temperature, the elevation considered to be 0.01ft. JMP software was used to complete the analysis. Data from first week of September 2012, up to the first week of November 2012 were analyzed.

The best model was considered to be the model that shows no trend in the residuals plot, and contains the largest coefficient of determination, R-squared. R^2 provides some insight about the goodness of fit of the model, indicating the accuracy that the regression line fits the actual data. R^2 value of 1 shows that the regression line fits all the data points perfectly, and 0 indicates that the fitted model does not fit the data (no linear relationship). R^2 is mathematically defined as (46):

$$R^2 = \frac{SSR}{SST} = 1 - \frac{SSE}{SST}$$

Where:

$$SSR = Regression\ Sum\ of\ Sqares = \sum_i (\hat{y}_i - \bar{y})^2$$

$\bar{y}$: mean of the observed data $= \frac{1}{n}\sum_{i=1}^{n} y_i$

$$n: number\ of\ observations$$

$$\hat{y}_i: modelled\ value\ of\ actual\ values\ (y_i)$$

$$SST = the\ total\ sum\ of\ squares = \sum_i (y_i - \bar{y})^2$$

$$SSE = Residuals\ Sum\ of\ Squares = \sum_i (y_i - \hat{y}_i)^2$$

Table 14 shows the correlation between the variables. The high correlation, of 1 or -1, indicates that the two variables are directly or inversely proportional. In other words, it means that two variables are increasing in the same or opposite direction. As a result, if the correlation between two variables is high, one of the two may be excluded from the model. The red color values in the table indicate statistically high correlation.

Table 14 - Correlation of the Variables

Variable	Temperature	Time	Elevation	Wind Speed	Wind Direction	Humidity	Solar radiation	Albedo	Diffusivity
Temperature	1.0000	0.1727	-0.2210	0.5490	0.2213	-0.8439	0.7190	-0.0541	-0.0113
Time	0.1727	1.0000	-0.0000	-0.0334	0.3774	-0.3445	-0.1679	0.0000	0.0028
Elevation	-0.2210	-0.0000	1.0000	-0.0004	-0.0000	-0.0029	-0.0000	-0.0007	-0.0497
Wind Speed	0.5490	-0.0334	-0.0004	1.0000	0.0896	-0.4477	0.5457	0.0317	0.0518
Wind Direction	0.2213	0.3774	-0.0000	0.0896	1.0000	-0.1787	-0.0520	-0.0028	-0.0065
Humidity	-0.8439	-0.3445	-0.0029	-0.4477	-0.1787	1.0000	-0.4812	-0.0074	-0.0069
Solar Radiation	0.7190	-0.1679	-0.0000	0.5457	-0.0520	-0.4812	1.0000	-0.0014	-0.0026
Albedo	-0.0541	0.0000	-0.0007	0.0317	-0.0028	-0.0074	-0.0014	1.0000	0.6258
Diffusivity	-0.0113	0.0028	-0.0497	0.0518	-0.0065	-0.0069	-0.0026	0.6258	1.0000

The correlations between the independent variables appear to be reasonable. For example, the correlation between solar reflection and the albedo is really low (not significant as it is marked in black). This appears to be reasonable, because, solar radiation is the same for all different type of materials, but the albedo value for different surfaces is different. As it was mentioned earlier albedo is the ratio of the reflectivity of a surface to the incoming solar radiation. Although, in order to find albedo, solar reflection should be known, however they are not significantly correlated. On the other hand, the solar radiation and humidity are negatively correlated, indicating that as solar reflection increases the humidity decreases. This again appears to be reasonable. On a cloudy day where there is minimal incoming solar radiation, the humidity increases. In addition there is a relatively high correlation between Temperature and all other independent variables except albedo and diffusivity.

It is important to note that considering the correlation matrix alone, for determining the significant variables in the model, is not reasonable. This is because two variables may not have high correlation when they are compared, but the correlation between more than two of them may be significant. Therefore, all the variables were included for the regression model analysis. Table 15 provides a summary of the fitted model and Table 16 present the parameter estimates. Figure 22 shows the predicted vs. the actual values.

Table 15 - Summary of Fit

Multiple R^2	0.856184
Adjusted R^2	0.856171
F Ratio	65493.90
P> F	<0.0001
Root Mean Square Error	2.107411

Table 16 - Parameter Estimates (Regression Model)

N=88019	Regression Summary for Dependent Variable: TEMPERATURE			
	Estimate	Std Error	t Ratio	Prob>|t|
Intercept	32.31863	0.052834	611.71	<.0001
Time	0.0485324	0.00126	38.51	<.0001
Elevation	-0.046241	0.007153	-6.46	<.0001
Wind Speed	1.0578849	0.013499	78.37	<.0001
Wind Direction	0.0089236	7.177e-5	124.33	<.0001
Humidity	-0.238362	0.00073	-326.7	<.0001
Solar Radiation	0.0066652	3.238e-5	205.83	<.0001
Albedo	0.1525197	0.054035	2.82	0.0048
Diffusivity	-157742.9	54629.92	-2.89	0.0039

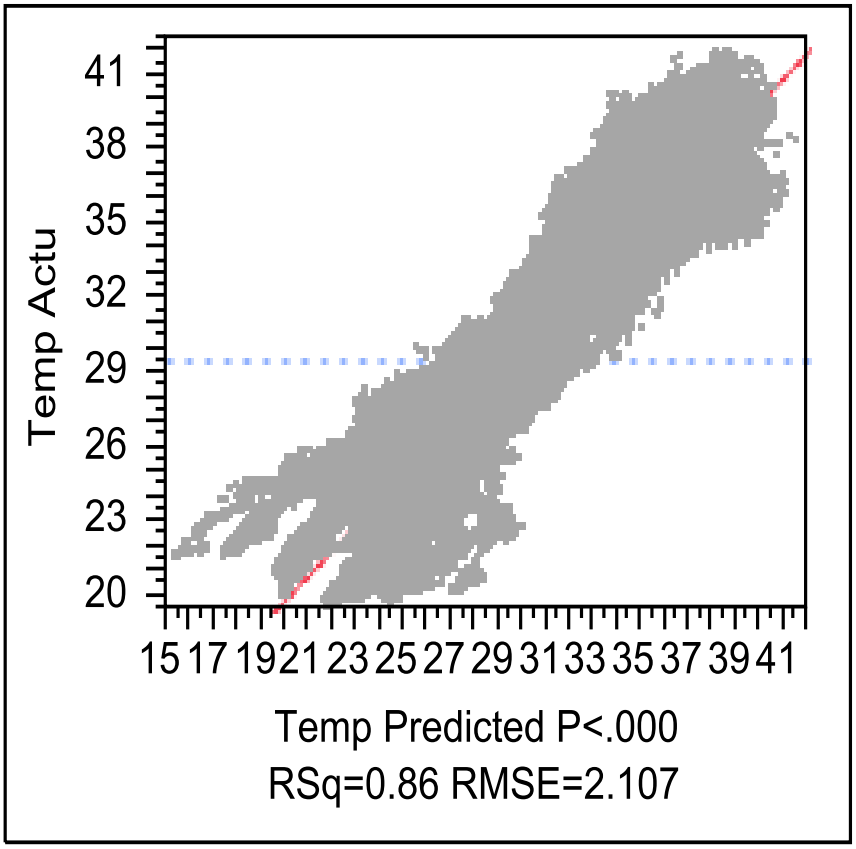

Figure 22 – Predicted vs. Observed Values (Multiple-Linear Regression)

According to the results, the following regression model is obtained:

$$T=32.31863+0.0485324 - 0.046241E + 1.0578849WS + 0.0089236WD – 0.238362H + 0.0066652SR +0.1525197A – 157742.9D$$

Where:

T: Temperature (˚C)

t: time of the day (military time, from 0-23.99)

E: elevation (ft)

WS: wind speed (m/s)

WD: wind direction (degree)

H: humidity (%)

SR: Solar Radiation (W/m^2)

A: Albedo

D: Diffusivity (m^2/s)

The statistics indicate that the model has very good goodness of fit: the P-values are less than 0.05; the predicted vs. Observed values, shows that all the data are close to the linear line. The R^2 is about 85.61%, the model can explain the major variability that exists in the data. In general, the higher number of variables corresponds with a higher R^2, the adjusted R^2 takes this fact into the considerations. However, the difference in R^2 is negligible.

The coefficients of the regression model appear to be rational. For example, as the elevation (from the surface) increases the temperature decreases, therefore a negative coefficient is expected. On the other hand, as solar radiation increase, temperature is expected to increases as it is shown in the model. Although it is difficult to examine the time, temperature tends to increase from the sunrise to the sunset and therefore a positive correlation, as it is shown in the model, is expected. It is noted that the model above is based on a multiple-linear regression analysis. Although a large number of data was available for humidity at 3' and 5'; however, such measurement was missing at the surface level. A power model was also examined with a slightly higher R^2 and it is shown in APPENDIX F. Due to the nature of the power model, the model is only valid when all the input parameters are greater than zero. As a result, there is a limited use for such model, since some of the input parameter such as wind speed could have a zero value.

CHAPTER 7

7.1 PHASE II - PAVEMENT NEAR SURFACE TEMPERATURE

As it was mentioned earlier, thermocouple sensors were installed in each slab and directly under the artificial turf surface. In the pavement slabs and gravel, sensors depths were 1", 2.5" and 4" from the surface. Data are summarized in Figure 23 through Figure 25. It is noted that the sensors in the HMA stopped working one week after construction, which may have been the result of exposure to high compaction temperature followed by a rain event shortly thereafter. In addition, the Turf and Gravel section were not constructed during that one-week, where the HMA temperature data are available. Therefore, the first comparison does not include the Turf or the Gravel and the second comparison does not include the HMA.

Figure 23 indicates that the HMA and PHMA had the highest daytime temperatures (~153°F / ~67.2°C), which are expected. However, the porous HMA had the lowest nighttime temperature (~95°F / ~35°C) compared to the other three pavement types (~104-106°F / ~40-41.1°C). This trend corresponds with literature and is a result of the unique lower specific heat and thermal conductivity properties of the porous materials. Figure 24 and Figure 25 show similar trends at 2.5" and 4" depth, respectively. It is important to note that the temperature decrease as the depth increases. As the result the difference in the temperature decreases across all types of the pavements.

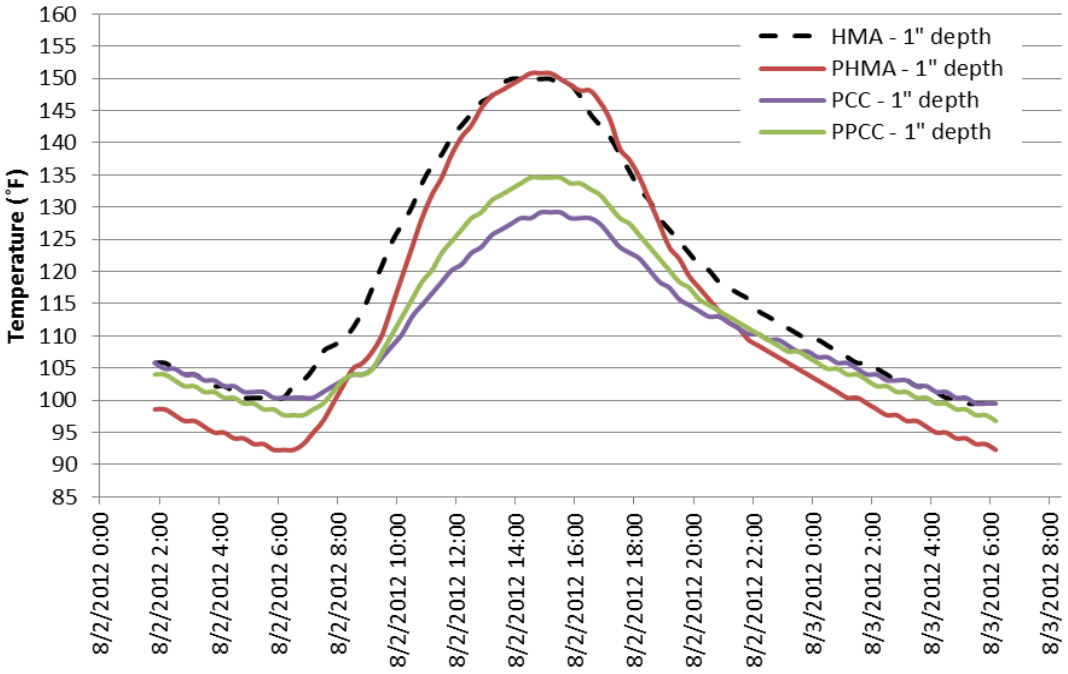

Figure 23 – Comparison of Diurnal 1" Below Surface Pavement Temperatures

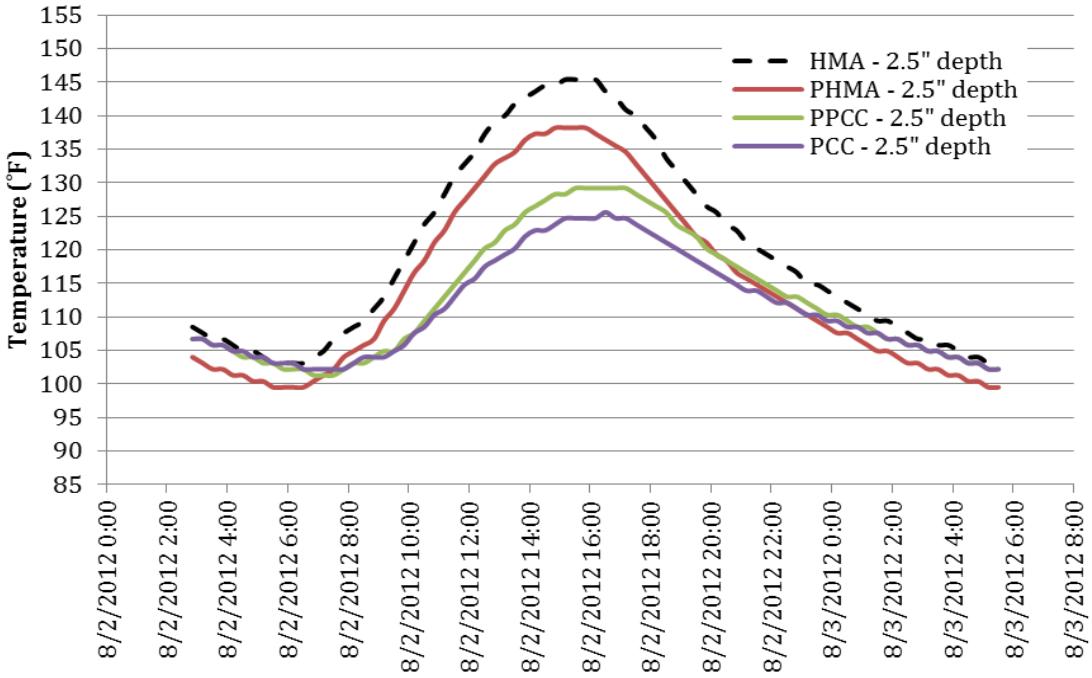

Figure 24 - Comparison of Diurnal 2.5" Below Surface Pavement Temperatures

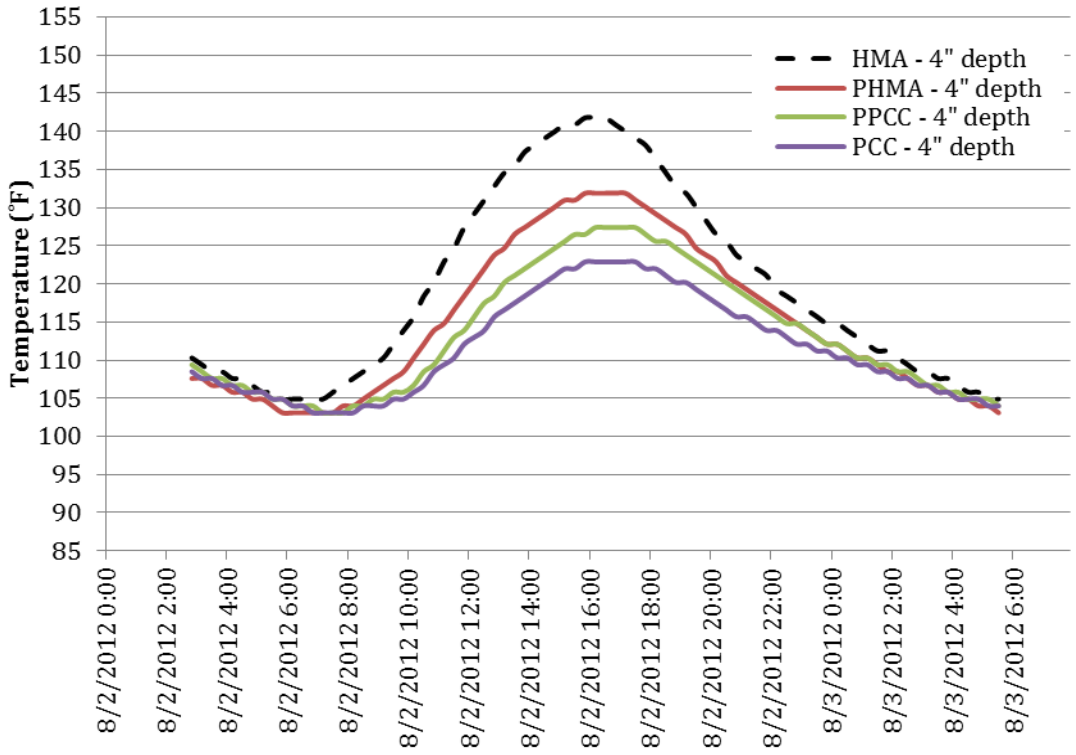

Figure 25 - Comparison of Diurnal 4" Below Surface Pavement Temperatures

Figure 26 indicates that all pavement slabs had similar nighttime temperatures despite PHMA having the highest daytime temperature. In comparison, the gravel slab had similar daytime temperatures as the porous HMA but exhibited the lowest nighttime temperature. Note that in this Figure, PHMA has a higher nighttime temperature compared to the gravel, PPCC, PCC and turf. One contributing factor could be the change in season and solar radiation. Figure 23 - Figure 25 represent the data early August when the air temperature is at its maximum in Arizona, with high solar reflectivity. However, Figure 26-Figure 28 represent the in mid/late September of the same year, where the solar reflectivity is less and the air temperature has cooled down.

However, the overall data shows similar trend, with an increase in the depth the temperature decreases, thus the difference across all types of the pavement decreases.

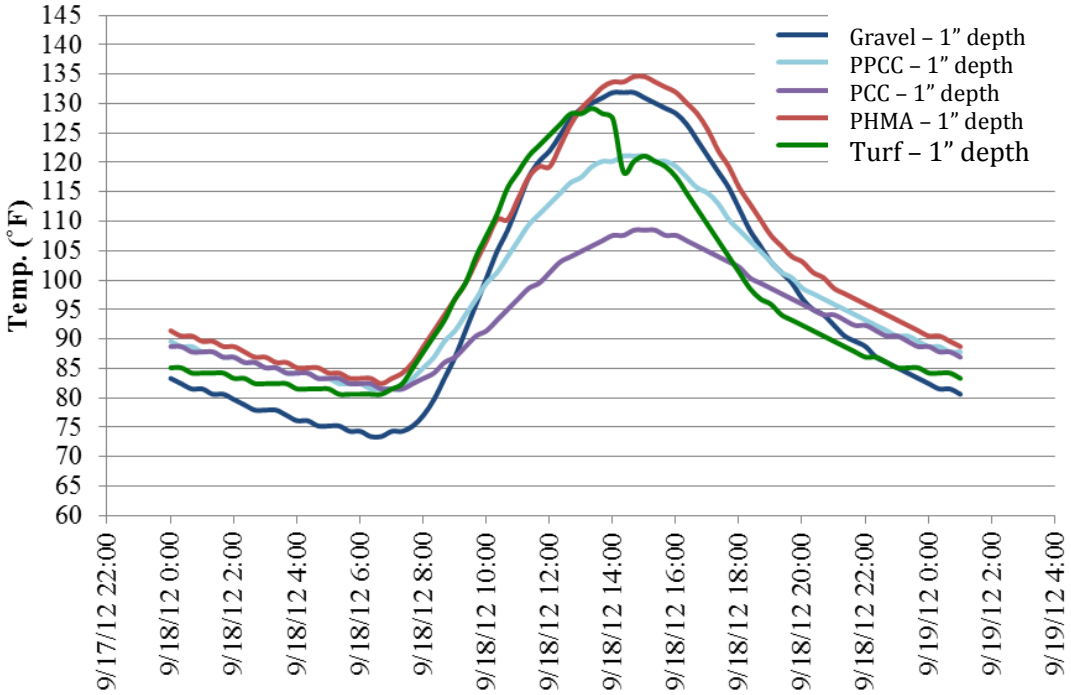

Figure 26 - Comparison of Diurnal 1" Below Surface Pavement Temperatures

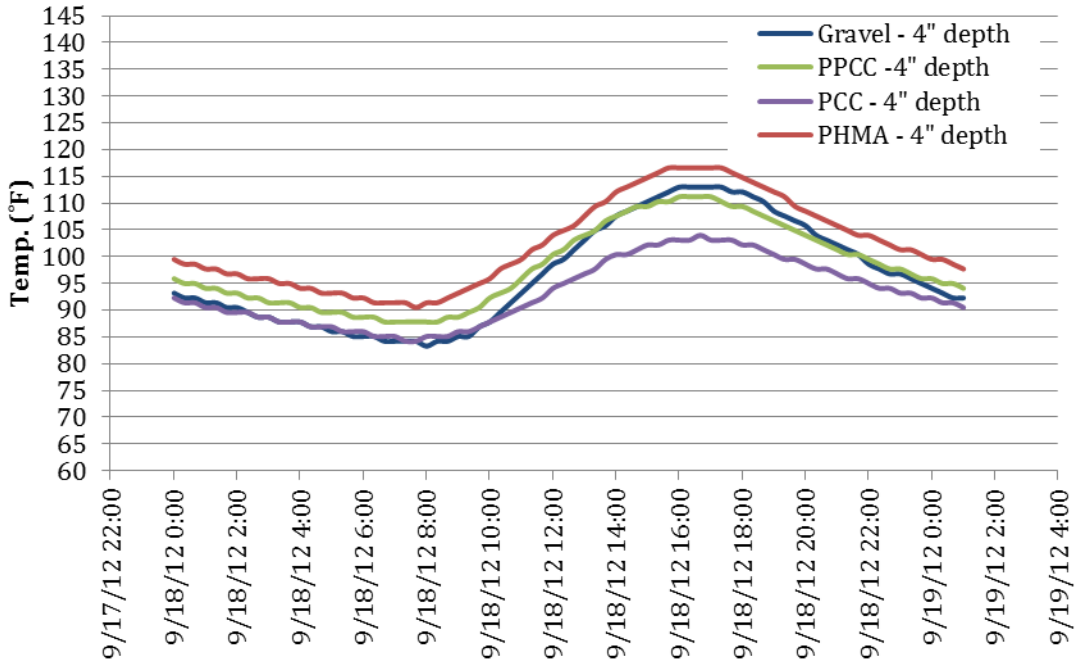

Figure 27 - Comparison of Diurnal 2.5" Below Surface Pavement Temperatures

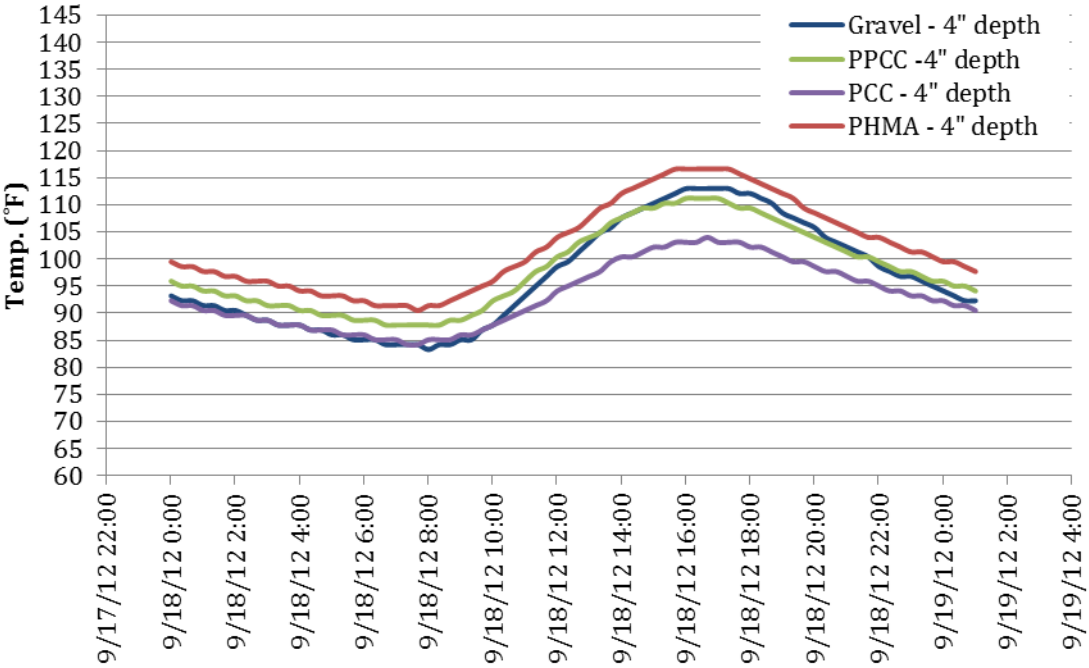

Figure 28 - Comparison of Diurnal 4" Below Surface Pavement Temperatures

7.2 PHASE II – ASU MODEL VERIFICATION

Using the collected data from the site, such as air temperature at 5', solar radiation, wind speed and humidity, a verification analysis was conducted using the ASU Pavement Temperature model. In Phase I, Sky harbor Weather station (AZMET) data was used. However, it is important to note that the air temperature reported from the Sky Harbor weather station is not exactly the same air temperature measured at the site. This is due to small variations in environmental factors (wind, shade, adjacent building, roads and etc.) and the location of the experimental site in comparison to the Sky Harbor weather station. This quick verification analysis used the onsite weather station data to predict pavement temperatures. This is the model that was originally used in Phase I.

The material properties used for this analysis, are based on the typical average values and the measured albedo values during Phase II. The albedo values used in the model for PHMA and PPCC were slightly higher than the actual measured values in the field due to reasons explained earlier. Table 17 provides a summary of the pavement properties used in this analysis.

Figure 29, Figure 30 and Figure 31 show examples of such analysis; the pavement temperature at 1", 2.5" and 4" depth is modeled for both PCC and PHMA (additional plots can be found in Appendix G).

Table 17 - Materials Input Properties

Structure		1	2	3	4
Layer 1					
Material	-	HMA	PHMA	PCC	PPCC
Albedo	-	0.1	0.09	0.5	0.4
Emissivity	-	0.91	0.91	0.91	0.91
Density	(kgm^{-3})	2238	2146	2350	2100
Specific Heat	($Jkg^{-1}K^{-1}$)	921	800	1000	950
Conductivity	($Wm^{-1}K^{-1}$)	1.2	0.4	1.5	0.95
Thickness	(in)	5	5	5	5
Interface Resistance	-	0.001	0.001	0.001	0.001
Layer 2(Ground)					
Material	-	Dry Clay	Dry Clay	Dry Clay	Dry Clay
Density	(kgm^{-3})	1700	1700	1700	1700
Specific Heat	($Jkg^{-1}K^{-1}$)	920	920	920	920
Conductivity	($Wm^{-1}K^{-1}$)	0.9	0.9	0.9	0.9
Additional Factors					
Sky View Factor	-	0.95	0.95	0.95	0.95
Solar View Factor	-	0.85	0.85	0.85	0.85

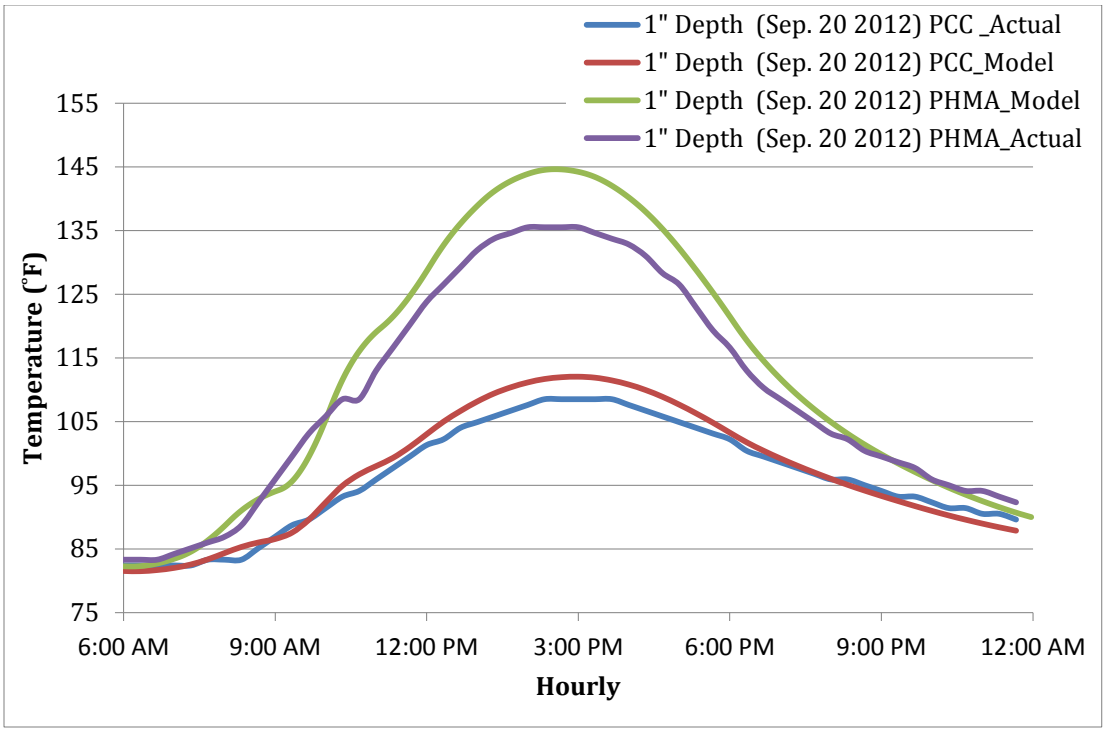

Figure 29 – Pavement Temperature at 1" Depth: Actual vs. Predicted Values

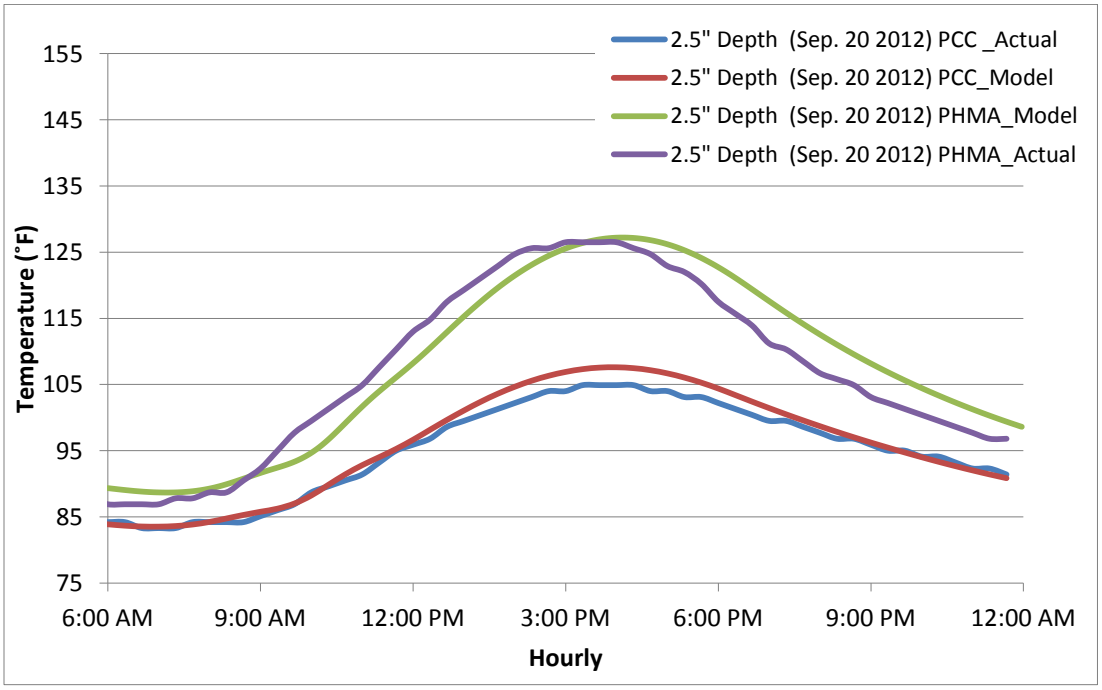

Figure 30 – Pavement Temperature at 2.5" Depth: Actual vs. Predicted Values

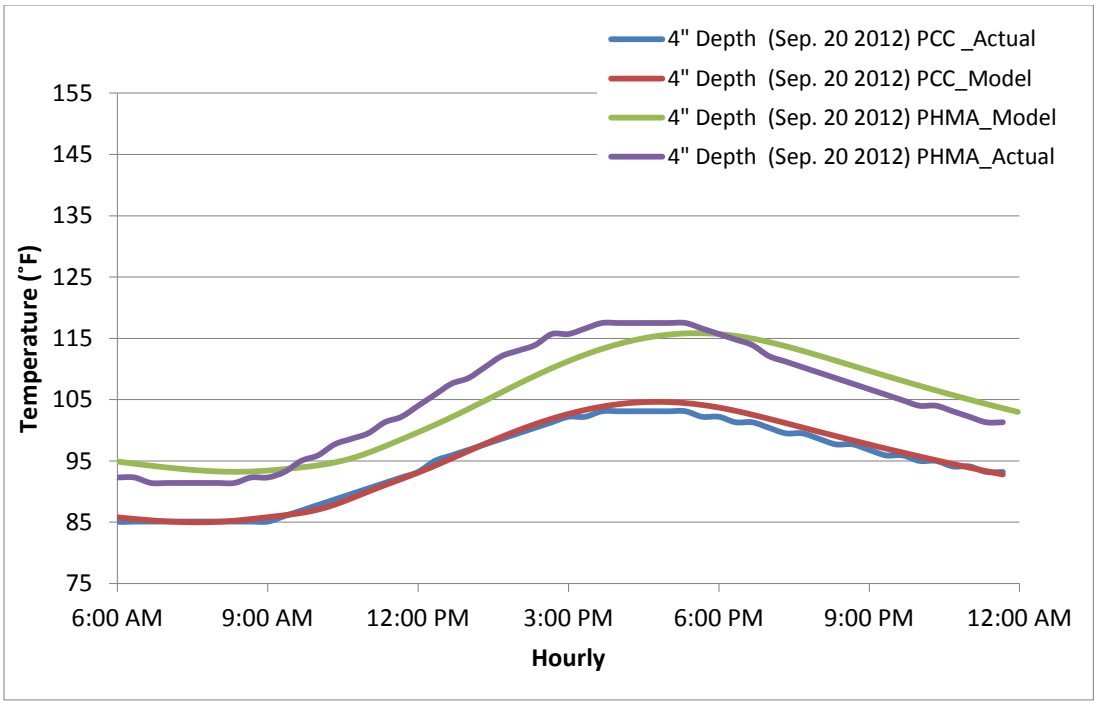

Figure 31 – Pavement Temperature at 4" Depth: Actual vs. Predicted Values

According to the graphs, the model predicts a similar trend in the actual values. However predicted values do not exactly match the actual measurements. In addition, the predicted temperature values appear to be shifted by a few degrees. However, the difference between the actual and the predicted values decreases as the depth increases. The assumptions made for the properties of the pavement material and the subgrade may have contributed to these differences. Based on the findings, the model may need to be adjusted when dealing with porous materials as it overestimates the heat captured near the surface for such materials. The model values and the actual values for the PCC appear to be almost the same. Data for HMA are not available as the sensors imbedded in the pavement were lost shortly after the construction. However the pavement temperature data is available for the prior week while the weather data is not available during those

weeks (weather stations were not installed). Therefore, further analysis and validation using the specific material properties and climatic data are required.

CHAPTER 8

8.1 SUMMARY AND CONCLUSIONS

In the recent years exploring different ways to mitigate the effects of UHI has gained the attention of the researchers, industry and public officials. In the past, recommendations such as use of larger vegetation area and increasing the albedo of the construction materials have been suggested. Many researchers believe that replacement of the darker materials with a lighter one (higher albedo or solar-reflectivity) is the key to reduce the UHI effect. However, other studies have shown that the problem may be more complex, and that solar reflectivity may not be the only important factor to evaluate the ability of a pavement to mitigate UHI.

This study explored the influence of different types of pavement materials on the near surface air temperature and extent at which the surrounding air temperature will be affected.

8.1.2 Phase I Effort

Phase I explored the extent to which porous hot-mix asphalt (PHMA) pavements influence pavement temperatures and contribute to the overall UHI effect. Three sample porous asphalt mixtures were obtained and subjected to thermal conductivity testing. The samples were compacted (cylindrical shape) at the ASU advanced materials laboratory. The thermal conductivity test developed at ASU, revealed that the thermal conductivity parameter of asphalt materials is very complex. Therefore, the use of the general k-values found in the literature may affect the analysis of the paving material resulting in improper conclusions.

A one-dimensional pavement temperature model (ASU) was used to model surface pavement temperature for PHMA, HMA (Hot Mix Asphalt) and PCC (Portland Cement Concrete). Through series of studies it was found that although lower albedo results in a higher maximum daily surface temperature, the type of materials and the pavement structure have a greater impact on the minimum nighttime temperature. It was found that PHMA has the highest predicted daytime surface temperature and lowest nighttime temperature. This concluded that the pavement surface temperature is a complex study that is not only affected by albedo, but by the material type, pavement thickness and subgrade properties.

A pilot study was completed to analyze the effect of pavement surface temperature on near-surface air temperatures. Air temperature was measured at 1-foot interval above the pavement surface. It was noted that there is not a significant difference after 5' level. The data was collected at different locations and differences in weather conditions and surrounding conditions (buildings, etc.) made comparison of air temperatures and pavement surface temperatures impractical. Although the results were promising, it led to further investigation and construction of pavement test sections.

8.1.3 Phase II

Six full-scale pavement slabs (12' x 12' x 5") consisting of Turf, Gravel, HMA, PHMA, PCC and PPCC (Pervious Portland Cement Concrete) were constructed in Tempe, Arizona in the summer of 2012. During construction, pavement temperature sensors were installed into the pavements at 1", 2.5", and 4" depth. Small weather stations capable of measuring air temperature, surface temperature and humidity were installed on top of each section. Air temperature was measured at 1', 3' and 5' above

each test section. In addition, wind speed/direction, rain and solar reflection was measured on the site. The data was collected and monitored wirelessly and it was accessible through a website. Weather stations were installed in late September 2012 and data was collected until late November 2012.

8.1.4 Near Surface Air Temperature Data Analysis

Albedo was measured from about 7am until 5pm once, hourly. Data revealed that there was not a significant difference in the albedo reading throughout the day. It was found that PCC has the highest albedo followed by PPCC and gravel, Turf, HMA and PHMA. It was interesting to note that PPCC and Gravel had similar Albedo value although different in color and structure. This could be due to the open structure of the PPCC and the inconsistent intensity and direction of the solar reflection.

Near surface air temperature was measured above all 6-test sections at different elevations. However, due to utilizing different sensors and data collection system, data collected at 1' across all 6 slabs were not analyzed in this study. Data collected form the weather stations showed no significant difference between air temperature at 3' and 5' regardless of the pavement type. It was also found that the turf maximum surface temperature can be hotter than HMA during the day, although it has a higher albedo value. On the other hand, the turf minimum surface temperature is the coolest compared to PPCC, PCC, HMA, PHMA and gravel. General trend for the min and maximum surface temperature are the following:

Minimum Surface temperature, Cool> Hot: Turf, Gravel, PHMA and PPCC, PCC, HMA

Maximum Surface temperature, Hot>Cool: Gravel and HMA, PHMA, PPCC, PCC, Turf

It appears that although HMA, PCC and Turf could be at the extreme ends when considering both minimum and maximum surface temperature, the porous materials (PHMA, and PPCC) tend to be somewhere in between. This again is due to the structure of the material and their insulation affect, not allowing the surface temperature to fluctuate extremely throughout the day.

In addition, it was found that there was no significant difference in the air temperature with respect to the change in the elevation after 3'. Regression analysis was completed to mathematically model the relationship between the different pavement parameters for each of the test sections and air temperature above the surface.

8.1.5 Pavement Near Surface Temperature and ASU Model Verification

Pavement temperature sensors indicated that PHMA has the highest near surface temperature during the day compared to HMA, PCC, and PPCC. However, it exhibits a lower night time temperature. The actual measured near surface temperature of PPCC, PHMA, and PCC were compared to the predicted values using the ASU pavement temperature model used in phase I. This model uses the weather information data and pavement material properties as the input to predict near surface temperature of the pavement. The predicted values although follow the same trend are a few degrees shifted form the actual values for the porous materials. It is important to note that this difference decreases as the depth increases. Based on the findings, the model may need to be adjusted when analyzing porous materials as it overestimates the heat captured near the surface during the day for such materials. Therefore, further analysis and validation are required.

8.2 RECOMMENDATIONS

Phase I of this study considered only hot weather scenarios in Phoenix, Arizona. Follow up studies should consider pavement temperature modeling for cooler climatic conditions. The pavement temperature modeling indicated that PHMA has a higher daytime surface temperature, which may be beneficial in cold weather climates. In addition, the literature indicated that the subgrade temperatures under porous pavements may remain warmer later into the fall season due to the insulating effect of this material. These effects should further evaluated in subsequent studies.

Future research should be conducted to develop additional thermal and physical properties of PHMA or HMA mixtures to better capture the range of data variations for the different mixes. Research should be also directed to further study the effects of aggregates and subgrade material properties on pavement surface temperatures. The moisture content, mineral content and evapotranspiration will play a significant role in the thermal behavior of porous asphalt pavements and should be considered in future analysis.

Phase II of this study considered only the weather scenarios during September through November in Phoenix, Arizona. The near surface air temperature analysis suggested that there is no significant difference between 3' and 5' level air temperature, indicating that the air temperature reaches an equilibrium at a lower elevation, below 3'. The near surface pavement temperature measurement suggested that the PHMA could be the coolest or the warmest during the night, depending on the environmental factors. Follow up studies should consider near surface air temperature and near surface pavement temperature modeling for year round climatic conditions. In addition, future

study should consider analyzing air temperature and humidity data below 3' during different seasons. Such data can then be used to re-evaluate the regression model that was reported in this study.

It is important to note that the rain measurement was not significant during the study period, and thus it was not considered for this statistical analysis. Literature reviews suggested that the porous materials such as PHMA and PPCC would result in lower air temperature during wet-conditions that corresponds to lower energy consumption of the adjacent buildings. Future studies should focus on the effect of rain on the pavement temperature, near surface air temperature and its effect on the adjacent buildings energy consumptions. Also, in this study wind was measured only at one level. In future studies wind measurement should also be conducted at different levels to investigate the effect of wind circulation on near surface air temperature.

Based on the finding of this study, the UHI mitigation process is definitely complex and needs to be inclusive of many pavement properties and climatic conditions. The best approach for identifying the best methods to mitigate the urban heat island effect is a well-balanced design that considers all of the factors discussed in this study.

REFERENCE

1. Barnes K., Morgan J., Roberge M. (2001). "Impervious Surfaces and the Quality of Natural and Built Environment", Department of Geography and Environmental Planning, Towson University, Baltimore, Maryland.

2. Oke T.R. (1987) Boundary Layer Climate, 2nd edition, Routledge, London.

3. Rosenfeld A.H., Akbari H., Bretz S., Fishman B.L., Kurn D.M., Sailor D., & Taha H. (1995). "Mitigation of urban heat islands: materials, utility programs, updates," Energy and Buildings, Vol. 22, pp. 255 – 265.

4. EPA, U. *Green Infrastructure Programs*. 2010 [cited 2011 Mar.10]; Available from: http://cfpub.epa.gov/npdes/greeninfrastructure/gicasestudies.cfm.

5. Navigant Consulting Inc., B.T.P., *Building Technologies Program, Assessment of International Urban Heat Island Research - Literature Review of International Studies on Urban Heat Island Countermeasures. Draft Report,* 2011, Office of Energy Efficiency and Renewable Energy: USDOE: Washington, DC.

6. Haselbach, L., Boyer, M., Kevern, J., and Schaefer, V., (2011). Cyclic Heat Impacts in Traditional versus Pervious Concrete Pavement Systems. Proceedings of the 90th Annual Meeting of the Transportation Research Board, Transportation Research Board of the National Academies, Washington DC.

7. Stempihar, J., Pourshams-Manzouri, T., Kaloush., K., and Rodezno, M., (2012). Porous Asphalt Pavement Temperature Effects on Overall Urban Heat Island. Proceeding of the 91st Annual Meeting of the Transportation Research Board, Transportation Research Board of National Academies, Washington DC.

8. Haselbach, Liv. (2009) Pervious Concrete and Mitigation of the Urban Heat Island Effect, Proceedings; *Transportation Research Board Annual Meeting*, Transportation Research Board of the National Academies, Washington DC.

9. Taha, H. (1997) Urban Climates and Heat Islands: Albedo, Evapotranspiration and Anthropogenic Heat. Energy and Buildings, 25 (2), 99-103.

10. Liu, Q., Schlangen, E., Van de Ven, M., Garcia, A. (2010). "Healing of porous asphalt concrete via induction heating." *Road Materials and Pavement Design.* 11, 527-542.

11. National Asphalt Pavement Association (NAPA) (2008); Porous Asphalt Pavements for Stormwater Management, Design and Construction Maintenance Guide. Information Series 131.

12. Lin, Q., and D. Cao. Research on Material Composition and Performance of Porous Asphalt Pavement. *Journal of Materials in Civil Engineering*, Vol. 21, 2009, pp. 135-140.

13. Tan, S. A., Fwa, T.F. and Guwe, V.Y.K. "Laboratory Measurements and analysis of clogging mechanisms of porous asphalt mixes." *Journal of Testing Materials and Evaluations.* 28, 207-216.

14. Rose, L., H. Akbari, and H. Taha (2003), "Characterizing the Fabric of Urban Environment: A Case Study of Metropolitan Houston, Texas," Lawrence Berkeley National Laboratory, LBNL-51448.

15. Cahill, T., M. Adams, and M. Courtney (2005), "Stormwater Management with Porous Pavements," Government Engineering, 14.

16. Kandhal, P.S.. Asphalt pavements mitigate tire/pavement noise. Hot Mix Asphalt Technology, 2004. http://www.flexiblepavements.org/images/kandhalnoiseart.pdf.

17. Kevern, John T., V. Schaefer, and K. Wang. (2009) Temperature Behavior of a Pervious Concrete System, Proceedings; *Transportation Research Board Annual Meeting*, Transportation Research Board of the National Academies, Washington DC.

18. Kevern, J. (2006), Mix Design Development for Pervious Concrete in Cold Weather Climates, Proceedings; *Transportation Research Board Annual Meeting*, Transportation Research Board of the National Academies, Washington DC.

19. Incropera, F. and DeWitt, D. (1996). Fundamentals of Heat and Mass Transfer, 4th edition. John Wiley & Sons, Inc., New York.

20. Pommerantz, M., Pon, B., Akbari, H. and Chang, S-C. (2000). The Effect of Pavement's Temperatures on Air Temperatures in Large Cities. Berkeley, CA: Lawerence Berkeley National Laboratory, LBNL-43442.

21. Cahill, T., M. Adams, and C. Marm. (2003). Porous asphalt: The right choice for porous pavements. Hot Mix Asphalt Technology, September/October: 26-40.

22. Somayaji, S. (2001). Civil Engineering Materials. Prentice Hall, NJ.

23. Zalba, B., Marín, J. M., Cabeza, L. F., and Mehling, H. (2003). Review on thermal energy storage with phase change: materials, heat transfer analysis and applications. *Applied thermal engineering*, *23*(3), 251-283.

24. Gui, J., Phelan, P.E., Kaloush, K. E., and Golden, J. S. (2007). Impact of Pavement Thermophysical Properties on Surface Temperatures. Journal of Materials in Civil Engineering, 19(8), 683-690

25. Hedquis, B. (2010). Microscale Evaluation of the Urban Heat Island in Phoenix, Arizona. A Dissertation (PHD) Arizona State University.

26. Al-Tamimi, N. A., and Fadzil, S. F. S. (2011). The Potential of Shading Devices for Temperature Reduction in High-Rise Residential Buildings in the Tropics. *Procedia Engineering*, *21*, 273-282.

27. Li, H., Harvey, J., and Jones, D. (2012). Cooling Effect of Permeable Asphalt Pavement under Both Dry and Wet Conditions, Proceedings; *Transportation Research Board Annual Meeting*, Transportation Research Board of the National Academies, Washington DC. TRB #13-1115.

28. Wang, ZH, Bou-Zeid, E and Smith, JA, 2011, A spatially-analytical scheme for surface temperatures and conductive heat fluxes in urban canopy models,*Boundary-Layer Meteorology*, 138:171-193.

29. Wang, ZH, Bou-Zeid, E and Smith, JA. (2013). A coupled energy transport and hydrological model for urban canopies evaluated using a wireless sensor network,*Quarterly Journal of the Royal Meteorological Society*, DOI:10.1002/qj.2032.

30. Carlson, J., Bhardwaj, R., Phelan, P., Kaloush, K and Golden, J.S. (2010). "Determining Thermal Conductivity of Paving Materials Using Cylindrical Sample Geometry". ASCE Journal of Materials in Civil Engineering, 22 (2) 186-195.

31. Kaloush, K., Carlson, J., Golden, J. and Phelan, P. (2008). The Thermal and Radiative Characteristics of Concrete Pavements in Mitigating Urban Heat Island Effects. ASU National Center of Excellence. Final Report Submitted to American Concrete Paving Association.

32. Belshe, M., Kaloush, K., Golden, J and Mamlouk, M. (2008). The Urban Heat Island Effect and Impact of Asphalt Rubber Friction Course Overlays on Portland Cement Concrete Pavements in the Phoenix Area. *In ASCE Conference, GeoCongress2008: Geosustainability and GeoHazard Mitigation* (GSP 178), Vol. 310, No. 129, 2008.

33. National Asphalt Pavement Association. Porous Asphalt Pavement, National Asphalt Pavement Association, Lanham Maryland, (2003).

34. Somayaji, S.. Civil Engineering Materials. (2001). Prentice Hall, New Jersey.

35. Nakayama T., and Fujita, T. (2010). Cooling Effect of Water-holding Pavements Made of New Materials on Water and Heat Budgets in Urban Areas*, Landscape and Urban Planning*, Vol. 96, pp. 57–67.

36. Highter, W. H., and Wall, D. J.. (1984). Thermal Properties of Some Asphaltic Concrete Mixes. In *Transportation Research Record: Journal of the Transportation Research Board,* No. 968, Transportation Research Board of the National Academies, Washington, D.C., pp. 38–45.

37. Luca, J., & Mrawira, D. (2005). New Measurement of Thermal Properties of Superpave Asphalt Concrete. *Journal of Materials in Civil Engineering*, Vol.17, No.1, pp. 72-79.

38. American Concrete Paving Association. Albedo: A Measure of Pavement Surface Reflectance. R&T Update, Concrete Pavement Research and Technology, No. 3.05, 2002. Accessed at: *www.pavement.com/Downloads/RT/RT3.05.pdf*

39. Corlew, J.S., and P.F. Dickson. Methods for Calculating Temperature Profiles of Hot-Mix Asphalt Concrete as Related to the Construction of Asphalt Pavements, *In Asphalt Paving Technology: Association of Asphalt Paving Technologists Technical Sessions*, Vol. 37, 1968, pp. 101-140.

40. Wolfe, R. K., Heath, G. L., and D. C. Colony. University of Toledo Time–Temperature Model Laboratory Field Validation. Publication FHWA-OH-80-006, FHWA, U.S. Department of Transportation, 1980.

41. Calson, J., Kaloush, K. et al.. Evaluation of In Situ Temperatures, Water Infiltration and Regional Feasibility of Pervious Concrete Pavements. *International Journal of Pavements*, Vol. 7, No. 1-2-3, 2006, pp. 1-13.

42. Asaeda, T. Ca, and V. T.. Characteristics of Permeable Pavement During Hot Summer Weather and Impact on the Thermal Environment; *Building and Environment*, Vol. 35, 2000, pp. 363-375.

43. JFE Steel Corporation. Experimental Data of Performance Test of Water-Holding Block, 2006.

44. Andersland, O. Frozen Ground Engineering, 2nd Edition. John Wiley & Sons, Inc., Hoboken, New Jersey, 2004.

45. Montgomery, D. C. (2008). Design and analysis of experiments. Wiley.

46. Montgomery, D. C., Peck, E. A., and Vining, G. G. (2012). Introduction to linear regression analysis, Wiley, Vol. 821.

APPENDIX A

HOURLY ALBEDO MEASUREMENTS:
PCC
PPCC
HMA
PHMA
GRAVEL
TURF

Hourly albedo measurements

PCC

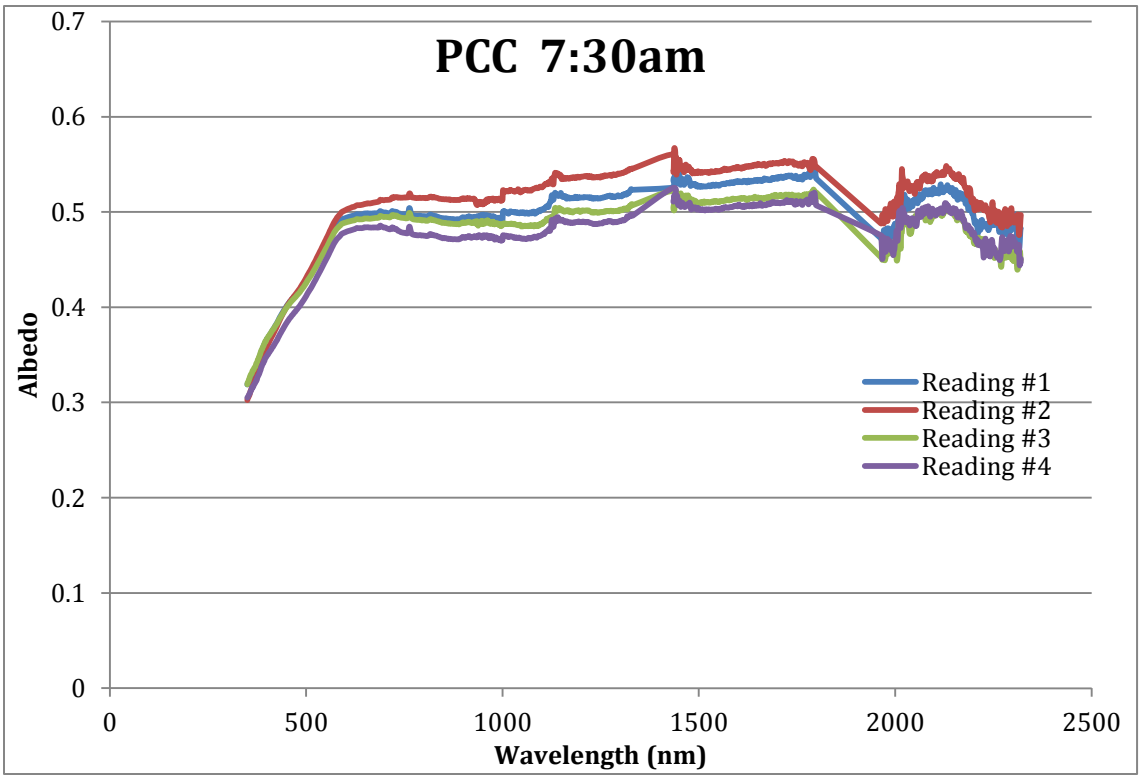

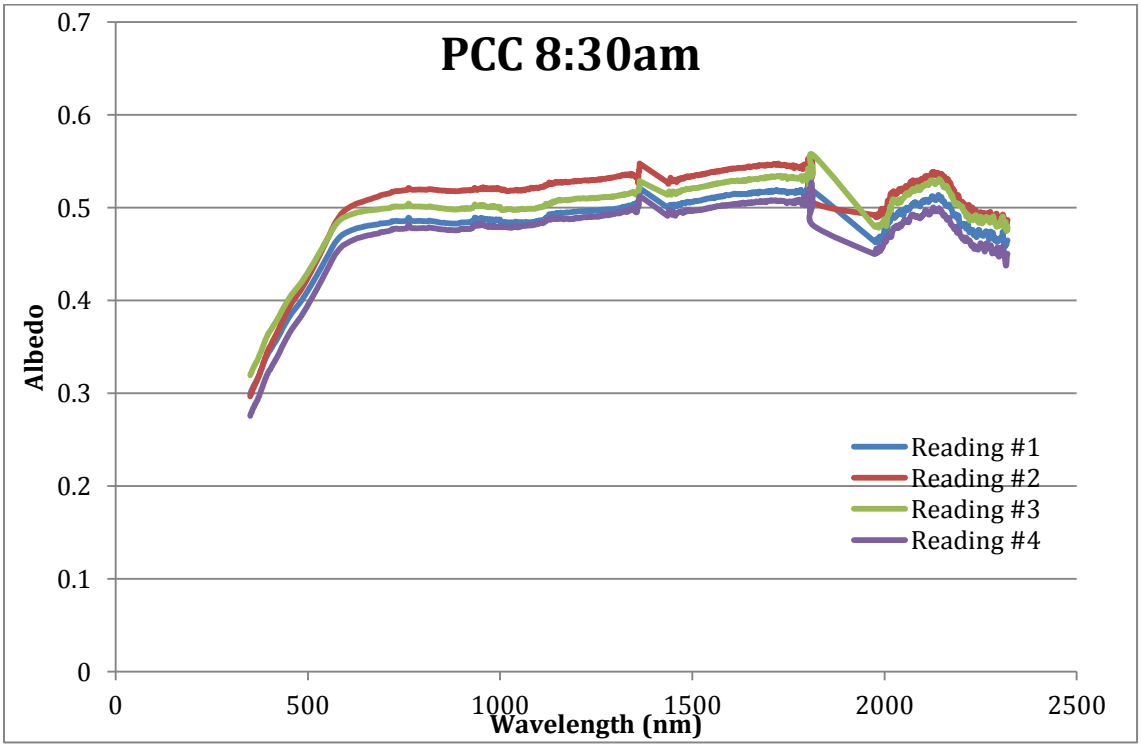

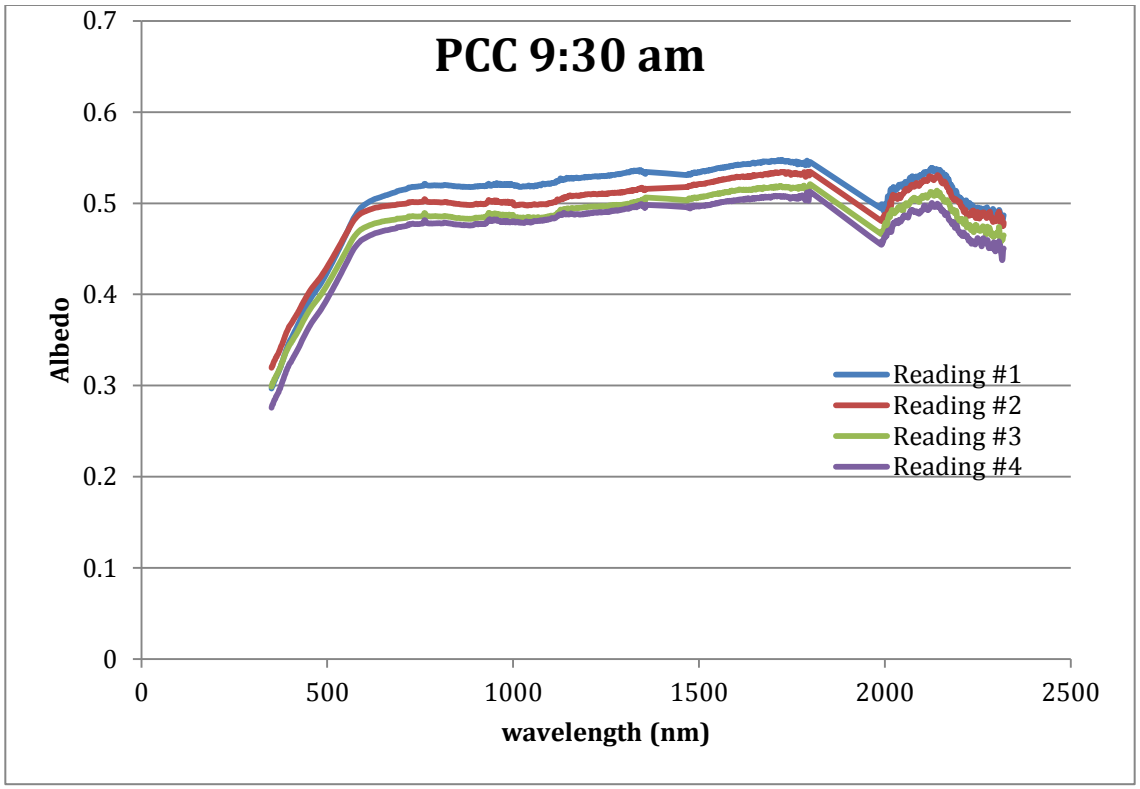
PCC 9:30 am
Albedo
0.7
0.6
0.5
0.4
0.3
0.2
0.1
0
0
500
1000
1500
2000
2500
wavelength (nm)
Reading #1
Reading #2
Reading #3
Reading #4

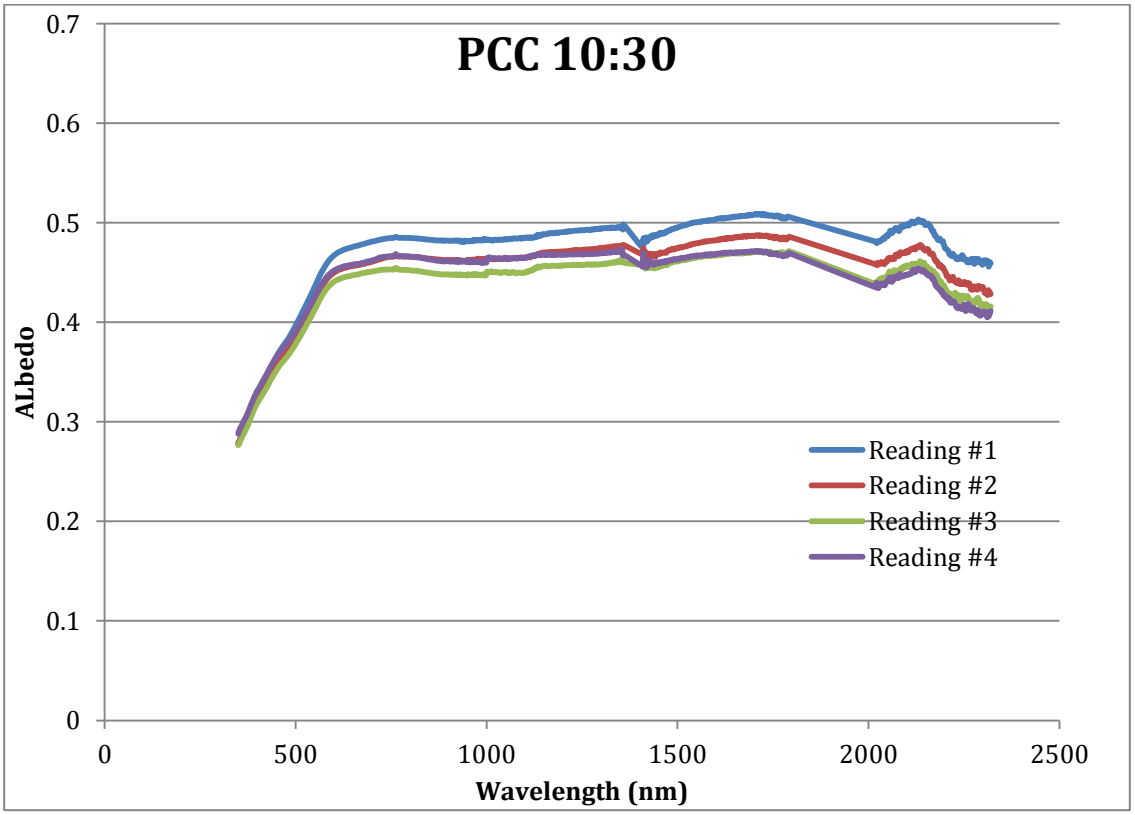
PCC 10:30
ALbedo
0.7
0.6
0.5
0.4
0.3
0.2
0.1
0
0
500
1000
1500
2000
2500
Wavelength (nm)
Reading #1
Reading #2
Reading #3
Reading #4

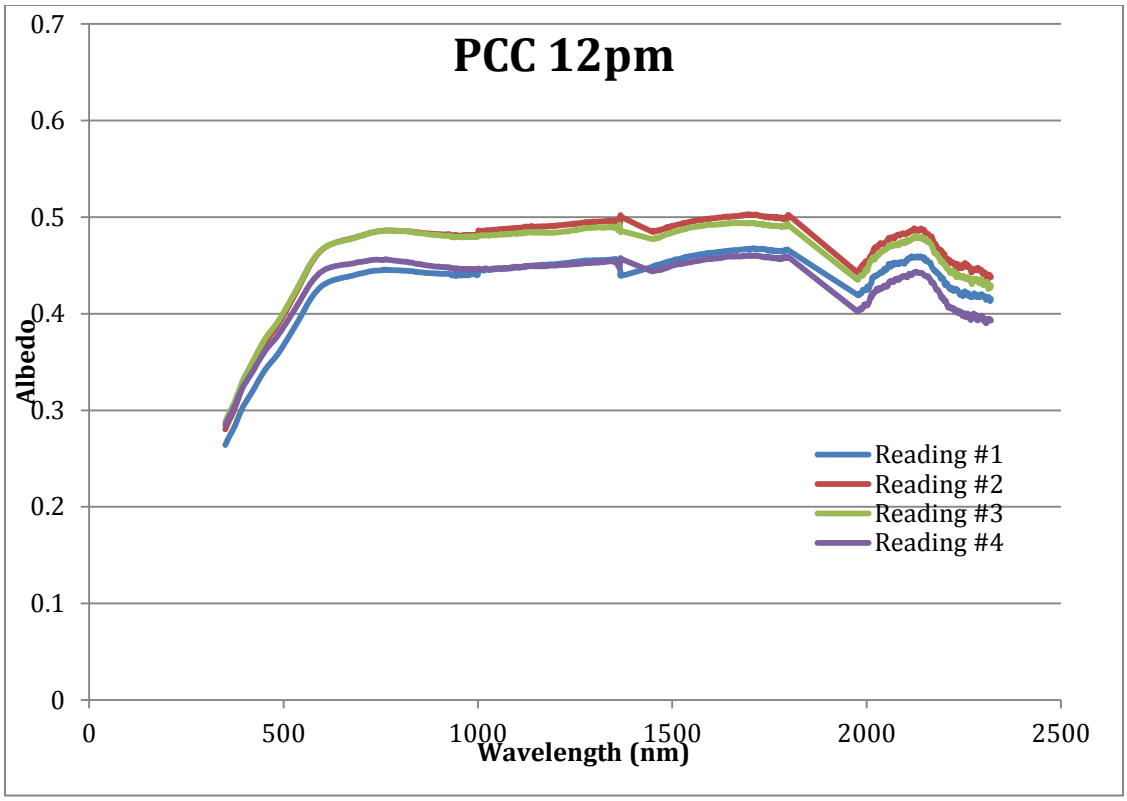
PCC 12pm
Albedo
0.7
0.6
0.5
0.4
0.3
0.2
0.1
0
0
500
1000
1500
2000
2500
Wavelength (nm)
Reading #1
Reading #2
Reading #3
Reading #4

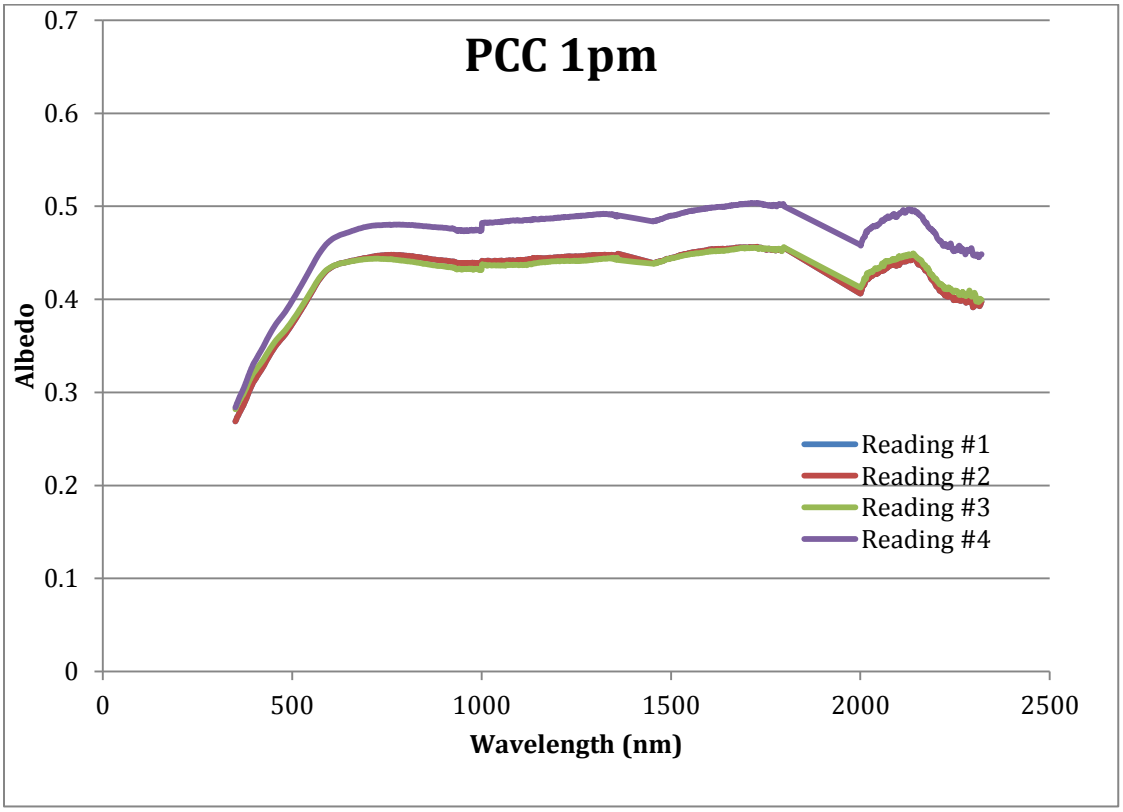
PCC 1pm
Albedo
0.7
0.6
0.5
0.4
0.3
0.2
0.1
0
0
500
1000
1500
2000
2500
Wavelength (nm)
Reading #1
Reading #2
Reading #3
Reading #4

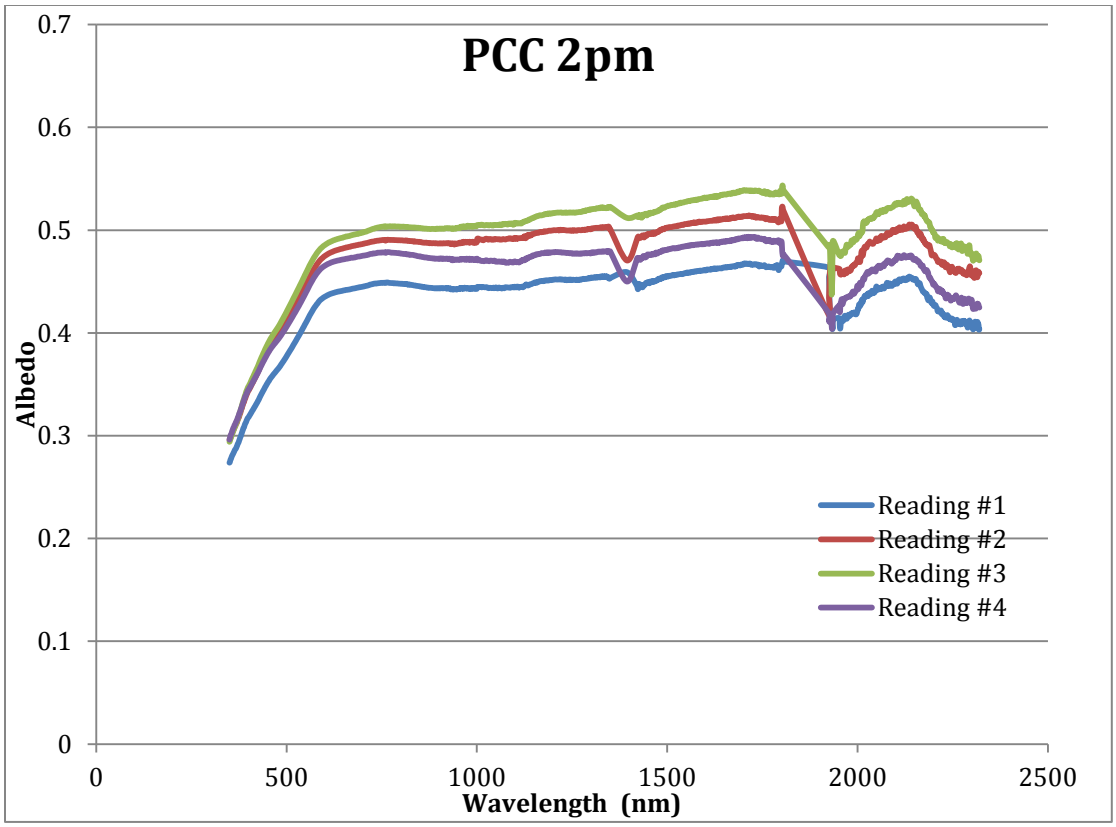
PCC 2pm
Albedo
0.7
0.6
0.5
0.4
0.3
0.2
0.1
0
0
500
1000
1500
2000
2500
Wavelength (nm)
Reading #1
Reading #2
Reading #3
Reading #4

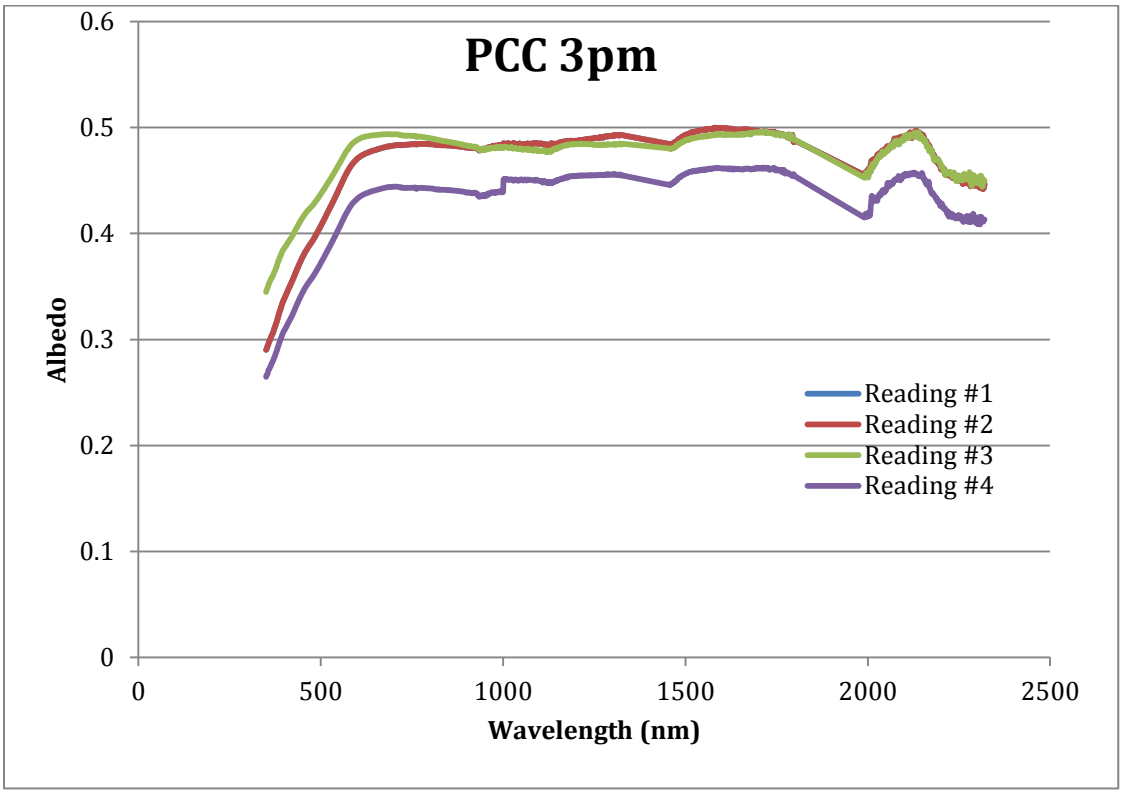
PCC 3pm
Albedo
0.6
0.5
0.4
0.3
0.2
0.1
0
0
500
1000
1500
2000
2500
Wavelength (nm)
Reading #1
Reading #2
Reading #3
Reading #4

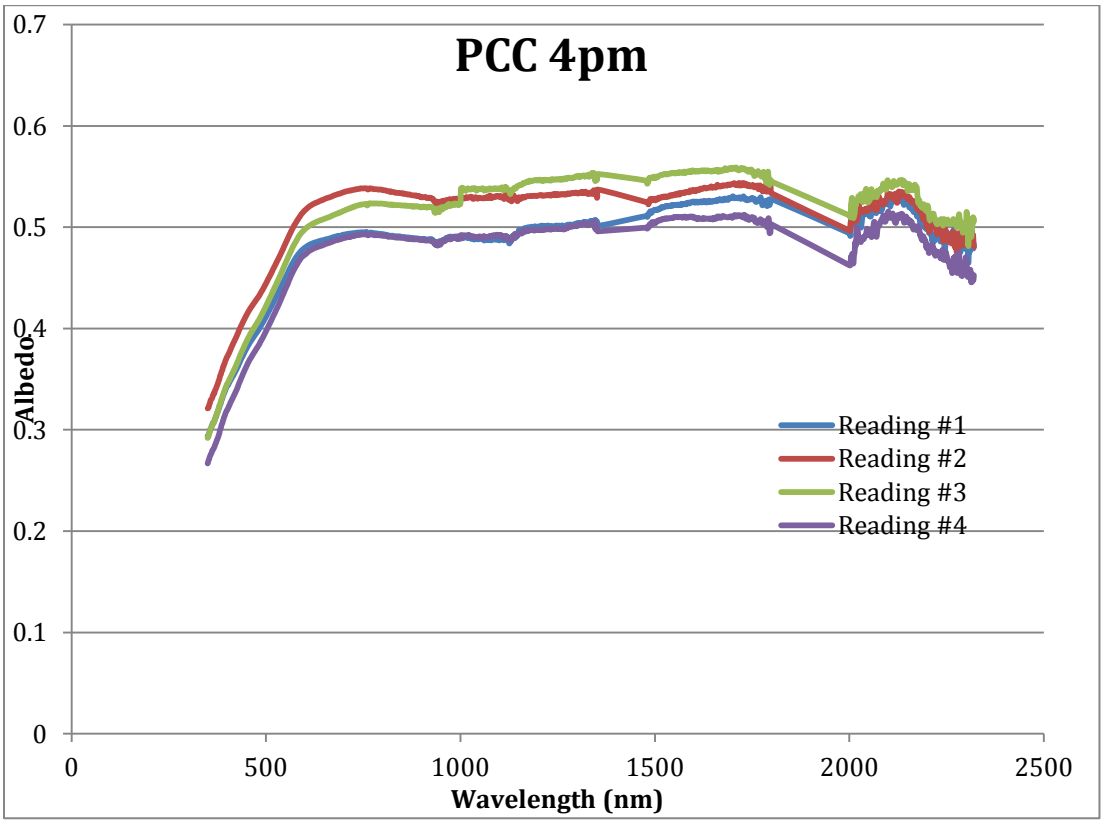
PCC 4pm
0.7
0.6
0.5
0.4
0.3
0.2
0.1
0
Albedo
0
500
1000
1500
2000
2500
Wavelength (nm)
Reading #1
Reading #2
Reading #3
Reading #4

Turf

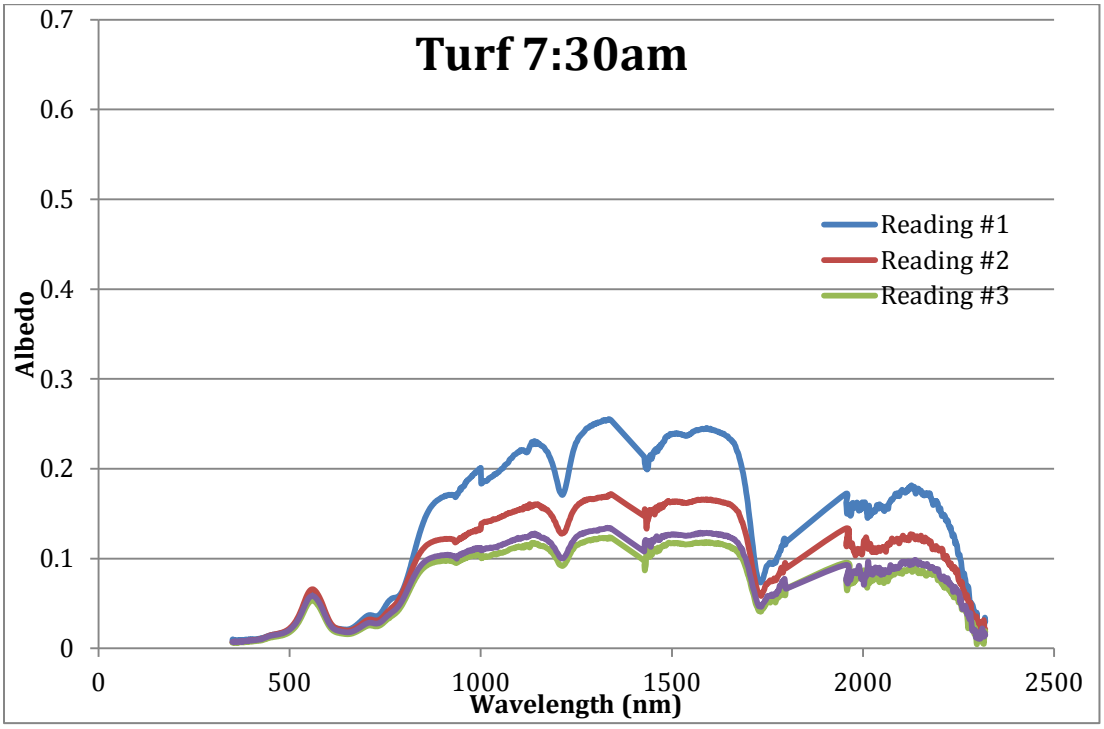
Turf 7:30am
Albedo
Wavelength (nm)
Reading #1
Reading #2
Reading #3
0.7
0.6
0.5
0.4
0.3
0.2
0.1
0
0
500
1000
1500
2000
2500

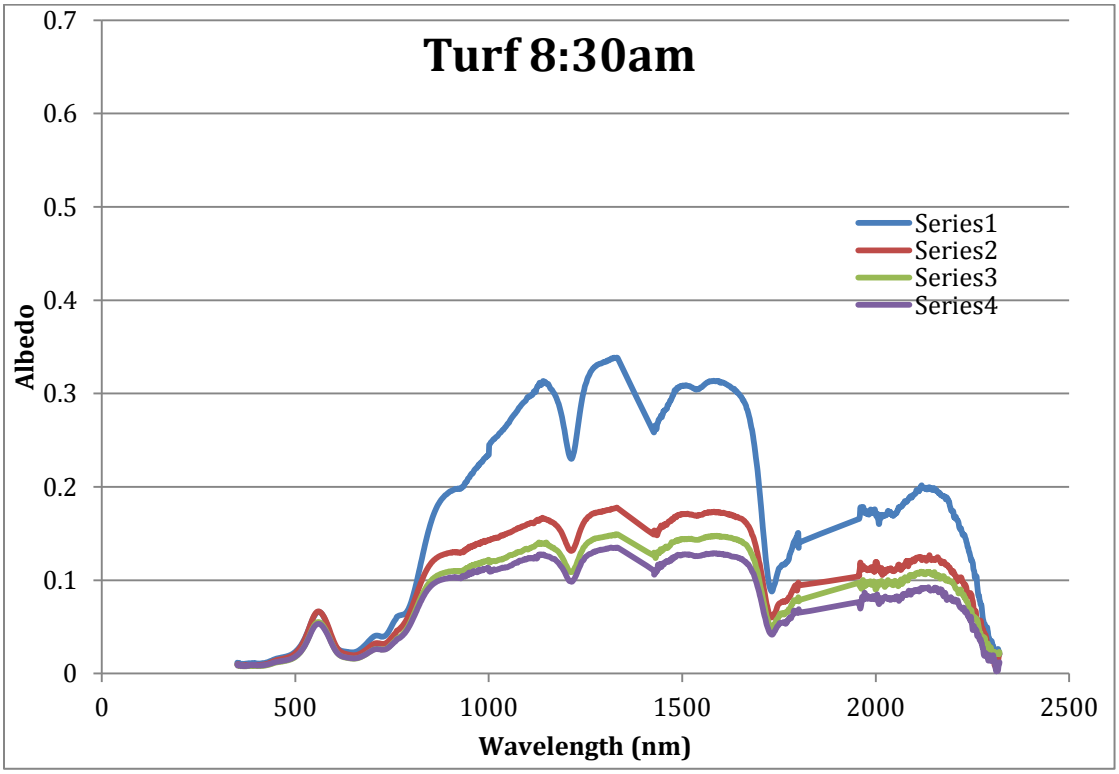
Turf 8:30am
Albedo
Wavelength (nm)
Series1
Series2
Series3
Series4
0.7
0.6
0.5
0.4
0.3
0.2
0.1
0
0
500
1000
1500
2000
2500

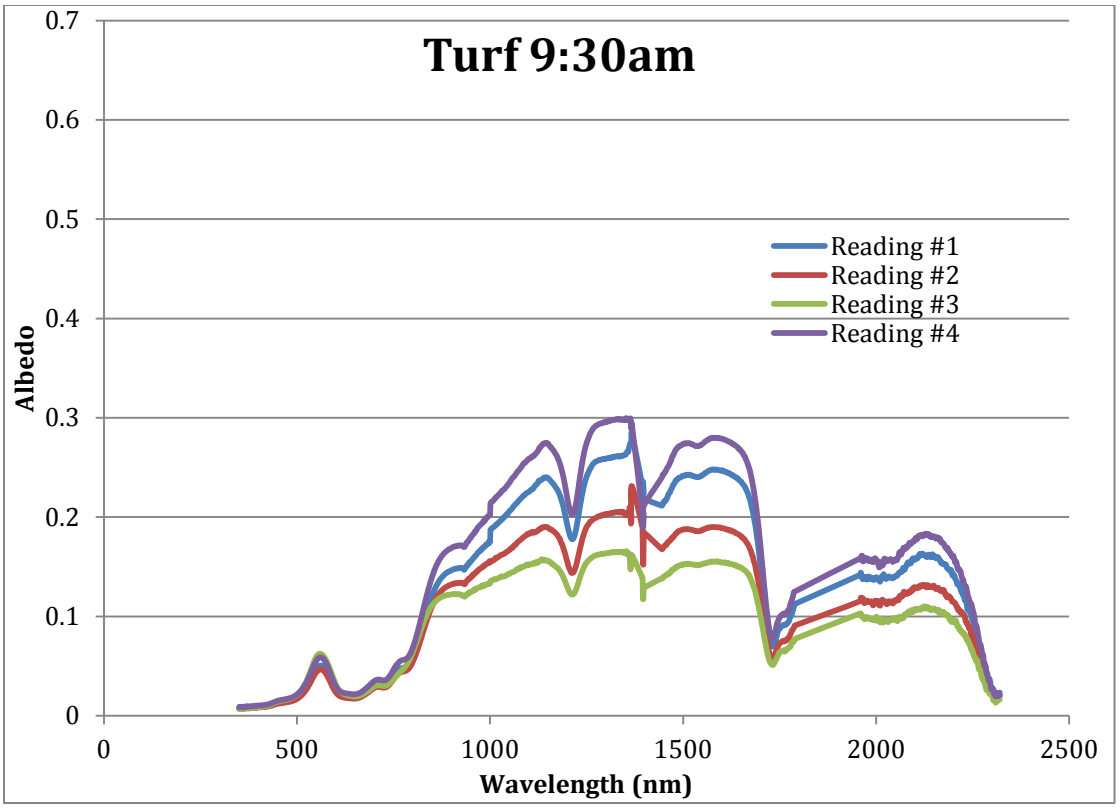
Turf 9:30am
Albedo
Wavelength (nm)
Reading #1
Reading #2
Reading #3
Reading #4
0.7
0.6
0.5
0.4
0.3
0.2
0.1
0
0
500
1000
1500
2000
2500

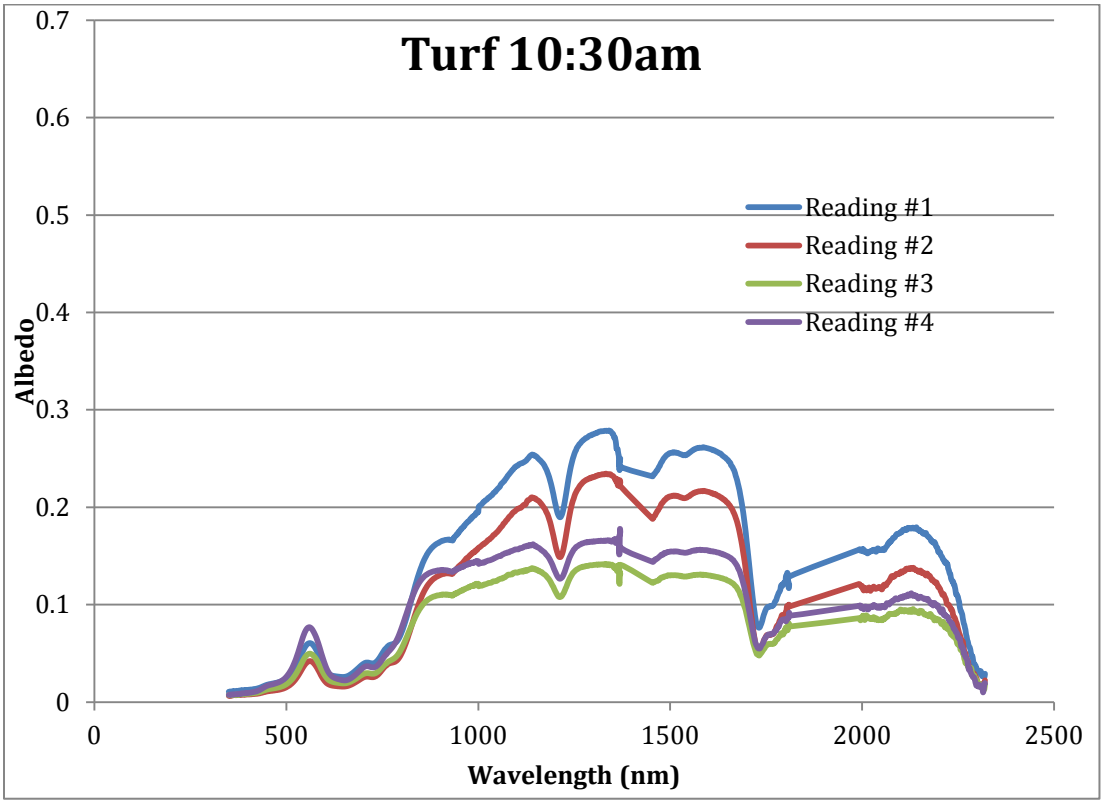
Turf 10:30am
Albedo
Wavelength (nm)
Reading #1
Reading #2
Reading #3
Reading #4
0.7
0.6
0.5
0.4
0.3
0.2
0.1
0
0
500
1000
1500
2000
2500

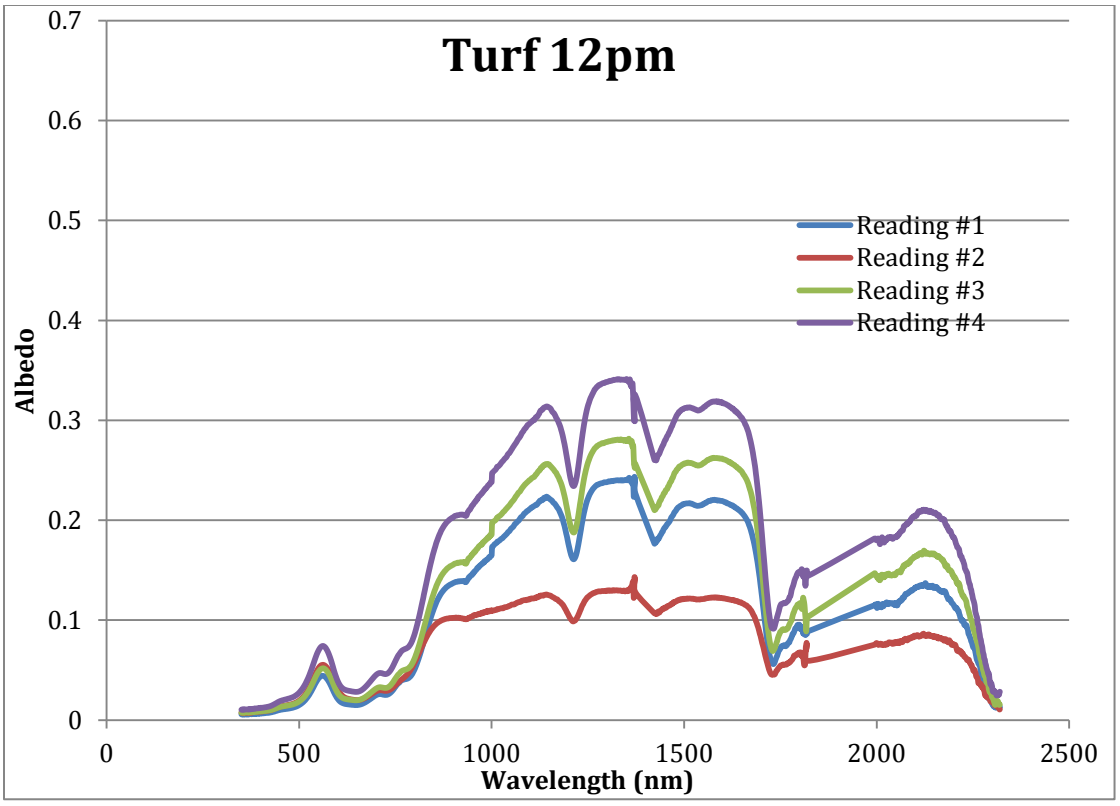
Turf 12pm
Albedo
Wavelength (nm)
Reading #1
Reading #2
Reading #3
Reading #4
0.7
0.6
0.5
0.4
0.3
0.2
0.1
0
0
500
1000
1500
2000
2500

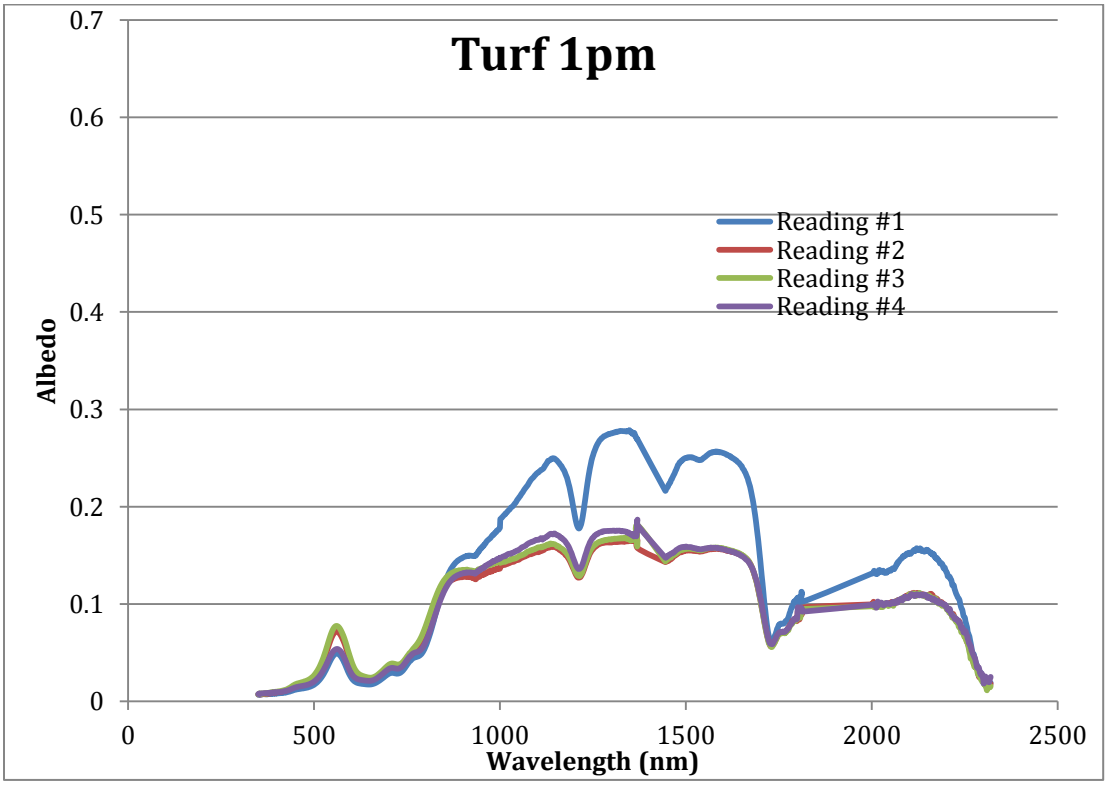
Turf 1pm
Albedo
Wavelength (nm)
Reading #1
Reading #2
Reading #3
Reading #4
0.7
0.6
0.5
0.4
0.3
0.2
0.1
0
0
500
1000
1500
2000
2500

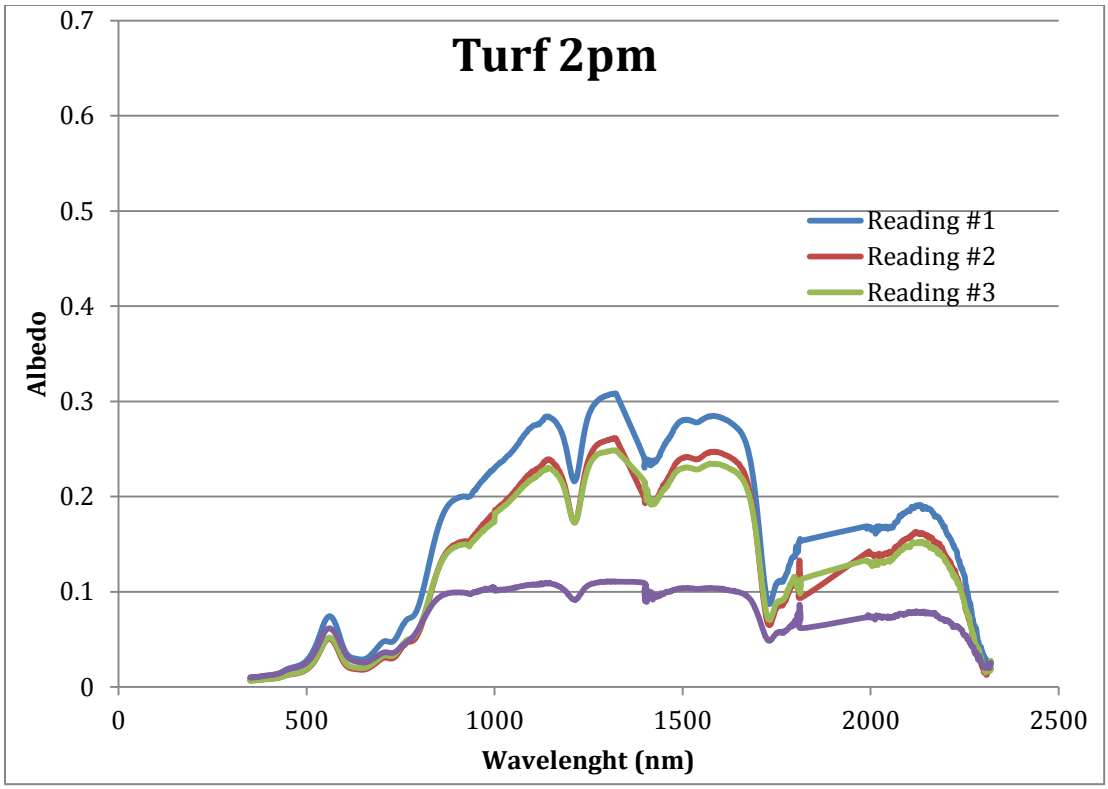
Turf 2pm
Albedo
0.7
0.6
0.5
0.4
0.3
0.2
0.1
0
0
500
1000
1500
2000
2500
Wavelenght (nm)
Reading #1
Reading #2
Reading #3

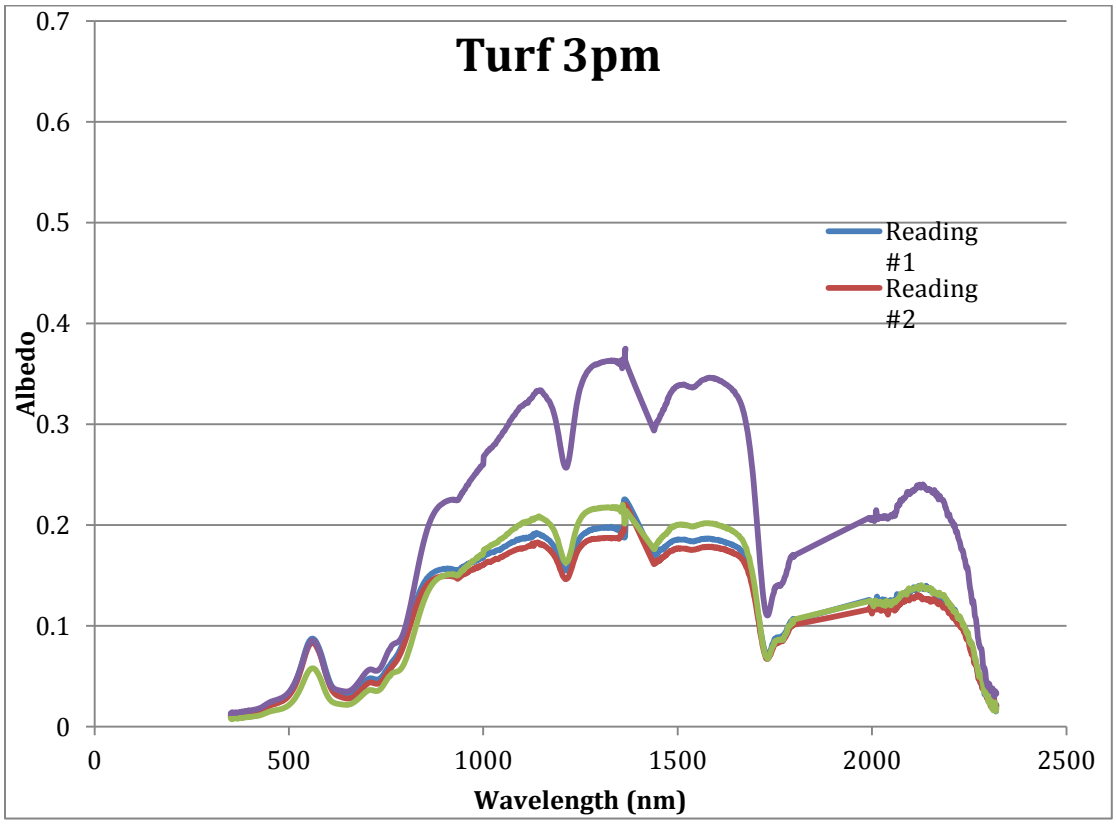
Turf 3pm
Albedo
0.7
0.6
0.5
0.4
0.3
0.2
0.1
0
0
500
1000
1500
2000
2500
Wavelength (nm)
Reading #1
Reading #2

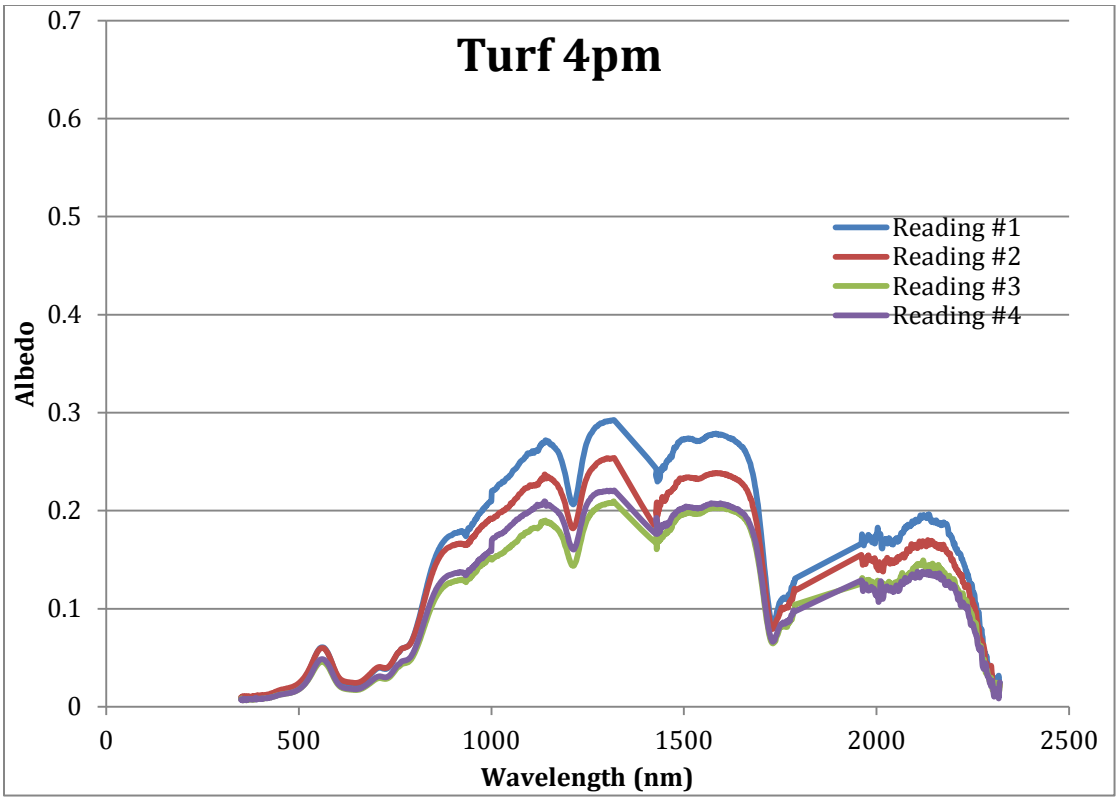
Turf 4pm
Albedo
0.7
0.6
0.5
0.4
0.3
0.2
0.1
0
0
500
1000
1500
2000
2500
Wavelength (nm)
Reading #1
Reading #2
Reading #3
Reading #4

Gravel

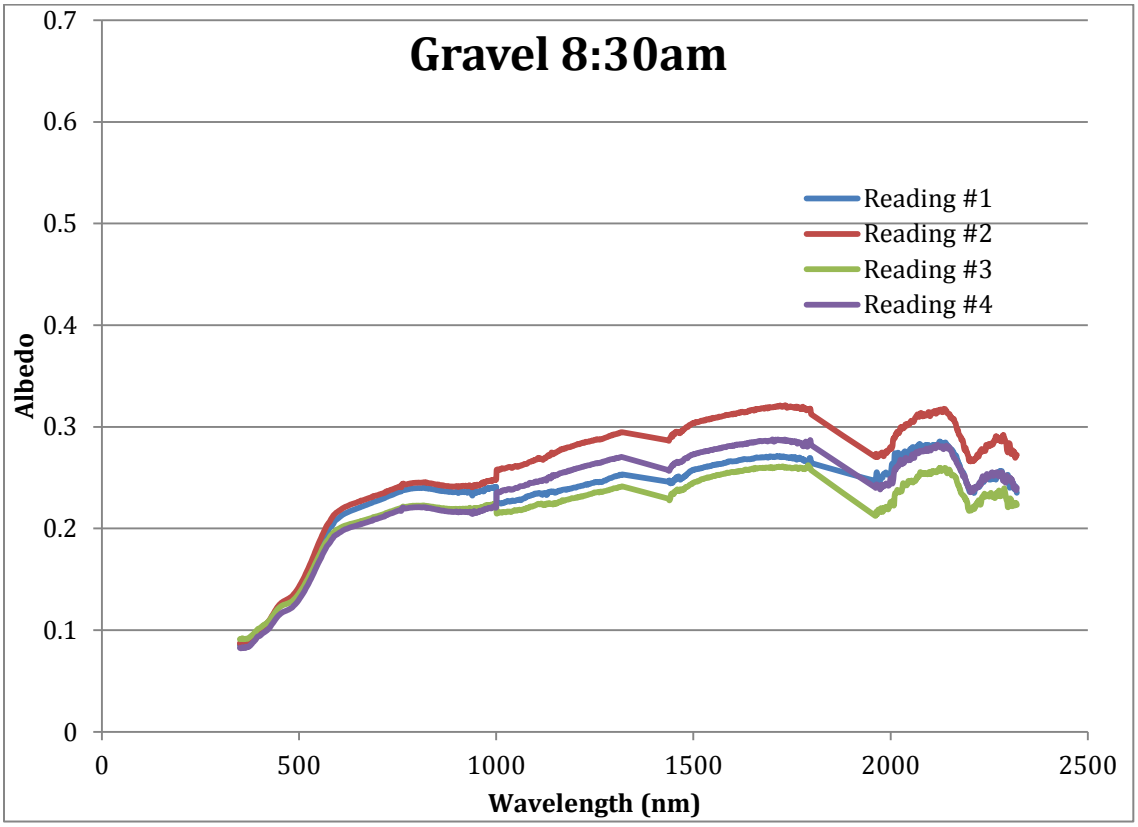
Gravel 8:30am
Albedo
Wavelength (nm)
Reading #1
Reading #2
Reading #3
Reading #4
0.7
0.6
0.5
0.4
0.3
0.2
0.1
0
0
500
1000
1500
2000
2500

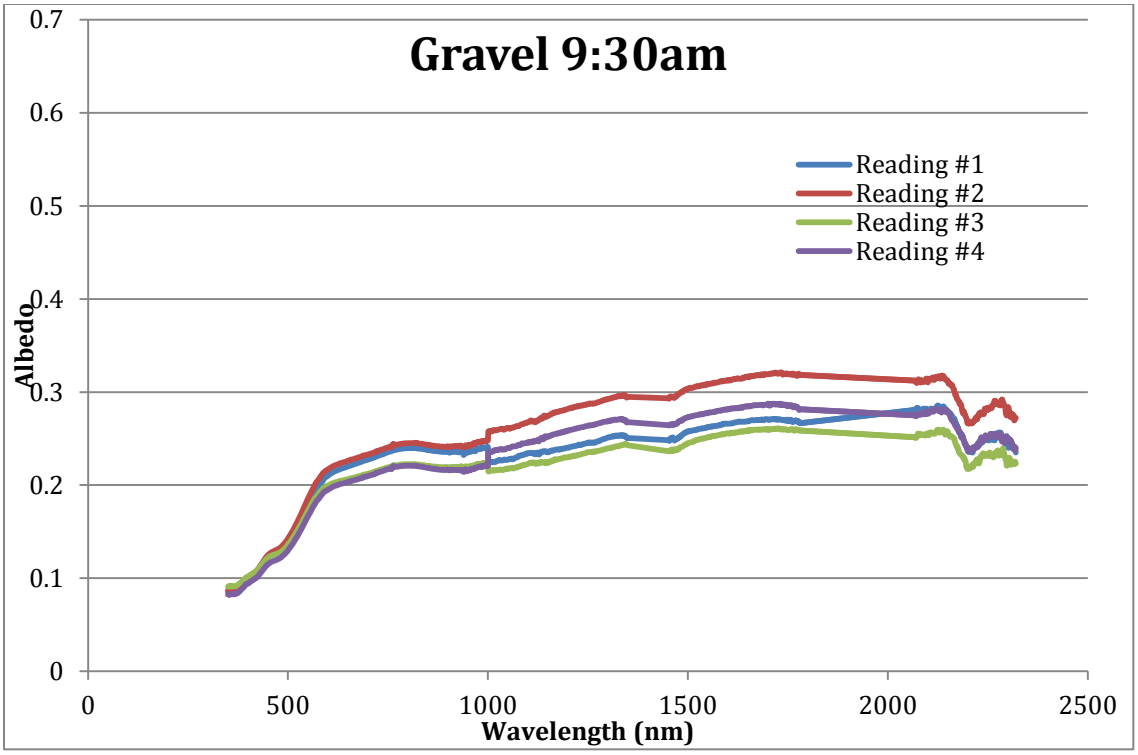
Gravel 9:30am
Albedo
Wavelength (nm)
Reading #1
Reading #2
Reading #3
Reading #4
0.7
0.6
0.5
0.4
0.3
0.2
0.1
0
0
500
1000
1500
2000
2500

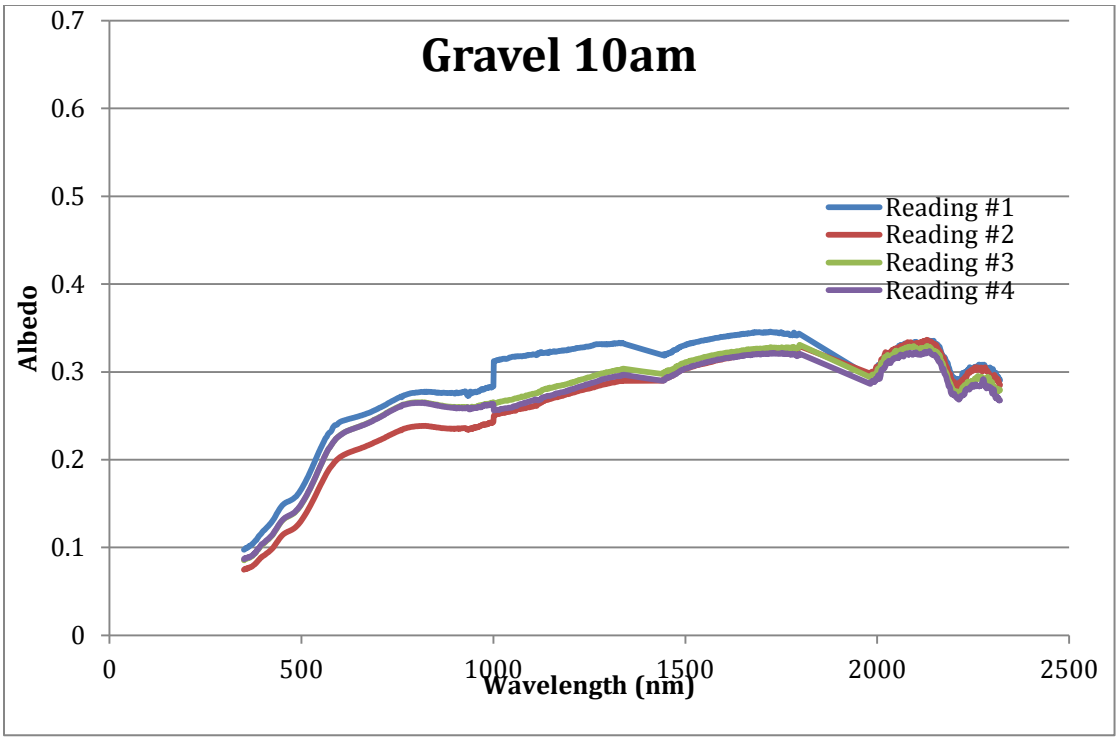
Gravel 10am
Albedo
Wavelength (nm)
Reading #1
Reading #2
Reading #3
Reading #4
0.7
0.6
0.5
0.4
0.3
0.2
0.1
0
0
500
1000
1500
2000
2500

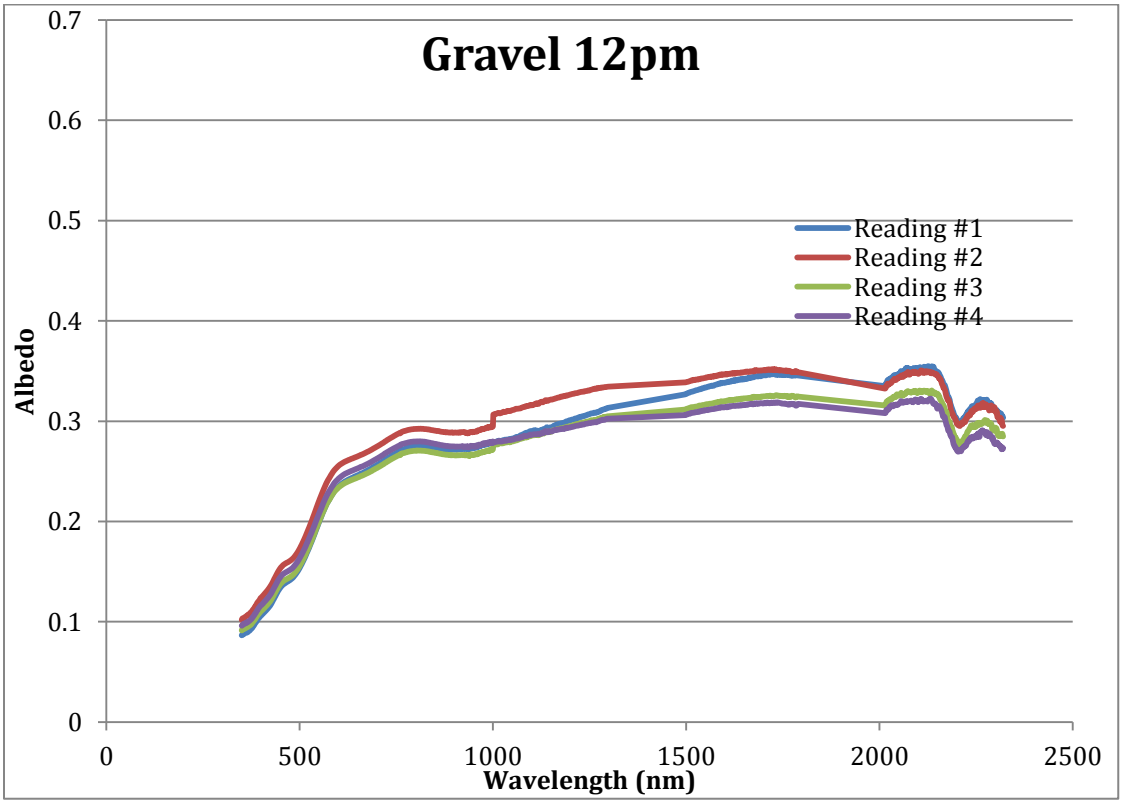
Gravel 12pm
Albedo
Wavelength (nm)
Reading #1
Reading #2
Reading #3
Reading #4
0.7
0.6
0.5
0.4
0.3
0.2
0.1
0
0
500
1000
1500
2000
2500

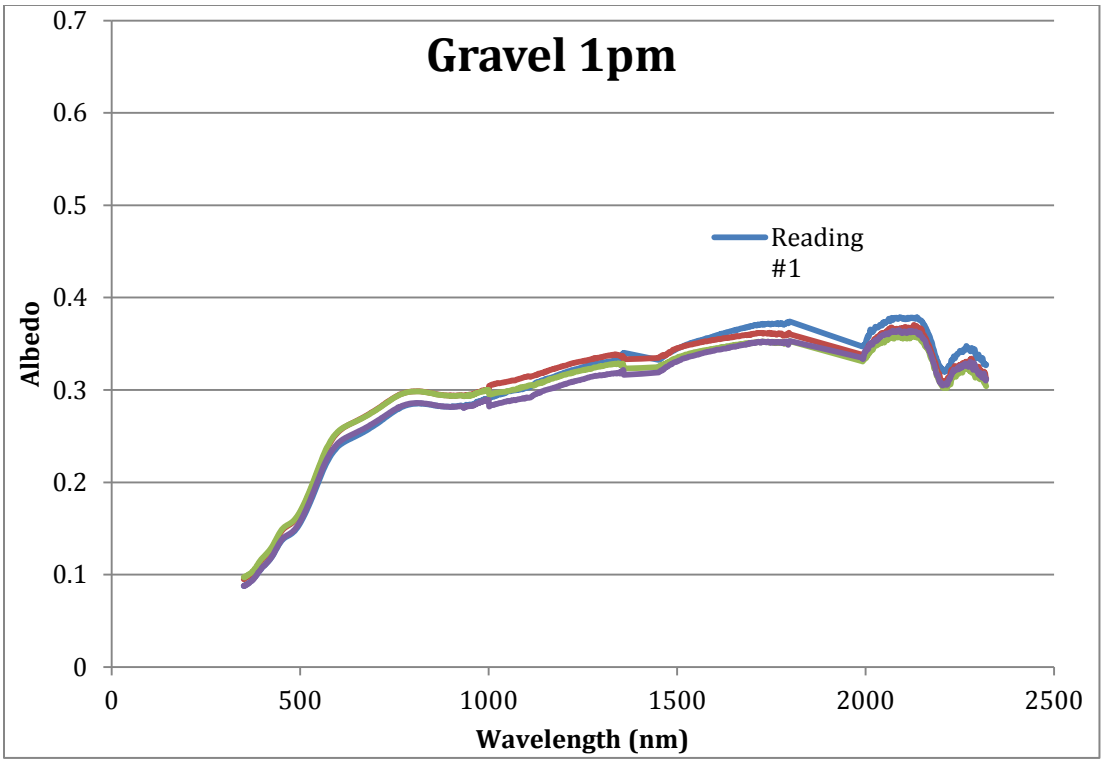
Gravel 1pm
Albedo
Wavelength (nm)
Reading #1
0.7
0.6
0.5
0.4
0.3
0.2
0.1
0
0
500
1000
1500
2000
2500

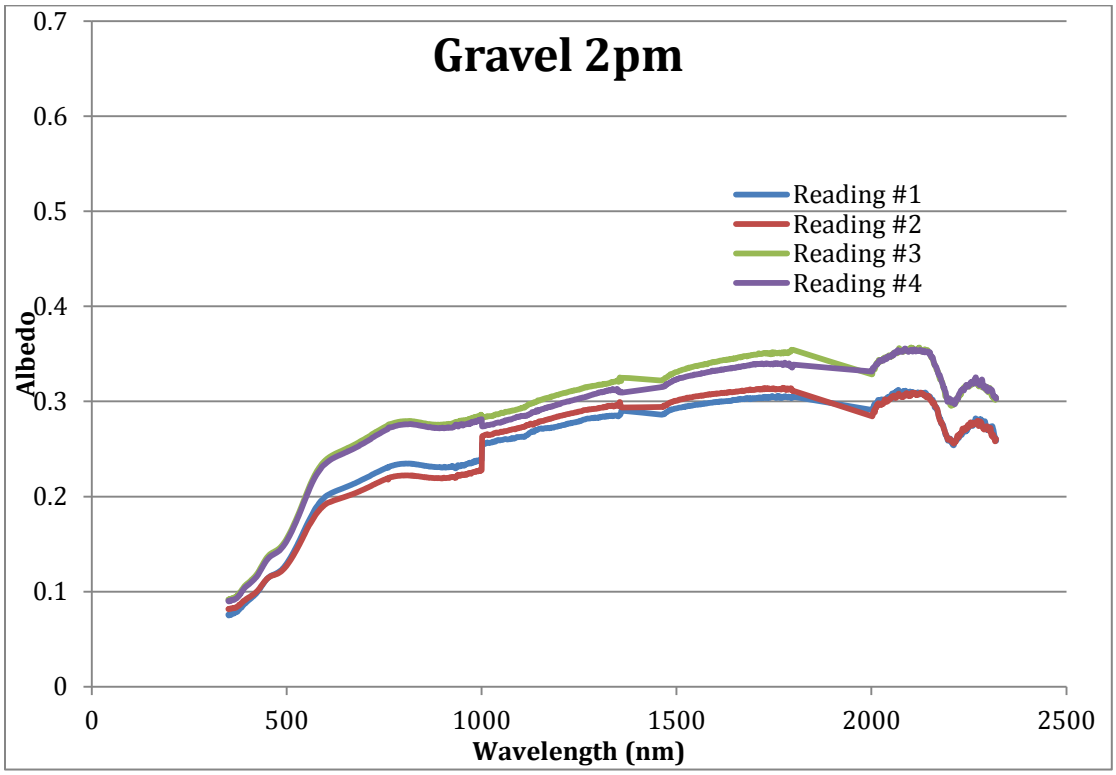
Gravel 2pm
Albedo
Wavelength (nm)
Reading #1
Reading #2
Reading #3
Reading #4
0.7
0.6
0.5
0.4
0.3
0.2
0.1
0
0
500
1000
1500
2000
2500

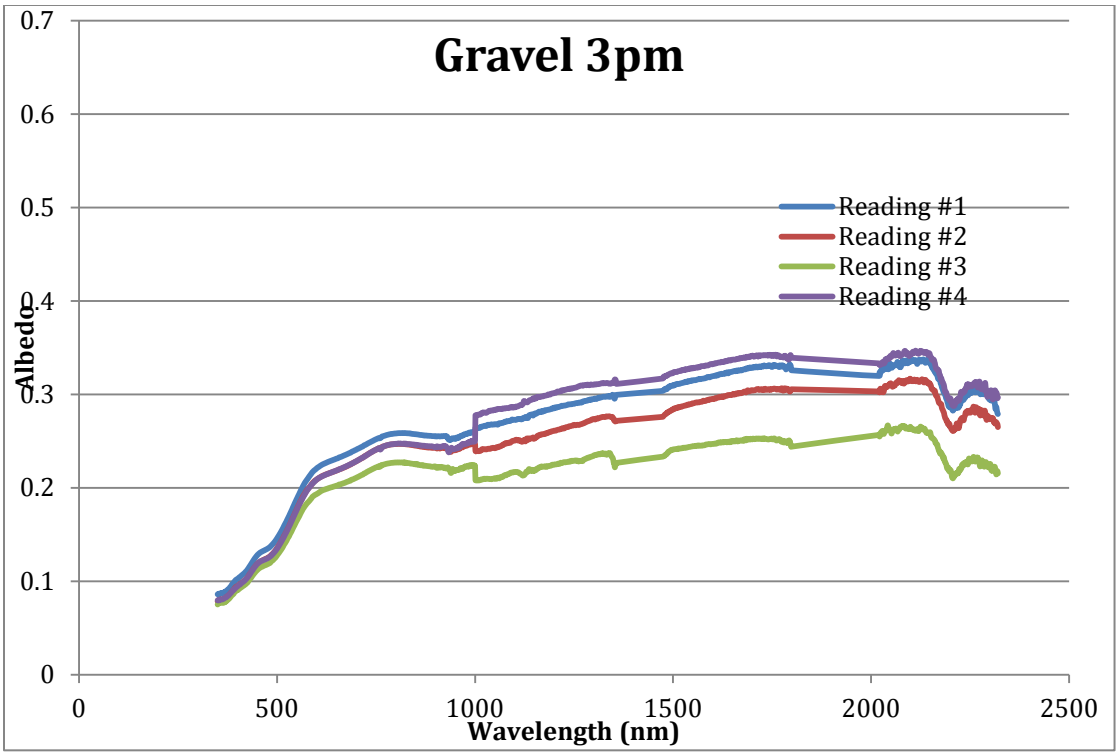
Gravel 3pm
Albedo
Wavelength (nm)
Reading #1
Reading #2
Reading #3
Reading #4
0.7
0.6
0.5
0.4
0.3
0.2
0.1
0
0
500
1000
1500
2000
2500

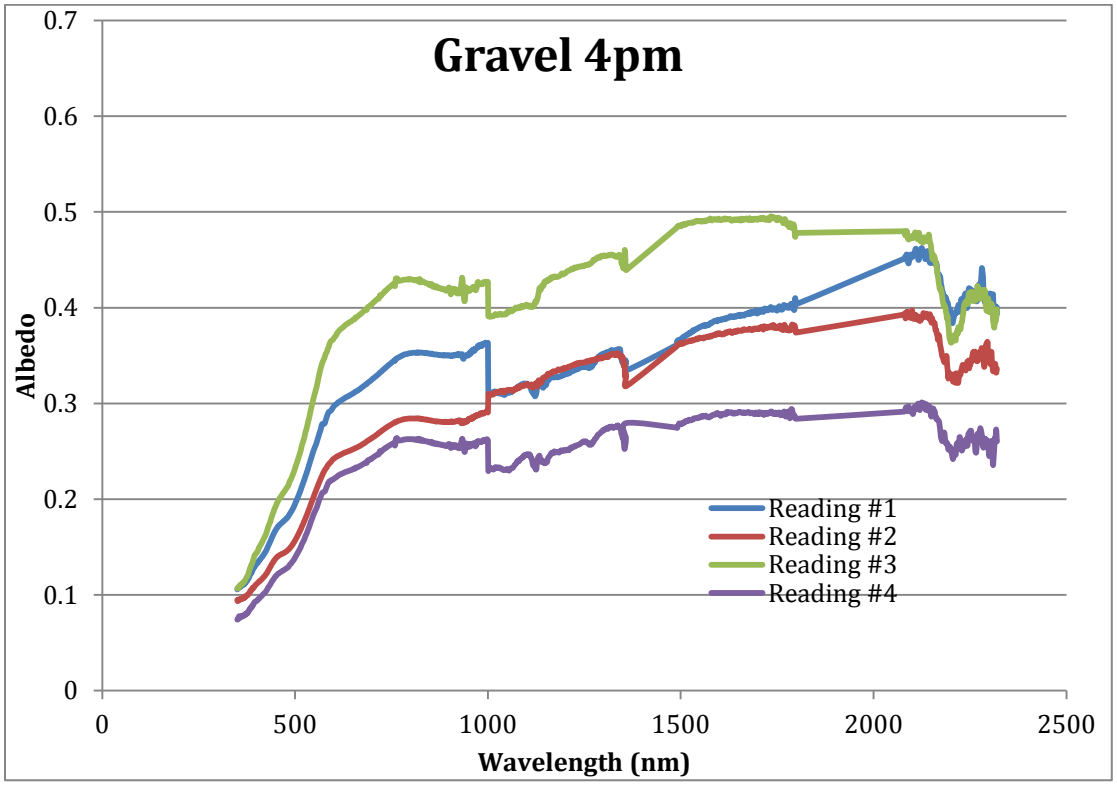
Gravel 4pm
Albedo
Wavelength (nm)
Reading #1
Reading #2
Reading #3
Reading #4
0.7
0.6
0.5
0.4
0.3
0.2
0.1
0
0
500
1000
1500
2000
2500

HMA

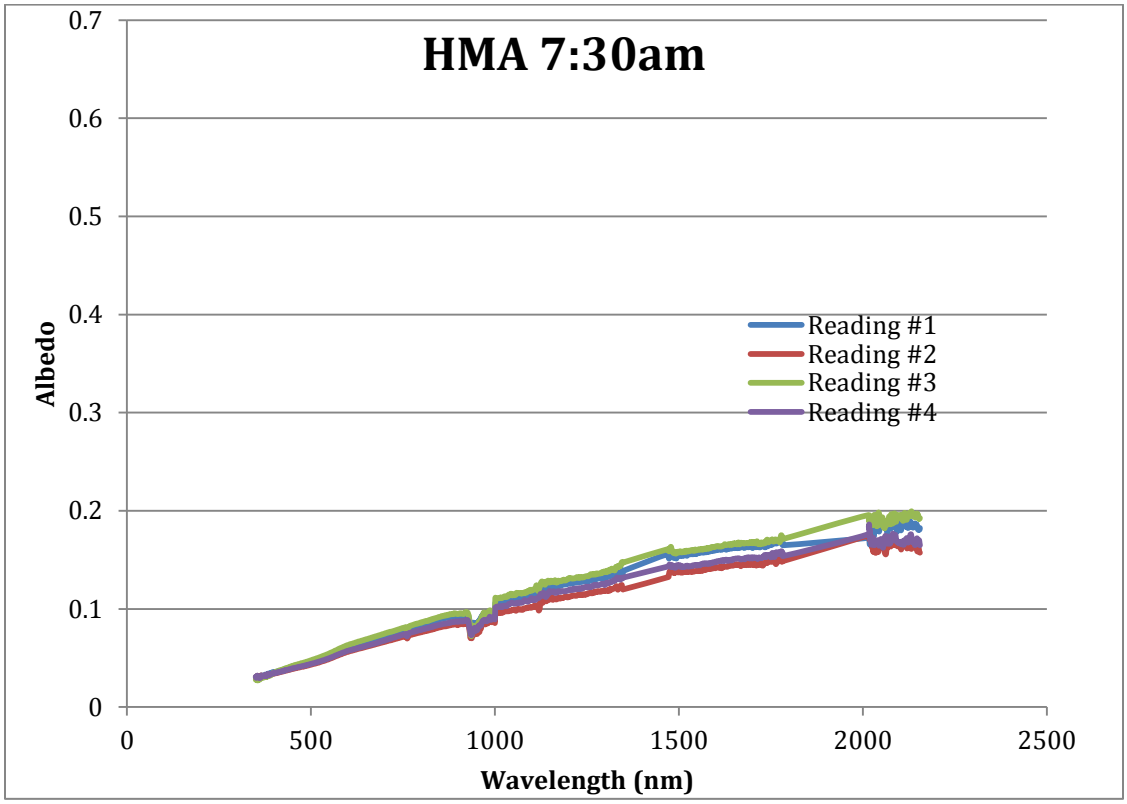
HMA 7:30am
Albedo
0.7
0.6
0.5
0.4
0.3
0.2
0.1
0
0
500
1000
1500
2000
2500
Wavelength (nm)
Reading #1
Reading #2
Reading #3
Reading #4

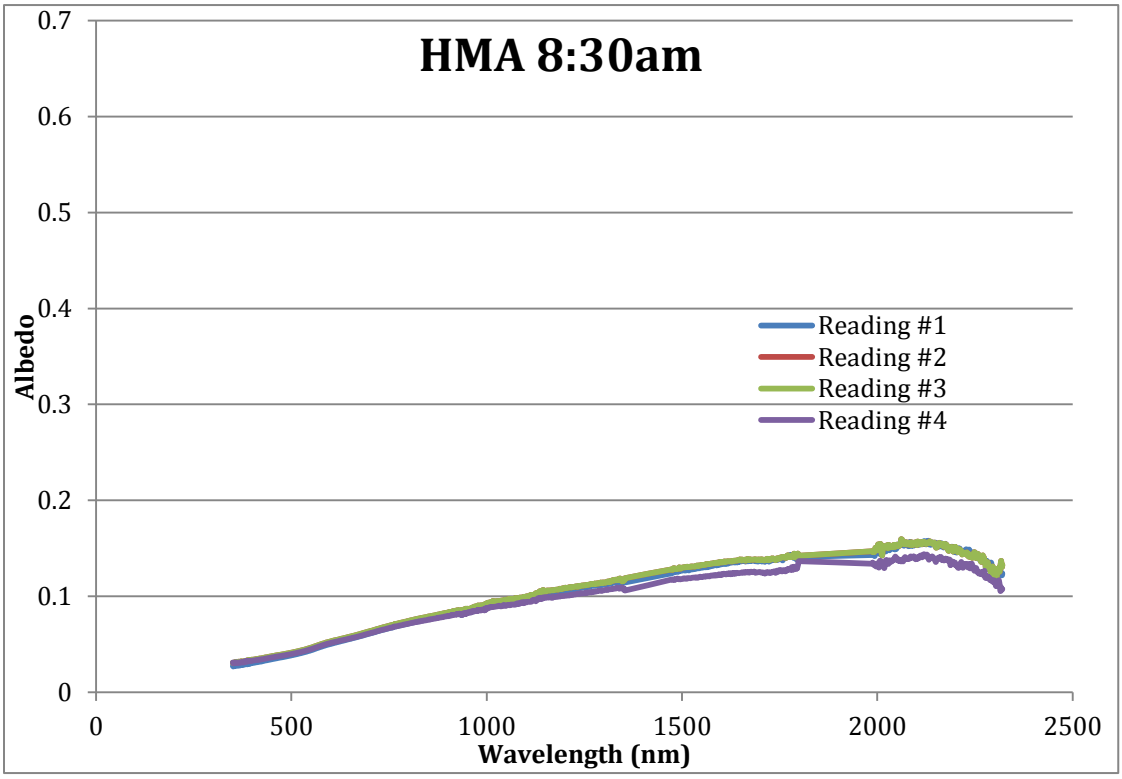
HMA 8:30am
Albedo
0.7
0.6
0.5
0.4
0.3
0.2
0.1
0
0
500
1000
1500
2000
2500
Wavelength (nm)
Reading #1
Reading #2
Reading #3
Reading #4

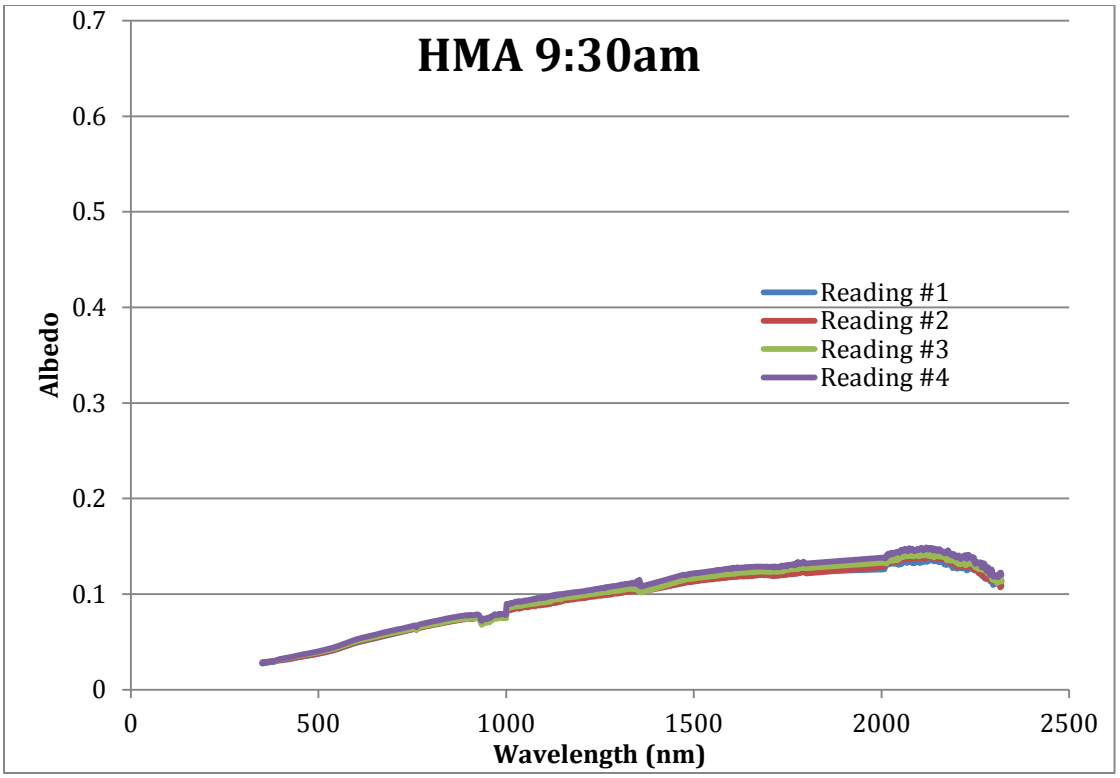
HMA 9:30am
Albedo
Wavelength (nm)
Reading #1
Reading #2
Reading #3
Reading #4
0.7
0.6
0.5
0.4
0.3
0.2
0.1
0
0
500
1000
1500
2000
2500

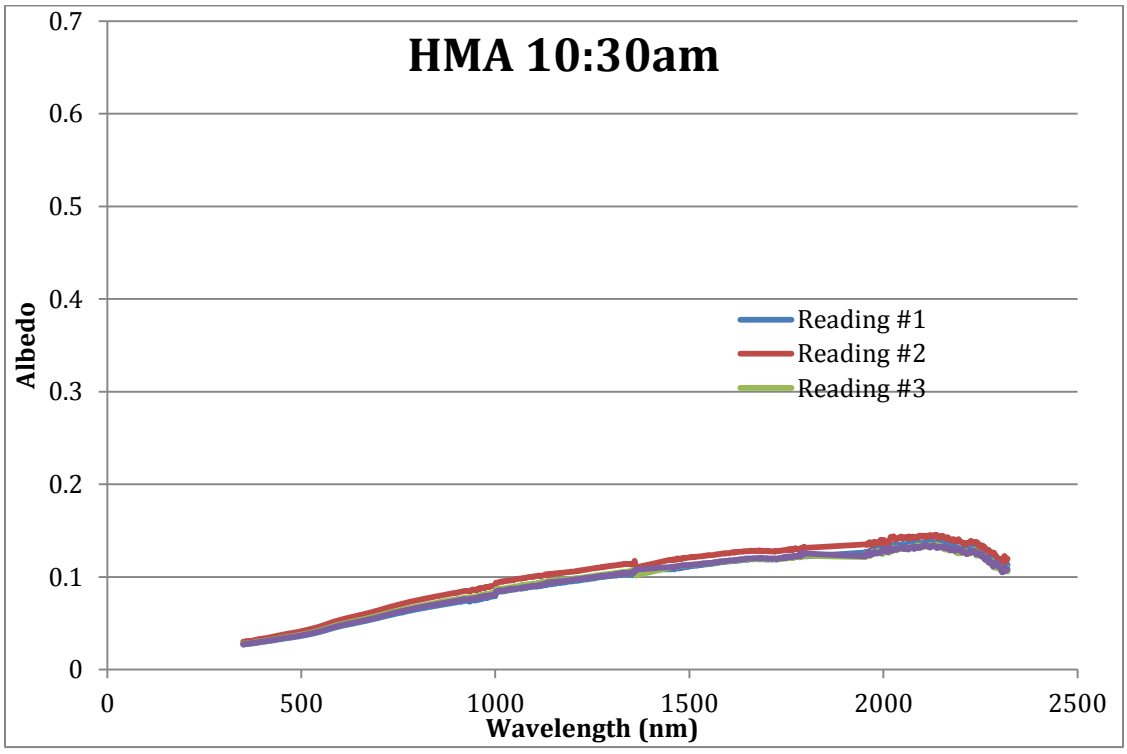
HMA 10:30am
Albedo
Wavelength (nm)
Reading #1
Reading #2
Reading #3
0.7
0.6
0.5
0.4
0.3
0.2
0.1
0
0
500
1000
1500
2000
2500

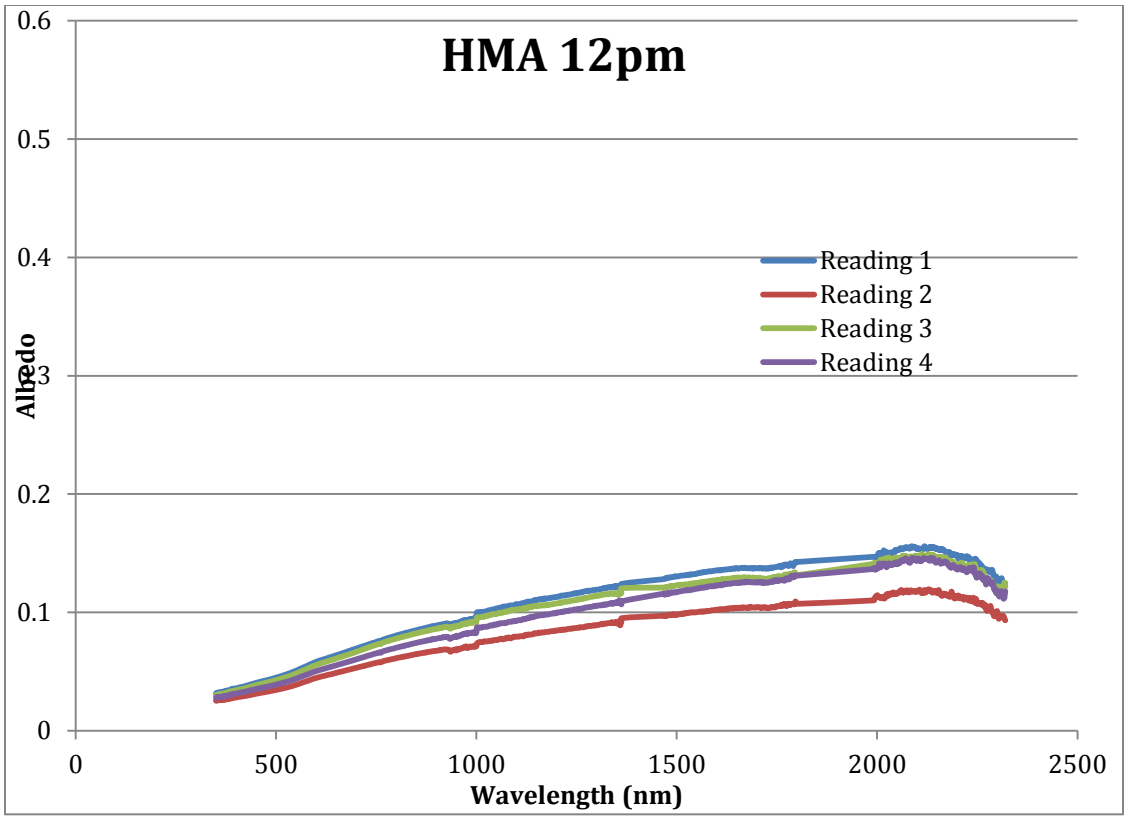
HMA 12pm
Albedo
Wavelength (nm)
Reading 1
Reading 2
Reading 3
Reading 4
0.6
0.5
0.4
0.3
0.2
0.1
0
0
500
1000
1500
2000
2500

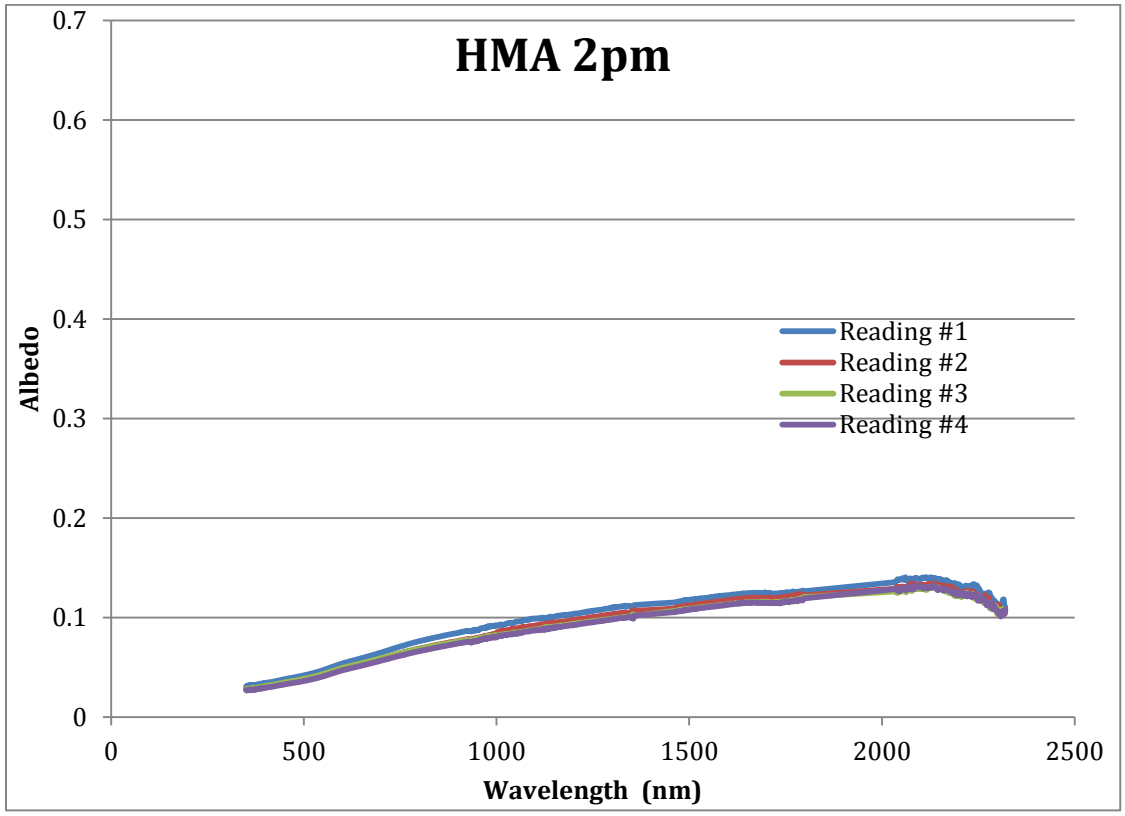
HMA 2pm
Albedo
Wavelength (nm)
Reading #1
Reading #2
Reading #3
Reading #4
0.7
0.6
0.5
0.4
0.3
0.2
0.1
0
0
500
1000
1500
2000
2500

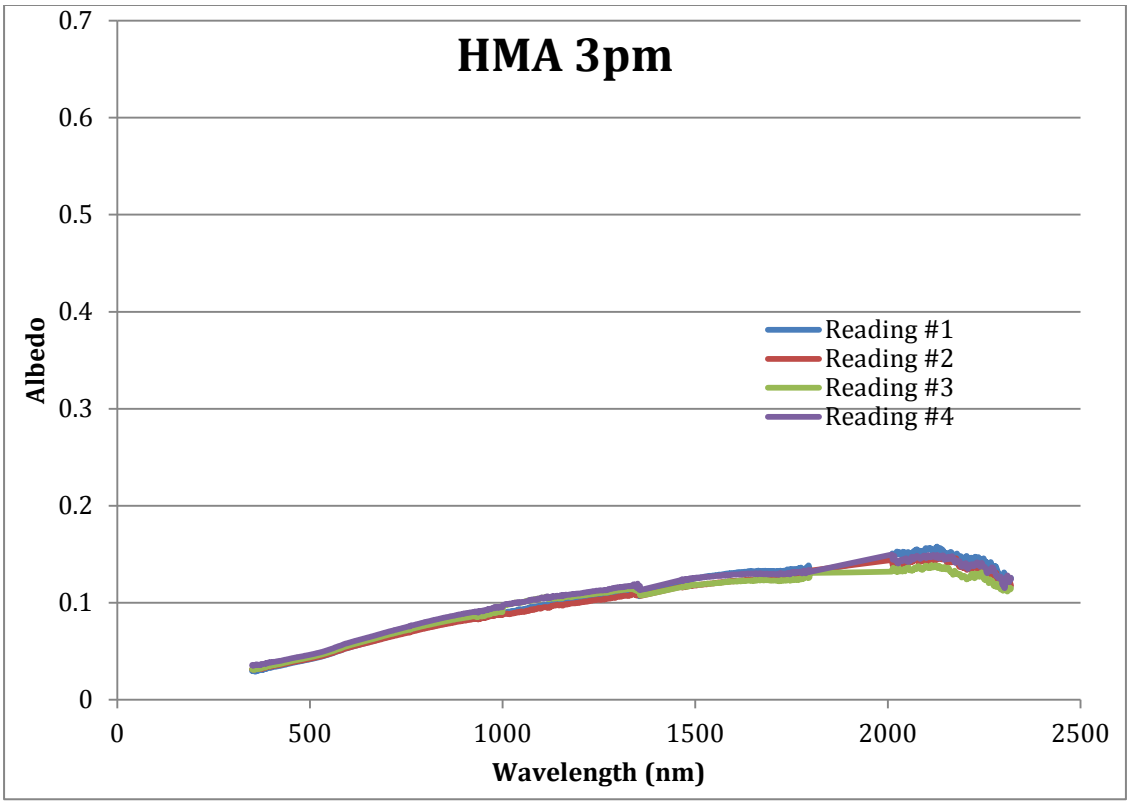
HMA 3pm
Albedo
0.7
0.6
0.5
0.4
0.3
0.2
0.1
0
0
500
1000
1500
2000
2500
Wavelength (nm)
Reading #1
Reading #2
Reading #3
Reading #4

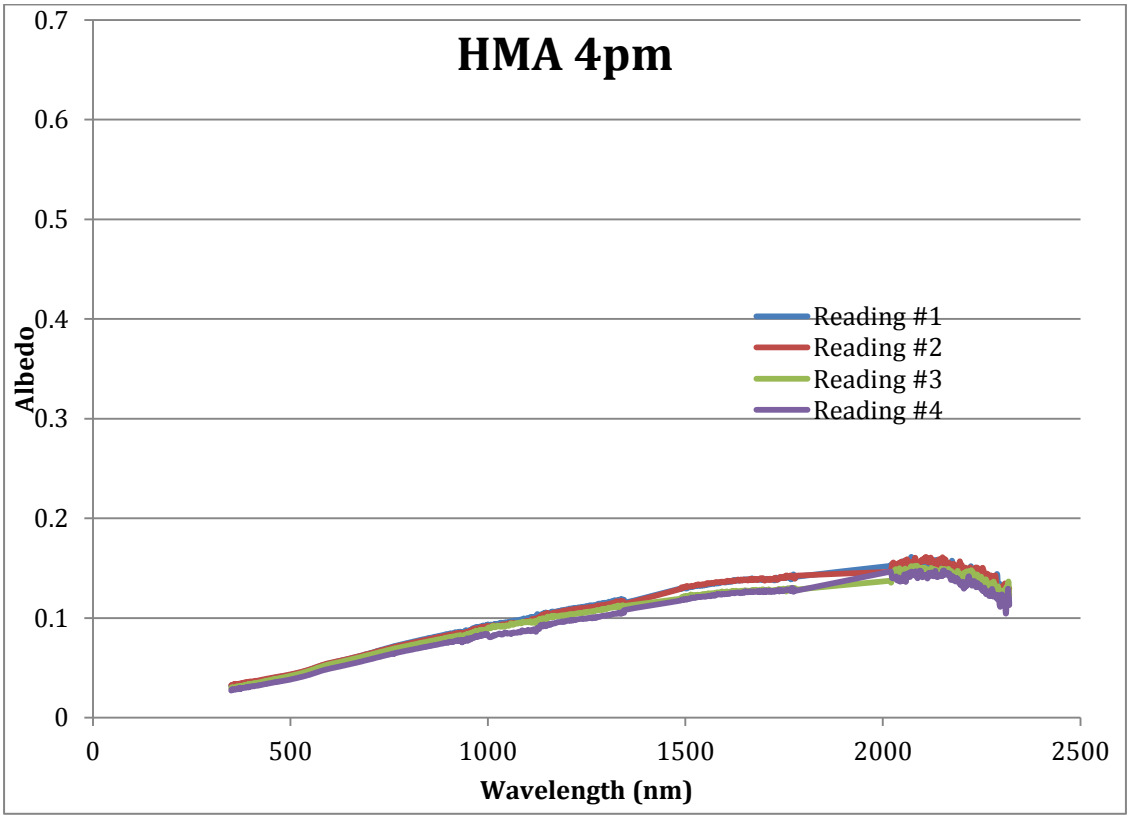
HMA 4pm
Albedo
0.7
0.6
0.5
0.4
0.3
0.2
0.1
0
0
500
1000
1500
2000
2500
Wavelength (nm)
Reading #1
Reading #2
Reading #3
Reading #4

PHMA

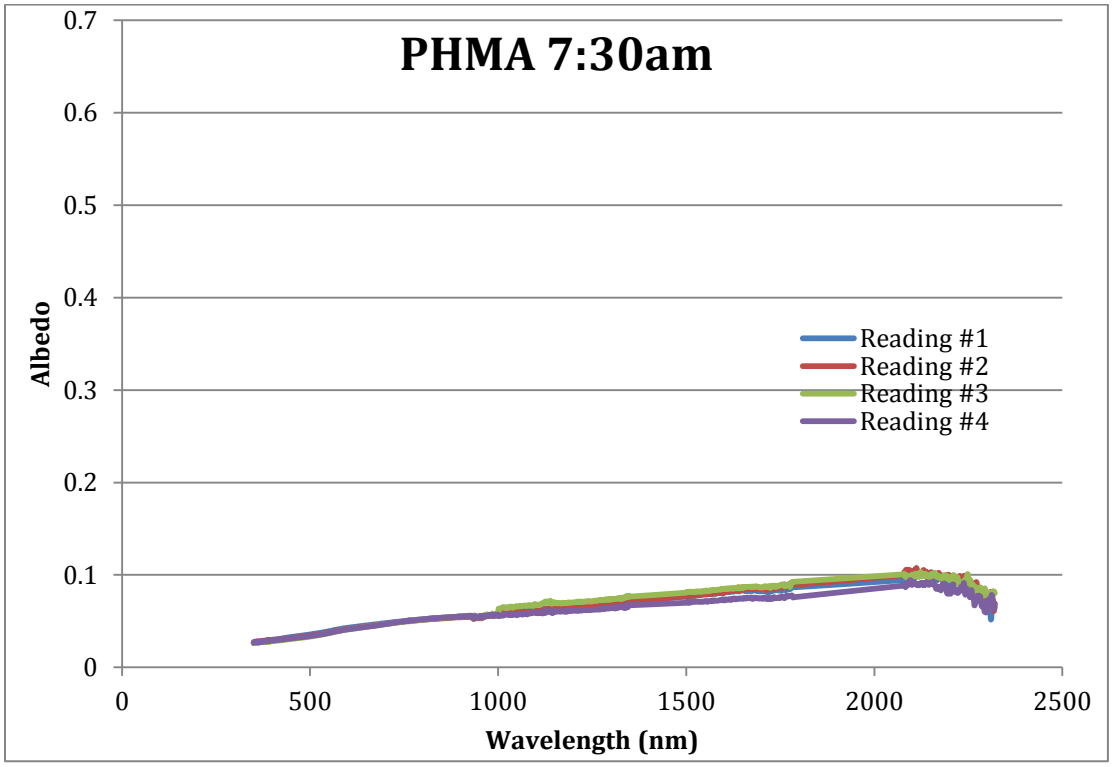
PHMA 7:30am
0.7
0.6
0.5
0.4
0.3
0.2
0.1
0
Albedo
0
500
1000
1500
2000
2500
Wavelength (nm)
Reading #1
Reading #2
Reading #3
Reading #4

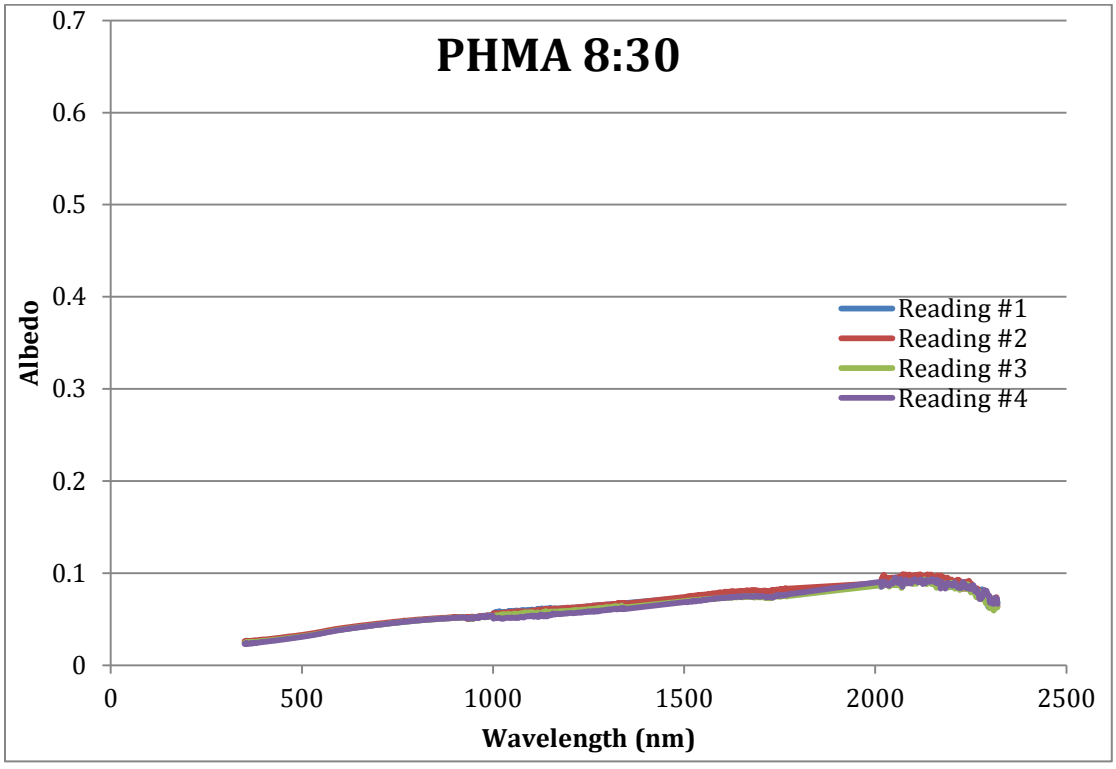
PHMA 8:30
0.7
0.6
0.5
0.4
0.3
0.2
0.1
0
Albedo
0
500
1000
1500
2000
2500
Wavelength (nm)
Reading #1
Reading #2
Reading #3
Reading #4

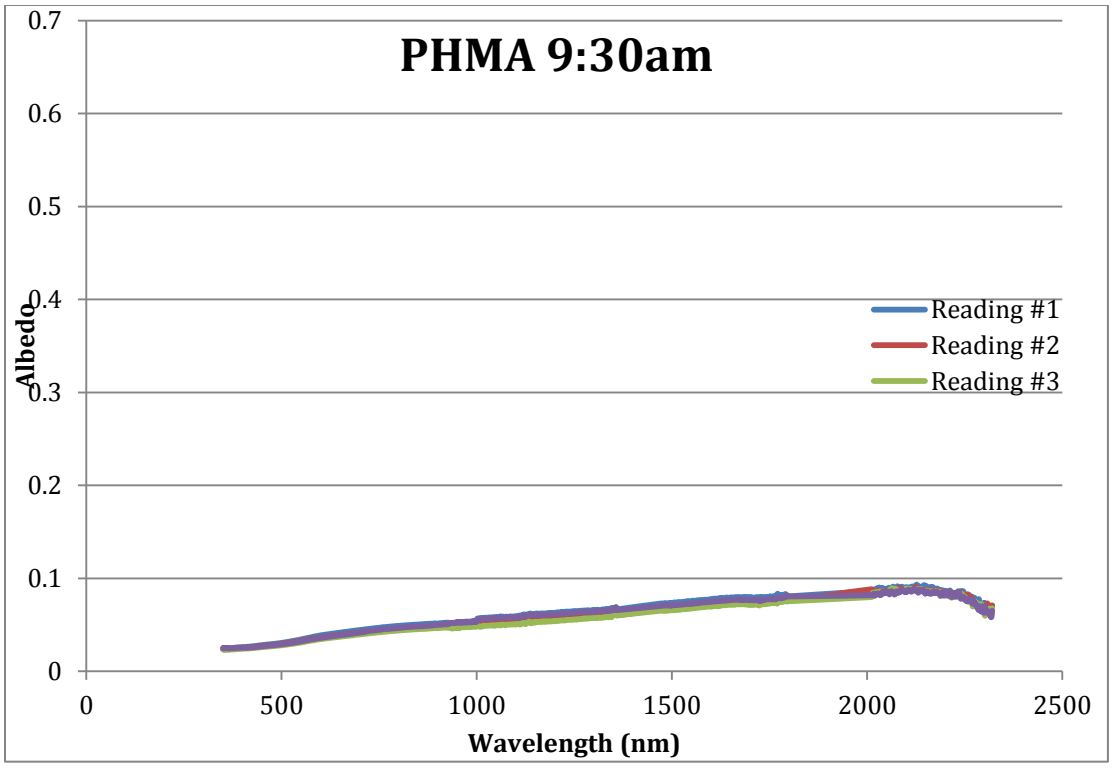
PHMA 9:30am
Albedo
Wavelength (nm)
Reading #1
Reading #2
Reading #3
0.7
0.6
0.5
0.4
0.3
0.2
0.1
0
0
500
1000
1500
2000
2500

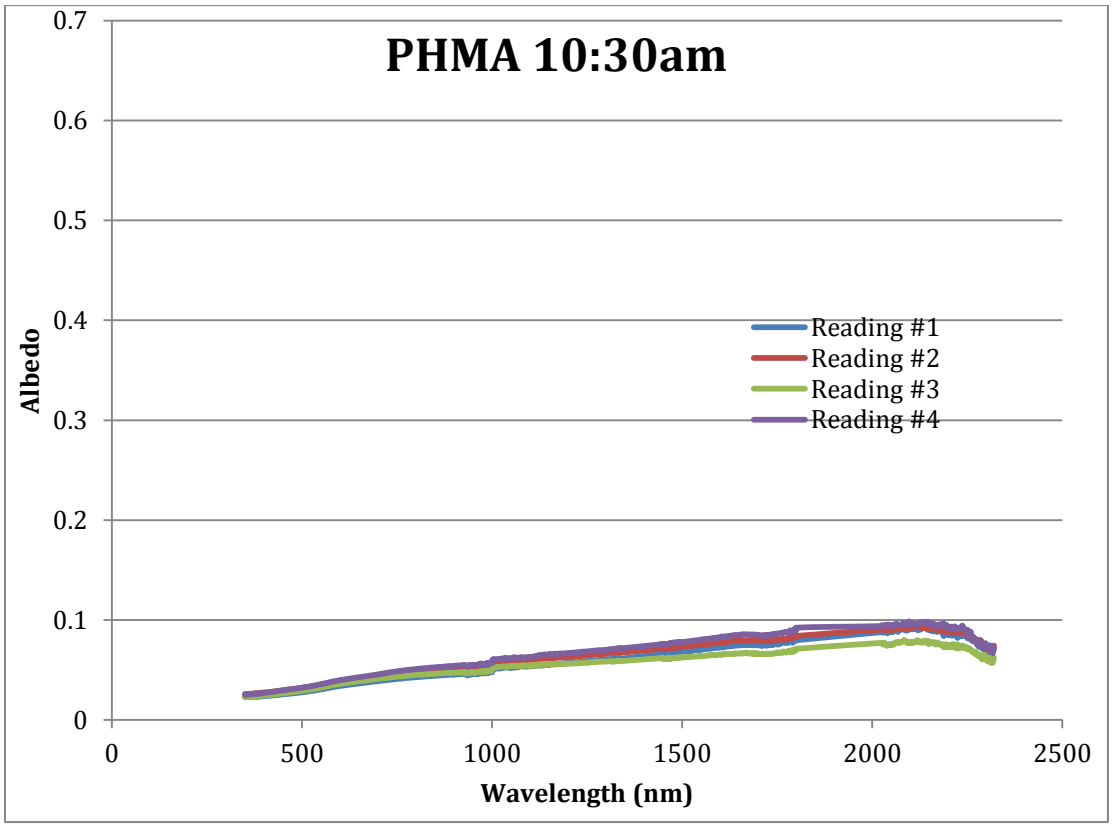
PHMA 10:30am
Albedo
Wavelength (nm)
Reading #1
Reading #2
Reading #3
Reading #4
0.7
0.6
0.5
0.4
0.3
0.2
0.1
0
0
500
1000
1500
2000
2500

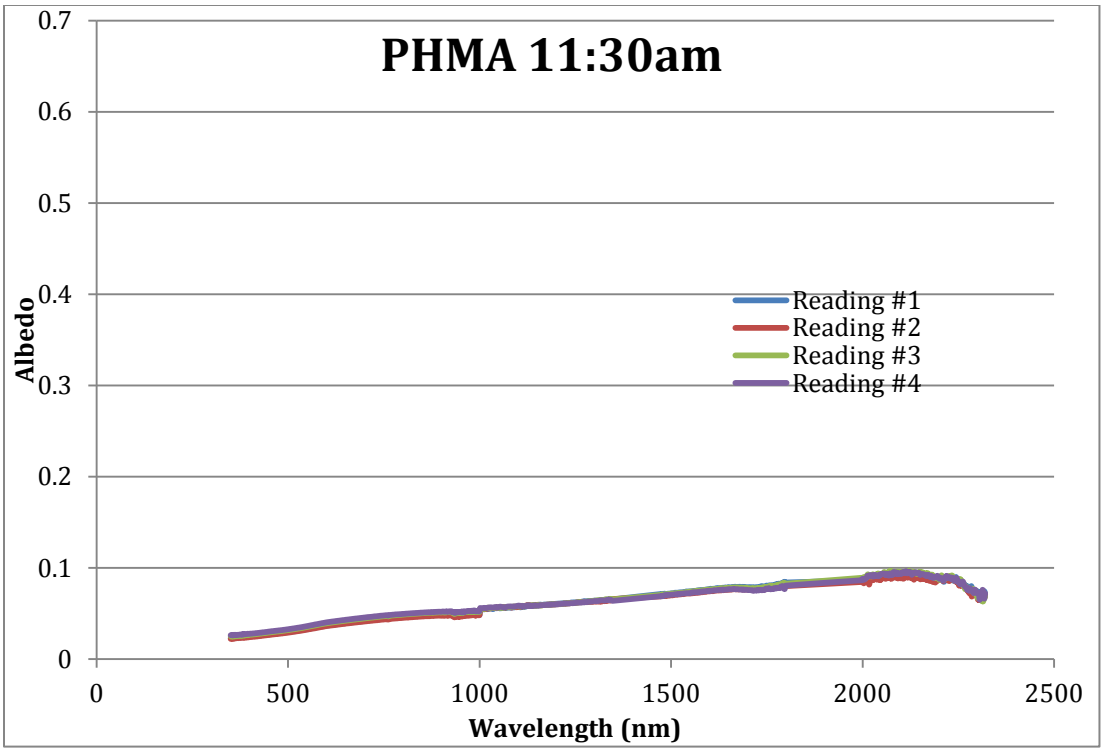
PHMA 11:30am
Albedo
Wavelength (nm)
Reading #1
Reading #2
Reading #3
Reading #4
0.7
0.6
0.5
0.4
0.3
0.2
0.1
0
0
500
1000
1500
2000
2500

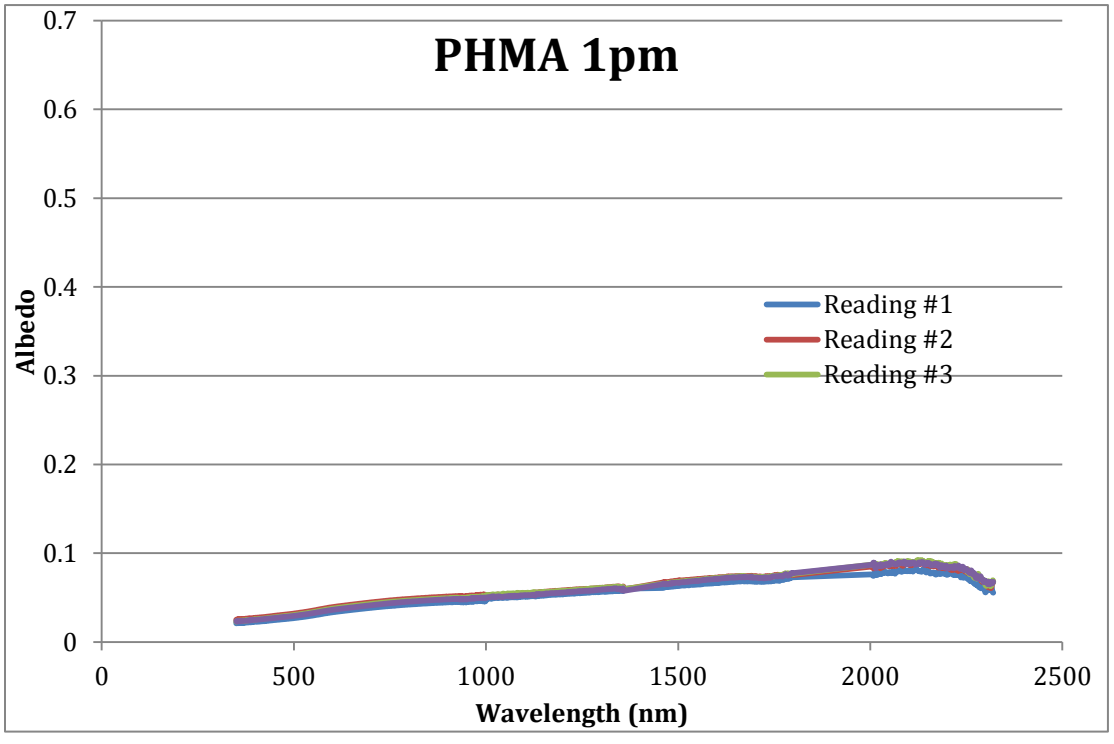
PHMA 1pm
Albedo
Wavelength (nm)
Reading #1
Reading #2
Reading #3
0.7
0.6
0.5
0.4
0.3
0.2
0.1
0
0
500
1000
1500
2000
2500

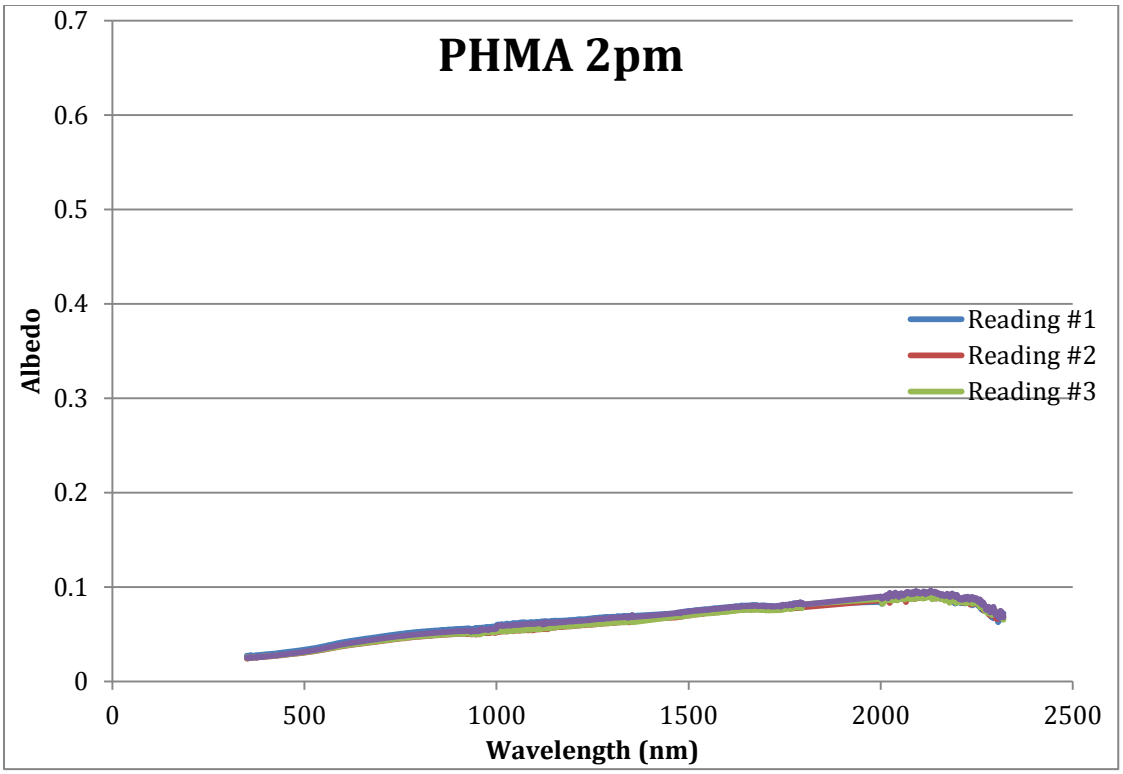
PHMA 2pm
Albedo
0.7
0.6
0.5
0.4
0.3
0.2
0.1
0
0
500
1000
1500
2000
2500
Wavelength (nm)
Reading #1
Reading #2
Reading #3

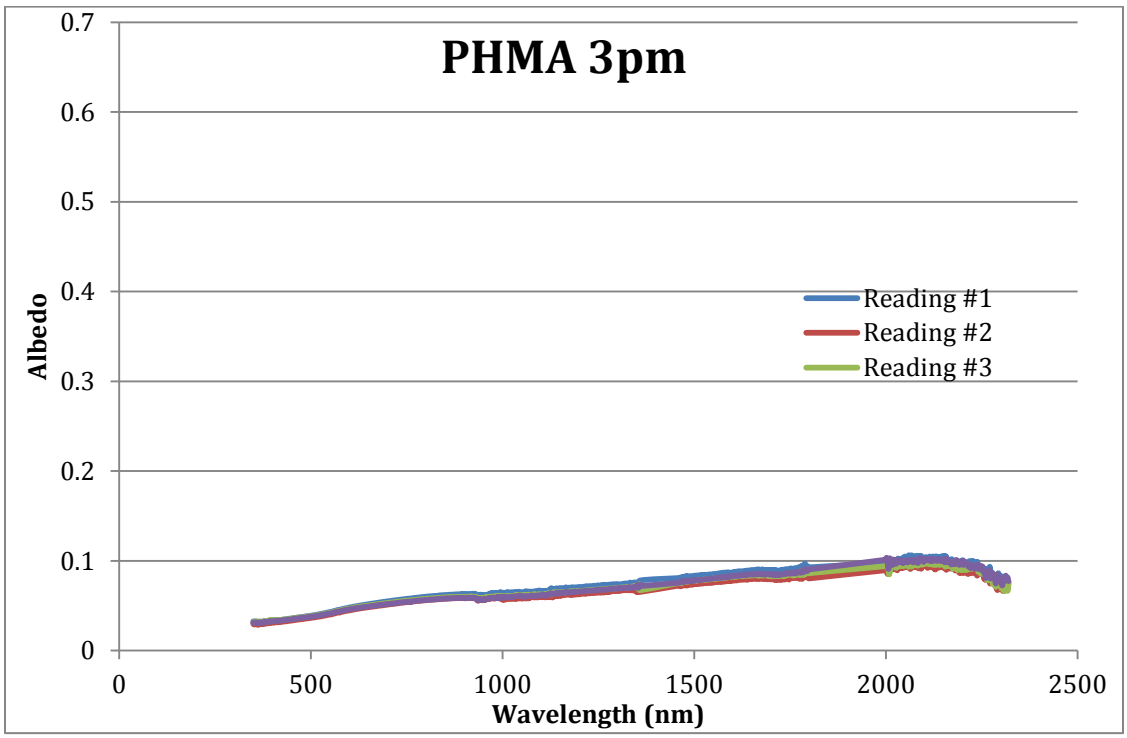
PHMA 3pm
Albedo
0.7
0.6
0.5
0.4
0.3
0.2
0.1
0
0
500
1000
1500
2000
2500
Wavelength (nm)
Reading #1
Reading #2
Reading #3

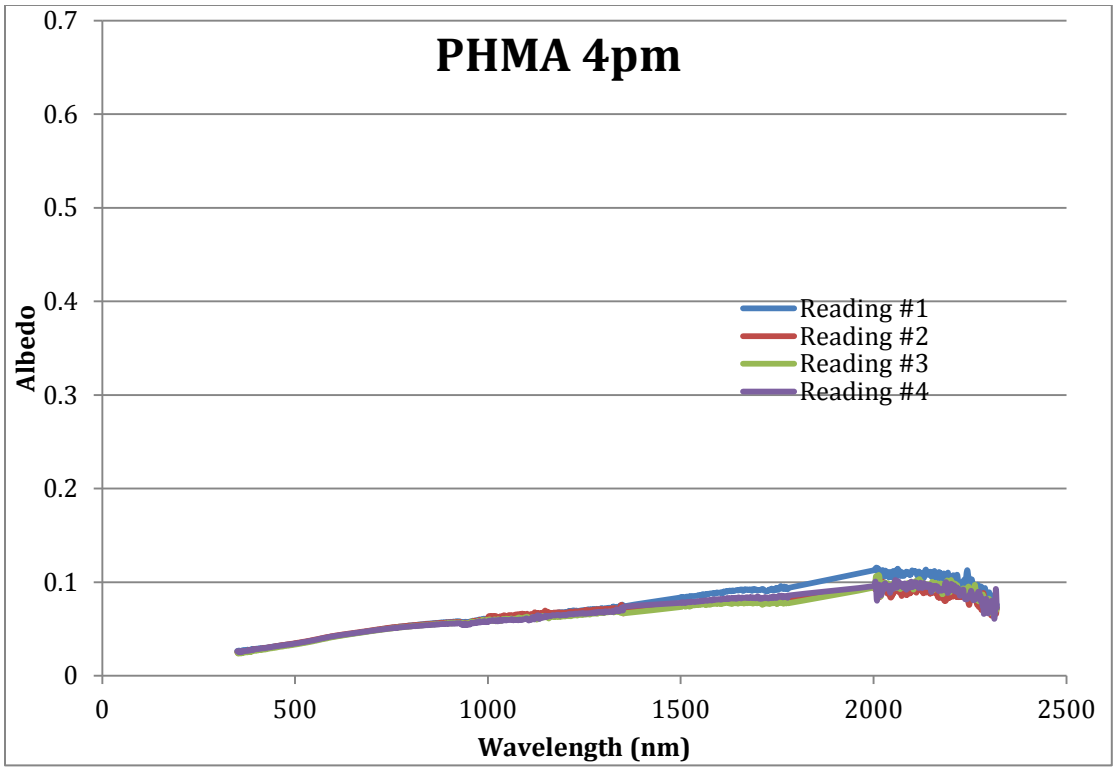
PHMA 4pm
Albedo
0.7
0.6
0.5
0.4
0.3
0.2
0.1
0
0
500
1000
1500
2000
2500
Wavelength (nm)
Reading #1
Reading #2
Reading #3
Reading #4

PPCC

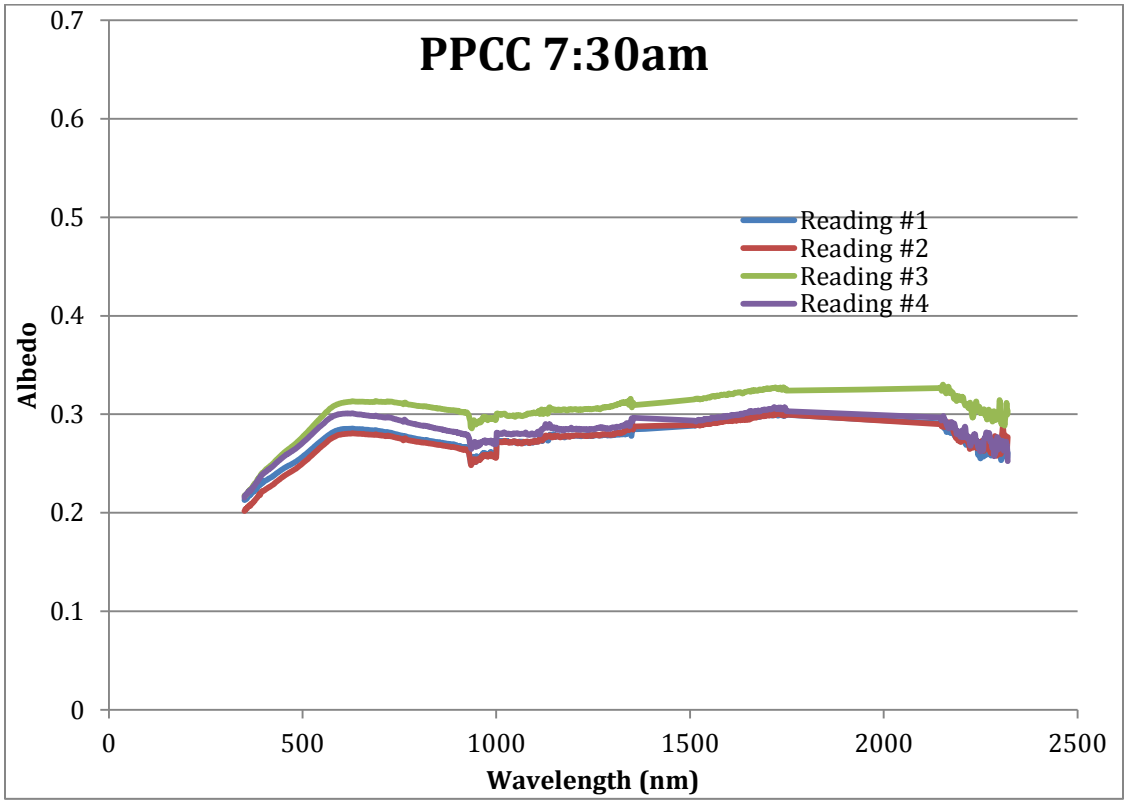
PPCC 7:30am
Albedo
Wavelength (nm)
Reading #1
Reading #2
Reading #3
Reading #4
0.7
0.6
0.5
0.4
0.3
0.2
0.1
0
0
500
1000
1500
2000
2500

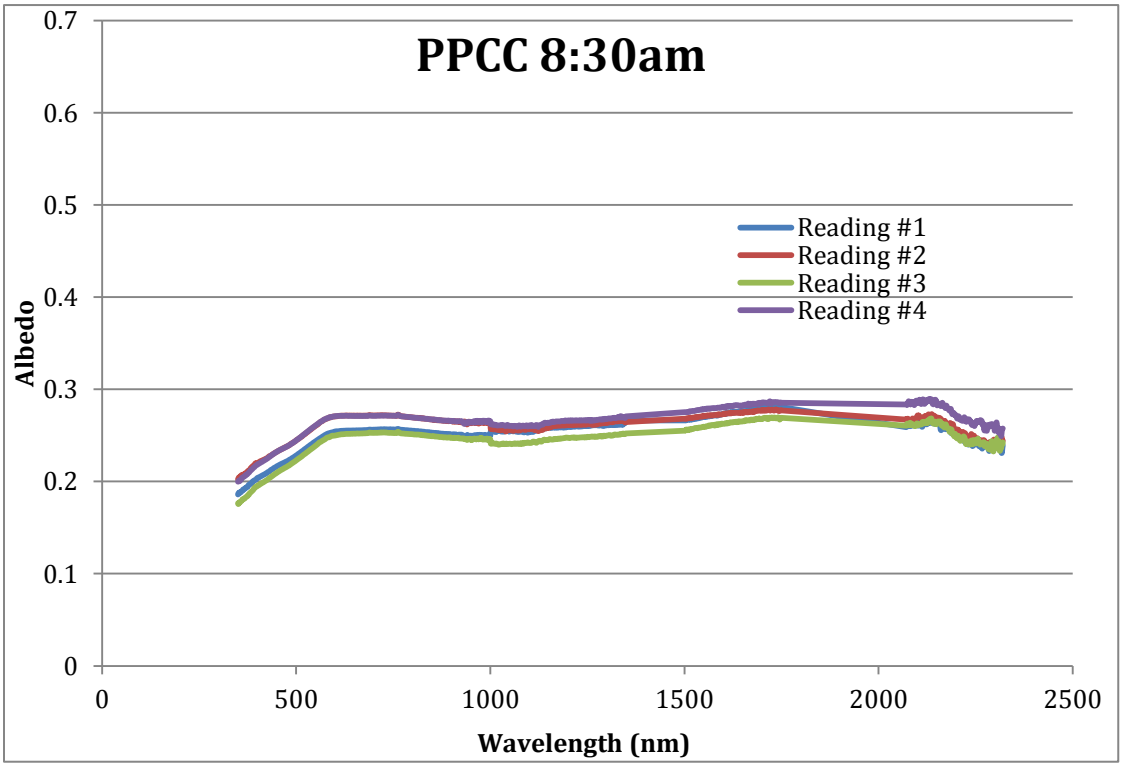
PPCC 8:30am
Albedo
Wavelength (nm)
Reading #1
Reading #2
Reading #3
Reading #4
0.7
0.6
0.5
0.4
0.3
0.2
0.1
0
0
500
1000
1500
2000
2500

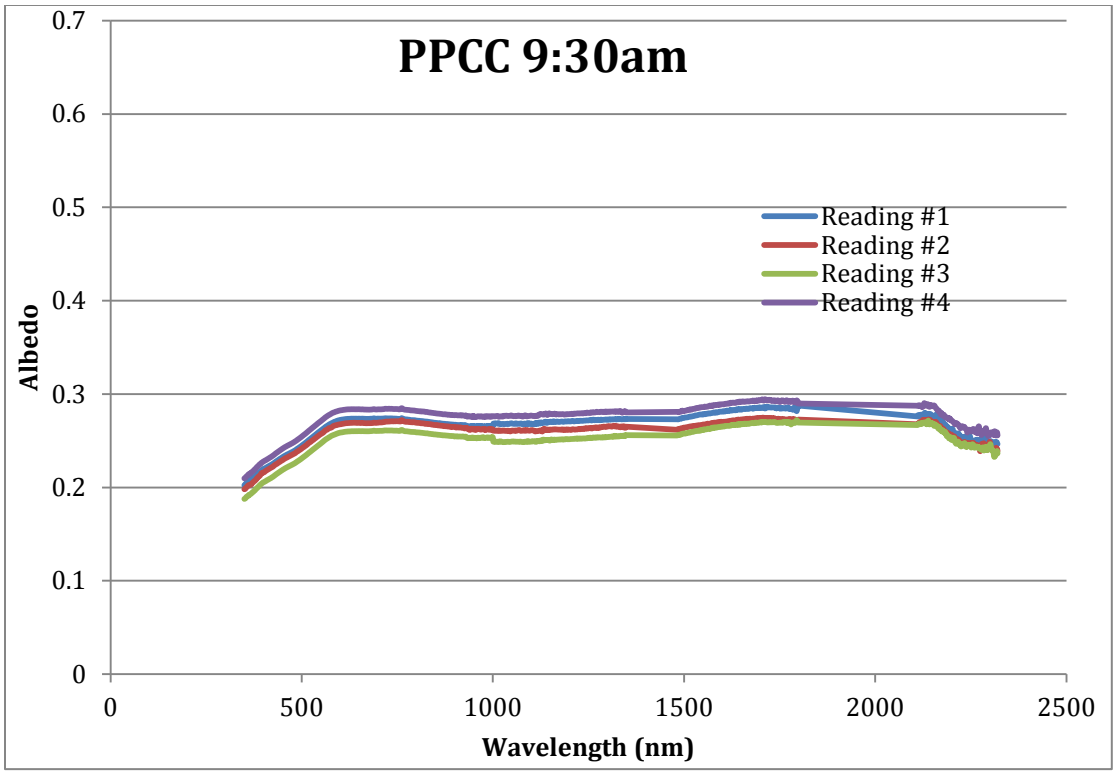
PPCC 9:30am
Albedo
Wavelength (nm)
Reading #1
Reading #2
Reading #3
Reading #4
0.7
0.6
0.5
0.4
0.3
0.2
0.1
0
0
500
1000
1500
2000
2500

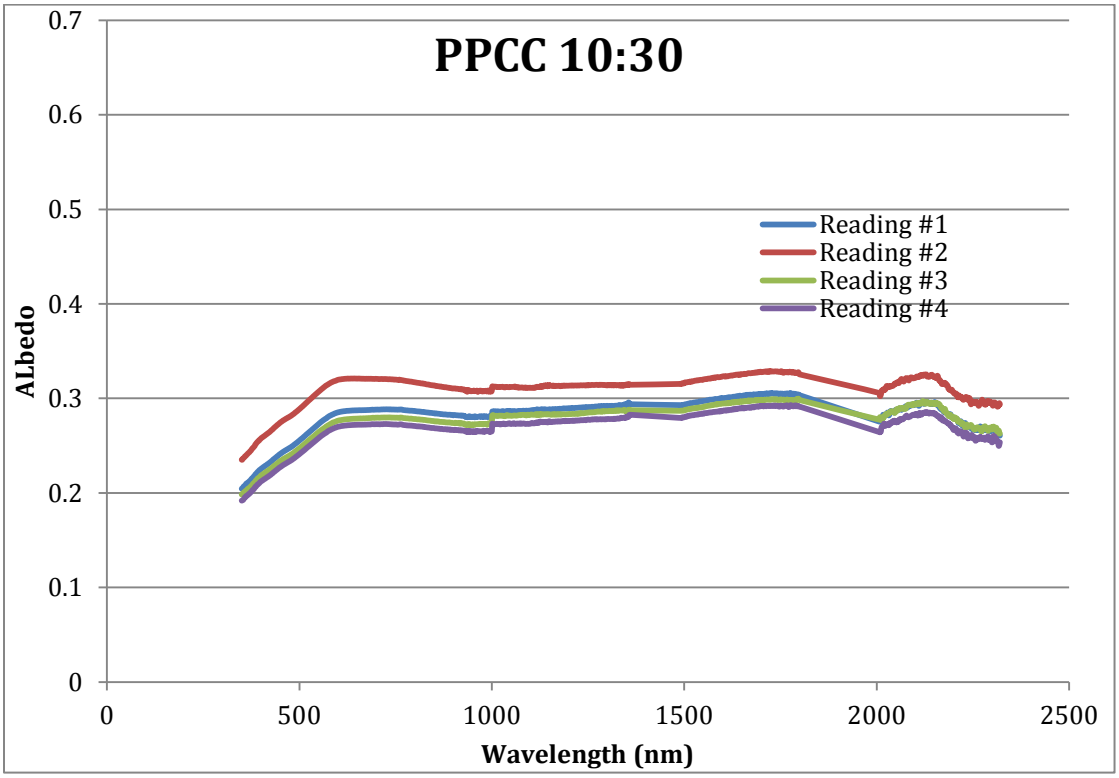
PPCC 10:30
ALbedo
Wavelength (nm)
Reading #1
Reading #2
Reading #3
Reading #4
0.7
0.6
0.5
0.4
0.3
0.2
0.1
0
0
500
1000
1500
2000
2500

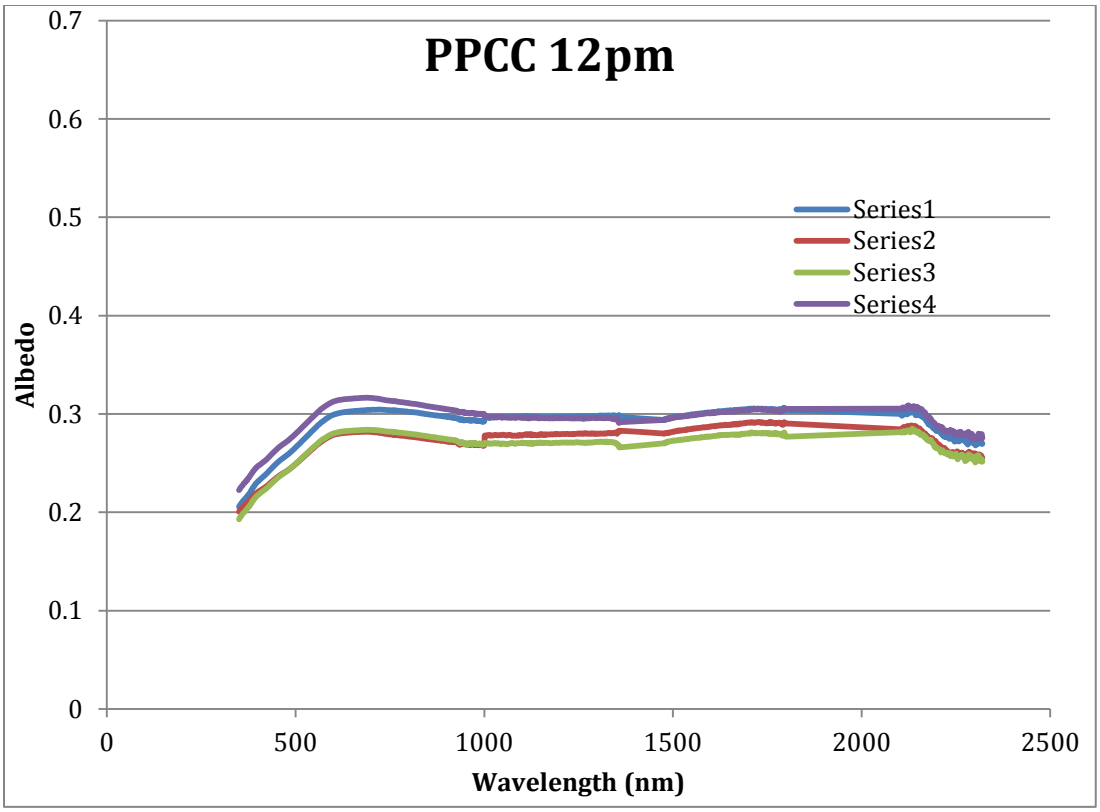
PPCC 12pm
Albedo
Wavelength (nm)
0.7
0.6
0.5
0.4
0.3
0.2
0.1
0
0
500
1000
1500
2000
2500
Series1
Series2
Series3
Series4

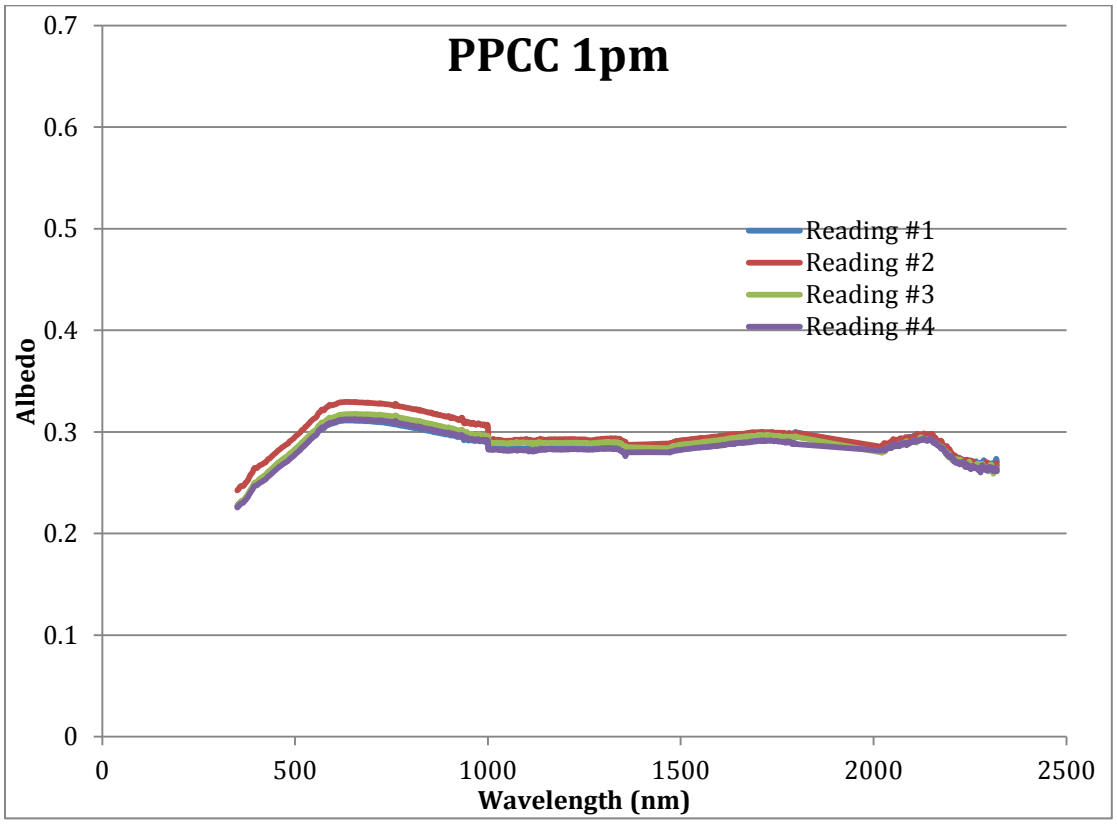
PPCC 1pm
Albedo
Wavelength (nm)
0.7
0.6
0.5
0.4
0.3
0.2
0.1
0
0
500
1000
1500
2000
2500
Reading #1
Reading #2
Reading #3
Reading #4

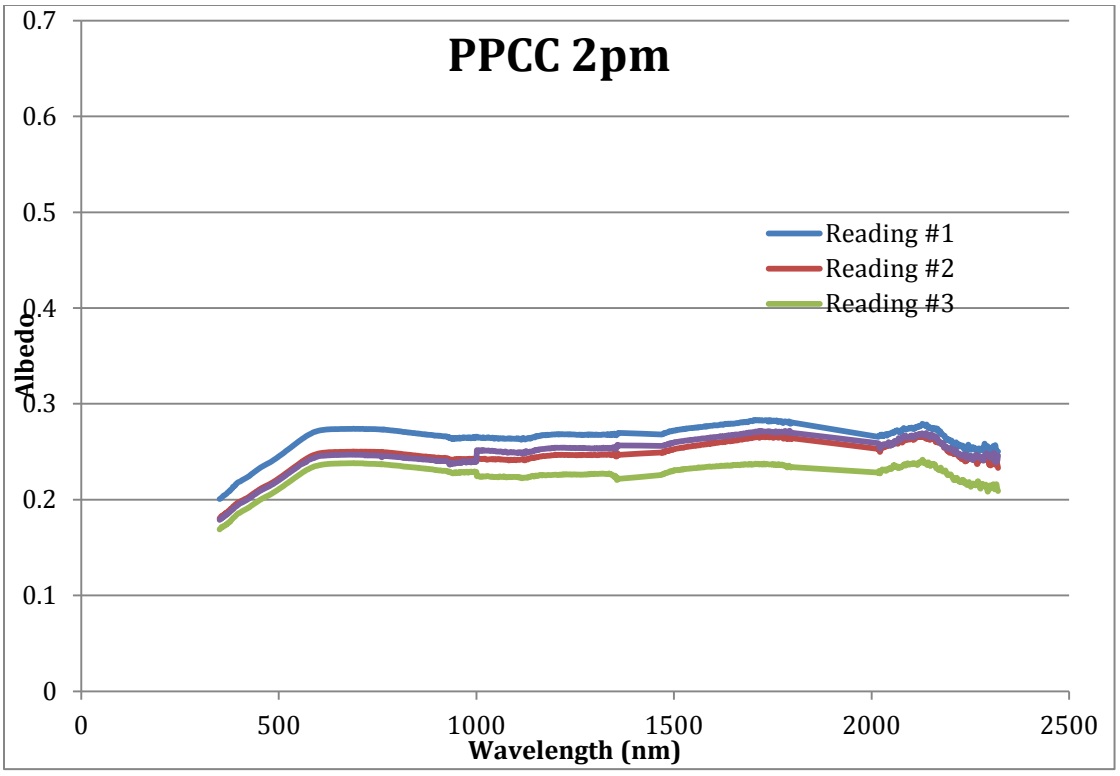
PPCC 2pm
Albedo
Wavelength (nm)
Reading #1
Reading #2
Reading #3
0.7
0.6
0.5
0.4
0.3
0.2
0.1
0
0
500
1000
1500
2000
2500

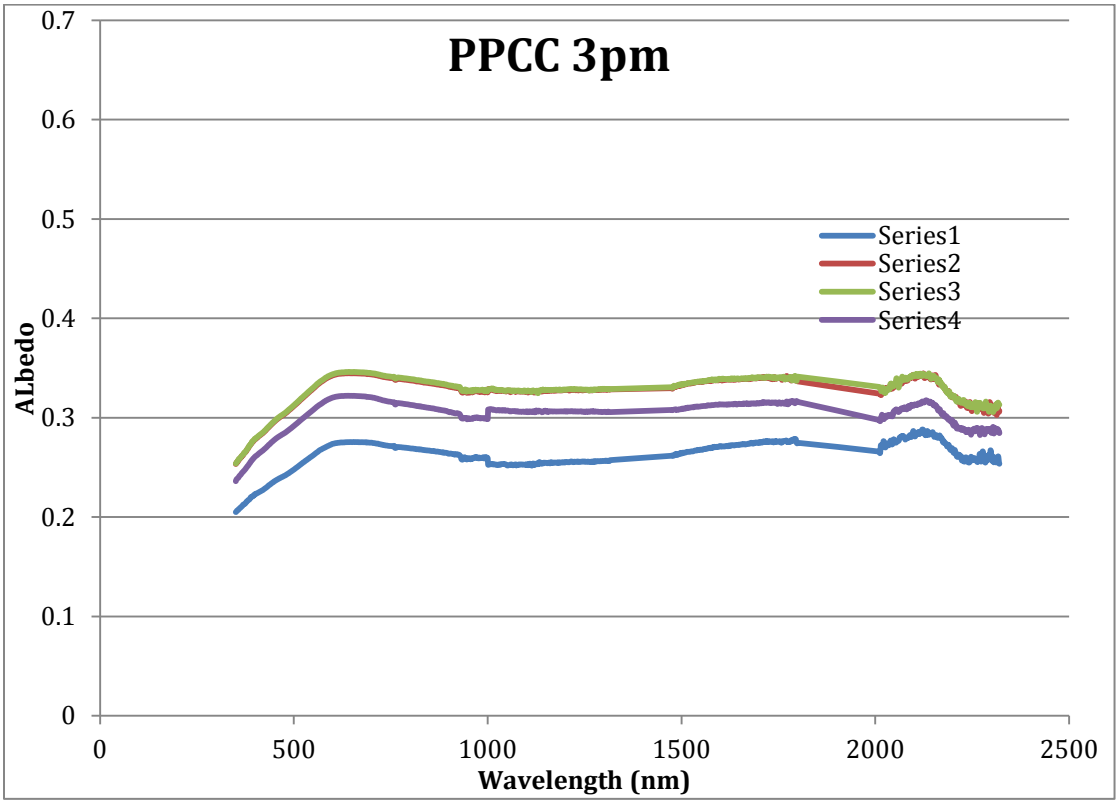
PPCC 3pm
ALbedo
Wavelength (nm)
Series1
Series2
Series3
Series4
0.7
0.6
0.5
0.4
0.3
0.2
0.1
0
0
500
1000
1500
2000
2500

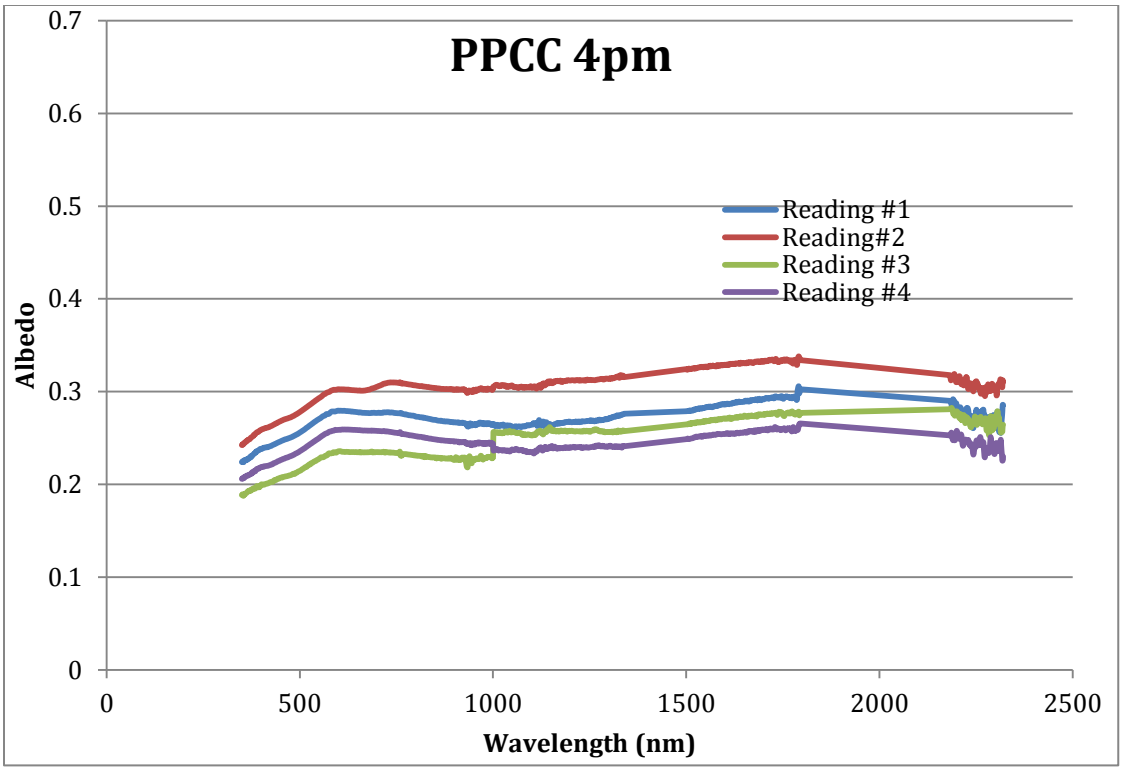
PPCC 4pm
Albedo
Wavelength (nm)
Reading #1
Reading#2
Reading #3
Reading #4
0.7
0.6
0.5
0.4
0.3
0.2
0.1
0
0
500
1000
1500
2000
2500

APPENDIX B

EXAMPLE CLIMAPS DATA OUT-PUT

AZ Time Zone	Wind Speed	Wind Direction	PHMA/ Surface Temperature	PHMA /~1.5'-2.5'/ Air Temperature	PHMA / Temperature 3'	PHMA / Temperature 5'	PHMA / Humidity 3'	PHMA/ Humidity 5'
9/25/2012 0:00	0.7376	86.3457	26.6	25.475	26.07	25.98	32.5332	32.8066
9/25/2012 0:01	0.82141	82.8316	26.475	25.4125	26.06	25.96	32.7082	33.0156
9/25/2012 0:02	0.60349	76.9451	26.4125	25.4125	26.01	25.91	32.8795	33.1515
9/25/2012 0:03	0.40233	75.4466	26.5375	25.35	25.98	25.88	33.0173	33.3241
9/25/2012 0:04	0.35203	75.6489	26.35	25.2875	25.93	25.83	33.1182	33.4248
9/25/2012 0:05	0.30174	82.888	26.2875	25.225	25.88	25.78	33.219	33.4903
9/25/2012 0:06	0.20116	74.6646	26.4125	25.225	25.82	25.74	33.3538	33.6617
9/25/2012 0:07	0	70.2912	26.35	25.1	25.76	25.68	33.4185	33.6913
9/25/2012 0:08	0.03353	70.3209	26.2875	25.0375	25.7	25.62	33.5532	33.8956
9/25/2012 0:09	0.10058	70.3506	26.2875	24.975	25.63	25.55	33.6868	34.0987
9/25/2012 0:10	0.10058	70.3209	26.1625	24.975	25.56	25.48	33.7853	34.1621
9/25/2012 0:11	0.06705	70.4694	26.1625	24.9125	25.51	25.43	34.0252	34.2621
9/25/2012 0:12	0	70.5881	26.2875	24.85	25.44	25.37	34.1584	34.4656
9/25/2012 0:13	0	70.5881	26.2875	24.7875	25.38	25.31	34.2924	34.6341
9/25/2012 0:15	0	70.5881	26.0375	24.6625	25.26	25.18	34.4903	34.9001
9/25/2012 0:16	0.08382	70.5881	26.1625	24.6	25.2	25.12	34.6935	35.0333

APPENDIX C

SAMPLE AIR TEMPERATURE AT 4AM, NOON AND 5PM:

SURFACE (WITH WIND)
1’ (WITH WIND)
3’ (WITH WIND)
5’ (WITH SOLAR RADIATION)

Sample Air Temperature (3 Different Weeks During Sep. – Nov.)

Surface and Wind

4am:

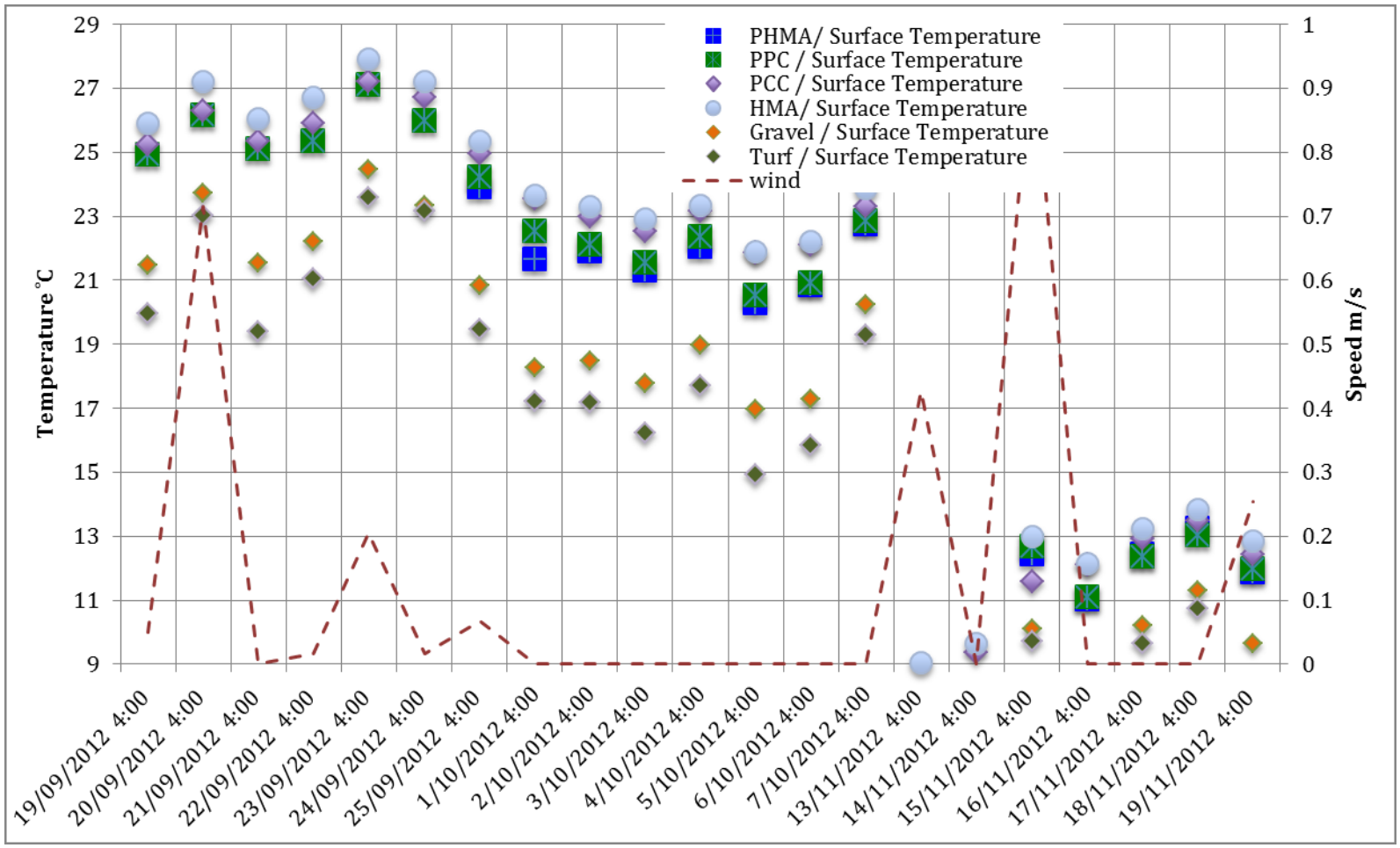

Surface and Wind

12pm:

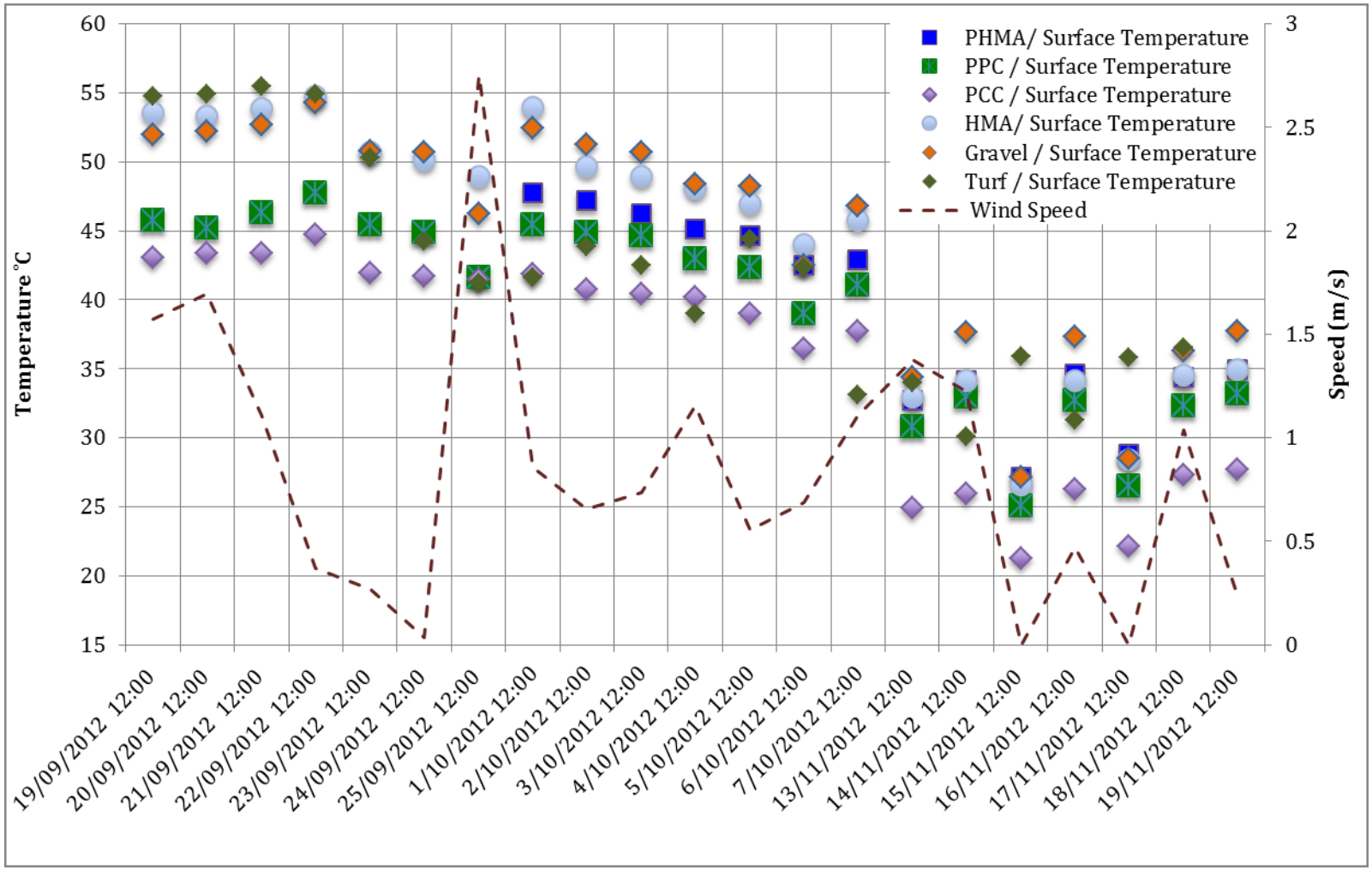

Surface and Wind

5 pm:

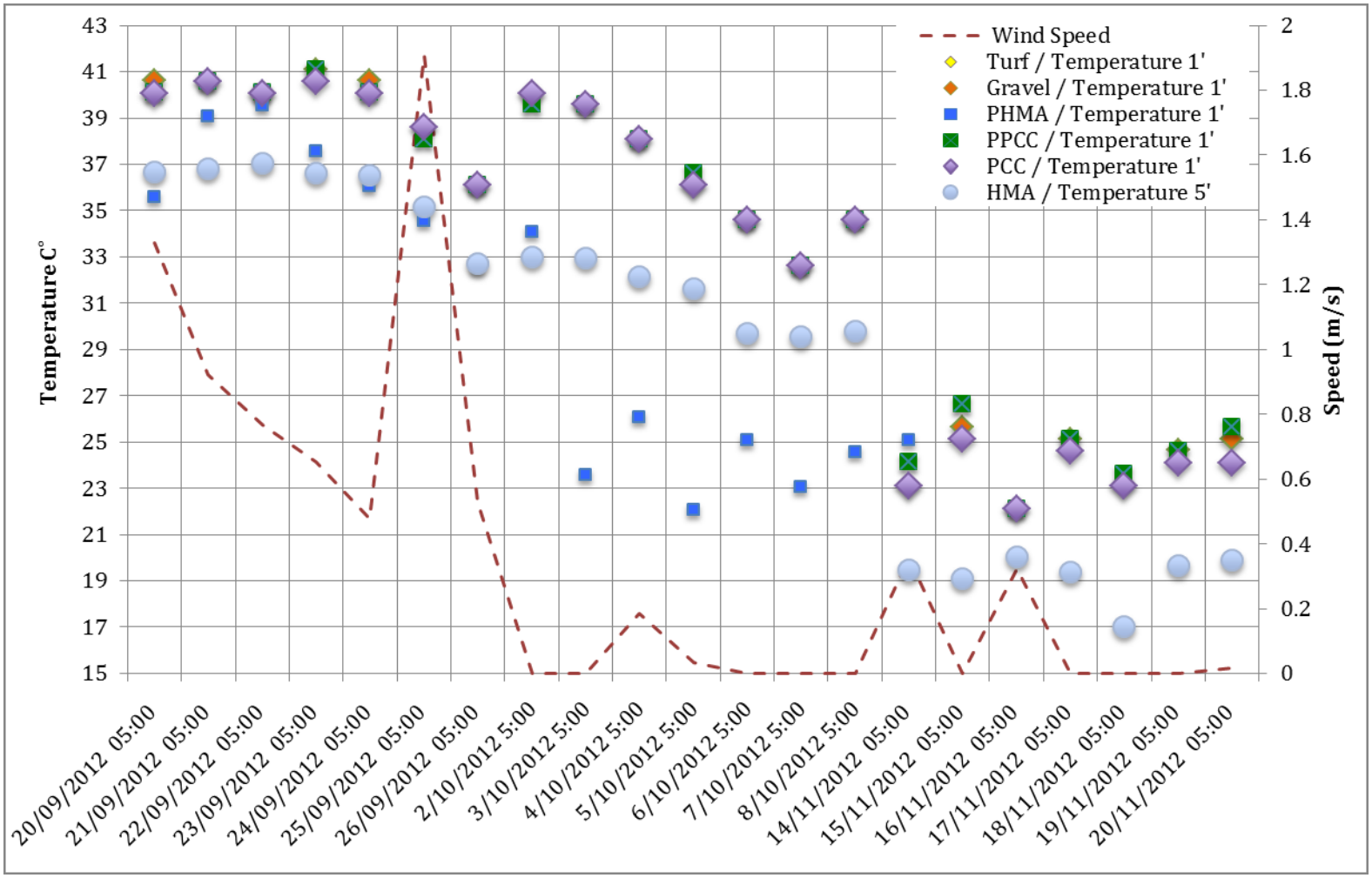

3 Feet Level (Air Temperature and Wind Speed)

4 am:

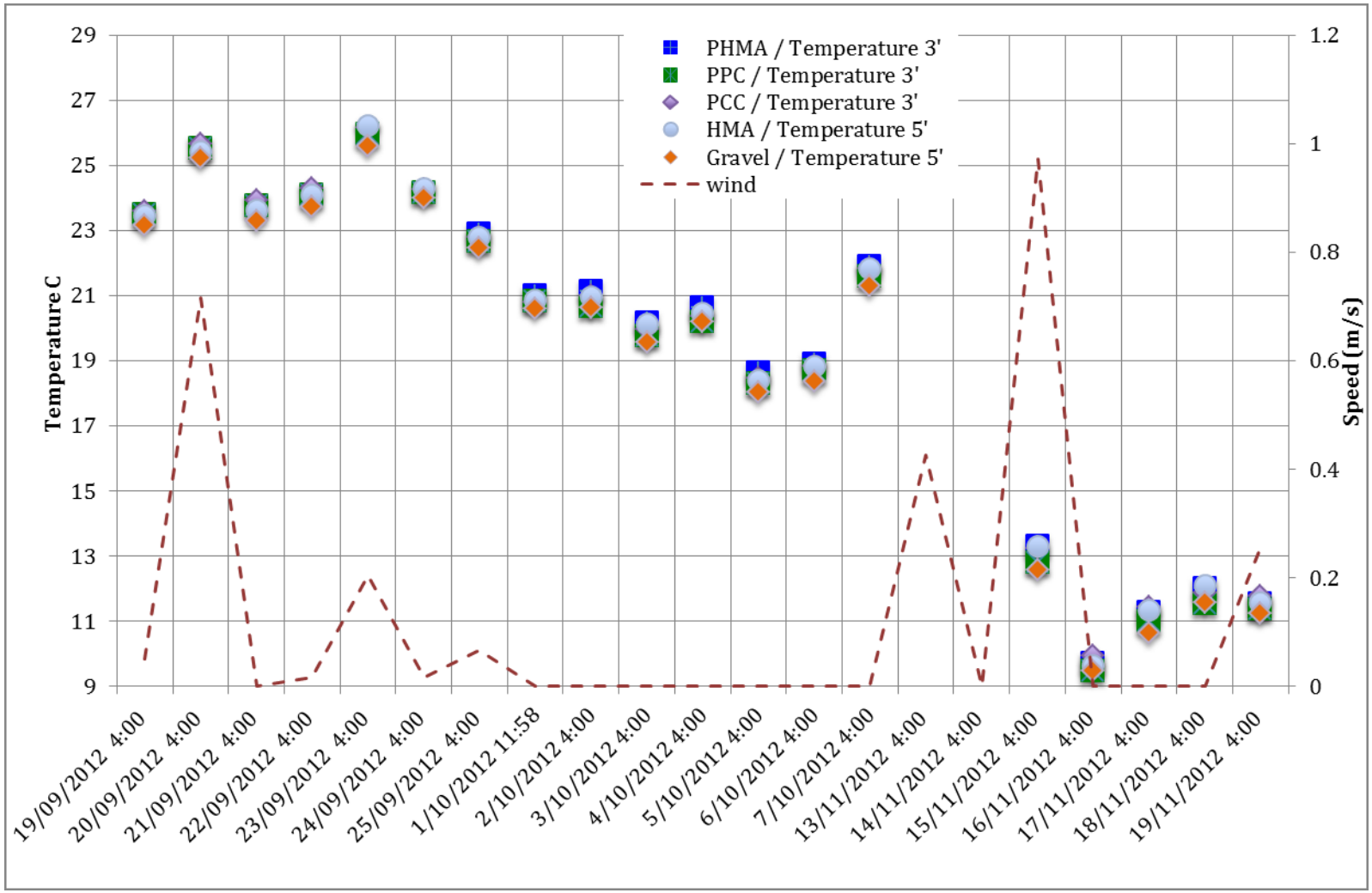

3 Feet Level (Air Temperature and Wind Speed)

12 pm:

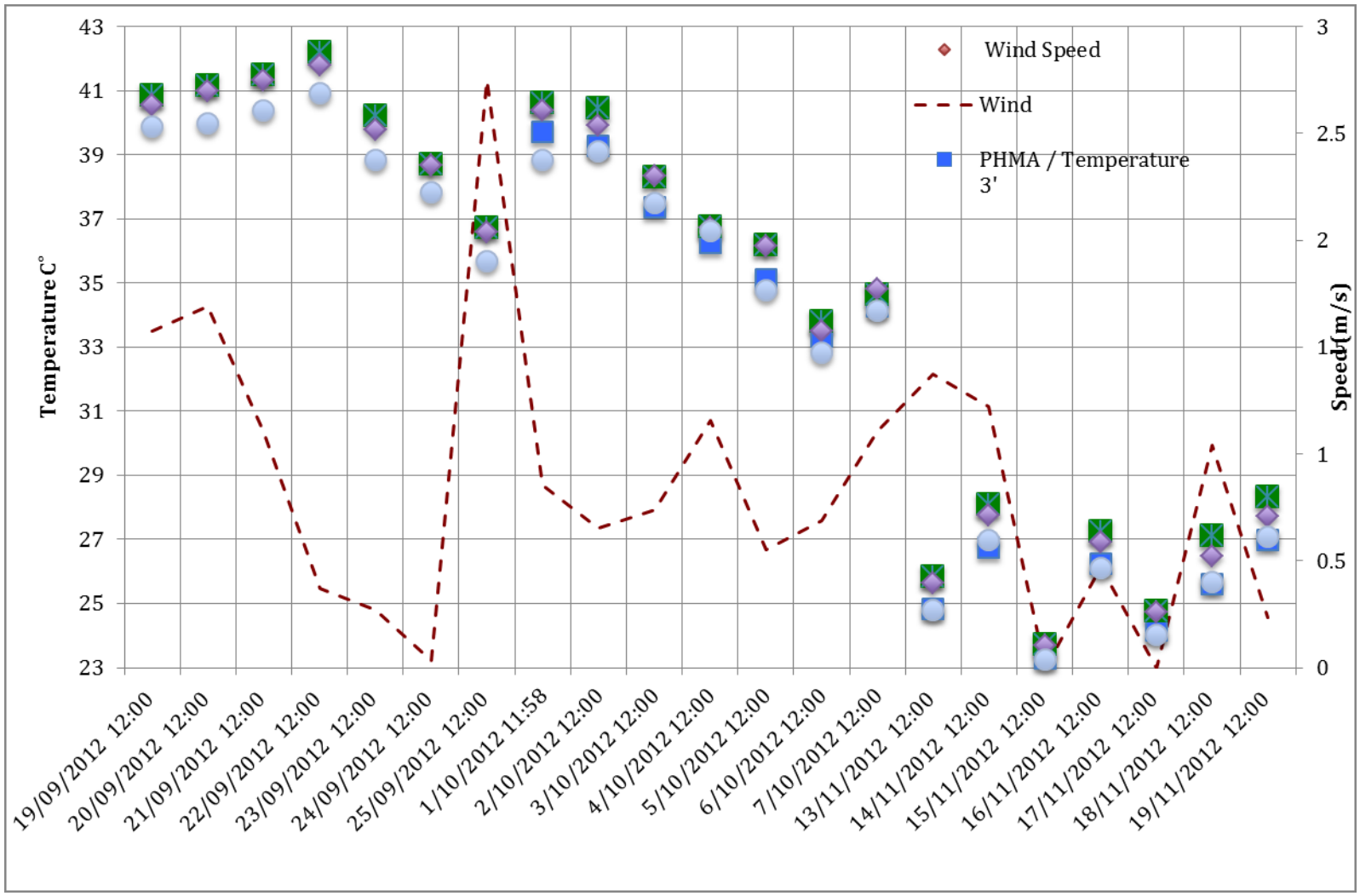

3 Feet Level (Air Temperature and Wind Speed)

5 pm:

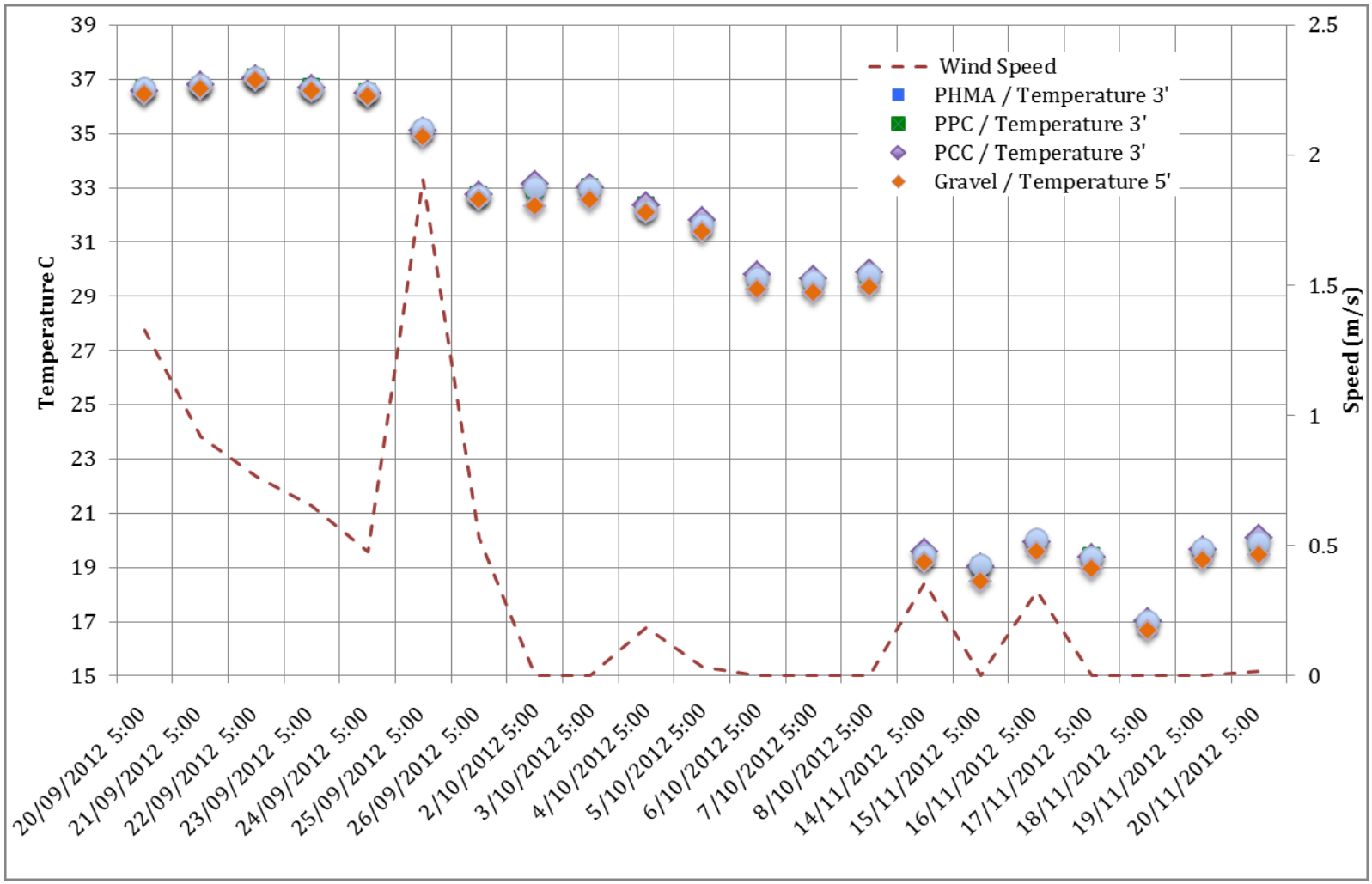

5 Feet Level (Air Temperature and Solar Radiation)

4am:

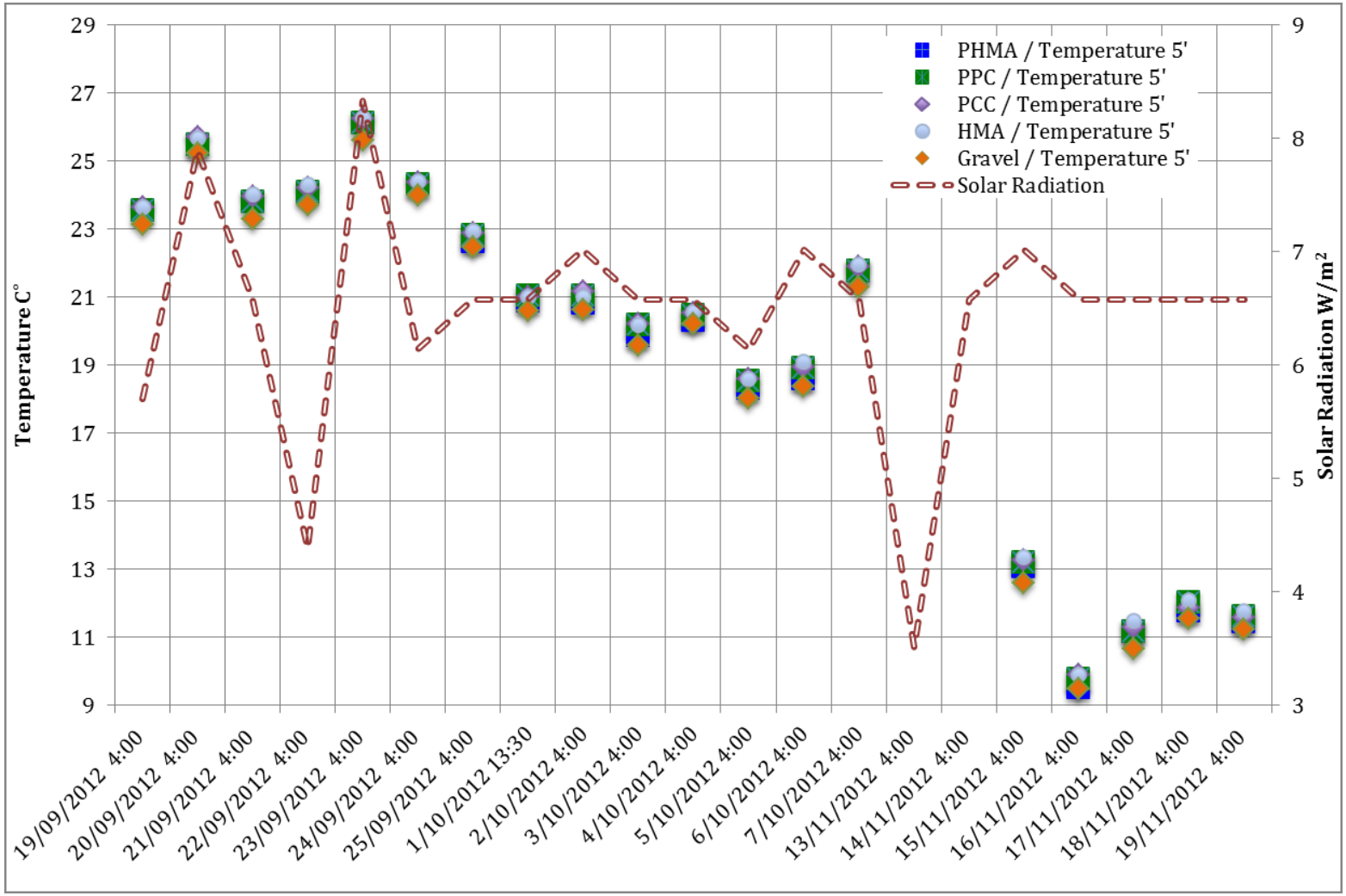

5 Feet Level (Air Temperature and Solar Radiation)

12pm:

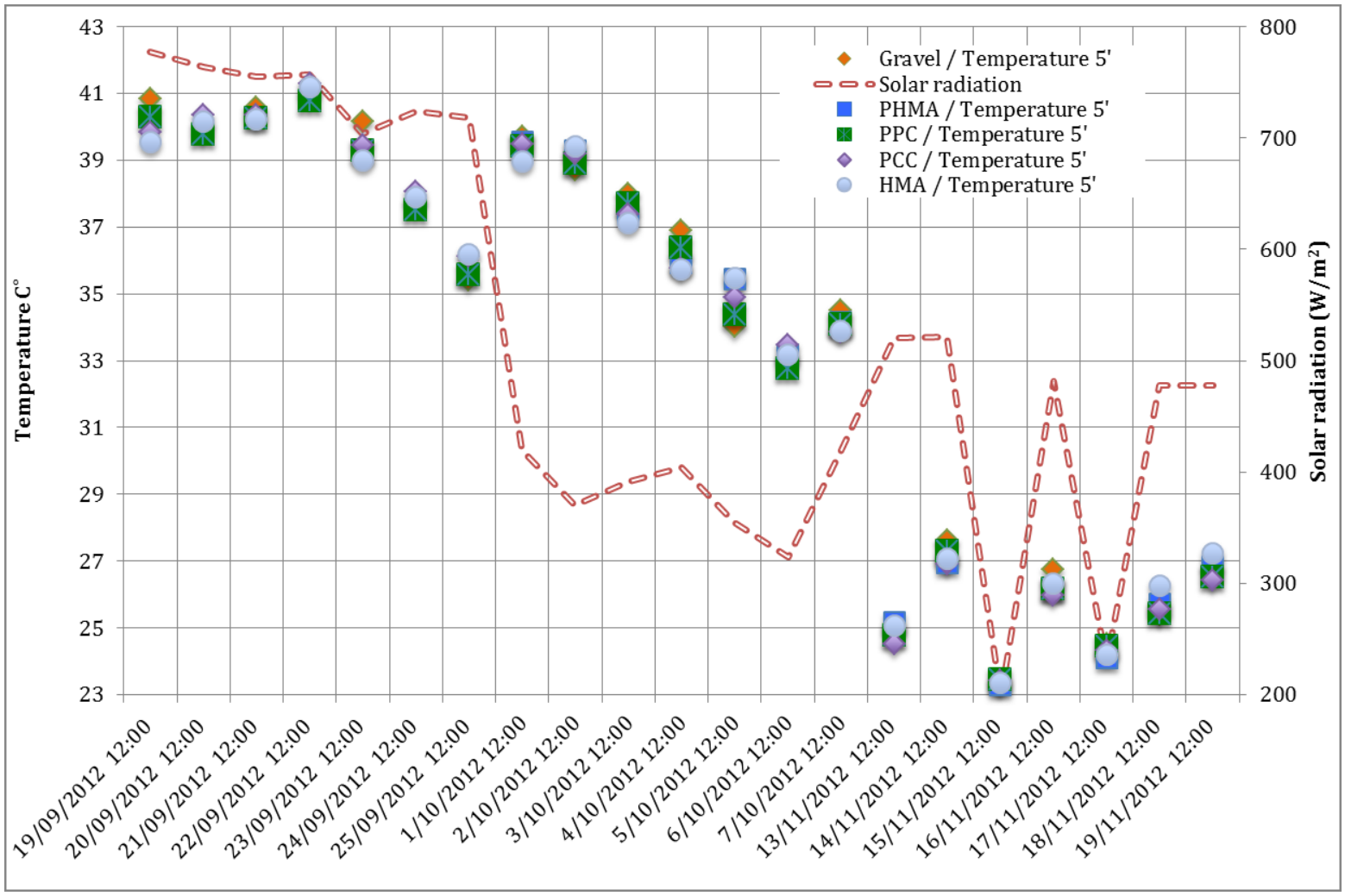

5 feet level (Air Temperature and Solar Radiation)

5pm:

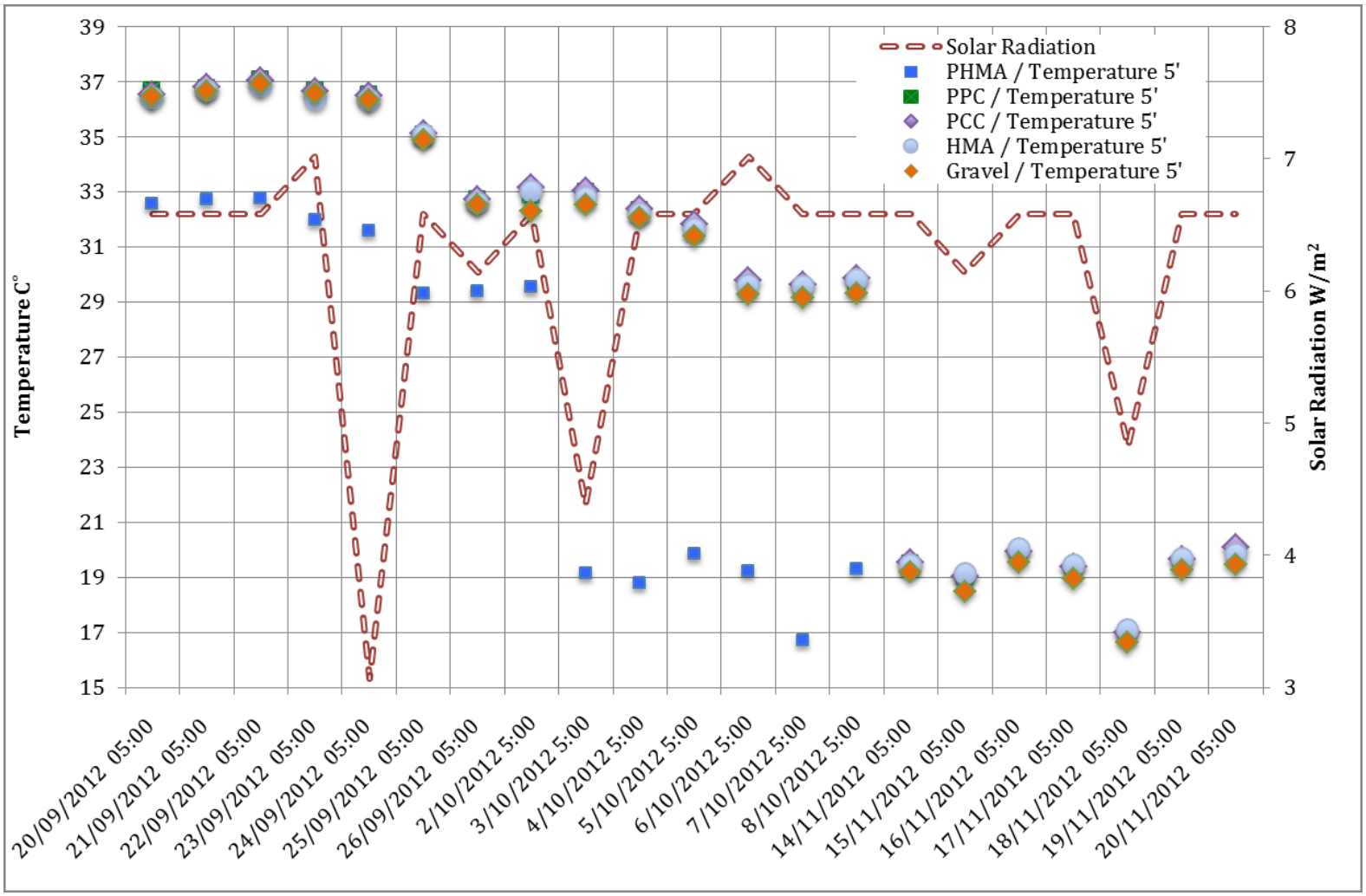

APPENDIX D

DELTA T, MAXIMUM AND MINIMUM TEMPERATURE

Temperature before sunset(4:00am)

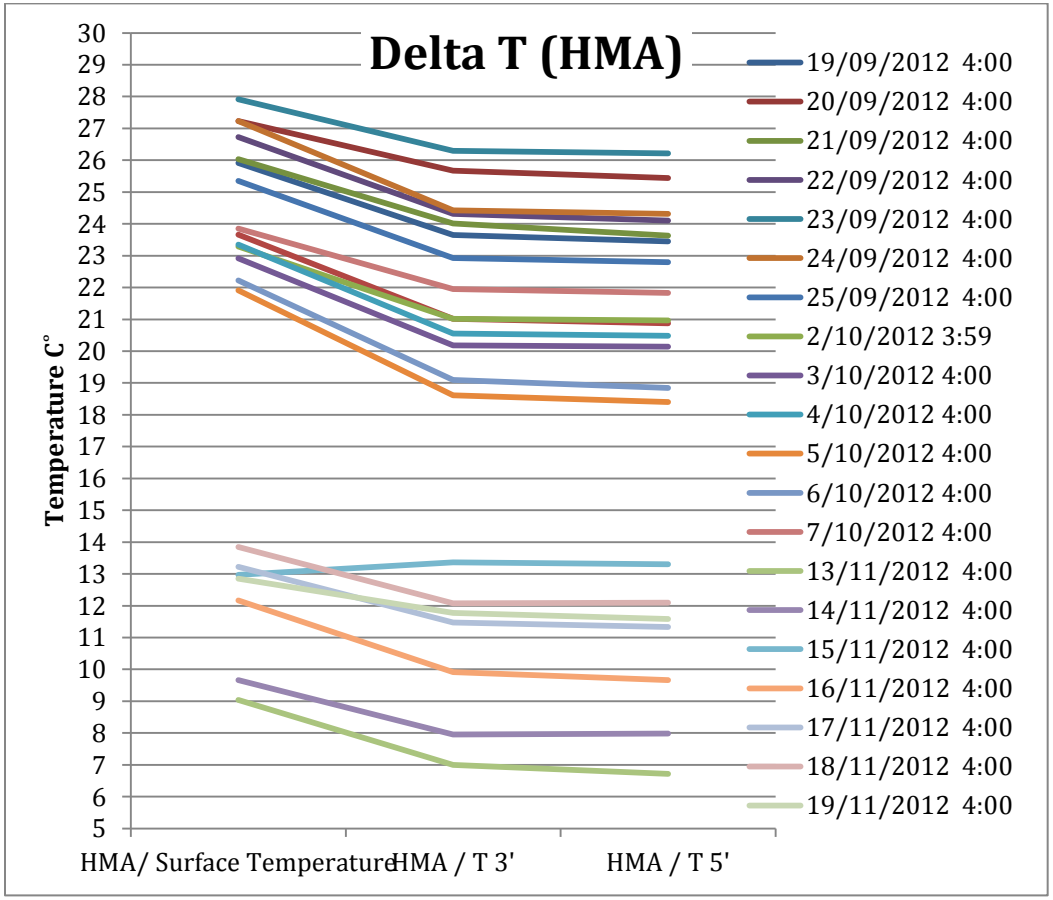

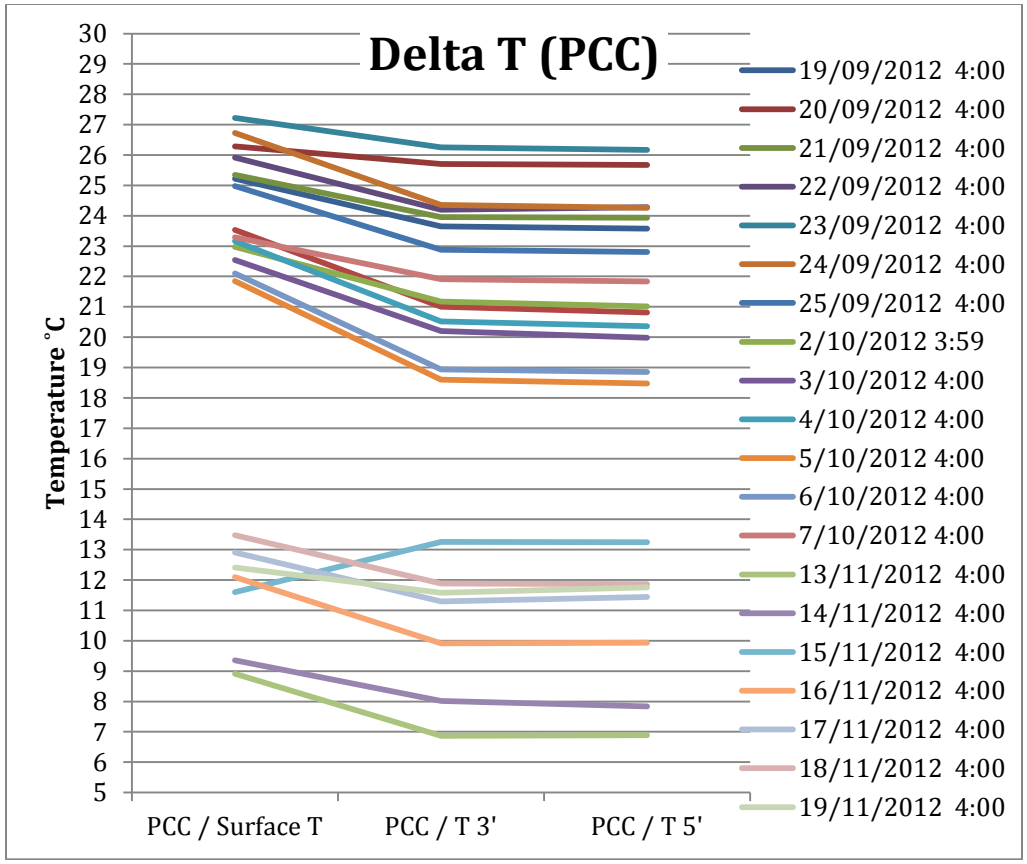
Delta T (PCC)
Temperature °C
30
29
28
27
26
25
24
23
22
21
20
19
18
17
16
15
14
13
12
11
10
9
8
7
6
5
PCC / Surface T
PCC / T 3'
PCC / T 5'
19/09/2012 4:00
20/09/2012 4:00
21/09/2012 4:00
22/09/2012 4:00
23/09/2012 4:00
24/09/2012 4:00
25/09/2012 4:00
2/10/2012 3:59
3/10/2012 4:00
4/10/2012 4:00
5/10/2012 4:00
6/10/2012 4:00
7/10/2012 4:00
13/11/2012 4:00
14/11/2012 4:00
15/11/2012 4:00
16/11/2012 4:00
17/11/2012 4:00
18/11/2012 4:00
19/11/2012 4:00

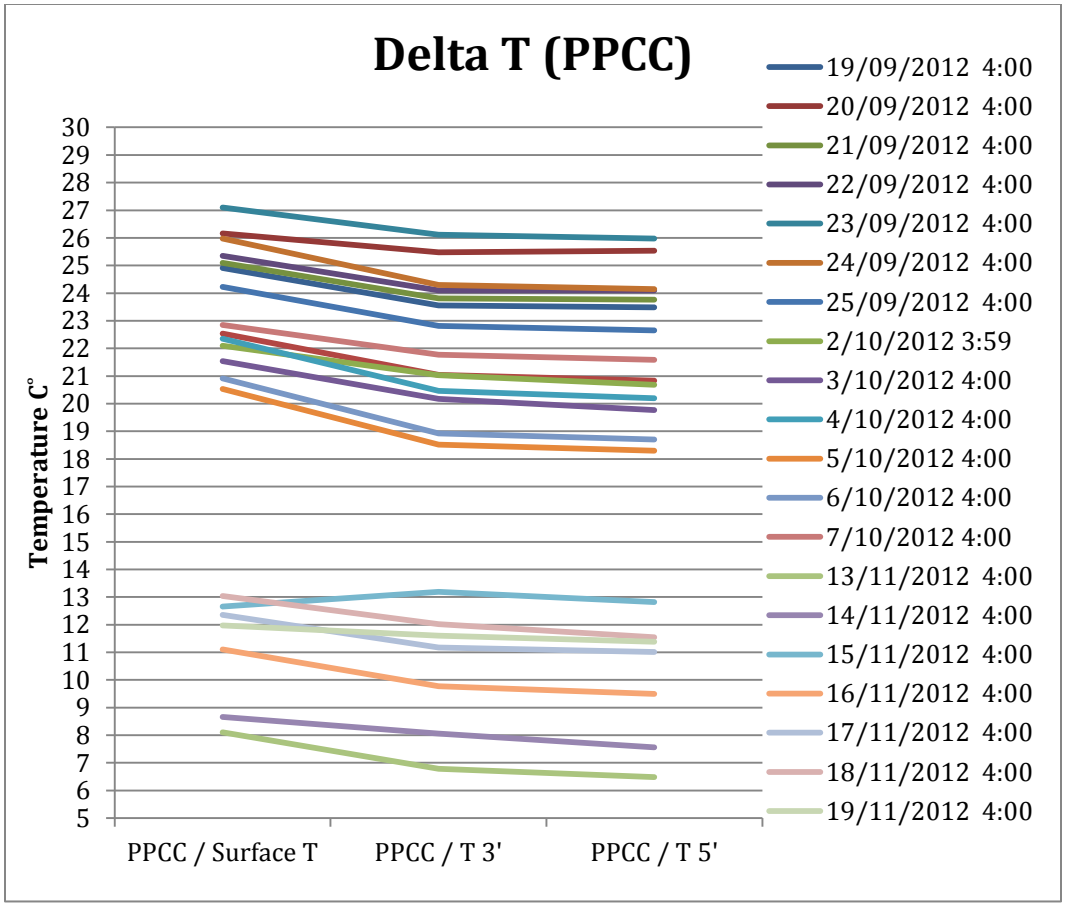
Delta T (PPCC)
Temperature C°
30
29
28
27
26
25
24
23
22
21
20
19
18
17
16
15
14
13
12
11
10
9
8
7
6
5
PPCC / Surface T
PPCC / T 3'
PPCC / T 5'
19/09/2012 4:00
20/09/2012 4:00
21/09/2012 4:00
22/09/2012 4:00
23/09/2012 4:00
24/09/2012 4:00
25/09/2012 4:00
2/10/2012 3:59
3/10/2012 4:00
4/10/2012 4:00
5/10/2012 4:00
6/10/2012 4:00
7/10/2012 4:00
13/11/2012 4:00
14/11/2012 4:00
15/11/2012 4:00
16/11/2012 4:00
17/11/2012 4:00
18/11/2012 4:00
19/11/2012 4:00

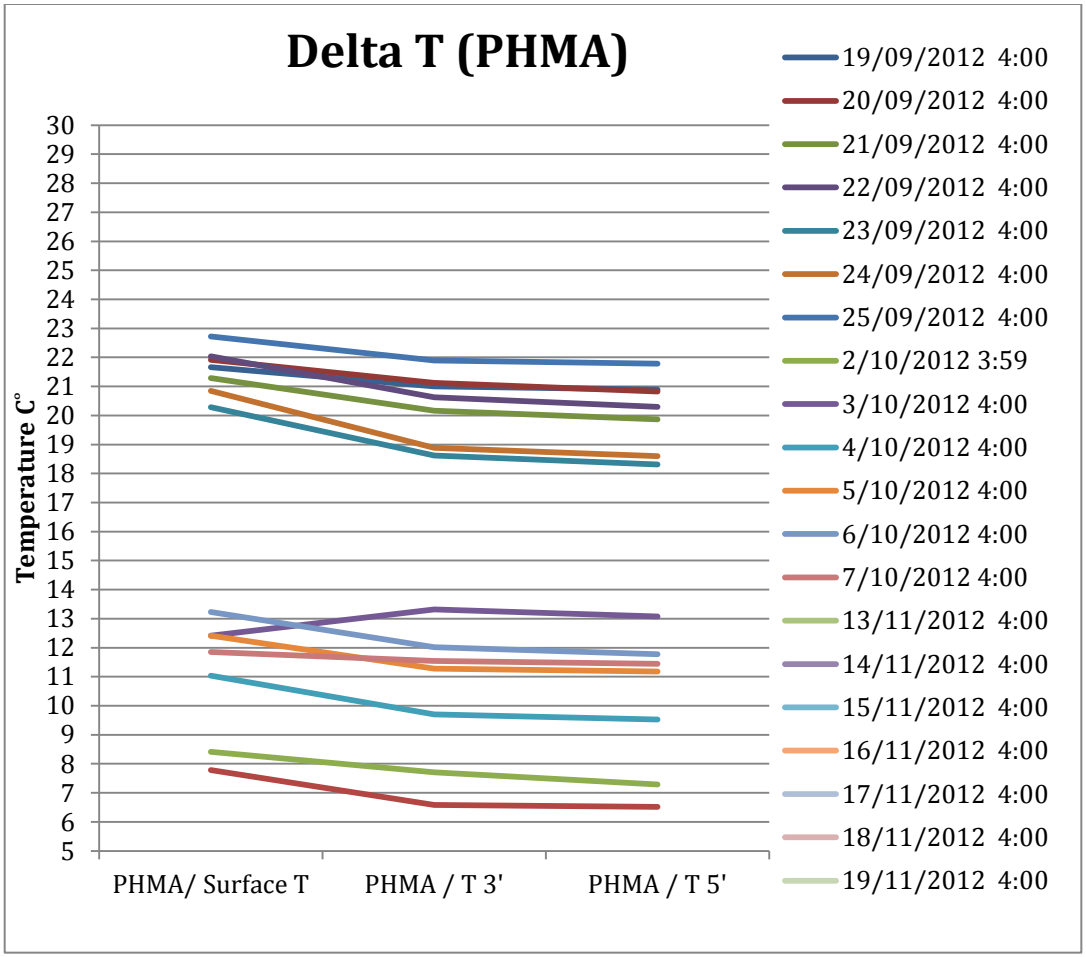
Delta T (PHMA)
Temperature C°
30
29
28
27
26
25
24
23
22
21
20
19
18
17
16
15
14
13
12
11
10
9
8
7
6
5
PHMA/ Surface T
PHMA / T 3'
PHMA / T 5'
19/09/2012 4:00
20/09/2012 4:00
21/09/2012 4:00
22/09/2012 4:00
23/09/2012 4:00
24/09/2012 4:00
25/09/2012 4:00
2/10/2012 3:59
3/10/2012 4:00
4/10/2012 4:00
5/10/2012 4:00
6/10/2012 4:00
7/10/2012 4:00
13/11/2012 4:00
14/11/2012 4:00
15/11/2012 4:00
16/11/2012 4:00
17/11/2012 4:00
18/11/2012 4:00
19/11/2012 4:00

Temperature at noon (12:00pm)

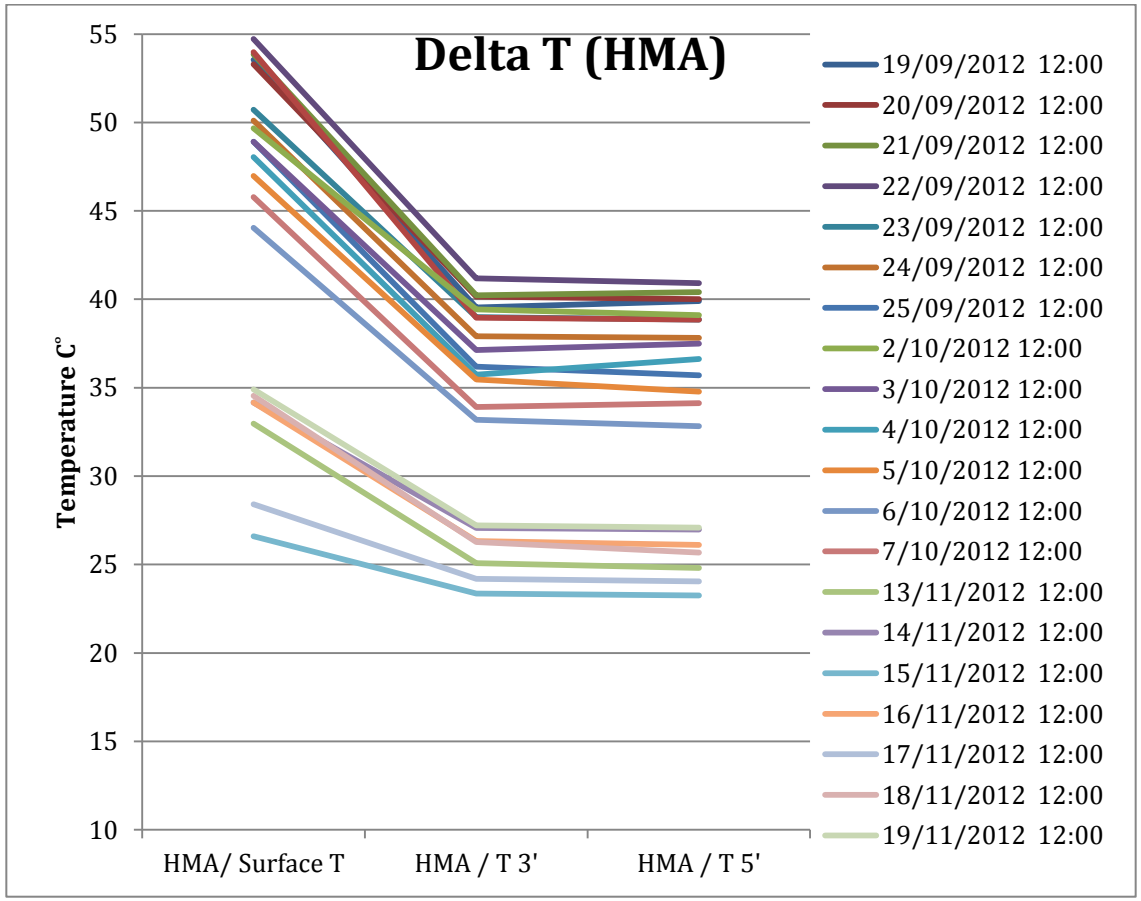

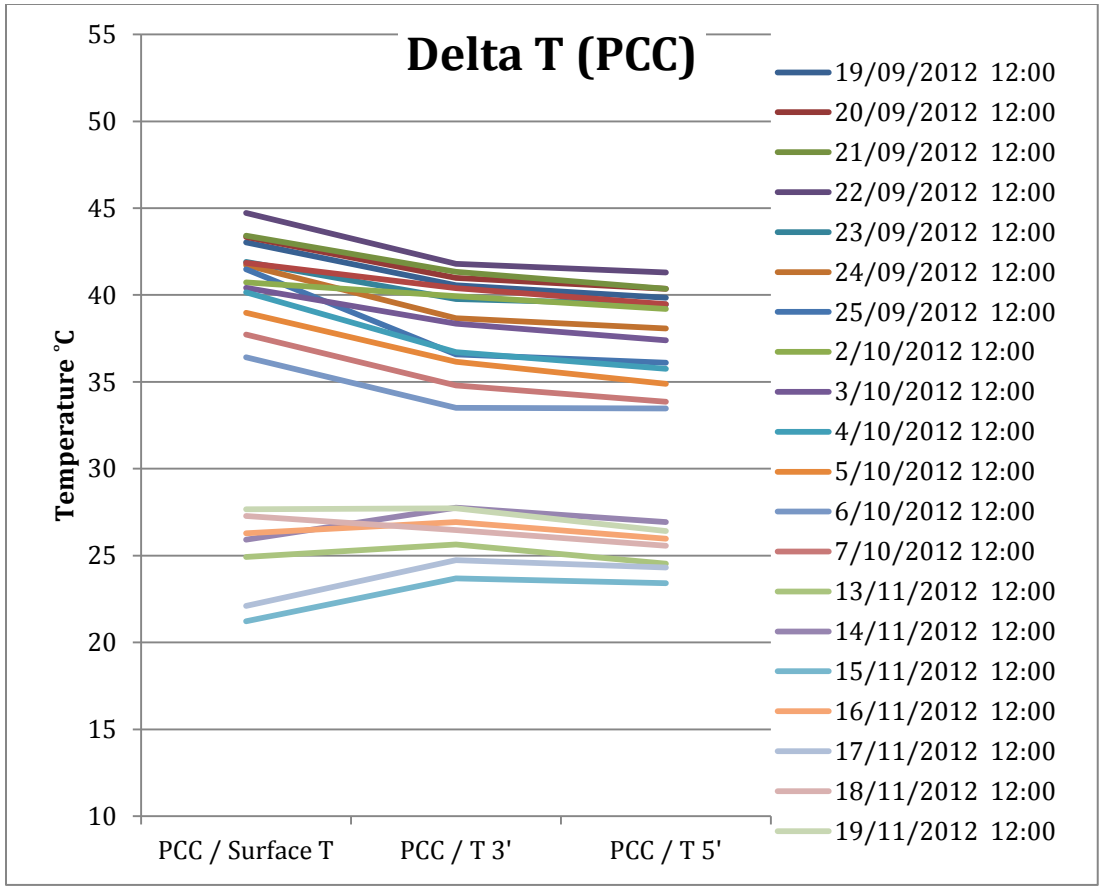
Delta T (PCC)
Temperature °C
55
50
45
40
35
30
25
20
15
10
PCC / Surface T
PCC / T 3'
PCC / T 5'
19/09/2012 12:00
20/09/2012 12:00
21/09/2012 12:00
22/09/2012 12:00
23/09/2012 12:00
24/09/2012 12:00
25/09/2012 12:00
2/10/2012 12:00
3/10/2012 12:00
4/10/2012 12:00
5/10/2012 12:00
6/10/2012 12:00
7/10/2012 12:00
13/11/2012 12:00
14/11/2012 12:00
15/11/2012 12:00
16/11/2012 12:00
17/11/2012 12:00
18/11/2012 12:00
19/11/2012 12:00

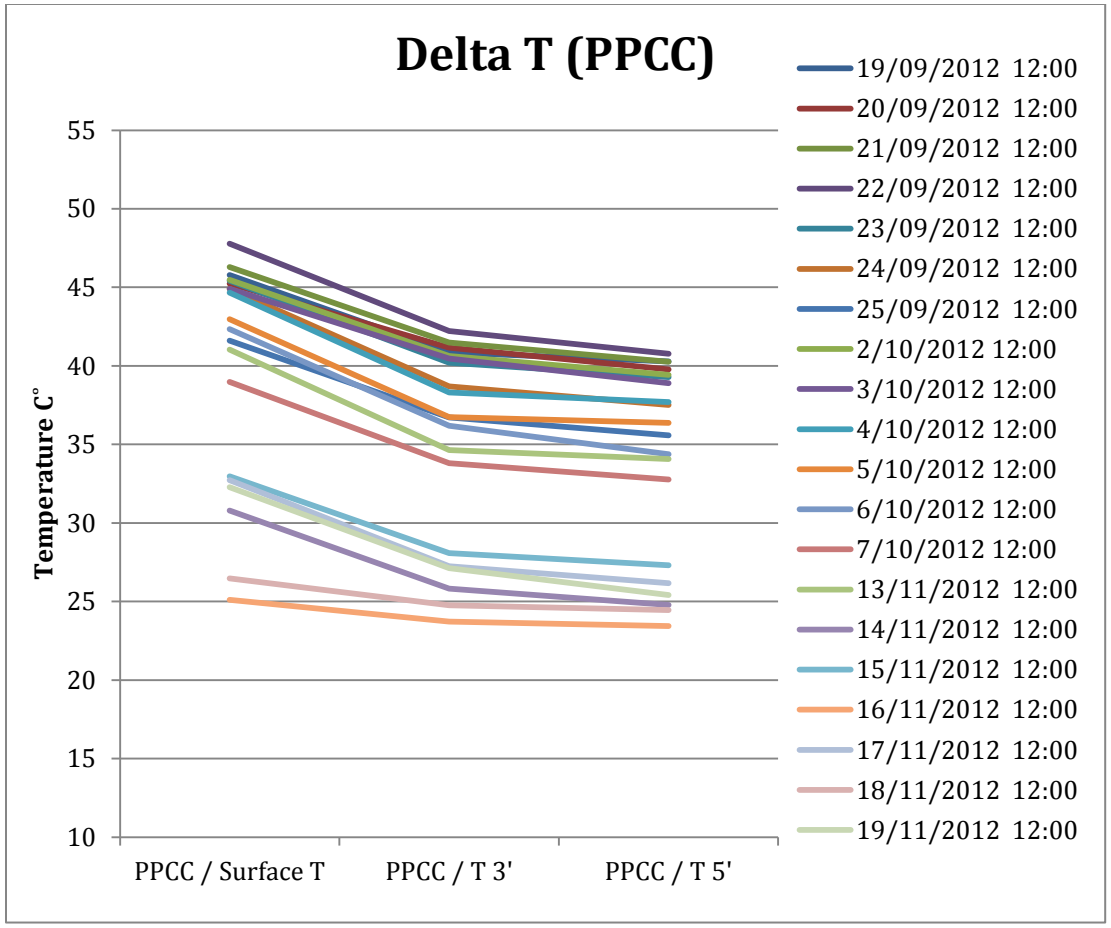
Delta T (PPCC)
Temperature C°
55
50
45
40
35
30
25
20
15
10
PPCC / Surface T
PPCC / T 3'
PPCC / T 5'
19/09/2012 12:00
20/09/2012 12:00
21/09/2012 12:00
22/09/2012 12:00
23/09/2012 12:00
24/09/2012 12:00
25/09/2012 12:00
2/10/2012 12:00
3/10/2012 12:00
4/10/2012 12:00
5/10/2012 12:00
6/10/2012 12:00
7/10/2012 12:00
13/11/2012 12:00
14/11/2012 12:00
15/11/2012 12:00
16/11/2012 12:00
17/11/2012 12:00
18/11/2012 12:00
19/11/2012 12:00

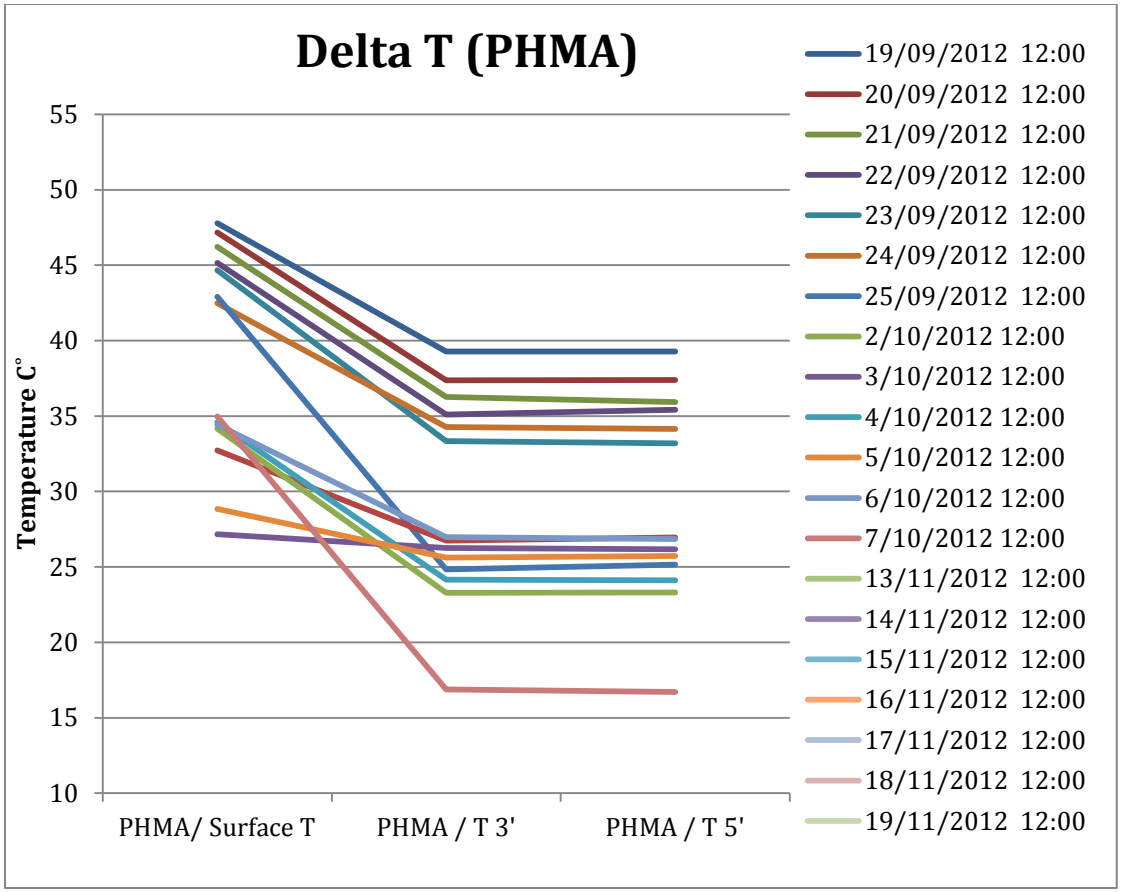
Delta T (PHMA)
Temperature C°
55
50
45
40
35
30
25
20
15
10
PHMA/ Surface T
PHMA / T 3'
PHMA / T 5'
19/09/2012 12:00
20/09/2012 12:00
21/09/2012 12:00
22/09/2012 12:00
23/09/2012 12:00
24/09/2012 12:00
25/09/2012 12:00
2/10/2012 12:00
3/10/2012 12:00
4/10/2012 12:00
5/10/2012 12:00
6/10/2012 12:00
7/10/2012 12:00
13/11/2012 12:00
14/11/2012 12:00
15/11/2012 12:00
16/11/2012 12:00
17/11/2012 12:00
18/11/2012 12:00
19/11/2012 12:00

Temperature after sunset (5:00pm)

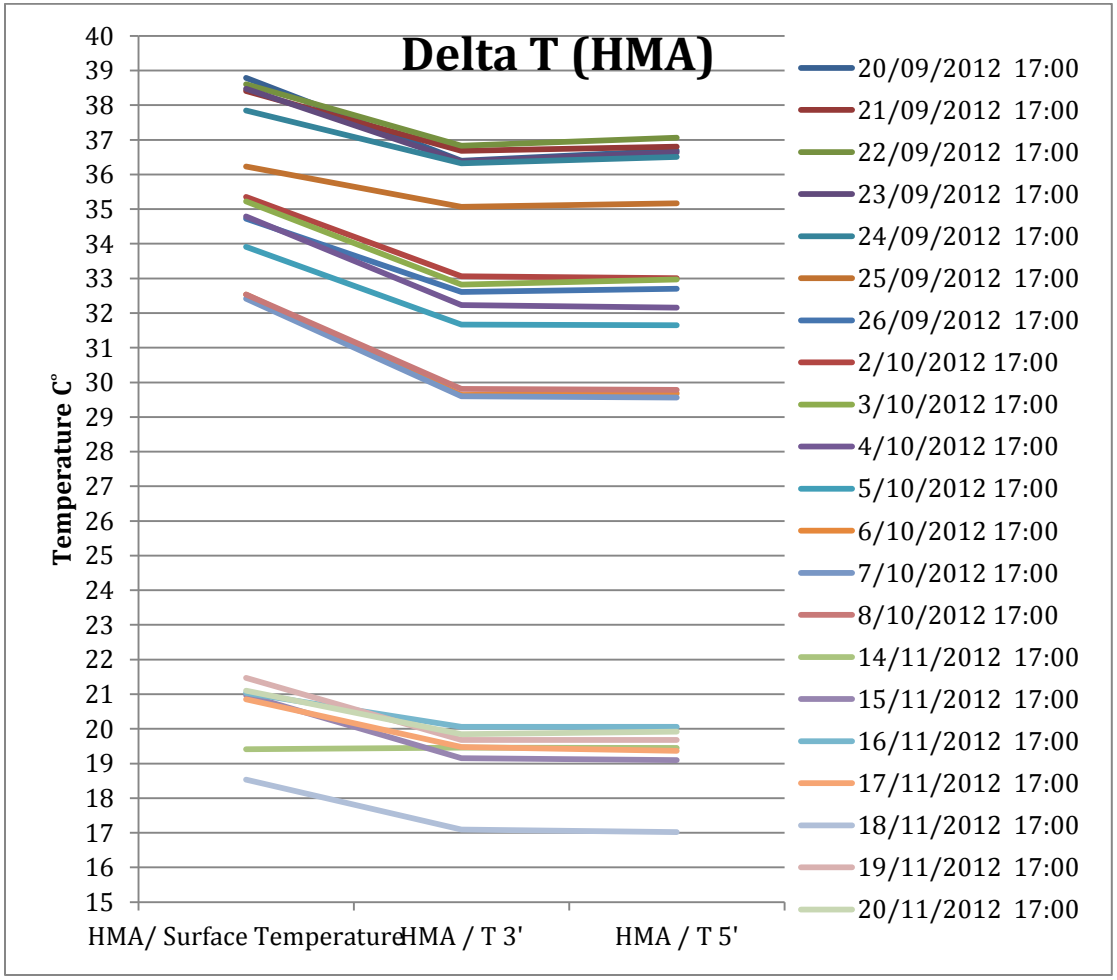

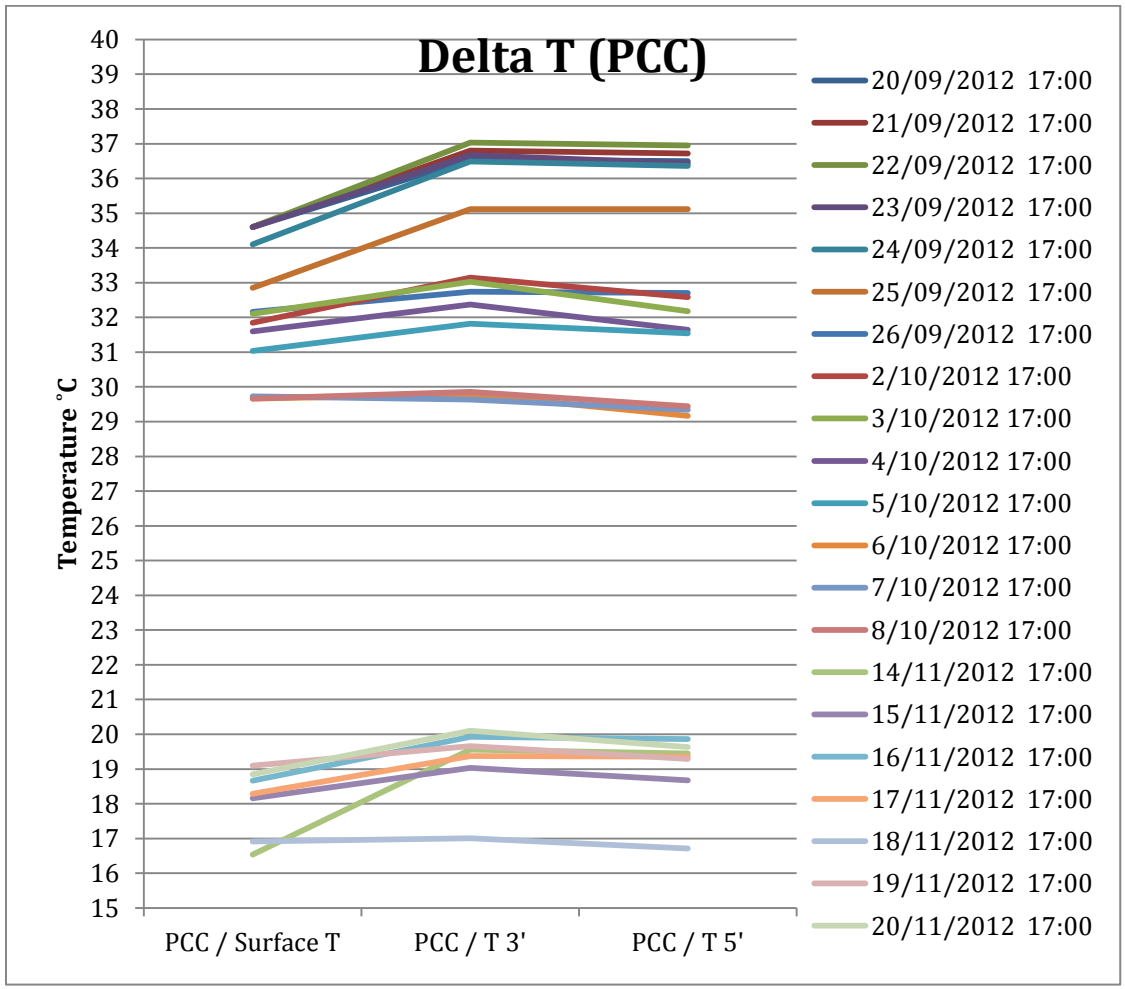
Delta T (PCC)
Temperature °C
40
39
38
37
36
35
34
33
32
31
30
29
28
27
26
25
24
23
22
21
20
19
18
17
16
15
PCC / Surface T
PCC / T 3'
PCC / T 5'
20/09/2012 17:00
21/09/2012 17:00
22/09/2012 17:00
23/09/2012 17:00
24/09/2012 17:00
25/09/2012 17:00
26/09/2012 17:00
2/10/2012 17:00
3/10/2012 17:00
4/10/2012 17:00
5/10/2012 17:00
6/10/2012 17:00
7/10/2012 17:00
8/10/2012 17:00
14/11/2012 17:00
15/11/2012 17:00
16/11/2012 17:00
17/11/2012 17:00
18/11/2012 17:00
19/11/2012 17:00
20/11/2012 17:00

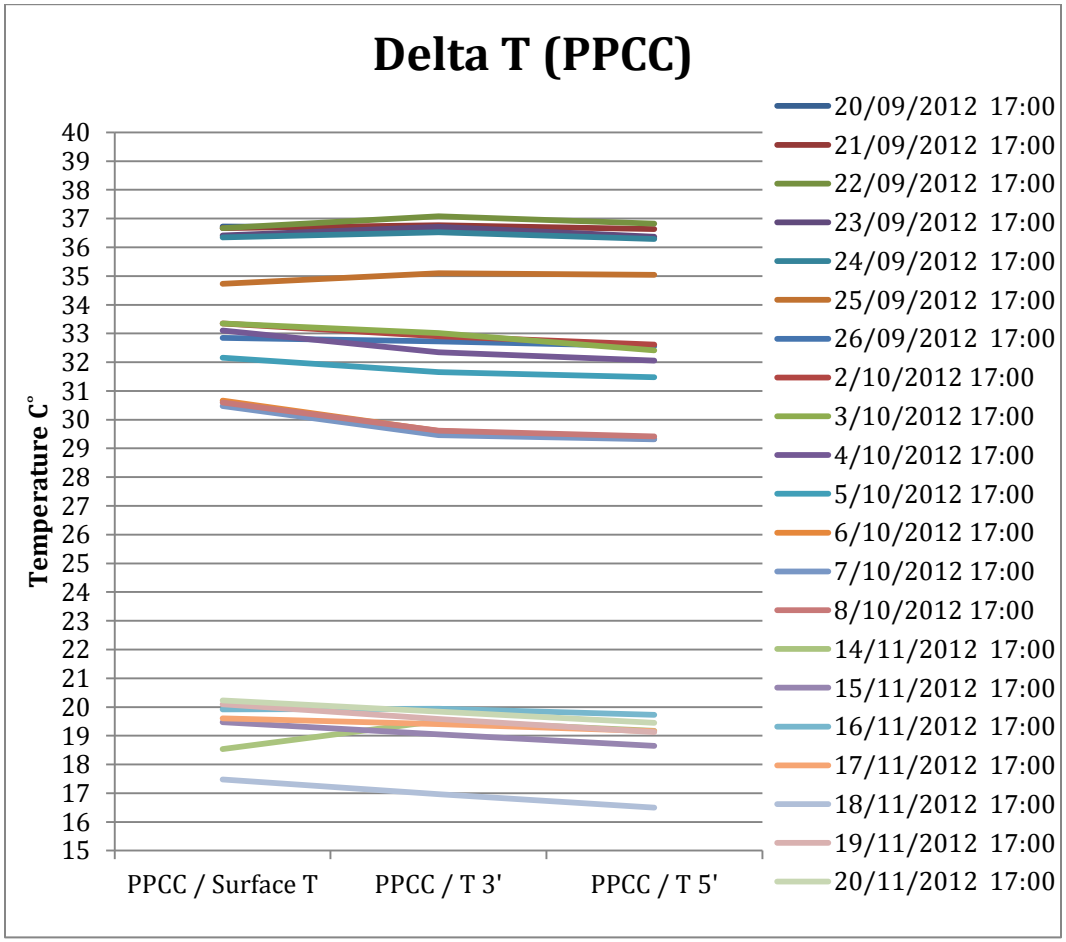
Delta T (PPCC)
Temperature C°
40
39
38
37
36
35
34
33
32
31
30
29
28
27
26
25
24
23
22
21
20
19
18
17
16
15
PPCC / Surface T
PPCC / T 3'
PPCC / T 5'
20/09/2012 17:00
21/09/2012 17:00
22/09/2012 17:00
23/09/2012 17:00
24/09/2012 17:00
25/09/2012 17:00
26/09/2012 17:00
2/10/2012 17:00
3/10/2012 17:00
4/10/2012 17:00
5/10/2012 17:00
6/10/2012 17:00
7/10/2012 17:00
8/10/2012 17:00
14/11/2012 17:00
15/11/2012 17:00
16/11/2012 17:00
17/11/2012 17:00
18/11/2012 17:00
19/11/2012 17:00
20/11/2012 17:00

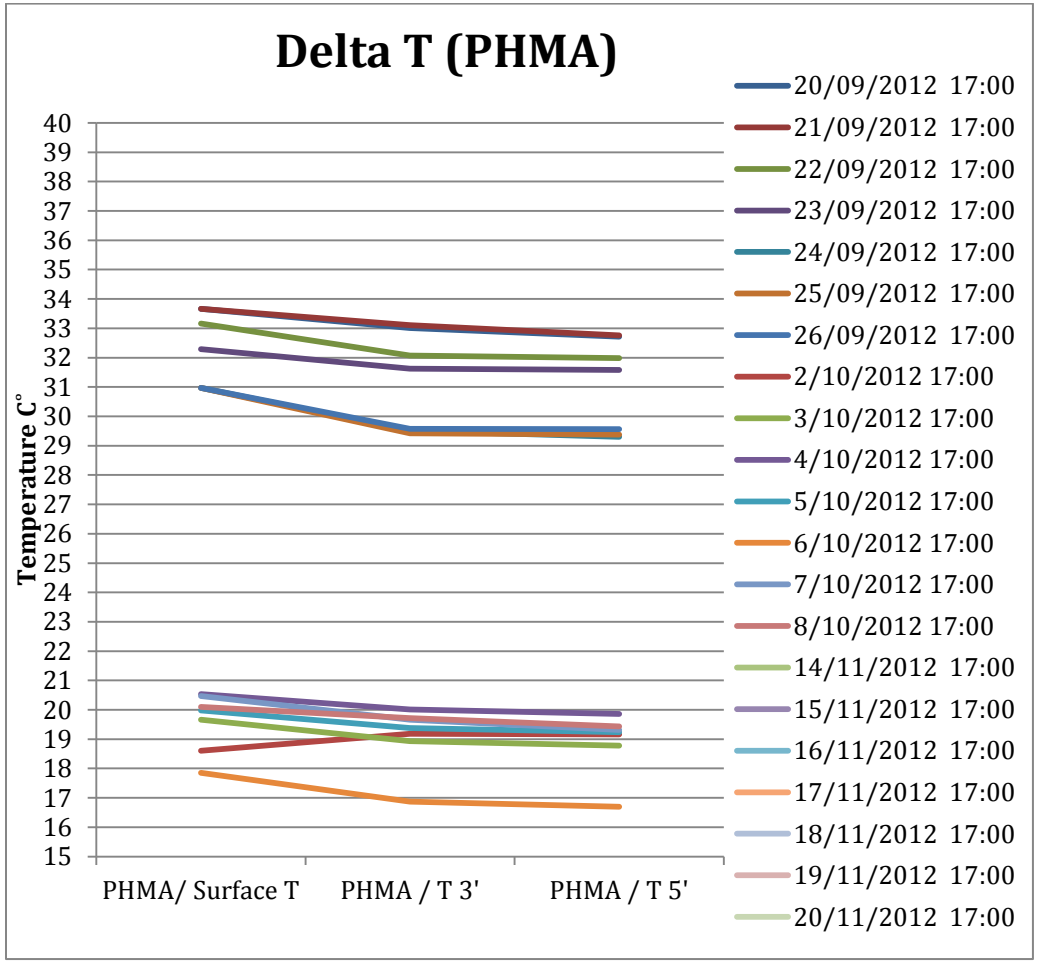
Delta T (PHMA)
Temperature C°
40
39
38
37
36
35
34
33
32
31
30
29
28
27
26
25
24
23
22
21
20
19
18
17
16
15
PHMA/ Surface T
PHMA / T 3'
PHMA / T 5'
20/09/2012 17:00
21/09/2012 17:00
22/09/2012 17:00
23/09/2012 17:00
24/09/2012 17:00
25/09/2012 17:00
26/09/2012 17:00
2/10/2012 17:00
3/10/2012 17:00
4/10/2012 17:00
5/10/2012 17:00
6/10/2012 17:00
7/10/2012 17:00
8/10/2012 17:00
14/11/2012 17:00
15/11/2012 17:00
16/11/2012 17:00
17/11/2012 17:00
18/11/2012 17:00
19/11/2012 17:00
20/11/2012 17:00

Min and Max Temperatures (random days)

	Min Temperature C°								
	2-Oct			4-Nov			26-Nov		
	Surface	3'	5'	Surface	3'	5'	Surface	3'	5'
HMA	23.04	20.58	20.75	14.85	11.84	12.19	11.35	8.72	9
PCC	22.73	20.49	20.76	14.73	12.02	12.02	11.29	8.82	8.92
PPC	21.98	20.64	20.31	13.66	11.83	11.62	10.2	8.42	8.85
PHMA	21.66	20.79	20.44	13.54	11.9	11.82	10.16	8.76	8.43
Turf	16.537	21.1517		8.91	12.63	12.08	5.54	9.62	9.07
Gravel	18.225	21.1	20.09	10.6	12.58	11.5	7.35	9.57	8.32

	Max Temperature C°								
	2-Oct			4-Nov			4-Nov		
	Surface	3'	5'	Surface	3'	5'	Surface	3'	5'
HMA	52.85	40.17	39.97	42.04	32.8	32.75	33.91	27.36	27.17
PCC	42.413	40.98	40.14	33.41	32.72	32.23	26.47	27.28	26.53
PPC	46.23	40.25	40.82	38.91	32.57	32.97	32.5	27.22	27.1
PHMA	50.48	40.68	40.64	41.41	32.71	32.51	34.16	27.19	27.16
Turf	62.975	40.62		49.725	33.14	32.59	39.35	27.65	27.09
Gravel	52.91	40.58	40.42	44.48	33.09	32.39	36.725	28.1	27.12

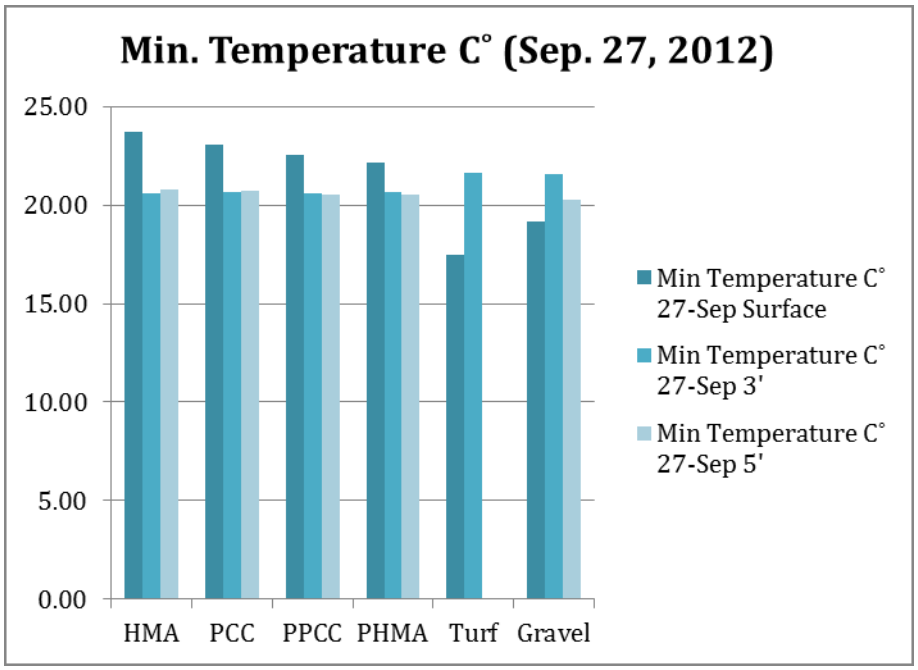
Min. Temperature C° (Sep. 27, 2012)
25.00
20.00
15.00
10.00
5.00
0.00
HMA
PCC
PPCC
PHMA
Turf
Gravel
Min Temperature C° 27-Sep Surface
Min Temperature C° 27-Sep 3'
Min Temperature C° 27-Sep 5'

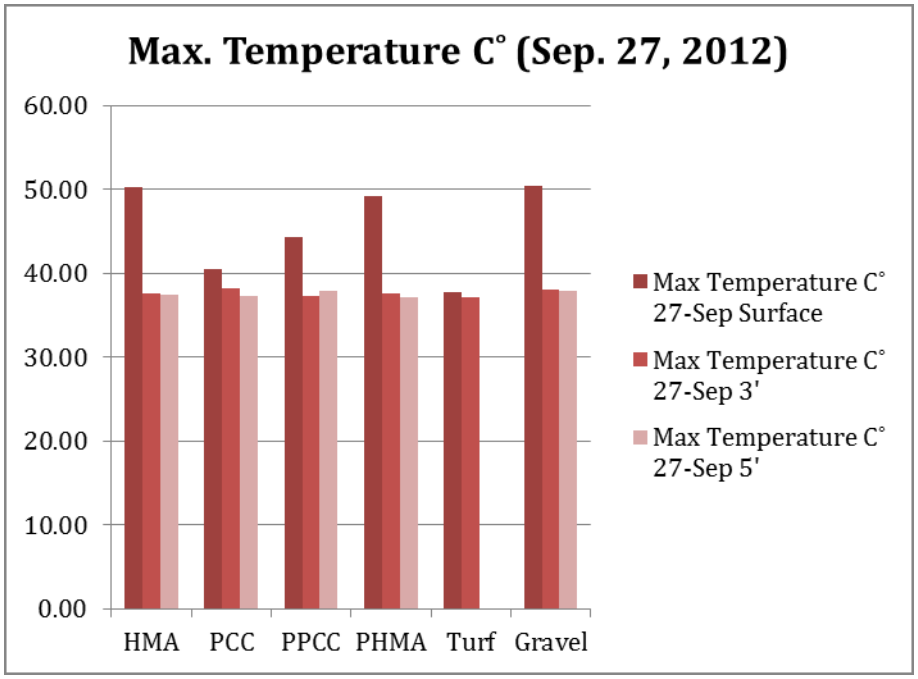
Max. Temperature C° (Sep. 27, 2012)
60.00
50.00
40.00
30.00
20.00
10.00
0.00
HMA
PCC
PPCC
PHMA
Turf
Gravel
Max Temperature C° 27-Sep Surface
Max Temperature C° 27-Sep 3'
Max Temperature C° 27-Sep 5'

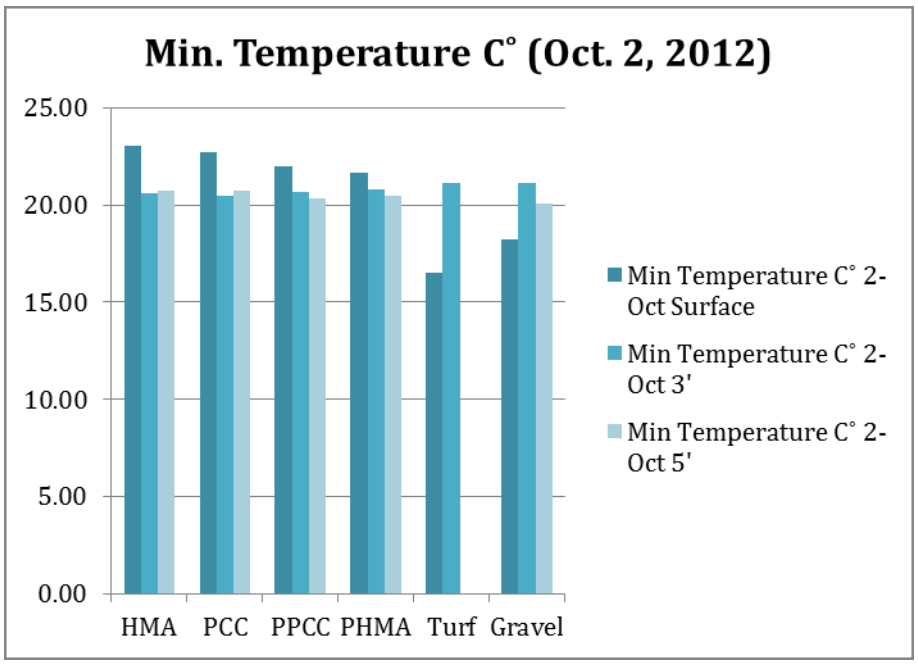
Min. Temperature C° (Oct. 2, 2012)
25.00
20.00
15.00
10.00
5.00
0.00
HMA
PCC
PPCC
PHMA
Turf
Gravel
Min Temperature C° 2-Oct Surface
Min Temperature C° 2-Oct 3'
Min Temperature C° 2-Oct 5'

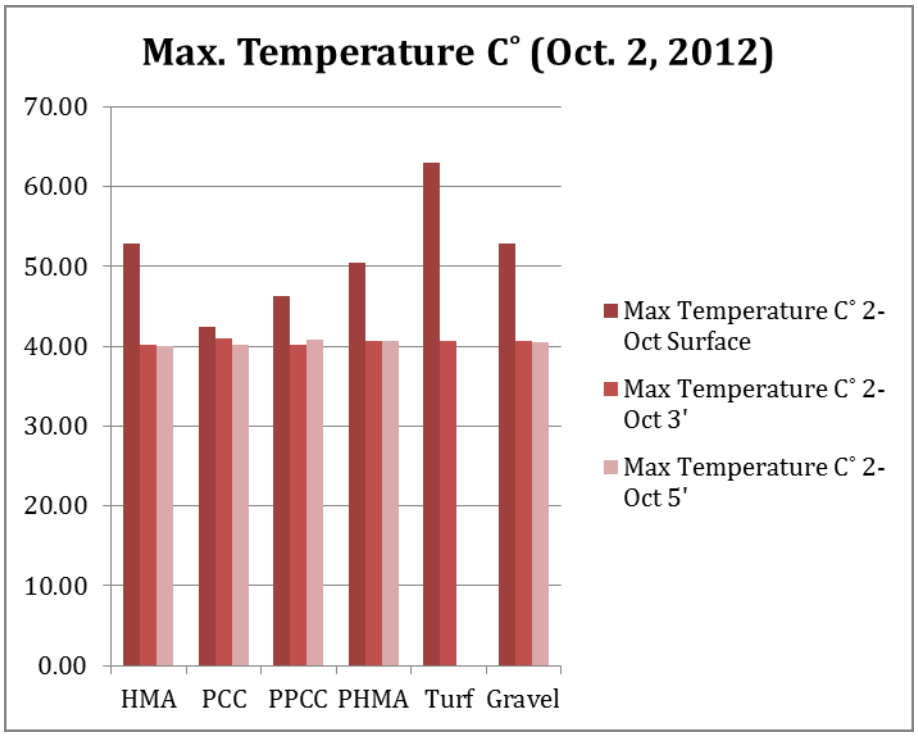
Max. Temperature C° (Oct. 2, 2012)
70.00
60.00
50.00
40.00
30.00
20.00
10.00
0.00
HMA
PCC
PPCC
PHMA
Turf
Gravel
Max Temperature C° 2-Oct Surface
Max Temperature C° 2-Oct 3'
Max Temperature C° 2-Oct 5'

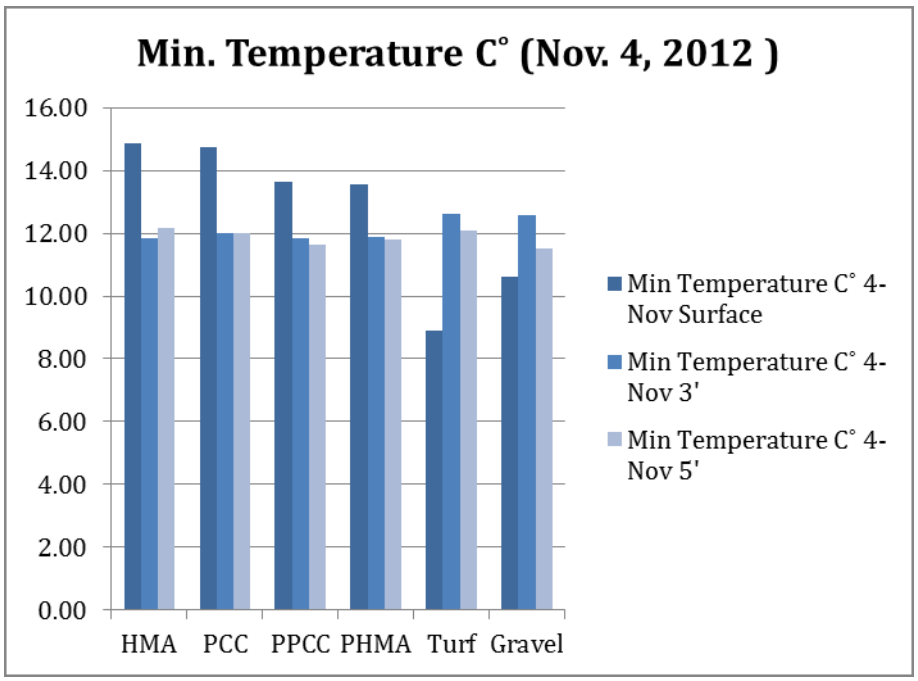
Min. Temperature C° (Nov. 4, 2012)
16.00
14.00
12.00
10.00
8.00
6.00
4.00
2.00
0.00
HMA
PCC
PPCC
PHMA
Turf
Gravel
Min Temperature C° 4-Nov Surface
Min Temperature C° 4-Nov 3'
Min Temperature C° 4-Nov 5'

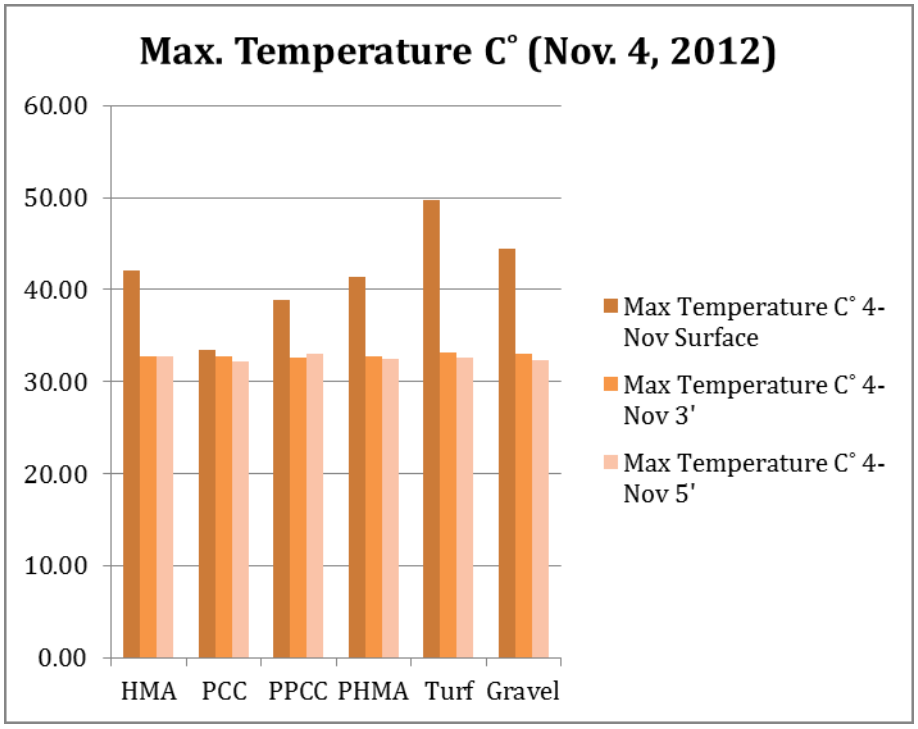
Max. Temperature C° (Nov. 4, 2012)
60.00
50.00
40.00
30.00
20.00
10.00
0.00
HMA
PCC
PPCC
PHMA
Turf
Gravel
Max Temperature C° 4-Nov Surface
Max Temperature C° 4-Nov 3'
Max Temperature C° 4-Nov 5'

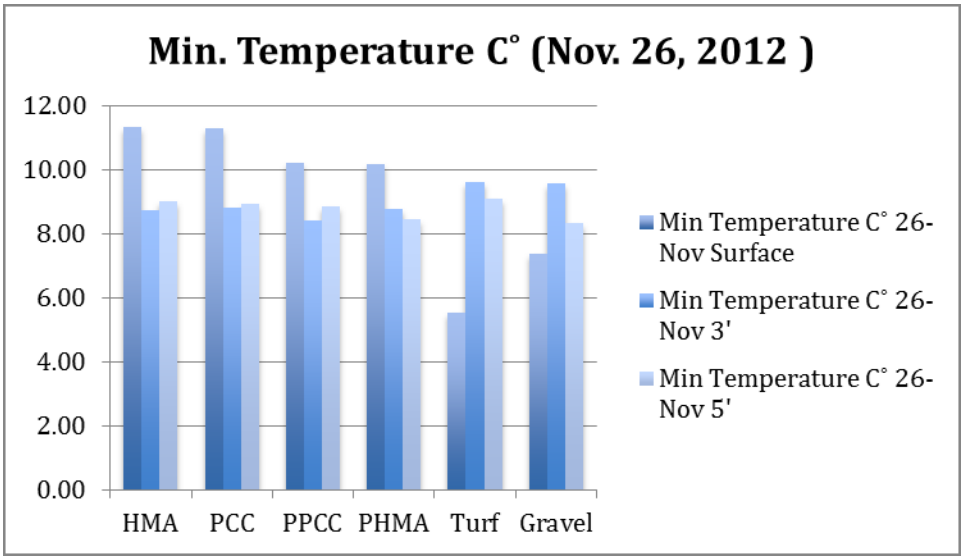
Min. Temperature C° (Nov. 26, 2012)
12.00
10.00
8.00
6.00
4.00
2.00
0.00
HMA
PCC
PPCC
PHMA
Turf
Gravel
Min Temperature C° 26-Nov Surface
Min Temperature C° 26-Nov 3'
Min Temperature C° 26-Nov 5'

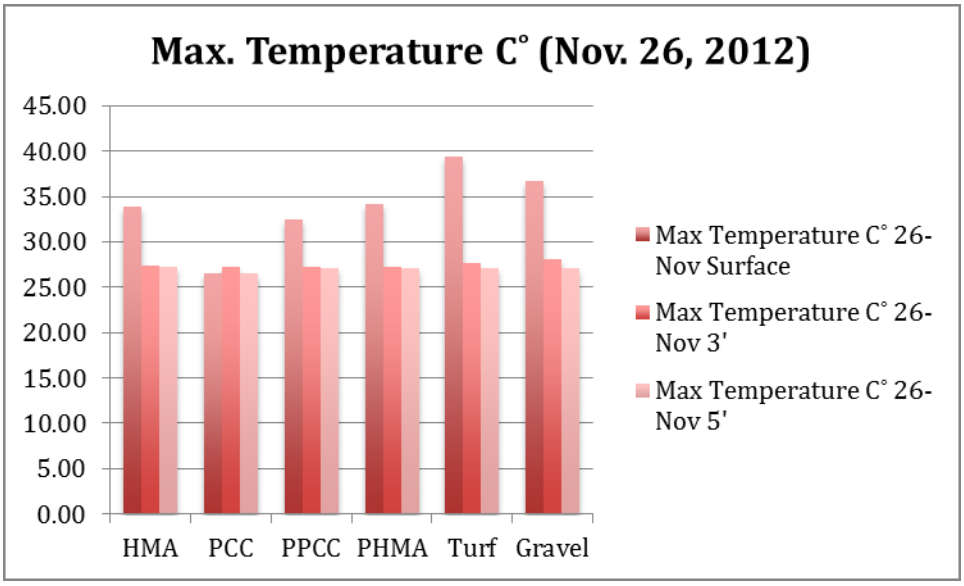
Max. Temperature C° (Nov. 26, 2012)
45.00
40.00
35.00
30.00
25.00
20.00
15.00
10.00
5.00
0.00
HMA
PCC
PPCC
PHMA
Turf
Gravel
Max Temperature C° 26-Nov Surface
Max Temperature C° 26-Nov 3'
Max Temperature C° 26-Nov 5'

APPENDIX E

T-PAIRED TEST OUT-PUT

Surface Temperature

Paired T-Test and CI: HMA/ Surface Temperature, PPCC / Surface Temperature

Paired T for HMA/ Surface Temperature - PPCC / Surface Temperature

	N	Mean	StDev	SE Mean
HMA/ Surface Temperature	62763	31.0653	9.4592	0.0378
PPCC / Surface Temperatu	62763	28.8915	8.3505	0.0333
Difference	62763	2.17383	2.09247	0.00835

95% lower bound for mean difference: 2.16009
T-Test of mean difference = 0.1 (vs > 0.1): T-Value = 248.29 P-Value = 0.000

Paired T-Test and CI: HMA/ Surface Temperature, PHMA/ Surface Temperature

Paired T for HMA/ Surface Temperature - PHMA/ Surface Temperature

	N	Mean	StDev	SE Mean
HMA/ Surface Temperature	53227	29.9619	9.1262	0.0396
PHMA/ Surface Temperatur	53227	29.0536	9.2718	0.0402
Difference	53227	0.9083	9.6755	0.0419

95% lower bound for mean difference: 0.8394
T-Test of mean difference = 0.1 (vs > 0.1): T-Value = 19.27 P-Value = 0.000

Paired T-Test and CI: HMA/ Surface Temperature, PCC / Surface Temperature

Paired T for HMA/ Surface Temperature - PCC / Surface Temperature

	N	Mean	StDev	SE Mean
HMA/ Surface Temperature	61341	31.0845	9.4623	0.0382
PCC / Surface Temperatur	61341	27.4896	6.7550	0.0273
Difference	61341	3.5949	3.1268	0.0126

95% lower bound for mean difference: 3.5741
T-Test of mean difference = 0.1 (vs > 0.1): T-Value = 276.83 P-Value = 0.000

Paired T-Test and CI: HMA/ Surface Temperature, Gravel / Surface Temperature

Paired T for HMA/ Surface Temperature - Gravel / Surface Temperature

	N	Mean	StDev	SE Mean
HMA/ Surface Temperature	63036	31.0922	9.4548	0.0377
Gravel / Surface Tempera	63036	27.9800	10.6054	0.0422
Difference	63036	3.1123	5.3398	0.0213

95% lower bound for mean difference: 3.0773
T-Test of mean difference = 0.1 (vs > 0.1): T-Value = 141.63 P-Value = 0.000

Paired T-Test and CI: HMA/ Surface Temperature, Turf / Surface Temperature

Paired T for HMA/ Surface Temperature - Turf / Surface Temperature

	N	Mean	StDev	SE Mean
HMA/ Surface Temperature	62863	31.0723	9.4570	0.0377
Turf / Surface Temperatu	62863	28.2594	14.0096	0.0559
Difference	62863	2.8128	17.2407	0.0688

95% lower bound for mean difference: 2.6997
T-Test of mean difference = 0.1 (vs > 0.1): T-Value = 39.45 P-Value = 0.000

Paired T-Test and CI: PPCC / Surface Temperature, Turf / Surface Temperature

Paired T for PPCC / Surface Temperature - Turf / Surface Temperature

	N	Mean	StDev	SE Mean
PPCC / Surface Temperatu	64327	28.8694	8.3476	0.0329
Turf / Surface Temperatu	64327	28.2851	14.0137	0.0553
Difference	64327	0.5842	16.8287	0.0664

95% lower bound for mean difference: 0.4751
T-Test of mean difference = 0.1 (vs > 0.1): T-Value = 7.30 P-Value = 0.000

Paired T-Test and CI: PPCC / Surface Temperature, Gravel / Surface Temperature

Paired T for PPCC / Surface Temperature - Gravel / Surface Temperature

	N	Mean	StDev	SE Mean
PPCC / Surface Temperatu	64142	28.9196	8.3351	0.0329
Gravel / Surface Tempera	64142	27.9918	10.6108	0.0419
Difference	64142	0.9278	5.9358	0.0234

95% lower bound for mean difference: 0.8893
T-Test of mean difference = 0.1 (vs > 0.1): T-Value = 35.32 P-Value = 0.000

Paired T-Test and CI: PPCC / Surface Temperature, PCC / Surface Temperature

Paired T for PPCC / Surface Temperature - PCC / Surface Temperature

	N	Mean	StDev	SE Mean
PPCC / Surface Temperatu	62757	28.8821	8.3542	0.0333
PCC / Surface Temperatur	62757	27.4696	6.7566	0.0270
Difference	62757	1.41247	2.31557	0.00924

95% lower bound for mean difference: 1.39726
T-Test of mean difference = 0.1 (vs > 0.1): T-Value = 141.99 P-Value = 0.000

Paired T-Test and CI: PPCC / Surface Temperature, PHMA/ Surface Temperature

Paired T for PPCC / Surface Temperature - PHMA/ Surface Temperature

	N	Mean	StDev	SE Mean
PPCC / Surface Temperatu	54476	27.8310	8.1030	0.0347
PHMA/ Surface Temperatur	54476	29.0442	9.2695	0.0397
Difference	54476	-1.2132	9.6935	0.0415

95% lower bound for mean difference: -1.2815
T-Test of mean difference = 0.1 (vs > 0.1): T-Value = -31.62 P-Value = 1.000

Paired T-Test and CI: PHMA/ Surface Temperature, PCC / Surface Temperature

Paired T for PHMA/ Surface Temperature - PCC / Surface Temperature

	N	Mean	StDev	SE Mean
PHMA/ Surface Temperatur	53174	29.0673	9.2626	0.0402
PCC / Surface Temperatur	53174	26.4740	6.4661	0.0280
Difference	53174	2.5933	8.8461	0.0384

95% lower bound for mean difference: 2.5302
T-Test of mean difference = 0.1 (vs > 0.1): T-Value = 64.99 P-Value = 0.000

Paired T-Test and CI: PHMA/ Surface Temperature, Gravel / Surface Temperature

Paired T for PHMA/ Surface Temperature - Gravel / Surface Temperature

	N	Mean	StDev	SE Mean
PHMA/ Surface Temperatur	54274	29.0757	9.2614	0.0398
Gravel / Surface Tempera	54274	26.9045	10.2620	0.0440
Difference	54274	2.1713	7.6712	0.0329

95% lower bound for mean difference: 2.1171
T-Test of mean difference = 0.1 (vs > 0.1): T-Value = 62.90 P-Value = 0.000

Paired T-Test and CI: PHMA/ Surface Temperature, Turf / Surface Temperature

Paired T for PHMA/ Surface Temperature - Turf / Surface Temperature

	N	Mean	StDev	SE Mean
PHMA/ Surface Temperatur	54534	29.0458	9.2672	0.0397
Turf / Surface Temperatu	54534	27.2018	13.6853	0.0586
Difference	54534	1.8440	15.1901	0.0650

95% lower bound for mean difference: 1.7370
T-Test of mean difference = 0.1 (vs > 0.1): T-Value = 26.81 P-Value = 0.000

Paired T-Test and CI: PCC / Surface Temperature, Gravel / Surface Temperature

Paired T for PCC / Surface Temperature - Gravel / Surface Temperature

	N	Mean	StDev	SE Mean
PCC / Surface Temperatur	62690	27.5242	6.7425	0.0269
Gravel / Surface Tempera	62690	28.0123	10.6187	0.0424
Difference	62690	-0.4881	6.2924	0.0251

95% lower bound for mean difference: -0.5294
T-Test of mean difference = 0.1 (vs > 0.1): T-Value = -23.40 P-Value = 1.000

Paired T-Test and CI: PCC / Surface Temperature, Turf / Surface Temperature

Paired T for PCC / Surface Temperature - Turf / Surface Temperature

	N	Mean	StDev	SE Mean
PCC / Surface Temperatur	62866	27.4751	6.7540	0.0269
Turf / Surface Temperatu	62866	28.3022	14.0174	0.0559
Difference	62866	-0.8270	15.7887	0.0630

95% lower bound for mean difference: -0.9306
T-Test of mean difference = 0.1 (vs > 0.1): T-Value = -14.72 P-Value = 1.000

Paired T-Test and CI: Gravel / Surface Temperature, Turf / Surface Temperature

Paired T for Gravel / Surface Temperature - Turf / Surface Temperature

	N	Mean	StDev	SE Mean
Gravel / Surface Tempera	64250	27.9956	10.6076	0.0418
Turf / Surface Temperatu	64250	28.3131	14.0142	0.0553
Difference	64250	-0.3175	16.0690	0.0634

95% lower bound for mean difference: -0.4218
T-Test of mean difference = 0.1 (vs > 0.1): T-Value = -6.59 P-Value = 1.000

Temperature at 3'

Paired T-Test and CI: HMA T3, PPCC T3

Paired T for HMA T3 - PPCC T3

	N	Mean	StDev	SE Mean
HMA T3	63773	26.0638	6.7114	0.0266
PPCC T3	63773	26.1056	7.0612	0.0280
Difference	63773	-0.04181	0.67393	0.00267

95% lower bound for mean difference: -0.04620
T-Test of mean difference = 0.1 (vs > 0.1): T-Value = -53.14 P-Value = 1.000

Paired T-Test and CI: HMA T3, PHMA T3

Paired T for HMA T3 - PHMA T3

	N	Mean	StDev	SE Mean
HMA T3	53915	25.0467	6.3988	0.0276
PHMA T3	53915	25.1584	6.5041	0.0280
Difference	53915	-0.1117	6.2778	0.0270

95% lower bound for mean difference: -0.1561
T-Test of mean difference = 0.1 (vs > 0.1): T-Value = -7.83 P-Value = 1.000

Paired T-Test and CI: HMA T3, PCC T3

Paired T for HMA T3 - PCC T3

	N	Mean	StDev	SE Mean
HMA T3	63332	26.0749	6.7103	0.0267
PCC T3	63332	26.2032	6.9491	0.0276
Difference	63332	-0.12836	0.66028	0.00262

95% lower bound for mean difference: -0.13267
T-Test of mean difference = 0.1 (vs > 0.1): T-Value = -87.04 P-Value = 1.000

Paired T-Test and CI: PPCC T3, PHMA T3

Paired T for PPCC T3 - PHMA T3

	N	Mean	StDev	SE Mean
PPCC T3	54472	25.0406	6.7617	0.0290
PHMA T3	54472	25.1514	6.4967	0.0278
Difference	54472	-0.1108	6.5871	0.0282

95% lower bound for mean difference: -0.1572
T-Test of mean difference = 0.1 (vs > 0.1): T-Value = -7.47 P-Value = 1.000

Paired T-Test and CI: PPCC T3, PCC T3

Paired T for PPCC T3 - PCC T3

	N	Mean	StDev	SE Mean
PPCC T3	63944	26.0815	7.0645	0.0279
PCC T3	63944	26.1690	6.9527	0.0275
Difference	63944	-0.08750	0.84903	0.00336

95% lower bound for mean difference: -0.09302
T-Test of mean difference = 0.1 (vs > 0.1): T-Value = -55.84 P-Value = 1.000

Paired T-Test and CI: PHMA T3, PCC T3

Paired T for PHMA T3 - PCC T3

	N	Mean	StDev	SE Mean
PHMA T3	54053	25.1650	6.4906	0.0279
PCC T3	54053	25.1429	6.6421	0.0286
Difference	54053	0.0221	6.1383	0.0264

95% lower bound for mean difference: -0.0213
T-Test of mean difference = 0.1 (vs > 0.1): T-Value = -2.95 P-Value = 0.998

Temperature at 5'

Paired T-Test and CI: HMA T5, PPCC T5

Paired T for HMA T5 - PPCC T5

	N	Mean	StDev	SE Mean
HMA T5	62507	26.0075	6.7892	0.0272
PPCC T5	62507	26.0236	6.7920	0.0272
Difference	62507	-0.01613	0.59092	0.00236

95% lower bound for mean difference: -0.02002
T-Test of mean difference = 0.1 (vs > 0.1): T-Value = -49.13 P-Value = 1.000

Paired T-Test and CI: HMA T5, PHMA T5

Paired T for HMA T5 - PHMA T5

	N	Mean	StDev	SE Mean
HMA T5	52698	24.9756	6.4705	0.0282
PHMA T5	52698	25.0642	6.5600	0.0286

Difference	52698	-0.0886	6.4587	0.0281

95% lower bound for mean difference: -0.1348
T-Test of mean difference = 0.1 (vs > 0.1): T-Value = -6.70 P-Value = 1.000

Paired T-Test and CI: HMA T5, PCC T5

Paired T for HMA T5 - PCC T5

	N	Mean	StDev	SE Mean
HMA T5	60609	26.0165	6.7942	0.0276
PCC T5	60609	26.1199	6.7717	0.0275
Difference	60609	-0.10335	0.51881	0.00211

95% lower bound for mean difference: -0.10681
T-Test of mean difference = 0.1 (vs > 0.1): T-Value = -96.49 P-Value = 1.000

Paired T-Test and CI: HMA T5, PCC T5

Paired T for HMA T5 - PCC T5

	N	Mean	StDev	SE Mean
HMA T5	60609	26.0165	6.7942	0.0276
PCC T5	60609	26.1199	6.7717	0.0275
Difference	60609	-0.10335	0.51881	0.00211

95% lower bound for mean difference: -0.10681
T-Test of mean difference = 0.1 (vs > 0.1): T-Value = -96.49 P-Value = 1.000

Paired T-Test and CI: HMA T5, Gravel T5

Paired T for HMA T5 - Gravel T5

	N	Mean	StDev	SE Mean
HMA T5	62701	26.0085	6.7908	0.0271
Gravel T5	62701	27.0817	8.5890	0.0343
Difference	62701	-1.0732	9.7611	0.0390

95% lower bound for mean difference: -1.1373
T-Test of mean difference = 0.1 (vs > 0.1): T-Value = -30.10 P-Value = 1.000

Paired T-Test and CI: PPCC T5, PHMA T5

Paired T for PPCC T5 - PHMA T5

	N	Mean	StDev	SE Mean

PPCC T5	54492	24.9629	6.4740	0.0277
PHMA T5	54492	25.0551	6.5558	0.0281
Difference	54492	-0.0922	6.6662	0.0286

95% lower bound for mean difference: -0.1392
T-Test of mean difference = 0.1 (vs > 0.1): T-Value = -6.73 P-Value = 1.000

Paired T-Test and CI: PPCC T5, PCC T5

Paired T for PPCC T5 - PCC T5

	N	Mean	StDev	SE Mean
PPCC T5	62651	26.0061	6.7998	0.0272
PCC T5	62651	26.0950	6.7743	0.0271
Difference	62651	-0.08899	0.85903	0.00343

95% lower bound for mean difference: -0.09463
T-Test of mean difference = 0.1 (vs > 0.1): T-Value = -55.07 P-Value = 1.000

Paired T-Test and CI: PPCC T5, Gravel T5

Paired T for PPCC T5 - Gravel T5

	N	Mean	StDev	SE Mean
PPCC T5	64307	26.0431	6.7810	0.0267
Gravel T5	64307	27.0661	8.5310	0.0336
Difference	64307	-1.0230	9.6343	0.0380

95% lower bound for mean difference: -1.0855
T-Test of mean difference = 0.1 (vs > 0.1): T-Value = -29.56 P-Value = 1.000

Paired T-Test and CI: PHMA T5, PCC T5

Paired T for PHMA T5 - PCC T5

	N	Mean	StDev	SE Mean
PHMA T5	52786	25.0729	6.5396	0.0285
PCC T5	52786	25.0461	6.4325	0.0280
Difference	52786	0.0268	6.2170	0.0271

95% lower bound for mean difference: -0.0177
T-Test of mean difference = 0.1 (vs > 0.1): T-Value = -2.70 P-Value = 0.997

Paired T-Test and CI: PHMA T5, Gravel T5

Paired T for PHMA T5 - Gravel T5

	N	Mean	StDev	SE Mean
PHMA T5	54115	25.0829	6.5462	0.0281

Gravel T5	54115	26.2397	8.6978	0.0374
Difference	54115	-1.1568	8.3033	0.0357

95% lower bound for mean difference: -1.2155
T-Test of mean difference = 0.1 (vs > 0.1): T-Value = -35.21 P-Value = 1.000

Paired T-Test and CI: PCC T5, Gravel T5

Paired T for PCC T5 - Gravel T5

	N	Mean	StDev	SE Mean
PCC T5	62336	26.1409	6.7619	0.0271
Gravel T5	62336	27.0814	8.5271	0.0342
Difference	62336	-0.9405	9.5358	0.0382

95% lower bound for mean difference: -1.0033
T-Test of mean difference = 0.1 (vs > 0.1): T-Value = -27.24 P-Value = 1.000

APPENDIX F

REGRESSION ANALYSIS

Response Temp
Summary of Fit

RSquare	0.886536
RSquare Adj	0.886521
Root Mean Square Error	0.060369
Mean of Response	3.430472
Observations (or Sum Wgts)	60473

Analysis of Variance

Source	**DF**	**Sum of Squares**	**Mean Square**	**F Ratio**
Model	8	1721.7251	215.216	59053.59
Error	60464	220.3557	0.003644	**Prob > F**
C. Total	60472	1942.0808		<.0001*

Parameter Estimates

Term	**Estimate**	**Std Error**	**t Ratio**	**Prob>|t|**
Intercept	3.5668785	0.011311	315.36	<.0001*
Elevation (E)	-0.011615	0.000969	-11.99	<.0001*
Wind Speed (WS)	0.0117781	0.000222	53.07	<.0001*
Wind Direction (WD)	0.0452289	0.00031	146.10	<.0001*
Humidity (H)	-0.170807	0.000556	-307.4	<.0001*
Solar Radiation (SR)	0.0293603	0.000155	189.39	<.0001*
Albedo (A)	0.0015701	0.00042	3.74	0.0002*
Diffusivity (D)	-0.000471	0.000783	-0.60	0.5477
Time (t)	0.0273729	0.000327	83.64	<.0001*

$T= e^{35668785}E^{-0.011615}WS^{0.0117781}WD^{0.0452289}H^{-0.170807}SR^{0.0293603}o^{0.0015701}D^{-0.000471}t^{0.0273729}$

t: time of the day, 0 to 23.99

Note that natural log of the data (ln), for dependent and independent variables was taken. After the regression analysis was completed, the regression model was converted into a power model. Due to the nature of this model, it is only valid when there is no zero as an input variable.

APPENDIX G

PAVEMENT TEMPERATURE MODEL

PCC

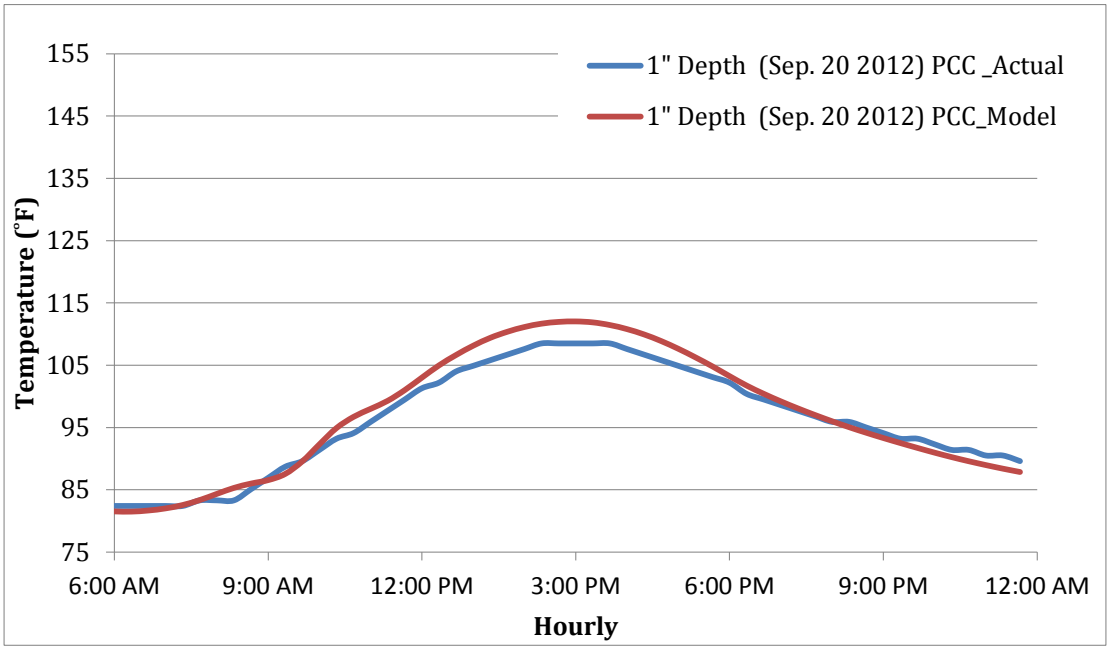
155
145
135
125
115
105
95
85
75
Temperature (°F)
1" Depth (Sep. 20 2012) PCC _Actual
1" Depth (Sep. 20 2012) PCC_Model
6:00 AM
9:00 AM
12:00 PM
3:00 PM
6:00 PM
9:00 PM
12:00 AM
Hourly

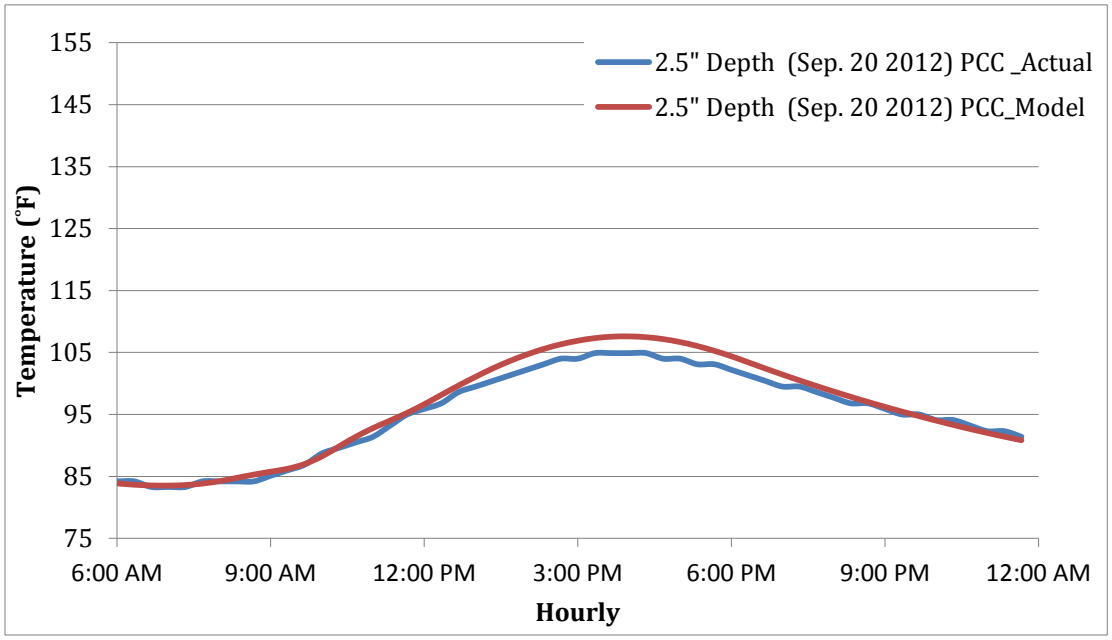
155
145
135
125
115
105
95
85
75
Temperature (°F)
2.5" Depth (Sep. 20 2012) PCC _Actual
2.5" Depth (Sep. 20 2012) PCC_Model
6:00 AM
9:00 AM
12:00 PM
3:00 PM
6:00 PM
9:00 PM
12:00 AM
Hourly

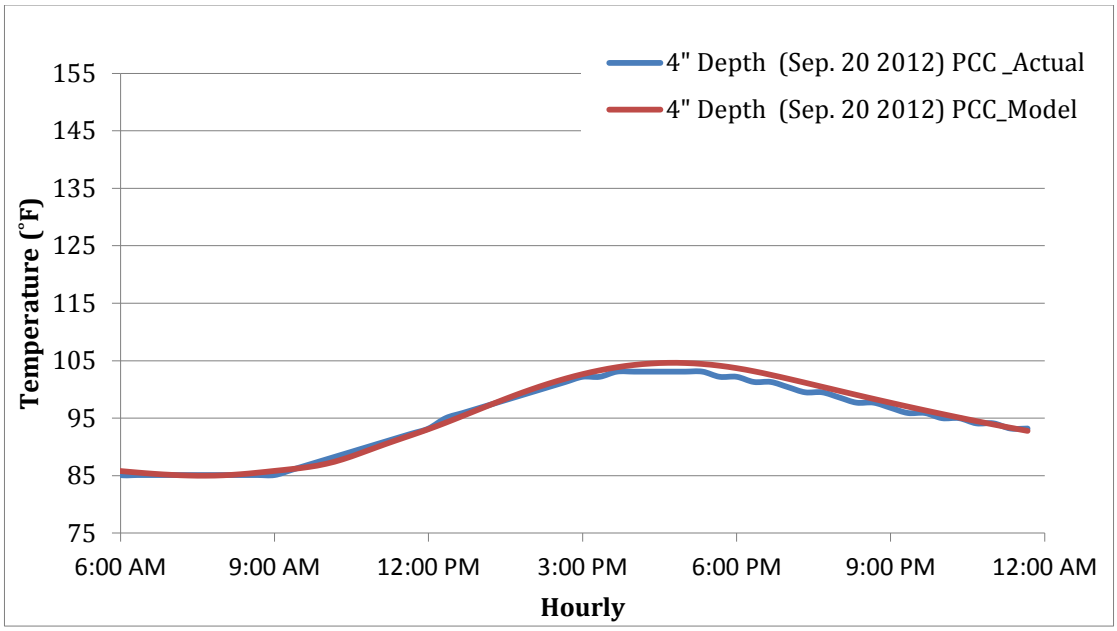
4" Depth (Sep. 20 2012) PCC _Actual
4" Depth (Sep. 20 2012) PCC_Model
155
145
135
125
115
105
95
85
75
Temperature (°F)
6:00 AM
9:00 AM
12:00 PM
3:00 PM
6:00 PM
9:00 PM
12:00 AM
Hourly

PHMA

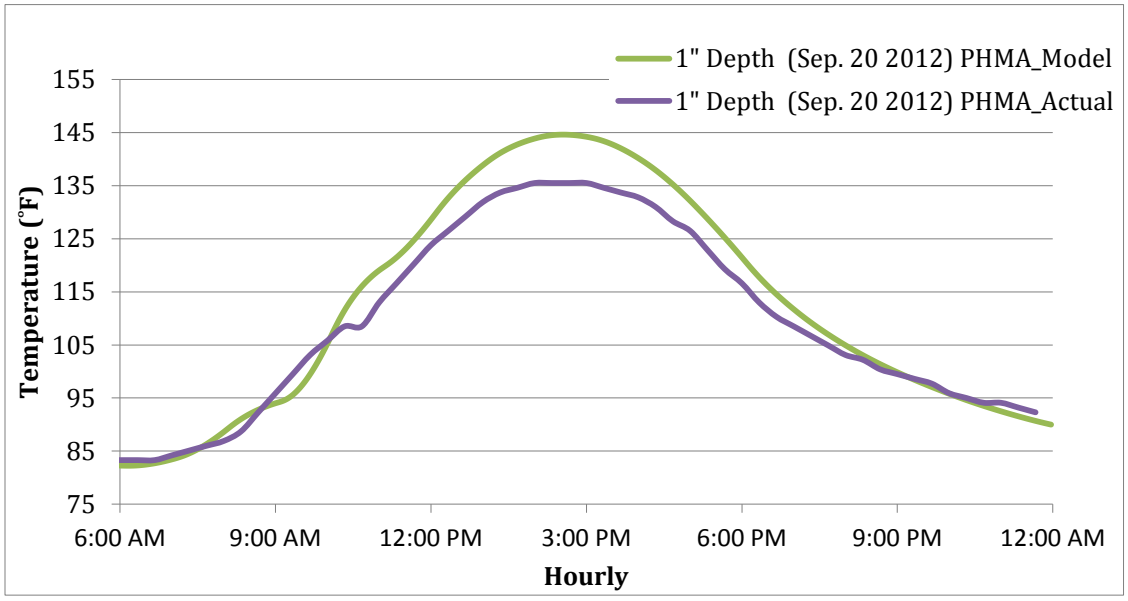
1" Depth (Sep. 20 2012) PHMA_Model
1" Depth (Sep. 20 2012) PHMA_Actual
155
145
135
125
115
105
95
85
75
Temperature (°F)
6:00 AM
9:00 AM
12:00 PM
3:00 PM
6:00 PM
9:00 PM
12:00 AM
Hourly

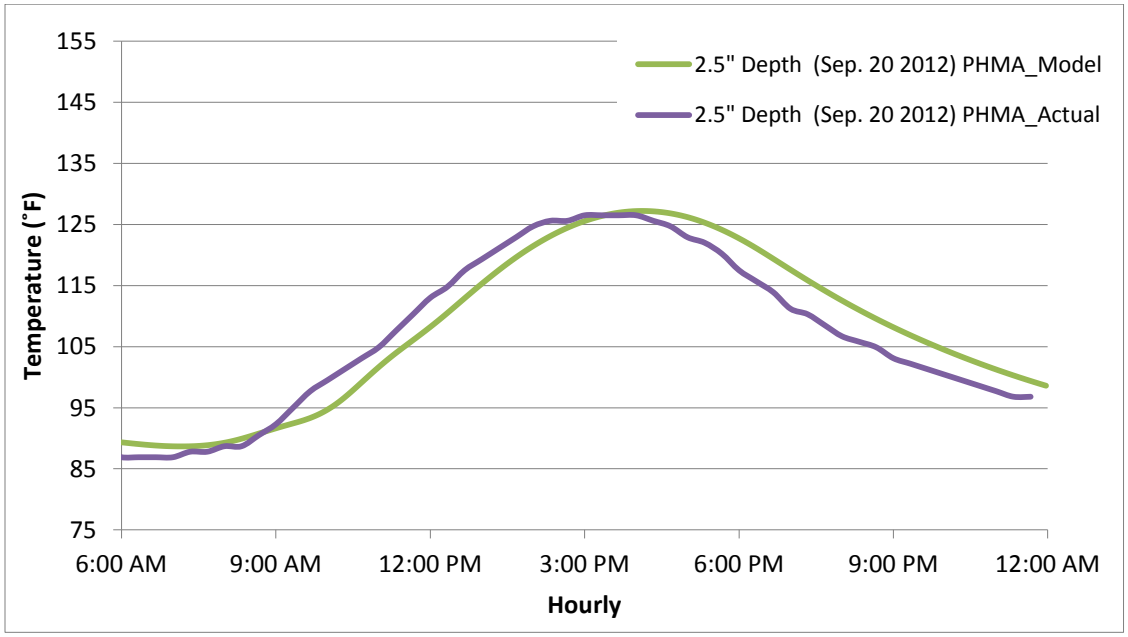
2.5" Depth (Sep. 20 2012) PHMA_Model
2.5" Depth (Sep. 20 2012) PHMA_Actual
155
145
135
125
115
105
95
85
75
Temperature (°F)
6:00 AM
9:00 AM
12:00 PM
3:00 PM
6:00 PM
9:00 PM
12:00 AM
Hourly

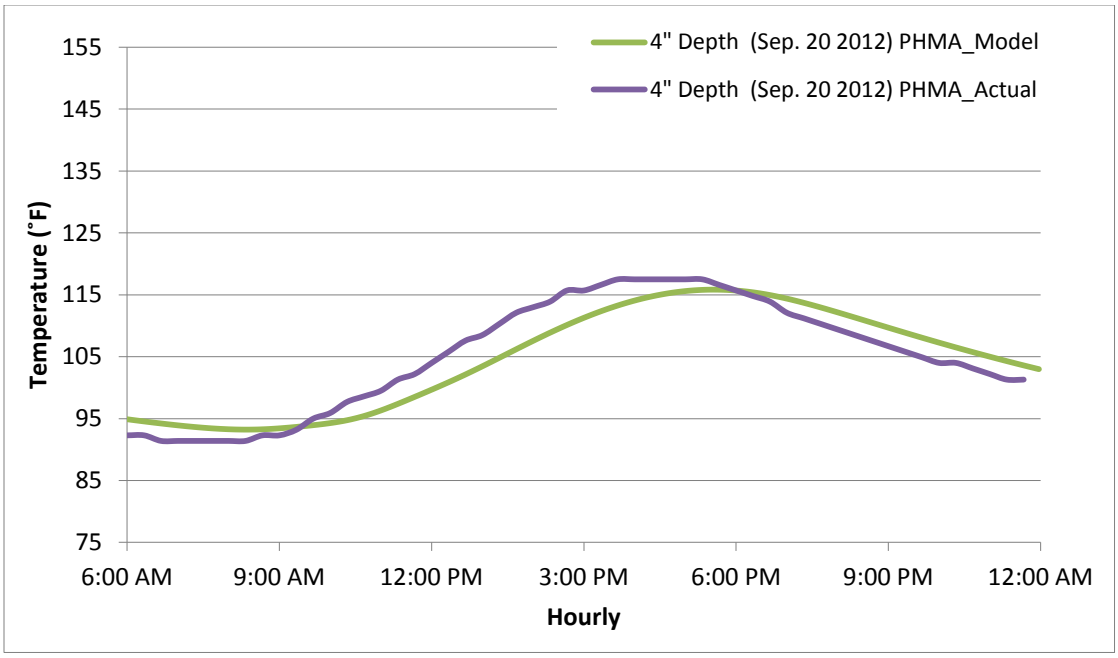
4" Depth (Sep. 20 2012) PHMA_Model
4" Depth (Sep. 20 2012) PHMA_Actual
155
145
135
125
115
105
95
85
75
Temperature (°F)
6:00 AM
9:00 AM
12:00 PM
3:00 PM
6:00 PM
9:00 PM
12:00 AM
Hourly

PPCC

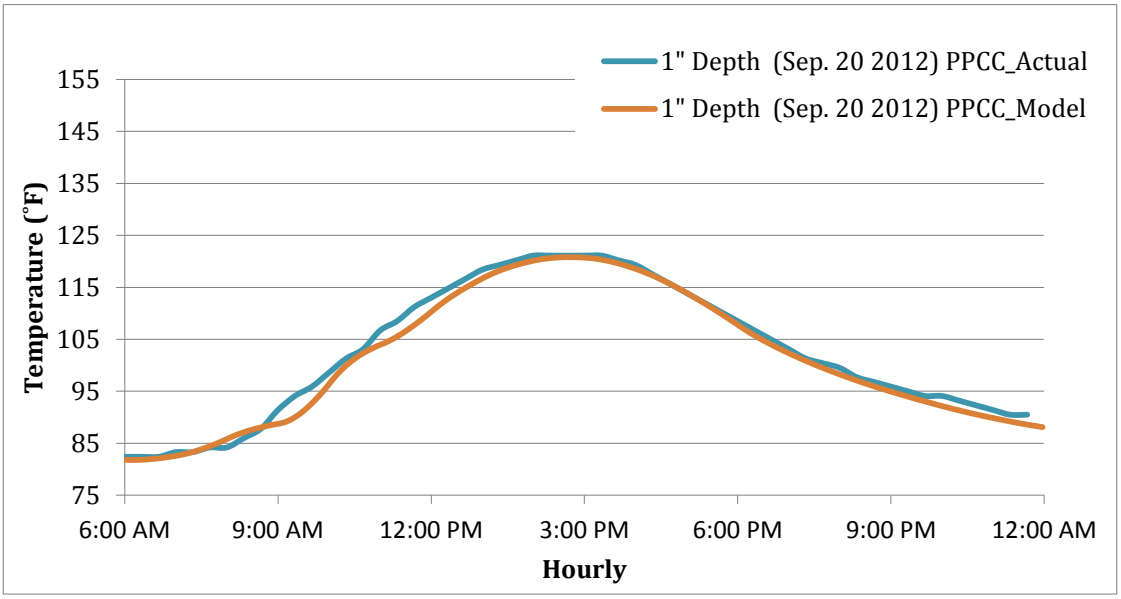
1" Depth (Sep. 20 2012) PPCC_Actual
1" Depth (Sep. 20 2012) PPCC_Model
155
145
135
125
115
105
95
85
75
Temperature (°F)
6:00 AM
9:00 AM
12:00 PM
3:00 PM
6:00 PM
9:00 PM
12:00 AM
Hourly

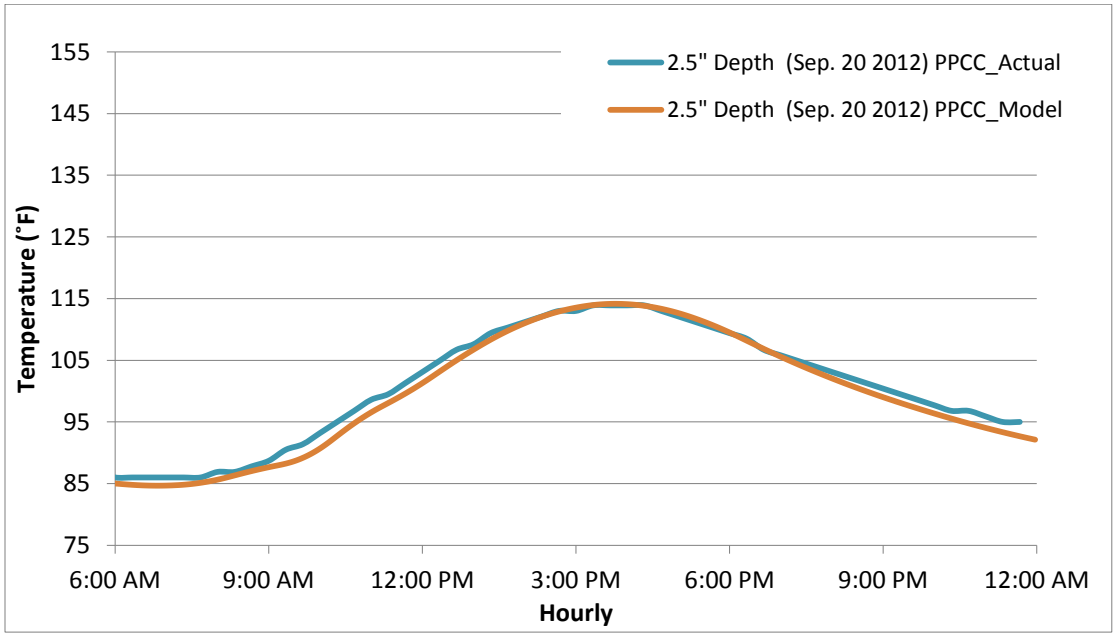
2.5" Depth (Sep. 20 2012) PPCC_Actual
2.5" Depth (Sep. 20 2012) PPCC_Model
155
145
135
125
115
105
95
85
75
Temperature (°F)
6:00 AM
9:00 AM
12:00 PM
3:00 PM
6:00 PM
9:00 PM
12:00 AM
Hourly

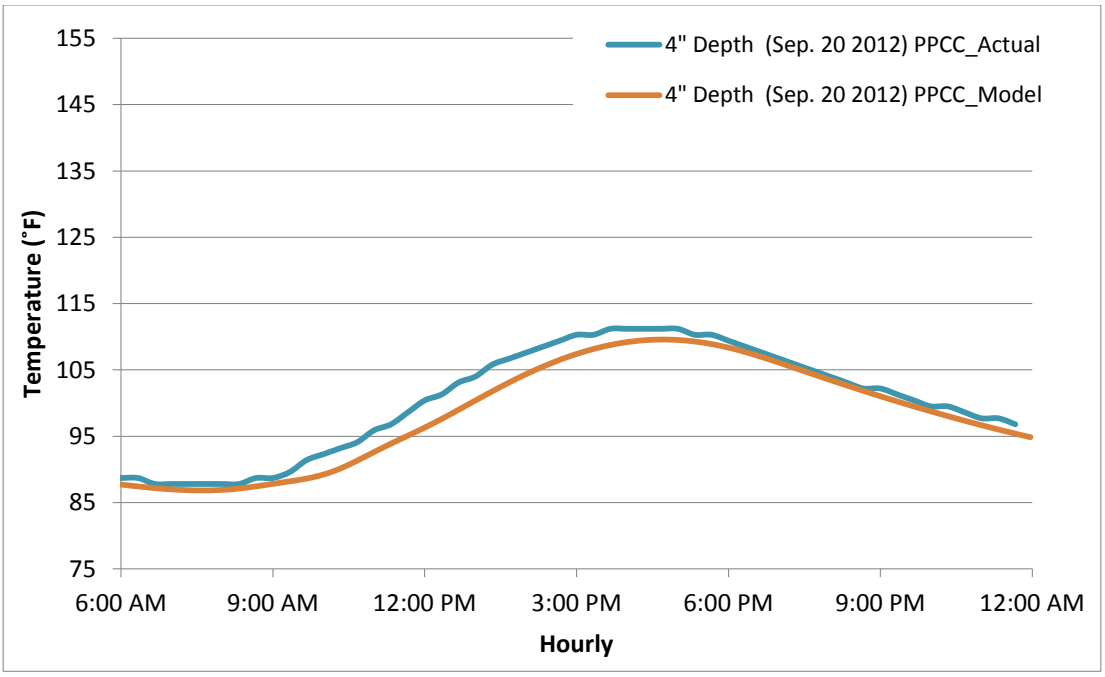
4" Depth (Sep. 20 2012) PPCC_Actual
4" Depth (Sep. 20 2012) PPCC_Model
155
145
135
125
115
105
95
85
75
Temperature (°F)
6:00 AM
9:00 AM
12:00 PM
3:00 PM
6:00 PM
9:00 PM
12:00 AM
Hourly